DISEÑO DE LACASAS FÚNGICAS ACTIVAS EN SANGRE MEDIANTE EVOLUCIÓN DIRIGIDA

MEMORIA

para optar al grado de Doctora en Química por la Universidad Autónoma de Madrid
presentada por:

DIANA MATÉ MATE

DIRECTORES:

Dr. Miguel Alcalde Galeote y Dr. Francisco José Plou Gasca

Instituto de Catálisis y Petroleoquímica (ICP)
Consejo Superior de Investigaciones Científicas, Madrid

TUTORA:

Dra. María Fernández Lobato

Departamento de Biología Molecular
Facultad de Ciencias
Universidad Autónoma de Madrid

MADRID, 2013

Miguel Alcalde Galeote, Dr. en Ciencias Biológicas, Científico Titular del CSIC, y Francisco José Plou Gasca, Dr. en Ciencias Químicas, Investigador Científico del CSIC.

CERTIFICAN:

Que el presente trabajo "*Diseño de lacasas fúngicas activas en sangre mediante evolución dirigida*" constituye la Memoria que presenta la Licenciada en Química por la Universidad Autónoma de Madrid, Diana Maté Mate, para optar al grado de Doctora, y que ha sido realizado bajo su dirección en el Departamento de Biocatálisis del Instituto de Catálisis y Petroleoquímica del CSIC, Madrid.

Y para que conste, firman el presente certificado en Madrid, a 10 de Mayo de 2013.

Dr. Miguel Alcalde Galeote

Dr. Francisco José Plou Gasca

A mis padres

A mi hermana

"Defiende tu derecho a pensar,
porque incluso pensar de manera errónea
es mejor que no pensar."
Hipatia de Alejandría

AGRADECIMIENTOS

La presente Tesis Doctoral, realizada en el Instituto de Catálisis y Petroleoquímica (ICP) del Consejo Superior de Investigaciones Científicas (CSIC), ha sido cofinanciada por una beca JAE-Predoc del CSIC, por el proyecto del Séptimo Programa Marco "*Three-dimensional nanobiostructure-based selfcontained devices for biomedical application*" (3D-NANOBIODEVICE, Ref. NMP4-SL-2009-229255) y por el proyecto del Plan Nacional "Evolución molecular dirigida de factorías celulares ligninolíticas en S*accharomyces cerevisiae*: aplicaciones medioambientales, industriales y energéticas" (EVOFACEL, Ref. BIO2010-19697).

Antes de que os sumerjáis en el fascinante mundo de la evolución dirigida de lacasas, me gustaría dedicar unas líneas para mostrar mi más sincero agradecimiento a las numerosas personas que, de una manera u otra, han contribuido con su cariño, apoyo y consejo a la realización de esta Tesis.

En primer lugar, a mis directores de Tesis, los Dres. Miguel Alcalde y Francisco José Plou, por darme la oportunidad de formar parte de su grupo de investigación, por su dedicación y apoyo durante estos cuatro años y por todo su esfuerzo, especialmente durante la fase de escritura de los artículos y de la Tesis.

A mi tutora de Tesis en el Dpto. de Biología Molecular de la Universidad Autónoma de Madrid (UAM), la Dra. María Fernández Lobato, por su interés y su excelente disposición.

Al Dr. Antonio Ballesteros, por su amabilidad y sabios consejos.

A la Dra. Susana Camarero, del Centro de Investigaciones Biológicas (CIB) del CSIC, por su cariño y amistad, por su ayuda cuando empecé en esto de la evolución dirigida y por los grandes momentos compartidos dentro y fuera del laboratorio.

A los Dres. Antonio López de Lacey y Marcos Pita, del ICP, por su colaboración en los estudios sobre electroquímica de lacasas.

Al Dr. Sergey Shleev, de la Universidad de Malmö (Suecia), y a los Dres. Roland Ludwig y Roman Kittl, de la Universidad de Recursos Naturales y Ciencias de la Vida (BOKU) de Viena (Austria), por permitirme llevar a cabo sendas estancias predoctorales en sus grupos de investigación. Gracias a Sergey por su paciencia y por enseñarme todo lo que sé sobre el complejo mundo de la espectroelectroquímica de lacasas, pero, sobre todo, gracias por su confianza y amistad. Gracias a Roland por sus consejos y su buen humor. Y especialmente gracias a Roman, por su supervisión, por toda la ayuda prestada en el clonaje y expresión de la

lacasa en *Pichia pastoris* y por los inolvidables momentos compartiendo cervezas y risas en el despacho tras días que parecían interminables.

Al Dr. Vicente Fernández, de la UAM, por ser un excelente profesor y por ponerme en su día en contacto con Miguel Alcalde.

Al Dr. Manuel Ferrer, del ICP, y a Iris Plumeier, del Centro Helmholtz para la Investigación de Infecciones (Braunschweig, Alemania) por los análisis de la secuencia N-terminal. A los Dres. Vivian de los Ríos y Francisco García Tabares, ambos del CIB, por los análisis de MALDI-TOF y de geles bidimensionales, respectivamente. Al servicio de Química de Proteínas del CIB por la síntesis de oligonucleótidos y la secuenciación de genes.

A mis compañeros del grupo de Biocatálisis Aplicada del ICP, mi "familia científica", por todo vuestro apoyo y cariño. Esta Tesis es también vuestra. Gracias a Miguel por confiar en mí, por enseñarme todo lo que sé sobre evolución dirigida de enzimas, por su paciencia en los momentos difíciles y por transmitirme el poder de la "Fuerza" día tras día. Porque además de gran científico y mejor persona, es un auténtico "Maestro Jedi". Gracias a Kiko por sus consejos, por su ayuda y orientación en tantos experimentos, por darme la oportunidad de ejercer como profesora de evolución dirigida en la Universidad Francisco de Vitoria de Madrid y por hacerme partícipe de las diversas actividades de divulgación de la ciencia que ha organizado. A Eva, por sus enseñanzas en mis inicios en el mundo de la Biología Molecular, por toda la ayuda prestada a lo largo de la Tesis y por los grandes momentos compartidos, tanto en el laboratorio como en los múltiples viajes a congresos a los que hemos tenido la oportunidad de asistir juntas. A David, por estar siempre dispuesto a ayudarme (especialmente, durante la fase de escritura), por su paciencia para explicarme todo lo que le preguntaba, por instruirme en el uso del PyMOL, pero sobre todo, gracias por su amistad y por los inolvidables momentos vividos juntos. A Patricia, por su alegría y buen humor, por animarme continuamente y por permitirme descubrir uno de los mejores dulces del país: los lazos de Soria. A Bernardo y Javier, por su alegría, por ser unos chicos estupendos. A Bárbara, mi "compi" de Máster y posteriormente de Tesis, por su desparpajo, por estar tan loquilla y sacarme siempre una sonrisa. A Lucía, Pamela y Paloma, por su cariño y optimismo, así como por todas las risas compartidas dentro y fuera del laboratorio. A las numerosas personas que durante este tiempo han pasado por el grupo, permitiéndome aprender sobre otras culturas y con los que he compartido buenos momentos: Mike, Gina, Xavi, Enrique, Paolo, Rafa, Alina, Laura, Mohammad, Paulina, Julia, Elisa, Cecilia, Ivanna y Berta.

A los compañeros del Dpto. de Biocatálisis del ICP (Víctor, Antonio, Manolo, Jaime, Nieves, Óscar, Cristina, Mónica, Rafa, Mercedes, María, Patricia, Álvaro y Jesús) por darme ánimos y por ser tan buena gente. En especial, gracias a Marcos por su cariño y por estar siempre dispuesto a escucharme, así como por revisar el apartado de "Aplicación de lacasas en biopilas

de combustible y biosensores" de esta Tesis. Gracias también especialmente a la Dra. Ana Bahamonde, por su apoyo durante este tiempo, por las confidencias compartidas y por todo el afecto mostrado.

A todos los trabajadores del ICP (personal de Almacén, Secretaría, Mantenimiento, Unidad de Apoyo, Biblioteca y las señoras de la limpieza, en especial a Carmen), por los servicios prestados durante este tiempo.

A todos mis compañeros durante las estancias en Malmö (Yana, Magnus, Viktor, Vida, Peter, Javier, Alejandro,…) y en Viena (Dagmar, Michael, Victoria, Daniel, Stefan, Alfons, Christoph, Cindy, Kawa,…), por los grandes momentos compartidos junto a ellos tanto dentro como fuera del laboratorio y por hacerme sentir como en familia estando lejos de casa.

A mis compañeras Isabel y Ana Isabel del CIB, por los buenos ratos vividos durante las reuniones del proyecto EVOFACEL; así como a todos los investigadores participantes en el proyecto europeo *3D-nanobiodevice*, por las enriquecedoras conversaciones que he compartido con ellos.

A mis amigos de Sanse: Alfonso, Lorena, Kike, Lucía, Álex, Marcos y Pablo, por su amistad y su apoyo continuo, por todos los buenos ratos vividos desde hace tantos años y que espero que sigamos compartiendo mucho tiempo. En especial, gracias a Laura y a Nerea. A Laura, por todo su cariño y por ser tan buena persona, porque siempre ha estado ahí cuando la he necesitado. Y a Nerea, por su amistad, por contagiarme su alegría y sus ganas de comerse el mundo y por todos los momentos geniales que hemos compartido desde que nos conocimos en la Facultad.

Por último, gracias de corazón a mi familia. A mi hermana Paloma, la otra Dra. Maté, por sus ánimos y motivación ☺. Y lo más importante: gracias a mis padres por su amor incondicional y su dedicación continua. A ti papá, por mimarme tanto desde siempre, y a ti mamá, por tu comprensión y por ser mi ejemplo a seguir en la vida. Todo lo que soy y todo lo que he conseguido ha sido gracias a vosotros.

ÍNDICE DE CONTENIDOS

ÍNDICE DE FIGURAS Y TABLAS ..... **VII**
LISTADO DE ABREVIATURAS Y ACRÓNIMOS ..... **XI**
SUMMARY **1**
ESTRUCTURA GENERAL **5**
1. INTRODUCCIÓN GENERAL **9**
1.1. EVOLUCIÓN MOLECULAR DIRIGIDA **11**
1.1.1. Aspectos generales 11
1.1.2. Elección del microorganismo hospedador 14
1.1.3. Creación de diversidad génica 16
1.1.4. Métodos de selección y *screening* 22
1.1.5. Diseño de estrategias evolutivas 25
1.2. LACASAS **28**
1.2.1. Distribución en la naturaleza y función biológica 28
1.2.2. Generalidades bioquímicas 30
1.2.3. Características estructurales y mecanismo catalítico 32
1.2.4. Lacasas no azules 34
1.2.5. Lacasas y potencial redox 36
1.2.6. Expresión de lacasas recombinantes 38
1.2.7. Aplicaciones industriales y biotecnológicas 42
1.2.8. Lacasas en biopilas de combustible y biosensores enzimáticos 43
1.2.9. La lacasa PM1 47
1.3. OBJETIVOS **48**
2. PUBLICACIONES **49**
2.1. CAPÍTULO 1 ..... **51**
2.1.1. SUMMARY 51
2.1.2. INTRODUCTION 51
2.1.3. RESULTS AND DISCUSSION 53
2.1.3.1. Point of departure for evolution: the construction of α-PM1 53
2.1.3.2. Laboratory evolution of α-PM1 53
2.1.3.3. Recovery of beneficial mutations 58
2.1.3.4. Mutational exchange with a related evolved HRPL 60

2.1.3.5. Directed evolution of the α-factor prepro-leader 60
2.1.3.6. Characterization of the OB-1 mutant 61
2.1.4. SIGNIFICANCE 67
2.1.5. EXPERIMENTAL PROCEDURES 69
2.1.5.1. Laboratory evolution: general aspects 69
2.1.5.2. First generation 69
2.1.5.3. Second generation 70
2.1.5.4. Third generation 70
2.1.5.5. Fourth generation 70
2.1.5.6. Fifth generation 70
2.1.5.7. Sixth generation 71
2.1.5.8. Site-directed mutagenesis 71
2.1.5.9. High-throughput screening 71
2.1.6. SUPPLEMENTAL EXPERIMENTAL PROCEDURES 71
2.1.6.1. Reagents and enzymes 71
2.1.6.2. Culture media 72
2.1.6.3. Construction of α-PM1 72
2.1.6.4. Site-directed mutagenesis approach 73
2.1.6.5. High-throughput screening assays: general aspects 75
2.1.6.6. Estimation of total activity improvement (TAI) 77
2.1.6.7. Production and purification of laccase 78
2.1.6.8. MALDI-TOF analysis 79
2.1.6.9. N-terminal analysis 79
2.1.6.10. Determination of thermostability 79
2.1.6.11. DNA sequencing 80
2.1.6.12. Protein modelling 80
2.1.7. SUPPLEMENTAL FIGURES AND TABLES 81
2.2. CAPÍTULO 2 89
2.2.1. SUMMARY 89
2.2.2. BACKGROUND 89
2.2.3. MATERIALS AND METHODS 91
2.2.3.1. Culture media 91
2.2.3.2. Library construction for laboratory evolution 92
2.2.3.3. High-throughput thermostability assay 93

2.2.3.4. Determination of thermostabilities in VP and HRPL parent types 95
2.2.3.5. DNA sequencing 95
2.2.3.6. Protein modelling 96
2.2.4. RESULTS AND DISCUSSION 96
2.2.4.1. Library construction 96
2.2.4.2. High-throughput screening assay 98
2.2.4.3. Library analysis 100
2.2.5. CONCLUSIONS 105
2.3. CAPÍTULO 3 109
2.3.1. SUMMARY 109
2.3.2. LACCASES: GENERAL FEATURES 109
2.3.3. DIRECTED EVOLUTION OF FUNGAL LACCASES 111
2.4. CAPÍTULO 4 123
2.4.1. SUMMARY 123
2.4.2. INTRODUCTION 124
2.4.3. MATERIAL AND METHODS 125
2.4.3.1. Materials 125
2.4.3.2. Culture media 125
2.4.3.3. Truncated variant (OB-1del mutant) 126
2.4.3.4. Production and purification of laccases 126
2.4.3.5. Estimation of copper content 128
2.4.3.6. MALDI-TOF analysis 128
2.4.3.7. Protein identification by peptide mass fingerprinting 128
2.4.3.8. pI determination 128
2.4.3.9. N-terminal analysis 129
2.4.3.10. Kinetic parameters 129
2.4.3.11. Determination of thermostability 129
2.4.3.12. Electrochemical characterization 130
2.4.3.13. Circular dichroism spectra 130
2.4.3.14. DNA sequencing 130
2.4.3.15. Protein modelling 131
2.4.4. RESULTS AND DISCUSSION 131
2.4.4.1. The yellow OB-1 mutant 131
2.4.4.2. Biochemical characterization 134

2.4.4.3. Laccase-mediator system 134
2.4.4.4. Spectro-electrochemical characterization 135
2.4.4.5. OB-1 truncated variant 139
2.4.4.6. Modification of the coordination sphere of the T1 Cu site 142
2.4.5. CONCLUSIONS 142
2.5. CAPÍTULO 5 145
2.5.1. SUMMARY 145
2.5.2. INTRODUCTION 145
2.5.3. RESULTS AND DISCUSSION 146
2.5.3.1. Laboratory evolution approach 146
2.5.3.2. Laccase mutant in blood 148
2.5.3.3. Inhibition by halides and hydroxides 149
2.5.3.4. Structural analysis of mutations 153
2.5.4. SIGNIFICANCE 154
2.5.5. EXPERIMENTAL PROCEDURES 156
2.5.5.1. Laboratory evolution 156
2.5.5.2. Screening assay and high-throughput protocol 158
2.5.5.3. Laccase production and purification 159
2.5.5.4. Measurement of laccase activity in human plasma and blood 159
2.5.5.5. Biochemical characterization 159
2.5.5.6. Spectro-electrochemical studies 160
2.5.5.7. Protein modelling 161
2.5.6. SUPPLEMENTAL RESULTS 161
2.5.7. SUPPLEMENTAL FIGURES AND TABLES 163
2.6. CAPÍTULO 6 169
2.6.1. SUMMARY 169
2.6.2. BACKGROUND 170
2.6.3. RESULTS AND DISCUSSION 172
2.6.3.1. Heterologous functional expression of blood tolerant laccases in *P. pastoris* 172
2.6.3.2. Biochemical characterization 173
2.6.4. CONCLUSIONS 183
2.6.5. METHODS 183
2.6.5.1. Strains and chemicals 183
2.6.5.2. Laccase functional expression in *P. pastoris* 183

2.6.5.3. Production and purification of the laccase expressed in *S. cerevisiae* 186
2.6.5.4. Biochemical characterization 186
2.6.5.5. Protein modelling 188
3. RESUMEN GENERAL 189
3.1. INTRODUCCIÓN 191
3.2. EVOLUCIÓN DIRIGIDA DE LA LACASA PM1 PARA EXPRESIÓN FUNCIONAL EN *S. cerevisiae* 191
3.2.1. Punto de partida 191
3.2.2. Diseño evolutivo 192
3.2.3. Buscando un compromiso entre actividad y estabilidad 194
3.2.4. Caracterización de la lacasa mutante de secreción OB-1 197
3.3. EVOLUCIÓN DIRIGIDA DE LA LACASA PM1 PARA SER ACTIVA EN SANGRE 201
3.3.1. Estrategia evolutiva 201
3.3.2. Caracterización de la lacasa mutante activa en sangre ChU-B 208
3.3.3. Sobreexpresión de ChU-B en *Pichia pastoris* 211
3.4. CONCLUSIONES 213
4. BIBLIOGRAFÍA 215
5. ANEXOS 243
5.1. ANEXO I: Producción científica de la doctoranda 245
5.2. ANEXO II: Secuencia de la lacasa α-PM1 249

ÍNDICE DE FIGURAS Y TABLAS

Figura 1.1. Esquema general de un experimento de evolución molecular dirigida. **12**

Figura 1.2. Número de artículos científicos sobre evolución dirigida publicados por año desde 1990 hasta Abril de 2013 inclusive **14**

Figura 1.3. Algunos de los métodos empleados en evolución dirigida y biología sintética para la creación de diversidad genética *in vivo* haciendo uso de *Saccharomyces cerevisiae* **23**

Figura 1.4. Ejemplos de herramientas HTS utilizadas en experimentos de evolución dirigida .. 25

Figura 1.5. Representación esquemática de la actividad lacasa en ausencia (**A**) o en presencia (**B**) de mediadores redox. **31**

Figura 1.6. Modelo tridimensional de la lacasa del basidiomiceto PM1 en base a la estructura cristalográfica de la lacasa de *Trametes trogii* **33**

Figura 1.7. Esquema de una biopila de combustible enzimática con transferencia electrónica directa **44**

Figura 1.8. Representación esquemática de un dispositivo autónomo con aplicaciones biomédicas **46**

Figure 2.1.1. Artificial evolution pathway for α-PM1 laccase **55**

Figure 2.1.2. Suggested crossovers events during the directed evolution of α-PM1 laccase. **57**

Figure 2.1.3. Rational approach to thermostability **59**

Figure 2.1.4. Biochemical characterization of OB-1 mutant **64**

Figure 2.1.5. Mutations in evolved laccase **66**

Figure 2.1.S1. Cloning strategy for the construction of α-PM1 ..... **81**

Figure 2.1.S2. Artificial evolution pathway for α-PcL **82**

Figure 2.1.S3. Partial alignment of the PM1 amino acid sequence and that of other highly related HRPLs **83**

Figure 2.1.S4. Characterization of OB-1 ..... **84**

Figure 2.1.S5. General structure of the OB-1 evolved laccase **85**

Figure 2.2.1. Schematic representation of methods employed for the construction of VP (**A**) and HRPL (**B**) mutant libraries. **97**

Figure 2.2.2. Validation of the colorimetric assay for the VP-library **99**

Figure 2.2.3. High-throughput protocol used for screening thermostability in VP- and HRPL-libraries **100**

Figure 2.2.4. Directed evolution landscapes **101**

Figure 2.2.5. Improved variants screened from VP-library **102**

Figure 2.2.6. (**A**) T_{50} for VP parent types and different mutants of the evolutionary process. (**B**) T_{50} for HRPL parent types and mutants of the *in vitro* evolution. **103**

Figure 2.2.7. Improved variants screened from HRPL-library **105**

Figure 2.2.8. Location and surroundings of stabilizing mutations in HRPL **107**

Figure 2.3.1. Different *in vivo* DNA recombination strategies based on *S. cerevisiae* **114**

Figure 2.3.2. Artificial evolution pathway for MtL in yeast. **116**

Figure 2.3.3. Amino acid substitutions accumulated in evolved laccases for functional expression in *S. cerevisiae* **117**

Figure 2.3.4. Combination of directed evolution and rational approaches for the engineering of HRPLs. **119**

Figure 2.3.5. Rational approach for thermostability during the evolution of PM1 laccase. **120**

Figure 2.4.1. Biochemical characterization. **133**

Figure 2.4.2. Dye decolourization by the laccase mediator system **137**

Figure 2.4.3. Spectro-electrochemical characterization **138**

Figure 2.4.4. The extra N-terminal extension in the OB-1 mutant **140**

Figure 2.4.5. Generation of the truncated OB-1del mutant by *in vivo* overlap extension (IVOE) deletion mutagenesis **141**

Figure 2.4.6. The coordination sphere of the T1 Cu site **143**

Figure 2.5.1. Directed laccase evolution **147**

Figure 2.5.2. Activity in physiological fluids and spectro-electrochemical characterization. **150**

Figure 2.5.3. Biochemical characterization **152**

Figure 2.5.4. Mutations in evolved laccase **155**

Figure 2.5.S1. pH activity profiles of the parental laccase and the best mutants of each round of evolution **163**

Figure 2.5.S2. Overview of the mutations in the laccase structure **164**

Figure 2.5.S3. Saturation mutagenesis at residue 454 **165**

Figure 2.6.1. Mutations in the ChU-B mutant fusion gene. **172**

Figure 2.6.2. Cloning strategy for the construction of pPICZαChU-B, pGAPZαChU-B, pPICZα*ChU-B and pGAPZα*ChU-B plasmids **174**

Figure 2.6.3. Laccase expression in *P. pastoris* **175**

Figure 2.6.4. Biochemical characterization of ChU-B mutant **178**

Figure 2.6.5. Inhibition of ChU-B by halides **180**

Figure 2.6.6. Location of the two mutations responsible for blood tolerance in the ChU-B mutant (**B**) compared with the corresponding residues in the parental type OB-1 (**A**) **181**

Figura 3.1. Rutas evolutivas artificiales de las lacasas α-PM1 (**A**) y α-PcL (**B**) hacia expresión funcional en *S. cerevisiae*. **194**

Figura 3.2. Perfil de actividad frente al pH utilizando DMP como sustrato reductor **195**

Figura 3.3. Evolución dirigida del citocromo $P450_{BM-3}$ para hidroxilación de alcanos. **196**

Figura 3.4. Perfiles de actividad frente al pH de los mutantes OB-1 (parental), 27C7 (3G) y 1B1-D205N (4G) empleando ABTS (**A**) y DMP (**B**) como sustratos. **204**

Figura 3.5. Análisis estructural de la Ala389 **205**

Tabla 1.1. Resumen de las características y herramientas genéticas disponibles para la bacteria *Escherichia coli* y las levaduras *Saccharomyces cerevisiae* y *Pichia pastoris*. **15**

Tabla 1.2. Frecuencia y tipo de mutaciones de los métodos mutagénicos basados en el empleo de DNA polimerasas **19**

Tabla 1.3. Oxidorreductasas ligninolíticas producidas por hongos de podredumbre blanca. **29**

Tabla 1.4. Potenciales redox y alineamiento de la secuencia del sitio T1 de lacasas producidas por diferentes organismos **37**

Tabla 1.5. Lacasas fúngicas expresadas en levaduras **40**

Tabla 1.6. Lacasas fúngicas expresadas en hongos filamentosos, en plantas y en bacterias **41**

Tabla 1.7. Preparados comerciales que contienen lacasas. **43**

Table 2.1.1. Comparison of the kinetic parameters of PM1 mutants expressed in *S. cerevisiae* and of the highly related *Trametes* sp. C30 and *Trametes trogii* laccases. **62**

Table 2.1.2. Mutations in mature OB-1 variant. **68**

Table 2.1.S1. Mutations introduced in the directed evolution of α-PM1 **86**

Table 2.1.S2. Activities improvements for mutants at position 9 and 10 of the α-factor pre-leader. **87**

Table 2.2.1. HRPL selected mutants generated by IvAM. **106**

Table 2.4.1. Biochemical and spectrochemical features of PM1L-wt and the PM1 mutants. **133**

Table 2.4.2. Purification of the OB-1 mutant. **134**

Table 2.4.3. Comparison of the kinetic parameters of PM1 mutants expressed in *S. cerevisiae* and wild type PM1 expressed in fungus. **136**

Table 2.4.4. CD analysis. **139**

Table 2.5.S1. Mutations introduced during the directed evolution process **166**

Table 2.5.S2. Parental and ChU-B mutant I_{50} values for different halides. **167**

Table 2.5.S3. Maximum turnover rates for the parental laccase and ChU-B mutant under optimum conditions and in blood buffer. **167**

Table 2.5.S4. Mutations introduced into the mature laccase during the directed evolution process. **167**

Table 2.5.S5. Primers employed in this project. **168**

Table 2.6.1. List of fungal laccases heterologously expressed in *P. pastoris* and *S. cerevisiae*. **171**

Table 2.6.2. Biochemical characteristics of ChU-B mutant produced in *P. pastoris* and *S. cerevisiae*. **176**

Table 2.6.3. I_{50} values (in mM) of sodium halides for ChU-B mutant produced in *P. pastoris* and *S. cerevisiae*. **179**

Table 2.6.4. Steady-state kinetic parameters of ChU-B mutant expressed in *P. pastoris* and *S. cerevisiae*. **182**

Tabla 3.1. T_{50} de la lacasa PM1, del mutante OB-1 y de otras lacasas de alto potencial redox... **199**

Tabla 3.2. Número de veces de mejora en la actividad total y T_{50} de la lacasa parental (mutante OB-1) y de las variantes que contienen la mutación F454S **206**

Tabla 3.3. T_{50} del mutante parental 27C7 (3G) y de las diferentes variantes obtenidas a partir de éste mediante mutagénesis saturada en la posición 454..... **207**

LISTADO DE ABREVIATURAS Y ACRÓNIMOS

AAO	Aril alcohol oxidasa
ABTS	2,2′-azino-bis(3-etilbenzotiazolin-6-sulfonato)
$_{ap}I_{50}Cl^-$	I_{50} aparente para el cloruro
BSA	Albúmina de suero bovino
CECT	Colección Española de Cultivos Tipo
CiP	Peroxidasa de *Coprinus cinereus*
CLERY	*Combinatorial Libraries Enhanced by Recombination in Yeast*
DMA	Dimetilacetamida
DMF	Dimetilformamida
DMP	2,6-dimetoxifenol
DMSO	Dimetilsulfóxido
DOGS	*Degenerate Oligonucleotide Gene Shuffling*
dITP	Desoxiinosina
dNTPs	Desoxirribonucleótidos
$E°_{T1}$	Potencial redox estándar del sitio de cobre T1
EC	Comisión de Enzimas; *Enzyme Commission*
ENH	Electrodo normal de hidrógeno
*ep*PCR	PCR propensa a error; *error-prone PCR*
EPR	Resonancia paramagnética electrónica; *Electronic Paramagnetic Resonance*
FPLC	Cromatografía líquida rápida de proteínas; *Fast Protein Liquid Chromatography*
HBT	1-hidroxibenzotriazol
hEGF	Factor de crecimiento epidérmico humano
HPLC	Cromatografía líquida de alta eficacia; *High-Performance Liquid Chromatography*
HRP	Peroxidasa de rábano picante
HRPLs	Lacasas de alto potencial redox; *High-Redox Potential Laccases*
HTS	*High-Throughput Screening*
ICP-OES	Espectrometría de emisión óptica con plasma de acoplamiento inductivo; *Inductively Coupled Plasma-Optical Emission Spectrometry*
ITCHY	*Incremental Truncation for the Creation of HYbrid enzymes*
IvAM	*In vivo Assembly of Mutant libraries with different mutational spectra*
IVOE	*In Vivo Overlap Extension*
k_{cat}	Constante catalítica

k_{cat}/K_m	Eficiencia catalítica
K_m	Constante de Michaelis-Menten
LiP	Lignina peroxidasa
MALDI-TOF	Desorción/ionización mediante láser asistida por matriz con un analizador de tiempo de vuelo; *Matrix-Assisted Laser Desorption/Ionization-Time Of Flight*
MAT	Mejora de actividad total
MnP	Manganeso peroxidasa
MSC	Mutagénesis saturada combinatorial
MtL	Lacasa de *Myceliophthora thermophila*
$P450_{BM-3}$	Citocromo P450 BM-3 de *Bacillus megaterium*
PACE	*Phage-Assisted Continuous Evolution*
PAHs	Hidrocarburos aromáticos policíclicos; *Polycyclic Aromatic Hydrocarbons*
P_{AOX1}	Promotor de la alcohol oxidasa 1 de *Pichia pastoris*
pb	Pares de bases
PCBs	Policlorobifenilos
PDB	Banco de datos de proteínas; *Protein Data Bank*
P_{GAP}	Promotor de la gliceraldehído-3-fosfato deshidrogenasa de *Pichia pastoris*
pI	Punto isoeléctrico
PcL	Lacasa de *Pycnoporus cinnabarinus*
RACHITT	*RAndom CHImeragenesis on Transient Templates*
RAISE	*RAndom Insertional-deletional Strand Exchange mutagenesis*
SDS-PAGE	Electroforesis en gel de poliacrilamida con dodecilsulfato sódico; *Sodium Dodecyl Sulfate-Polyacrylamide Gel Electrophoresis*
SHIPREC	*Sequence Homology-Independent Protein RECombination*
StEP	*Staggered Extension Process*
T_{50}	Temperatura a la que la enzima retiene el 50% de su actividad inicial tras 10 minutos de incubación
TED	Transferencia electrónica directa
TNT	2,4,6-trinitrotolueno
UPO	Peroxigenasa inespecífica o aromática
VP	Peroxidasa versátil
α-PcL	Gen del prepro-líder del factor α unido a la lacasa de *P. cinnabarinus* madura
α-PM1	Gen del prepro-líder del factor α unido a la lacasa PM1 madura
ε_λ	Coeficiente de extinción molar a la longitud de onda λ (en nm)

SUMMARY

The high-redox potential laccase from basidiomycete PM1 is a highly active and stable oxidoreductase with a broad spectrum of biotechnological applications. In particular, the use of high-redox potential laccases for the engineering of 3D-nanobiodevices working in physiological fluids (blood, plasma, salive) is arousing great interest. Unfortunately, fungal laccases are not active under the specific conditions of mammal blood (pH 7.4; strong chloride concentration) hampering the successful development of this kind of devices for implants in human beings.

Directed evolution is a suitable methodology to engineer enzymes beyond their natural limits. Through consecutives rounds of random mutation, DNA recombination and selection, new enzymes with improved or even novel properties can be created.

We have subjected the PM1 laccase to a comprehensive directed evolution experiment to be functional in blood. Firstly, the enzyme was evolved for functional expression in *Saccharomyces cerevisiae*, establishing a reliable platform for further developments. The native signal sequence was replaced by the α-factor prepro-leader and the whole fusion gene was evolved enhancing the laccase total activity 34,000-fold over the parental type. A series of *in vitro* and *in vivo* DNA recombination and/or mutagenic methods were employed. After exploring over 50,000 clones in 8 rounds of directed evolution, 15 mutations were accumulated both in the prepro-leader and in the mature protein, whilst the stability of the protein was conserved by a combined strategy which included: i) a HTS assay for thermostability, ii) the recovery of beneficial mutations, and iii) a mutational exchange approach. The characteristic blue colour of the enzyme switched to yellow as side-consequence of the evolution process but its biochemical properties were kept intact or even improved: the final mutant of this process (OB-1 variant) was readily secreted by *S. cerevisiae* (8 mg/L) showing enhanced kinetics values for phenolic and non-phenolic compounds and being also stable in terms of temperature, pH and organic co-solvents.

OB-1 was used as departure point to tailor a blood-tolerant laccase by 4 additional cycles of directed evolution. The laccase mutant was subjected to a customized directed evolution protocol in yeast, once again taking advantage of the physiology of *S. cerevisiae* to create DNA diversity. The inherent inhibition of laccases by the combined action of the high NaCl concentrations and the alkaline pH of blood was overcome with the help of an *ad-hoc* HTS assay based of these features in a buffer that simulated blood, albeit in the absence of coagulating agents and red blood cells. The ultimate mutant laccase (ChU-B variant) obtained through this evolutionary process was characterized comprehensively and its new features were tested on real human blood samples, revealing the mechanisms underlying this unprecedented improvement. Finally, ChU-B was cloned in *Pichia pastoris* and produced in a 42-L bioreactor (achieving production levels of 43 mg/L).

Concluding the whole mutational pathway, the PM1 laccase was sculptured by 12 rounds of directed evolution accumulating 22 mutations (8 silent) in the whole fusion gene. Beneficial mutations enhancing secretion or activity were located at the signal prepro-leader (5 mutations) and at the mature protein (7 mutations), respectively. Significantly, only two mutations located at the second coordination sphere of the T1 copper site were responsible of the conferred tolerance to blood. Therefore, the re-specialization to adapt the PM1 laccase to such inclement conditions only required of 0.4% of the amino acid sequence.

ESTRUCTURA GENERAL

La presente Tesis Doctoral consta de los siguientes apartados:

1. Introducción General y Objetivos.

2. Publicaciones. Recoge los trabajos de investigación que han dado lugar a esta Memoria de Tesis. El contenido de estos artículos se ha mantenido en el idioma en que fueron publicados y se ordenan en seis capítulos, titulados:

Capítulo 1: Laboratory evolution of high-redox potential laccases.

Capítulo 2: Evolving thermostability in mutant libraries of ligninolytic oxidoreductases expressed in yeast.

Capítulo 3: Directed evolution of fungal laccases.

Capítulo 4: Switching from blue to yellow: altering the spectral properties of a high-redox potential laccase by directed evolution.

Capítulo 5: Blood tolerant laccase by directed evolution.

Capítulo 6: Functional expression of a blood tolerant laccase in *Pichia pastoris*.

3. Resumen de los Resultados, Discusión y Conclusiones Finales.

4. Bibliografía

5. Anexos. Incluyen la producción científica de la doctoranda y la secuencia de la lacasa α-PM1.

Cada uno de los capítulos del Apartado II se compone de su propia sección de Resumen, Materiales y Métodos, Resultados, Discusión y Conclusiones. En el caso particular de los Capítulos 1 y 5, se adjunta el material suplementario anexado online en la publicación referida.

El **Capítulo 1** describe el proceso de evolución dirigida combinado con estudios semi-racionales que permitió la expresión funcional de la lacasa de alto potencial redox PM1 en *S. cerevisiae*. De cara a recuperar la termoestabilidad perdida por la acumulación de mutaciones a lo largo de la ruta evolutiva, el método de *high-throughput screening* (HTS) de evaluación de actividad se complementó con la incorporación de un protocolo HTS de termoestabilidad, tal y como se detalla en el **Capítulo 2**. A continuación, en el **Capítulo 3** se evalúan en mayor detalle las características bioquímicas y espectroscópicas del mutante final del proceso evolutivo (mutante OB-1), con el objetivo de elucidar las razones que dieron lugar al cambio de color de la enzima (de azul en la PM1 nativa a amarillo en OB-1) sin que ello afectara a las características cinéticas ni al potencial redox del sitio de Cu T1. El **Capítulo 4** constituye una revisión de lacasas fúngicas cuyas propiedades han sido mejoradas por evolución dirigida y empleando *S. cerevisiae* tanto como microorganismo hospedador como herramienta para la generación de diversidad genética *in vivo*. El **Capítulo 5** versa sobre la evolución dirigida en combinación con experimentos de mutagénesis dirigida y saturada del mutante OB-1 a fin de conseguir una lacasa tolerante a la sangre humana (mutante ChU-B). Finalmente, en el **Capítulo 6** se detalla el clonaje y la expresión de ChU-B en la levadura metanotrófica *P. pastoris*, empleándose dicho sistema para la producción de la enzima en un biorreactor.

1. INTRODUCCIÓN GENERAL Y OBJETIVOS

1.1. EVOLUCIÓN MOLECULAR DIRIGIDA

1.1.1. Aspectos generales

La evolución molecular dirigida o evolución *in vitro* es una poderosa metodología que permite la obtención de biocatalizadores con propiedades mejoradas o con nuevas funciones nunca antes requeridas en la naturaleza (Cherry y Fidantsef, 2003; Bloom *et al.*, 2005; Reetz *et al.*, 2008). Antes de la aparición de esta técnica a inicios de 1990, el diseño racional o mutagénesis dirigida, consistente en el cambio de aminoácidos concretos en base a modelos tridimensionales o estructuras cristalográficas, constituía la vía más frecuente para la creación de nuevas actividades enzimáticas. A pesar de los grandes avances en la elucidación estructural de proteínas mediante difracción de rayos X y espectroscopía de RMN, del desarrollo de métodos computacionales y predictivos para anticipar las interacciones enzima-sustrato (*p. ej.*, a través de simulaciones de dinámica molecular) (Braiuca *et al.*, 2006), o de la reconstrucción de genomas gracias a la disponibilidad de extensas bases de datos (Floudas *et al.*, 2012), el conocimiento acumulado sobre el plegamiento, mecanismo y función catalítica no es garantía suficiente para el diseño racional exitoso de biocatalizadores (Bershtein y Tawfik, 2008; Bloom y Arnold, 2009).

Por su parte, la evolución dirigida recrea en el laboratorio los principios darwinianos de evolución natural, permitiendo el diseño de enzimas con propiedades de alto interés biotecnológico en ausencia de información estructural o mecanística previa. En la evolución dirigida la presión selectiva es controlada por el científico en busca de una mejora en una propiedad enzimática concreta al tiempo que la escala temporal evolutiva se reduce a tan sólo meses, e incluso días, de trabajo en el laboratorio (Brakmann, 2001; Arnold, 2009; Dalby, 2011; Esvelt *et al.*, 2011; Alcalde, 2012).

Un experimento de evolución dirigida comienza con la generación de diversidad genética mediante mutagénesis aleatoria y/o recombinación de los genes que codifican para la proteína de interés. Esta variabilidad se expresa en un microrganismo hospedador adecuado y se explora bajo unas condiciones muy determinadas de cara a seleccionar aquellas variantes enzimáticas que presenten una mejora en la propiedad objeto de estudio. Finalmente, los genes que codifican para estas enzimas se aíslan con el fin de analizar las mutaciones introducidas y/o los procesos de recombinación que han tenido lugar. Los genes "ganadores" se someten a un nuevo ciclo de mutación/recombinación y selección o *screening*, lo que se traduce en incrementos acumulativos en las mejoras detectadas generación tras generación (**Figura 1.1.**). Este proceso se repite tantas veces como sean necesarias, de manera que la introducción, recombinación y transmisión de las mutaciones adquiridas a lo largo de las generaciones conducirá a la obtención del biocatalizador con las características deseadas (Jäckel y Hilvert, 2010; Wang *et al.*, 2012).

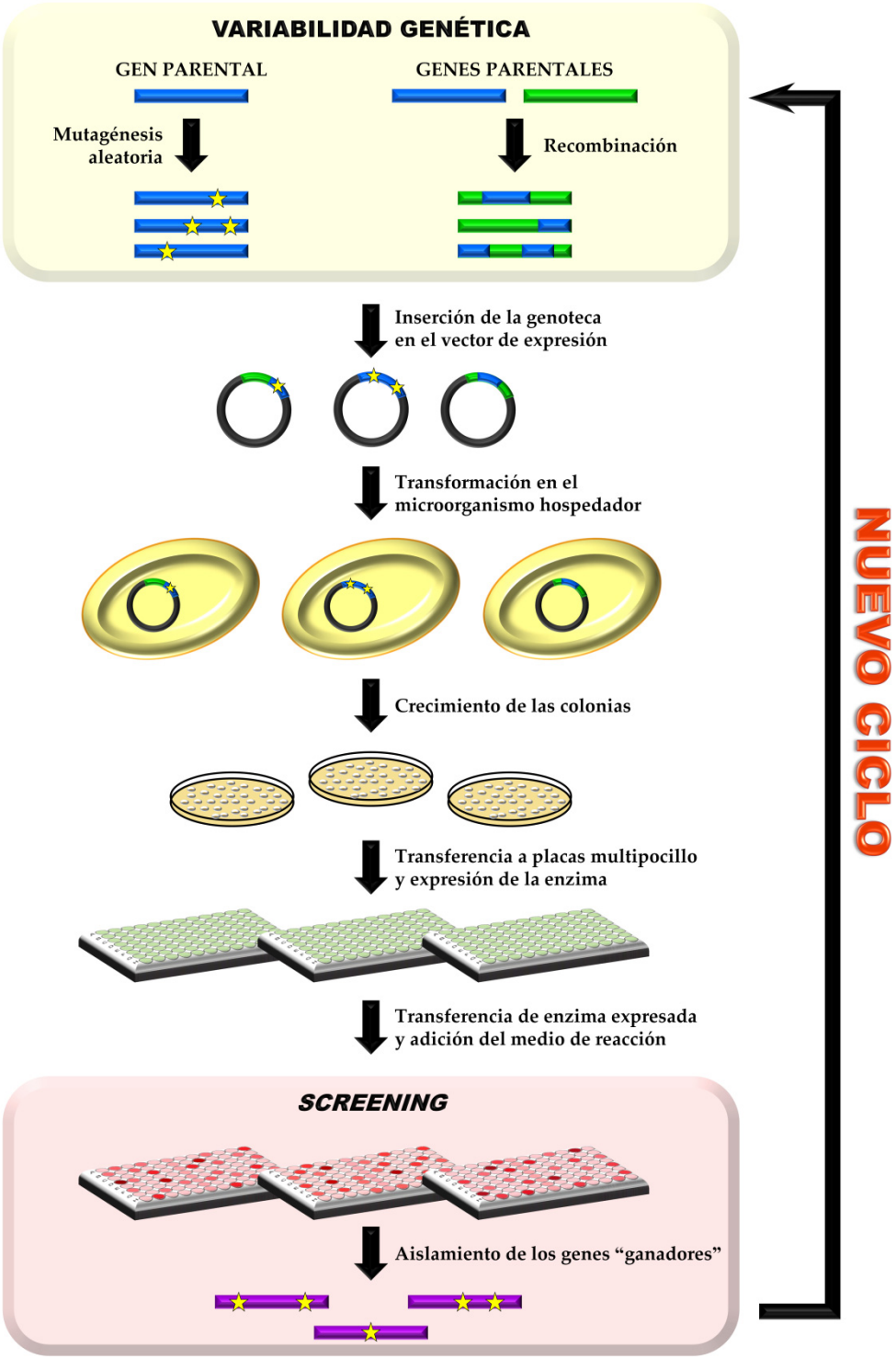

Figura 1.1. Esquema general de un experimento de evolución molecular dirigida. Las mutaciones están representadas como estrellas.

Las mutaciones beneficiosas descubiertas en experimentos de evolución *in vitro* se encuentran a menudo en zonas alejadas de los sitios catalíticos de interés, lo que permite descubrir regiones o posiciones determinadas que difícilmente podrían haberse anticipado mediante un enfoque racional (Arnold, 1996). No obstante, ambas herramientas de diseño de proteínas no son incompatibles, sino todo lo contrario. La combinación de estrategias que dirigen la mutagénesis a aminoácidos o regiones concretas de una proteína con la evolución dirigida de todo el gen puede facilitar la obtención de enzimas de gran interés biotecnológico (Cherry *et al.*, 1999; Miele *et al.*, 2010a). En este sentido, se han desarrollado numerosos algoritmos bioinformáticos (*p. ej.,* SCHEMA o ASRA, de *Adaptive Substituent Reordering Algorithm*) basados en el análisis computacional de conjuntos de datos de secuencias o de relaciones secuencia-función y que permiten el diseño de colecciones de mutantes en las que predominan las mutaciones beneficiosas frente a las perjudiciales (Feng *et al.*, 2012).

Tras más de 20 años de historia, la evolución dirigida se ha convertido en la herramienta más potente y versátil para el diseño de proteínas (Bloom y Arnold, 2009), habiéndose utilizado para mejorar un gran número de propiedades enzimáticas: la estereoselectividad (Reetz, 2011), la regioselectividad (Peters *et al.*, 2003), la quimioespecificidad (Iffland *et al.*, 2000; Glieder *et al.*, 2002), la termoestabilidad (Giver *et al.*, 1998; Zhao y Arnold, 1999; Cherry *et al.*, 1999), la estabilidad en disolventes orgánicos (You y Arnold, 1996; Moore y Arnold, 1996; Wong *et al.*, 2004a; Zumárraga *et al.*, 2007a), la estabilidad oxidativa (Cherry *et al.*, 1999; Morawski *et al.*, 2001; Oh *et al.*, 2002), la expresión funcional heteróloga (Morawski *et al.*, 2000; Sun *et al.*, 2001; Bulter *et al.*, 2003a; Roodveldt *et al.*, 2005; Rakestraw *et al.*, 2009; Camarero *et al.*, 2012; Garcia-Ruiz *et al.*, 2012), e incluso la luminiscencia y la fotoestabilidad de proteínas fluorescentes (Crameri *et al.*, 1996; Shaner *et al.*, 2008). Además, en el marco de la biología sintética, la evolución *in vitro* está facilitando la ingeniería de complejas rutas metabólicas y de genomas enteros (Johannes y Zhao, 2006; Cobb *et al.*, 2012). Recientemente se han desarrollado métodos de evolución *in vivo* como el PACE (*Phage-Assisted Continuous Evolution*) (Esvelt *et al.*, 2011) o técnicas basadas en el proceso de hipermutación somática que ocurre en los linfocitos B de mamíferos (Majors *et al.*, 2009). En estos métodos la función objeto de evolución está acoplada a una propiedad celular fácilmente detectable, como la supervivencia o la fluorescencia, y han permitido acelerar aún más el camino evolutivo, llevando a cabo docenas de generaciones en un solo día sin intervención del investigador en su desarrollo.

La importancia de la evolución dirigida queda demostrada por la tendencia exponencial creciente en el número de trabajos científicos publicados sobre el tema desde comienzos de 1990 (**Figura 1.2.**), por la disponibilidad en el mercado de diversos productos desarrollados mediante evolución en el laboratorio y por la inversión en proyectos de investigación sobre evolución dirigida de enzimas que realizan importantes empresas biotecnológicas como Novozymes, Maxygen y Codexis, entre otras (Alcalde, 2003).

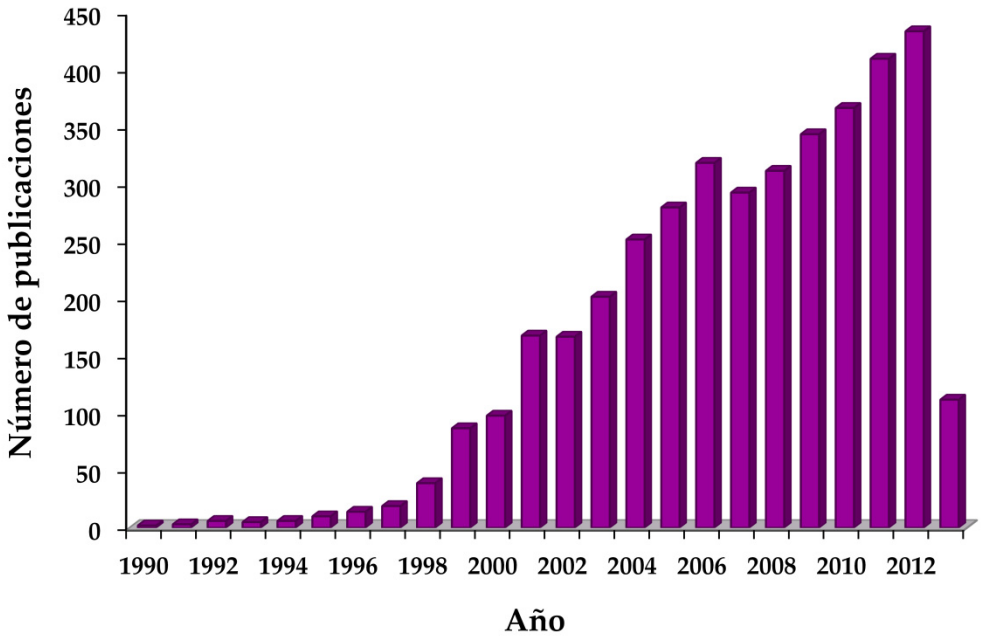

Figura 1.2. Número de artículos científicos sobre evolución dirigida publicados por año desde 1990 hasta Abril de 2013 inclusive. Información obtenida de la base de datos *Web of Science*.

1.1.2. Elección del microorganismo hospedador

La expresión funcional del gen que codifica para la proteína de interés es el primer requisito para llevar a cabo un experimento de evolución dirigida. Sin embargo, seleccionar un microorganismo hospedador adecuado para la expresión de un determinado gen es a menudo difícil ya que la expresión génica está controlada por numerosos factores a nivel transcripcional y traduccional cuyos efectos sobre el gen de interés son complicados de predecir (Romanos *et al.*, 1992). Aunque son muchos los microorganismo cultivables que podrían servir *a priori* como hospedadores en ensayos de evolución dirigida, hasta la fecha sólo se han utilizado varias especies bacterianas y de levadura así como contadas líneas celulares de insectos y de mamíferos (Pourmir y Johannes, 2012).

El microorganismo más empleado como hospedador es la bacteria Gram-negativa *Escherichia coli* debido a su alta eficiencia de transformación (10^8-10^{10} colonias por μg de DNA), su rápida tasa de crecimiento, su capacidad de mantener estable el DNA plasmídico, el detallado conocimiento de su genoma y la disponibilidad en el mercado de técnicas rutinarias de biología molecular que permiten su fácil manipulación (**Tabla 1.1.**) (Pourmir y Johannes, 2012). No obstante, la expresión bacteriana de genes eucarióticos a menudo se ve limitada por las diferencias entre los sistemas de expresión bacterianos y nativos (*p. ej.*, distinto uso de codones

o ausencia de chaperonas y de modificaciones post-traduccionales). Tales diferencias dan lugar a bajos niveles de expresión o a un plegamiento incorrecto de las proteínas, lo que origina su degradación o su acumulación en cuerpos de inclusión (Bulter *et al.*, 2003a). Estos inconvenientes pueden evitarse eligiendo hospedadores eucarióticos como las levaduras *Pichia pastoris* y *Saccharomyces cerevisiae*.

Tabla 1.1. Resumen de las características y herramientas genéticas disponibles para la bacteria *Escherichia coli* y las levaduras *Saccharomyces cerevisiae* y *Pichia pastoris*.

	Tiempo de duplicación (h)	Eficiencia de transformación (UFC[a]/μg de DNA)	Disponibilidad de plásmidos episómicos	Secreción de proteínas al medio extracelular
Bacteria				
E. coli	0.25-0.33	10^8-10^{10}	✓	✓*
Levadura				
S. cerevisiae	1.25-2.0	10^7-10^8	✓	✓
P. pastoris	1.5-2.0	10^5-10^6	×	✓

a. UFC = unidades formadoras de colonias. *Aunque el proceso de exportación de proteínas en *E. coli* ha sido ampliamente estudiado (Sahdev *et al.*, 2008; Yoon *et al.*, 2010), la mayoría de los experimentos de evolución dirigida llevados a cabo en esta bacteria requieren de un paso adicional de lisis celular.

Hasta la fecha, la levadura metanotrófica *Pichia pastoris* se ha utilizado para la producción heteróloga de más de 1000 proteínas, gracias a que, al ser un organismo eucariota, tiene la capacidad de producir proteínas solubles correctamente plegadas con las modificaciones post-traduccionales adecuadas y el correspondiente procesamiento proteolítico (Cregg *et al.*, 2000). Además, su cultivo en fermentadores en continuo da lugar a densidades celulares muy altas (>130 g de biomasa celular seca por litro de cultivo), permitiendo la secreción de grandes cantidades de proteína (Cereghino y Cregg, 2000). Sin embargo, la inmensa mayoría de los vectores disponibles para la expresión de proteínas heterólogas en *P. pastoris* son integrativos lo que constituye el principal obstáculo para el uso de esta levadura como hospedador en evolución dirigida (Gonzalez-Perez *et al.*, 2012) (**Tabla 1.1.**). Aunque se han desarrollado sistemas basados en la integración de *cassettes* de expresión mediante PCR de extensión por solapamiento (OE-PCR) para la generación de librerías de mutantes de hidroxinitril liasas (Liu *et al.*, 2008), la integración del plásmido en el genoma hace más laboriosa la recuperación de los genes y, por consiguiente, dificulta el proceso evolutivo.

Estos problemas pueden resolverse haciendo uso de la levadura *Saccharomyces cerevisiae* como microorganismo hospedador ya que tiene una mayor eficiencia transformación que *P. pastoris* (hasta 10^7-10^8 colonias por μg de DNA), también lleva a cabo modificaciones post-traduccionales, y dispone de un mecanismo muy eficaz de secreción de proteínas. Además, al contrario que *P. pastoris*, *S. cerevisiae* permite trabajar con diversos vectores episómicos multicopia que facilitan la recuperación de los genes seleccionados en el *screening* (Bulter *et al.*, 2003b; Pourmir y Johannes, 2012) (**Tabla 1.1.**). Una ventaja muy atractiva de *S. cerevisiae* es que, a diferencia de lo que ocurre en *E. coli* y *P. pastoris*, tiene una elevada frecuencia de recombinación homóloga que facilita la creación de diversidad genética *in vivo* a partir de varios genes parentales (Gonzalez-Perez *et al.*, 2012). Por otra parte, la ligación de los genes mutados en vectores de expresión es un paso crítico que requiere de PCRs adicionales pudiendo introducirse nuevas mutaciones en regiones no deseadas. El mecanismo reparador de huecos (*in vivo gap repair*) de *S. cerevisiae* permite sustituir la ligación *in vitro*, obteniendo *in vivo* plásmidos circulares de replicación autónoma por co-transformación del plásmido linearizado y de genes mutados que contienen secuencias homólogas (de entre 20 y 50 pares de bases, pb) con ambos extremos del plásmido (Alcalde, 2010).

Es importante señalar el frecuente empleo de sistemas de expresión en tándem para experimentos de evolución dirigida, donde *S. cerevisiae* albergaría todas las etapas de creación de diversidad genética y *screening* de la propiedad de interés, y una vez alcanzado el producto final, éste se sobreexpresaría en otros hospedadores como *P. pastoris* u hongos filamentosos del género *Aspergillus*. Ejemplos concretos se pueden encontrar en la evolución molecular de peroxidasas de bajo potencial redox como la peroxidasa de rábano picante (HRP) (Morawski *et al.*, 2000) o la peroxidasa de *Coprinus cinereus* (CiP) (Cherry *et al.*, 1999).

1.1.3. Creación de diversidad génica

El éxito de cualquier experimento de evolución dirigida depende, en gran medida, de la disponibilidad de una amplia gama de metodologías que permitan la creación de genotecas con un tamaño ajustado a la capacidad del ensayo de *screening* y con una calidad adecuada, la cual está determinada por la frecuencia de las mutaciones/recombinaciones y por el tipo de mutaciones introducidas.

Los procedimientos empleados típicamente en experimentos de evolución dirigida para generar variabilidad genética son los métodos mutagénicos y los basados en la recombinación del material genético (Wong *et al.*, 2007).

1.1.3.1. Métodos mutagénicos

a) Mutagénesis aleatoria

Aunque desde un punto de vista técnico todavía no se han optimizado muchas de las condiciones deseables para experimentos de mutagénesis al azar, el objetivo ideal de estas aproximaciones es el poder sustituir de forma aleatoria cualquier aminoácido de una cadena polipeptídica por los otros 19 aminoácidos de una manera estadística y sin limitar la expresión de la proteína en el organismo hospedador. Además, sería altamente conveniente que estos métodos cumplieran los siguientes requisitos: i) tener un espectro mutacional imparcial; ii) presentar una frecuencia mutacional controlable por el investigador; iii) dar lugar a sustituciones nucleotídicas consecutivas; iv) permitir mutagénesis en subconjuntos (*p. ej.*, introducir principalmente aminoácidos cargados positiva o negativamente); v) ser independientes de la longitud del gen, vi) ser reproducible y sencillo; y vii) ser de bajo coste (Wong *et al.*, 2006; Shivange *et al.*, 2009).

De cara a conseguir que un proyecto de evolución dirigida sea exitoso, es esencial el ajuste preciso de la frecuencia mutacional. Un cambio aminoacídico por gen parece la tasa mutacional más adecuada para la comprensión directa de las relaciones estructura-función. Sin embargo, la mayoría de los experimentos de evolución emplean frecuencias mutacionales que inducen de 1 a 4 cambios aminoacídicos (de 2 a 7 cambios nucleotídicos) por cada 1000 pb (Wong *et al.*, 2004a). La selección de estas condiciones es debida a que a menudo existen limitaciones de carácter práctico, ya que los laboratorios de muchos centros de investigación sólo pueden llevar a cabo la exploración de pequeñas librerías de mutantes (de entre 2000 y 20000 clones). Además, dicha tasa mutacional permite la detección de mutaciones beneficiosas, mucho menos frecuentes que las perjudiciales o neutras, como se explicará en el **Subapartado 1.1.5.**, pág. 25 (Moore y Arnold, 1996).

Con el objetivo de tener un número suficiente de clones activos, las tasas mutacionales se ajustan empíricamente para que el 40-60% de los clones retengan el 10% de la actividad del gen parental (Wong *et al.*, 2006). No obstante, existen casos excepcionales en los que se han obtenido anticuerpos con afinidades mejoradas a partir de librerías altamente mutagenizadas (con hasta 22.5 cambios nucleotídicos por gen) (Daugherty *et al.*, 2000).

El método más utilizado en evolución dirigida por su sencillez y eficacia para introducir mutaciones en el material genético es la reacción de PCR propensa a error (en inglés, *error-prone* PCR o *ep*PCR). Esta técnica hace uso de DNA polimerasas que exhiben baja fidelidad durante la amplificación génica. La DNA polimerasa *Taq* de la bacteria termófila *Thermus aquaticus* es la más empleada en reacciones de *ep*PCR. La *Taq* polimerasa es una enzima robusta que carece de actividad exonucleasa 3′→5′, lo que se traduce en una elevada frecuencia de error intrínseca (8.0

x 10^{-6} mutaciones por nucleótido y por duplicación) (Cline *et al.*, 1996). Sin embargo, dicha tasa mutacional es insuficiente para mutagenizar de forma efectiva genes que raramente superan las 5000 pb. Los métodos más destacados para aumentar la probabilidad de error son la adición de $MnCl_2$ y el uso de concentraciones desbalanceadas de los cuatro desoxirribonucleótidos (dNTPs) naturales (Cirino *et al.*, 2003). También tienen efectos mutagénicos el incremento del tiempo de extensión y de las concentraciones de *Taq* polimerasa y de $MgCl_2$ en la reacción, la disminución de la concentración de DNA molde (Leung *et al.*, 1989) o el uso de nucleótidos análogos a los dNTPs naturales (*p. ej.*, la desoxiinosina, dITP) (Wong *et al.*, 2004b).

Como alternativa a la variación de parámetros, es posible aumentar la falta de exactitud de la *Taq* polimerasa mediante ingeniería de proteínas (Patel *et al.*, 2001), o bien emplear DNA polimerasas con diferentes espectros mutacionales como son la Mutazima® (Cline y Hogrefe, 2000) o las DNA polimerasas humanas β, η y ι (Mondon *et al.*, 2007; Emond *et al.*, 2008) (**Tabla 1.2.**). De hecho, todas las DNA polimerasas descritas tienen una gran tendencia hacia las transiciones (cambios de bases púricas por púricas y pirimidínicas por pirimidínicas) frente a las transversiones (cambios de bases púricas por pirimidínicas y a la inversa), reduciendo la variedad de los cambios nucleotídicos e impidiendo la completa exploración del espacio proteico. No obstante, la probabilidad de que tengan lugar transversiones frente a transiciones puede aumentarse mediante el empleo de la *Taq* en presencia de $MnCl_2$ y concentraciones desequilibradas de dNTPs o usando la Mutazima® II (**Tabla 1.2.**). Además, los métodos de *ep*PCR están limitados por la degeneración del código genético, lo que hace que a menudo un cambio de nucleótido no dé lugar a cambio de aminoácido o bien que genere una mutación conservativa, esto es, el cambio de un aminoácido por otro de características bioquímicas similares. Como consecuencia, la sustitución de un nucleótido da lugar, en promedio, a sólo 5.7 cambios aminoacídicos frente a los 19 posibles (Kuchner y Arnold, 1997).

b) Mutagénesis saturada

Los métodos mutagénicos actualmente disponibles presentan la desventaja de que su uso impide la exploración de una parte importante del espacio proteico. Para paliar esta limitación se puede hacer uso de la mutagénesis saturada, estrategia consistente en el cambio de un único codón que codifica para un único aminoácido por todos los codones que codifican para los 20 aminoácidos naturales, con el objetivo de localizar el aminoácido óptimo para la función enzimática que se pretende mejorar. De esta manera se consigue aumentar el número de cambios aminoacídicos respecto a los accesibles por mutagénesis aleatoria convencional (Georgescu *et al.*, 2003), si bien es un método dirigido, no aleatorio, y por tanto, debe ser empleado dentro de un contexto semi-racional o híbrido (Chica *et al.*, 2005; Lutz, 2010).

Puede utilizarse también para mutagenizar varios codones (mutagénesis saturada combinatorial, MSC), tanto en bloques contiguos como en posiciones separadas, permitiendo la

Tabla 1.2. Frecuencia y tipo de mutaciones de los métodos mutagénicos basados en el empleo de DNA polimerasas. Ts/Tv: cociente transición/transversión. PolH: DNA polimerasa humana. n.d.: no determinado.

	***Taq* polimerasa**				**Mutazima® I**	**Mutazima® II**	**Método MutaGen**		
	dNTPs desequilibrados[a]	**$MnCl_2$/dNTPs equilibrados[b]**	**$MnCl_2$/dNTPs desequilibrados[c]**	**$MnCl_2$/dNTPs desequilibrados[d]**	**dNTPs equilibrados[e]**	**dNTPs equilibrados[f]**	**PolH β[g]**	**PolH η[h]**	**PolH η[i]**
Ts/Tv	3.7	2.9	1.1	0.8	1.2	0.8	3.7	6.0	2.1
Transiciones (%)									
A→G, T→C	57.2	63.2	35.0	27.6	10.3	17.5	43.9	72.9	54.1
G→A, C→T	21.3	9.5	17.5	13.6	43.7	25.5	34.8	8.8	13.1
Transversiones (%)									
A→T, T→A	14.9	16.1	37.5	40.9	11.1	28.5	6.6	6.5	13.1
A→C, T→G	2.4	4.0	5.0	7.3	4.2	4.7	4.2	2.3	6.5
G→T, C→A	2.8	3.3	5.0	4.5	20.0	14.1	9.0	1.8	4.9
G→C, C→G	1.4	1.4	0.0	1.4	8.8	4.1	1.4	3.0	8.1
Inserciones (%)	1.3	n.d.	0.0	0.3	0.8	0.7	2.7	2.7	2.9
Deleciones (%)									
De un nucleótido	3.1	1.5	0.0	4.2	1.1	4.8	1.8	4.8	2.9
De 2 o más nucleótidos	0.0	0.0	0.0	0.0	0.0	0.0	0.0	1.1	5.8

a. [dATP] = [dGTP] = 0.2 mM y [dTTP] = [dCTP] = 1 mM (Emond *et al.*, 2008).
b. [$MnCl_2$] = 0.25 mM y [dATP] = [dTTP] = [dGTP] = [dCTP] = 0.02 mM (Lin-Goerke *et al.*, 1997).
c. [$MnCl_2$] = 0.15 mM y [dATP] = [dGTP] = 0.2 mM y [dTTP] = [dCTP] = 1 mM (Shafikhani *et al.*, 1997).
d. [$MnCl_2$] = 0.5 mM y [dATP] = [dGTP] = 0.2 mM y [dTTP] = [dCTP] = 1 mM (Shafikhani *et al.*, 1997).
e. [dATP] = [dGTP] = [dTTP] = [dCTP] = 0.2 mM (Cline y Hogrefe, 2000).
f. [dATP] = [dGTP] = [dTTP] = [dCTP] = 0.2 mM (GeneMorph® II random mutagenesis kit, Stratagene).
g. Amplificación del gen entero y [dATP] = [dGTP] = 0.05 mM y [dTTP] = [dCTP] = 0.1 mM (Emond *et al.*, 2008).
h. Amplificación del gen entero y [dATP] = [dGTP] = [dTTP] = [dCTP] = 0.1 mM (Emond *et al.*, 2008).
i. Amplificación de la región del gen codificante para el dominio catalítico y [dATP] = [dGTP] = [dTTP] = [dCTP] = 0.1 mM (Emond *et al.*, 2008).

exploración de todas las posibles combinaciones de los aminoácidos de interés, de cara a optimizar sus interacciones para la propiedad proteica objeto de estudio. Aunque el uso combinado de la mutagénesis saturada con métodos de *high-throughput screening* (HTS) ha permitido la mejora de diferentes propiedades enzimáticas como la termoestabilidad, la especificidad de sustrato y la enantioselectividad (Chica *et al.*, 2005), nuevamente surgen limitaciones en la exploración, ya que los experimentos de MSC generan librerías con un gran número de mutantes. Si la mutagénesis saturada de las posiciones de interés tiene lugar al nivel de DNA por una "randomización" NNN (donde N representa una mezcla de A, C, T y G), la mutagénesis saturada de un único codón generaría 64 variantes, mientras que la mutagénesis saturada de dos y tres codones produciría 4096 y 262144 variantes diferentes, respectivamente. Una estrategia ampliamente utilizada para reducir el número de mutantes es la utilización de los codones NNG/C o NNA/T. Esta restricción da lugar a 32 codones codificantes para los 20 aminoácidos y con sólo 11 codones redundantes (es decir, que codifican para el mismo aminoácido) y un codón parada (Wong *et al.*, 2006).

1.1.3.2. Métodos de recombinación del DNA

El intercambio de material genético mediante recombinación durante los procesos de reproducción sexual constituye unas de las bases de la evolución de las especies, puesto que da lugar al aumento de la variabilidad genética de una población dada y a la eliminación del material genético de las mutaciones perjudiciales, traduciéndose en una mejor adaptación de los individuos a los cambios del entorno (Keightley y Eyre-Walker, 2000).

En la actualidad, existen numerosas técnicas que reproducen en el laboratorio los procesos de recombinación del DNA. En términos generales, la estrategia de recombinación de DNA es complementaria y sinérgica con la mutagénesis aleatoria, al facilitar la incorporación en un mismo gen de las mutaciones beneficiosas de diferentes genes parentales así como la eliminación de mutaciones neutras por cruzamiento de los genes descendientes con el gen parental (retrocruzamiento o *backcrossing*) (Alcalde, 2010).

Los métodos de recombinación utilizados en evolución dirigida se clasifican en dos grupos, dependiendo de si la recombinación tiene lugar mediante reacciones de PCR (recombinación *in vitro*) o en el interior de un microorganismo hospedador (recombinación *in vivo*).

a) Métodos de recombinación *in vitro*

En 1994 se describió la primera metodología de recombinación *in vitro*: el barajado *in vitro* del DNA (en inglés, *in vitro* DNA *shuffling*). Esta técnica consiste en la fragmentación aleatoria de los genes que se desea recombinar con una DNAsa, seguida de una reacción de PCR en ausencia de oligonucleótidos cebadores. Los fragmentos anillan entre ellos debido al alto grado

de homología y los ciclos sucesivos de anillamiento y extensión dan lugar a genes enteros cuyas secuencias son recombinaciones de las de los parentales. Estos genes enteros se utilizan como molde en una segunda reacción de PCR de cara a obtener suficiente cantidad para llevar a cabo el clonaje (Stemmer, 1994).

El éxito del *in vitro* DNA *shuffling* animó a la comunidad científica a desarrollar metodologías recombinantes diferentes, entre las que se pueden destacar: i) la recombinación homóloga mediante StEP (*Staggered Extension Process*) (Zhao *et al*., 1998) y RACHITT (*RAndom CHImeragenesis on Transient Templates*) (Coco *et al*., 2001); ii) la recombinación de genes de una misma familia o de genes relacionados con una homología de secuencia superior al 60% mediante DOGS (*Degenerate Oligonucleotide Gene Shuffling*) (Gibbs *et al*., 2001); iii) la recombinación de genes con una homología de secuencia inferior al 60% a través del ITCHY (*Incremental Truncation for the Creation of HYbrid enzymes*) (Ostermeier *et al*., 1999), del THIO-ITCHY (derivado del anterior, utiliza nucleótidos α-fosfotiolados) (Lutz *et al*., 2001a), del SHIPREC (*Sequence Homology-Independent Protein RECombination*) (Sieber *et al*., 2001) y del barajado *in vitro* de exones (*in vitro exon shuffling*) (Kolkman y Stemmer, 2001); y iv) el uso combinado del ITCHY con el barajado *in vitro* del DNA a través del SCRATCHY (Lutz *et al*., 2001b) y del *enhanced crossover* SCRATCHY (derivado del anterior, permite obtener un mayor número de clones con múltiples entrecruzamientos) (Kawarasaki *et al*., 2003).

b) Métodos de recombinación *in vivo*: *S. cerevisiae* como herramienta para la creación de diversidad

Las técnicas de recombinación *in vitro* del DNA requieren de reacciones de PCR adicionales para la amplificación de los genes completos y para la ligación de estos genes en el correspondiente vector de expresión, lo que a menudo genera la introducción de mutaciones no deseadas. Esto puede evitarse haciendo uso de *S. cerevisiae*, cuyo mecanismo de replicación de alta fidelidad permite la recombinación no mutagénica de los genes parentales, proceso conocido como barajado *in vivo* del DNA o *in vivo* DNA *shuffling* (Okkels, 2004). Esta levadura presenta además una alta frecuencia de recombinación homóloga habiéndose demostrado entrecruzamientos de fragmentos que tienen entre 20 y 200 pb de homología (Gibson, 2009). La longitud de los extremos solapantes en la región de entrecruzamiento entre el gen de interés y el plásmido linearizado es un factor clave que determina la eficiencia de la transformación. Así, regiones de homología con al menos 40 pb dan lugar a eficiencias de recombinación de alrededor del 70% (Oldenburg *et al*., 1997).

Estas propiedades convierten a *S. cerevisiae* en una herramienta ideal en evolución dirigida ya que permite la clonación y la recombinación *in vivo* de genotecas mutagénicas con el plásmido linearizado (Gonzalez-Perez *et al*., 2012). Para ello, el único requisito es la presencia de

30-40 pb de homología entre los extremos del gen de interés (o de los diferentes genes que se quieren recombinar) y del vector de expresión linearizado (Manivasakam *et al.*, 1995). El método IVOE o extensión por solapamiento *in vivo* (*In Vivo Overlap Extension*) permite crear librerías de mutantes para estudios de mutagénesis saturada (tanto simple como combinatorial), mutagénesis dirigida, mutagénesis de inserción y de deleción. En el IVOE se realizan dos o más reacciones de PCR con oligonucleótidos degenerados en la posición/posiciones de interés empleando cebadores que contienen secuencias homólogas con el plásmido linearizado, dando lugar a fragmentos de PCR homólogos entre sí y homólogos con respecto al vector linearizado. Finalmente se consigue la recombinación, ligación y clonaje en un único paso de transformación (Alcalde, 2010) (**Figura 1.3A**). El método IvAM (*In vivo Assembly of Mutant libraries with diferent mutational spectra*) consiste en la co-transformación en la levadura del plásmido linearizado con dos o más genotecas de mutantes obtenidas con DNA polimerasas que presentan distintas predisposiciones mutacionales (diferentes relaciones transición/transversión), lo que facilita la adquisición de una mayor riqueza mutacional en la librería (Zumárraga *et al.*, 2008a) (**Figura 1.3B**).

En el contexto de la biología sintética, se está realizando un exhaustivo empleo de *S. cerevisiae* para el ensamblaje *in vivo* de rutas metabólicas mediante diversas técnicas. Un ejemplo lo constituye el DNA *assembler*, el cual está basado en el autoensamblaje en la levadura de los diferentes *cassettes* que componen la ruta metabólica, expresando de manera funcional sus productos génicos (Shao *et al.*, 2009) (**Figura 1.3C**).

Por último, también se han desarrollado métodos que combinan las técnicas de recombinación *in vitro* e *in vivo*. Por ejemplo, el método CLERY (*Combinatorial Libraries Enhanced by Recombination in Yeast*) consiste en pasos consecutivos de *in vitro* e *in vivo* DNA *shuffling* (Abécassis *et al.*, 2000) (**Figura 1.3D**). De manera similar también se ha empleado recientemente la combinación de StEP mutagénico con *in vivo* DNA *shuffling* durante la evolución dirigida de peroxidasas versátiles (Garcia-Ruiz *et al.*, 2012) (**Figura 1.3E**).

1.1.4. Métodos de selección y *screening*

En todo experimento de evolución dirigida resulta determinante la puesta a punto de un método de detección sensible a la propiedad enzimática que se pretende evolucionar.

Los métodos basados en la selección biológica son aquellos en los que la función enzimática objeto de estudio está vinculada a la supervivencia o velocidad de crecimiento del microorganismo hospedador. De esta manera, sólo aquellos clones que producen una enzima mejorada sobreviven o crecen más rápidamente. Los métodos de selección son compatibles con librerías muy grandes (~10^9 clones) y no requieren instrumentación especial (Leemhuis *et al.*,

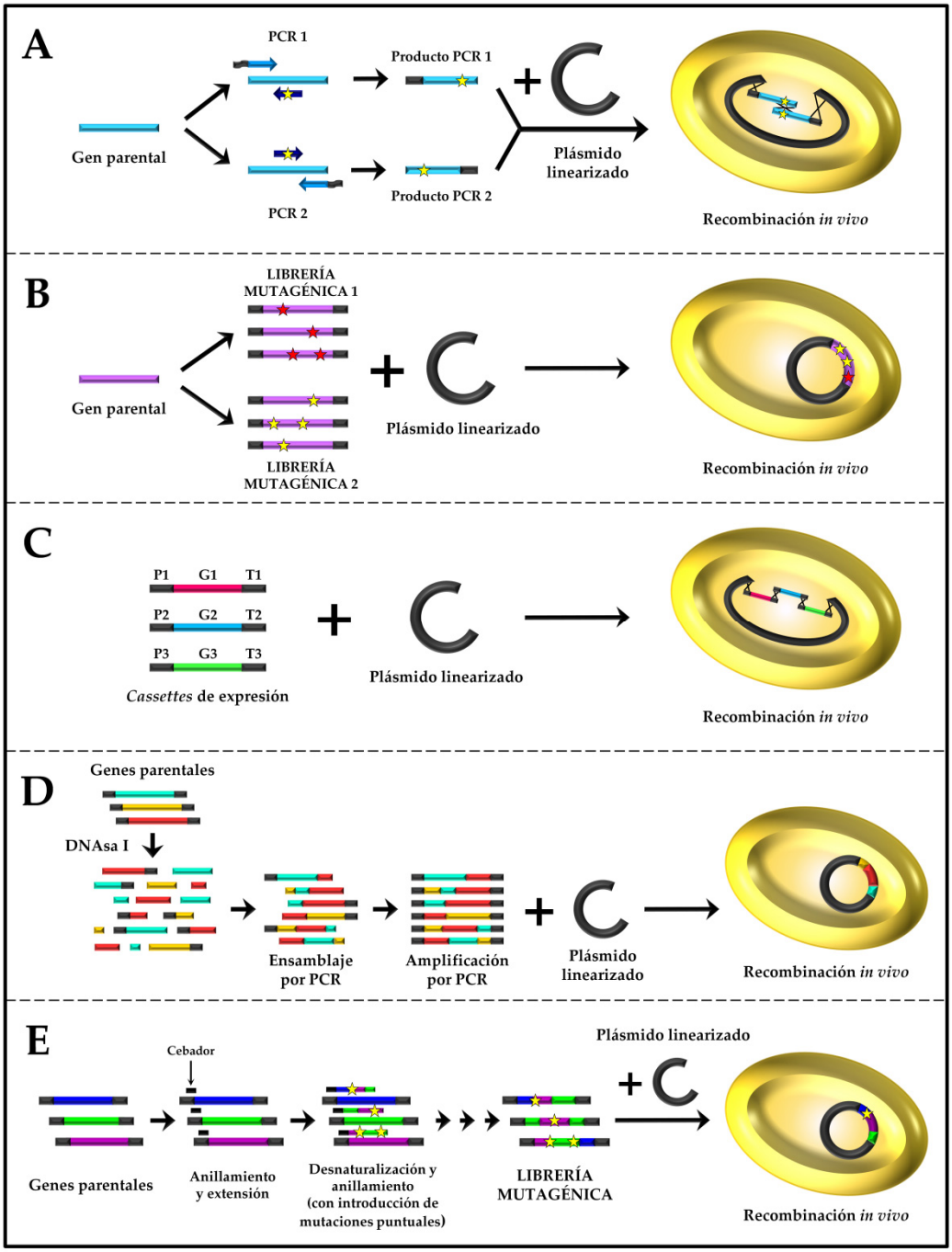

Figura 1.3. Algunos de los métodos empleados en evolución dirigida y biología sintética para la creación de diversidad genética *in vivo* haciendo uso de *Saccharomyces cerevisiae*. (**A**) IVOE. (**B**) IvAM. (**C**) DNA *assembler*. (**D**) CLERY. (**E**) StEP mutagénico + *in vivo* DNA *shuffling*. Las mutaciones están representadas como estrellas. Los promotores, genes y terminadores que componen los diferentes *cassettes* de expresión de la ruta metabólica están denominados como P, G y T, respectivamente.

2009). No obstante, suele tratarse de métodos muy específicos y difíciles de implementar lo que, combinado con el hecho de que la propiedad enzimática de interés no debe interferir en el complejo metabolismo celular y que debe ser distinguible del resto de reacciones celulares, hace que su uso en experimentos de evolución *in vitro* esté reducido a la ingeniería de enzimas detoxificantes o enzimas que sintetizan nutrientes esenciales para el crecimiento y la supervivencia celular (Arnold y Volkov, 1999; Leemhuis *et al.*, 2009).

En consecuencia, el interés de los investigadores se centra en el desarrollo de protocolos de *screening*, en los que cada miembro de la librería es analizado individualmente para la función objeto de estudio, a diferencia de los métodos de selección en los que sólo se estudian los clones supervivientes. El *screening* debe asegurar la detección de las pequeñas mejoras esperadas a partir de la sustitución de un único aminoácido. Con este fin, las condiciones del ensayo se ajustan de forma que la propiedad de la enzima nativa o parental está cerca (y nunca por debajo) del límite de detección.

El *screening* de la propiedad enzimática se lleva a cabo, de forma general, mediante la detección de absorbancia o emisión de fluorescencia. Algunos métodos de *screening* se realizan en fase sólida (placas de agar), donde los cambios de color se detectan directamente por visualización directa (aparición de halos en torno a las colonias o de color en el interior del hospedador) o por análisis de imágenes digitales. Los métodos en fase sólida requieren que el sustrato pueda ser aportado como parte del medio de crecimiento y han de ser los suficientemente sensibles como para que las colonias que expresan variantes con propiedades mejoradas muestren diferencias de color o fluorescencia con respecto a la enzima parental o a los clones inactivos (Tobias y Joern, 2003). Sin embargo, la mayoría de los protocolos de *screening* se llevan a cabo en fase líquida. Estos métodos implican la transferencia de colonias individuales a placas multipocillo que contienen medio de cultivo, el crecimiento de las células hasta alcanzar la fase estacionaria y la inducción de la proteína de interés (Salazar y Sun, 2003).

El principal inconveniente de los ensayos de *screening* es el limitado tamaño de las librerías de mutantes que pueden ser exploradas (~10^4 clones en los *screening* en fase líquida y ~10^5 clones en los *screening* en placas de agar). El desarrollo de tecnologías de *high-throughput screening* (HTS) ha permitido la exploración de librerías de mayor tamaño (~10^6 clones) (Aharoni *et al.*, 2005) (**Figura 1.4.**). Aunque los métodos HTS son cada vez más potentes (*p. ej.*, haciendo uso de FACS -*Fluorescence-Activated Cell Sorting*-), la todavía limitada capacidad de exploración que confieren estas herramientas sigue siendo el cuello de botella en evolución dirigida.

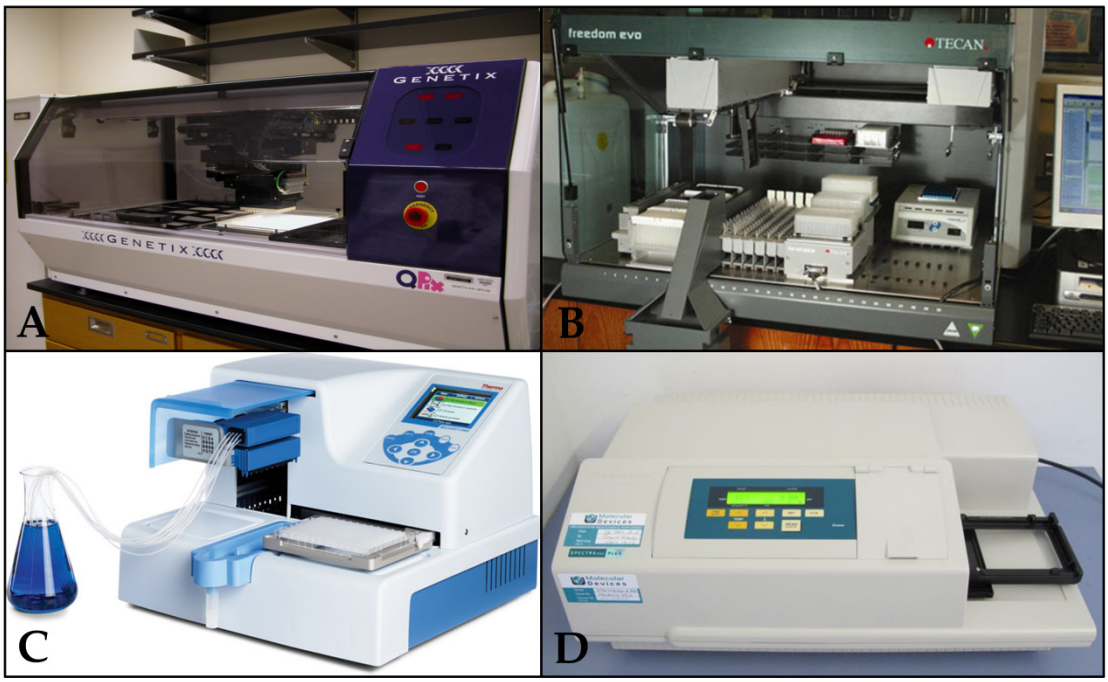

Figura 1.4. Ejemplos de herramientas HTS utilizadas en experimentos de evolución dirigida. (**A**) Robot picador de colonias. (**B**) Robot manipulador de líquidos. (**C**) Robot dispensador de líquidos. (**D**) Lector de microplacas.

1.1.5. Diseño de estrategias evolutivas

Lejos de lo trivial que pueda parecer un experimento de evolución dirigida, el éxito en este tipo de aproximaciones es directamente proporcional al planteamiento de la estrategia a emplear. La evolución dirigida no supone la mera introducción aleatoria de mutaciones o sus posibles recombinaciones, y en muchos casos esta corriente de pensamiento puede conducir a frustraciones científicas, sobre todo a la hora de abordar metas complejas (*p. ej.*, la creación de nuevas actividades o la superación de fuertes efectos inhibitorios intrínsecos al mecanismo catalítico).

Esto se debe en parte a la infinidad de posibilidades que existen al mutar una proteína: en un polipéptido virtual de 300 aminoácidos, se generarían 5700 posibles variantes a partir de la sustitución de un único residuo mientras que se llegarían a producir más de 16 millones de variantes en el caso de abordar la mutación en dos posiciones diferentes (Arnold, 1996). En la situación ideal de disponer de las herramientas moleculares, genéticas, robóticas y computacionales adecuadas (algo que se antoja del todo improbable en un presente-futuro cercano), la exploración completa de este espacio de secuencia proteica daría lugar a 20^{300} variantes que, como subraya la Prof. F. H. Arnold en muchos de sus trabajos, es un número de

combinaciones que incluso supera el número de átomos existentes en el universo (Arnold, 1996; Arnold, 2006). Sin embargo, lo más paradójico es que este espacio de secuencia proteica multidimensional se encuentra carente de función en la mayor parte de su contenido. Un reflejo experimental de esta aseveración se puede extraer del análisis mutacional llevado a cabo en diversos experimentos de evolución *in vitro*: de manera ordinaria, en torno al 30-50% de las mutaciones introducidas de manera aleatoria son perjudiciales, un 50-70% son neutras (no aportan función) y menos del 0.5-0.01% son beneficiosas (Bloom y Arnold, 2009).

Por este motivo, resulta obvio pensar que el descubrimiento de mutaciones beneficiosas es un evento poco frecuente, y la combinación de éstas, algo exclusivo. Es más, de estas mutaciones beneficiosas, sólo algunas se localizan en zonas o dominios que *a priori* podrían anticiparse de forma racional, mientras que muchas otras aparecen en zonas muy alejadas pero que, de alguna manera, afectan a la catálisis y función enzimática a través de suaves modificaciones en la geometría global proteica y en sus propiedades electrostáticas, y de manera particular en la dinámica de los aminoácidos del centro activo. El efecto combinado de estos eventos debe influir de manera precisa en el curso de la reacción, particularmente tras la formación del complejo intermediario de alta energía. Por último, no se deben obviar las interacciones epistáticas que tienen lugar cuando la presencia de una mutación influye sobre la contribución de otra en la función enzimática. Las formas extremas de epistasia se manifiestan como efectos epistáticos negativos, en los que la combinación de determinadas mutaciones puede resultar beneficiosa, aunque de manera independiente al menos una de estas mutaciones no lo sea.

En este complejo escenario de trabajo, queda probada la importancia que tiene un diseño evolutivo apropiado para poder conseguir la función deseada. En este sentido, la tendencia más exitosa es la denominada "*simple uphill walk*" o camino adaptativo, que defiende la introducción exclusiva de mutaciones beneficiosas de manera aleatoria, limitada y precisa (es decir, una por una, generación tras generación) (Bloom y Arnold, 2009). Empleando esta aproximación como punto de partida existen diferentes variaciones, todas ellas válidas y complementarias, para el diseño de nuevas actividades o funciones, a saber:

i) Incremento gradual de función. Esta opción se fundamenta en incrementar de manera progresiva la presión selectiva para alcanzar la actividad/función deseada, por ejemplo, mediante el empleo de sustratos intermediarios que pueden conducir finalmente a que la enzima trabaje eficientemente sobre el sustrato diana (Tracewell y Arnold, 2009).

ii) Diseño de enzimas generalistas y re-especialización enzimática. Las enzimas conocidas –con excepción de las enzimas sintéticas recientemente "resucitadas" de origen pre-cámbrico (Perez-Jimenez *et al.*, 2011)– son proteínas altamente especializadas debido a años de evolución natural en estrictos ambientes metabólicos. Para generar una nueva función, la

transformación de una enzima especialista en generalista (es decir, con una especificidad de sustrato más amplia que incluya una actividad marginal hacia el sustrato deseado) puede suponer una gran ventaja. Una vez ampliada su especificidad de sustrato, la actividad marginal creada se potencia, re-especializando la enzima en la dirección planeada. Cuando se obtiene la actividad en cuestión, puede ser interesante suprimir actividades laterales a través de la aplicación de procesos de *screening* o selección negativos y positivos para las actividades a anular y potenciar, respectivamente (Tracewell y Arnold, 2009). En este marco de trabajo puede resultar muy adecuado hacer uso de la deriva genética (*neutral drift*). Esta estrategia se basa en la acumulación de mutaciones neutras que no pongan en peligro la función proteica y que pueden conducir a un nuevo entorno evolutivo en el que se generan nuevas actividades catalíticas mediante dos vías diferentes: a) el incremento de la estabilidad proteica que facilita la tolerancia hacia nuevas mutaciones beneficiosas pero desestabilizantes, y b) el aumento de la promiscuidad en la función enzimática generando nuevos puntos de partida para actividades no identificadas en la enzima original (Bloom *et al.*, 2007; Bloom y Arnold, 2009).

iii) Evolución dirigida sorteando "vías muertas" (*dead ends*). En el camino adaptativo hacia la función enzimática, es frecuente encontrarse numerosos *dead ends* o "vías muertas", donde o bien la función se suprime o la enzima se desestabiliza siendo incapaz de tolerar nuevas mutaciones. Estas vías muertas pueden esquivarse mediante la incorporación de mutaciones estabilizantes o la exploración de rutas evolutivas múltiples y paralelas (Tracewell y Arnold, 2009).

iv) Evolución dirigida enfocada (*focused directed evolution*). Consiste en modificar posiciones concretas mediante mutagénesis dirigida y/o saturada en un enfoque híbrido o semi-racional. Dentro de esta alternativa también se podría incluir la denominada evolución dirigida de dominios, donde se exploran librerías mutagénicas aleatorias en dominios muy específicos mediante diversas estrategias (Wong *et al.*, 2007; Emond *et al.*, 2008; Hidalgo *et al.*, 2008; Shivange *et al.*, 2009). Esta aproximación, aunque muy válida para problemas concretos (*p. ej.*, rediseñar bolsillos catalíticos o superar problemas mecanísticos determinados), se encuentra impedida por el limitado conocimiento de la función proteica.

En resumen, no existe un camino exclusivo para el diseño de una propiedad enzimática y probablemente, lo más adecuado sea la combinación de diversos enfoques en función de la proteína y el reto que se plantee. En la presente Tesis Doctoral, como se deducirá de su lectura, se ha optado por un camino adaptativo que incluye la recombinación de mutaciones exclusivamente beneficiosas introducidas mediante mutagénesis aleatoria, su exploración por mutagénesis dirigida o saturada para optimizar los cambios más conservativos y el rodeo de *dead ends* a través de la incorporación de mutaciones estabilizantes así como la creación y análisis de rutas evolutivas paralelas.

1.2. LACASAS

1.2.1. Distribución en la naturaleza y función biológica

Las lacasas (EC 1.10.3.2., bencenodiol:oxígeno oxidorreductasas) son enzimas que catalizan la oxidación de diversos compuestos, principalmente aromáticos, utilizando el oxígeno molecular como aceptor final de electrones. Las lacasas presentan cuatro átomos de cobre: un cobre T1 donde tiene lugar la oxidación del sustrato reductor y un cobre T2 y dos cobres T3 que conforman un *cluster* trinuclear donde el oxígeno molecular es reducido a dos moléculas de agua. Las lacasas pertenecen a la familia de las oxidasas multicobre, en las que también se incluyen, entre otras, la ceruloplasmina de mamíferos y aves, la ascorbato oxidasa de plantas, la nitrito reductasa de bacterias, la bilirrubina oxidasa de hongos e insectos o la ferroxidasa de hongos (Messerschmidt, 1997; Hoegger *et al.*, 2006).

Desde que a finales del siglo XIX se extrajera de los exudados del árbol de la laca (*Toxicodendron vernicifluum* o anteriormente *Rhus vernicifera*) (Yoshida, 1883), se han descubierto lacasas en más de 20 especies bacterianas (Singh *et al.*, 2011), en varias especies de plantas superiores (Mayer y Staples, 2002) y de líquenes (Laufer *et al.*, 2009), e incluso se han descrito polifenol oxidasas con actividad lacasa en cutículas de insectos (Lang *et al.*, 2012) y en genotecas metagenómicas de muestras de rumen bovino (Beloqui *et al.* 2006). No obstante, es en hongos donde la presencia de estas enzimas es más abundante, habiéndose caracterizado lacasas en prácticamente todos los hongos examinados para ello, incluyendo mohos (*p. ej., Pennicillium*), setas (*p. ej., Agaricus*) y hongos de podredumbre blanca (*p. ej., Pleurotus*) (Hoegger *et al.*, 2006).

Las lacasas desempeñan funciones biológicas diversas que vienen determinadas por su origen y el estadio vital del organismo productor. En bacterias están implicadas en procesos de morfogénesis, pigmentación, oxidación de compuestos tóxicos y protección frente a la radiación ultravioleta y agentes oxidantes (Singh *et al.*, 2011). Las lacasas de plantas participan en la respuesta a heridas y en la polimerización de la lignina (Bao *et al.*, 1993; Davies y Ducros, 2002). Las polifenol oxidasas con actividad lacasa descubiertas en cutículas de insectos influyen en la esclerotización de las mismas (Miessner *et al.*, 1991). En hongos, las funciones de las lacasas son muy diversas, estando involucradas en procesos de morfogénesis, esporulación y patogénesis (Thurston, 1994; Gianfreda *et al.*, 1999; Zhu y Williamson, 2004). Además, en los hongos basidiomicetos y, más concretamente en los de podredumbre blanca de la madera, su principal objetivo es la degradación de la lignina (Alcalde, 2007).

La lignina es un polímero aromático de elevado peso molecular altamente insoluble y complejo que, junto con la celulosa y la hemicelulosa, constituye la pared celular de las plantas vasculares (Fengel y Wegener, 1984). Está formada por tres derivados fenilpropanoides

diferentes (los alcoholes *para*-hidroxicinámicos coniferílico, cumarílico y sinapílico), conectados entre sí mediante enlaces carbono-carbono y carbono-oxígeno no hidrolizables. El proceso de biodegradación de la lignina tiene lugar por la acción combinada de: i) los metabolitos de bajo peso molecular producidos por el hongo, que actúan como transportadores electrónicos difusibles y que, debido a su pequeño tamaño, pueden acceder al interior de la matriz lignocelulósica, iniciando la despolimerización; y ii) las enzimas ligninolíticas producidas por los hongos de podredumbre blanca (**Tabla 1.3.**). El consorcio de enzimas oxidorreductasas ligninolíticas está principalmente constituido, por un lado, por las lacasas y las peroxidasas de alto potencial redox (lignina peroxidasa, manganeso peroxidasa y peroxidasa versátil), encargadas de promover el proceso de mineralización de la lignina iniciado por los mediadores redox; y por otro lado, por enzimas auxiliares encargadas de la producción de H_2O_2 (aril-alcohol oxidasa y glioxal oxidasa) (Martínez *et al.*, 2005). Recientemente, se han incorporado a este grupo de oxidorreductasas la UPO (*unspecific peroxygenase*) y la DyP (*dye-decolorizing peroxidase*), lo que confiere una mayor plasticidad catalítica a este importante conjunto de enzimas (Hofrichter *et al.*, 2010).

Tabla 1.3. Oxidorreductasas ligninolíticas producidas por los hongos de la podredumbre blanca.

Enzima	Número E.C.	Función principal	Ejemplo de hongo productor
Aril-alcohol oxidasa (AAO)	1.1.3.7	Producción de H_2O_2	*Pleurotus eryngii*
Celobiosa deshidrogenasa	1.1.99.18	Oxidación de celobiosa y reducción de *orto*-quinonas y MnO_2	*Phanerochaete chrysosporium*
Glioxal oxidasa	1.2.3.5	Producción de H_2O_2	*Phanerochaete chrysosporium*
Lacasa	1.10.3.2	Oxidación de compuestos aromáticos	*Trametes versicolor*
Manganeso peroxidasa (MnP)	1.11.1.13	Oxidación de Mn^{2+} y compuestos fenólicos	*Phlebia radiata*
Lignina peroxidasa (LiP)	1.11.1.14	Oxidación de dímeros de lignina de tipo no fenólico y compuestos aromáticos de alto potencial redox	*Bjerkandera adusta*
Peroxidasa versátil (VP)	1.11.1.16	Oxidación de Mn^{2+} y compuestos aromáticos de alto, medio y bajo potencial redox	*Pleurotus eryngii*

Tabla 1.3. *(continuación)*. **Oxidorreductasas ligninolíticas producidas por los hongos de la podredumbre blanca.**

Enzima	Número E.C.	Función principal	Ejemplo de hongo productor
DyP	1.11.1.19	Oxidación de compuestos fenólicos y no fenólicos de bajo y medio potencial redox, así como de colorantes sintéticos de alto potencial redox derivados de antraquinonas	*Auricularia auricula-judae*
Peroxigenasa aromática o inespecífica (UPO)	1.11.2.1	Oxidación de compuestos de bajo, medio y alto potencial redox; reacciones de halogenación y de transferencia de oxígeno (hidroxilaciones, sulfoxidaciones, epoxidaciones) sobre sustratos aromáticos, heterocíclicos y alifáticos	*Agrocybe aegerita*

1.2.2. Generalidades bioquímicas

Las lacasas se suelen presentar como glicoproteínas extracelulares y monoméricas con masas moleculares comprendidas entre 50 y 130 kDa. Su grado de glicosilación compromete unidades de manosa, N-acetosamina y galactosa constituyendo en torno al 45% de la masa molecular en las lacasas de plantas y entre el 10 y el 20% en las lacasas fúngicas (Morozova *et al.*, 2007a). El punto isoeléctrico (pI) de las lacasas depende de su origen, de modo que mientras en las lacasas de hongos oscila entre 2.6 y 6.9 siendo 4.0 el valor típico, hay lacasas de plantas con pI de hasta 9.5 (Baldrian, 2006; Morozova *et al.*, 2007a).

La mayoría de las lacasas tienen temperaturas óptimas entre 50 y 70°C y potenciales redox estándar en el sitio T1 ($E°_{T1}$) comprendidos entre +430 y +790 mV (*vs.* Electrodo Normal de Hidrógeno, ENH) (Morozova *et al.*, 2007a; **Tabla 1.5.**). El espectro de sustratos de las lacasas es muy amplio, siendo capaces de oxidar compuestos aromáticos (*orto-* y *para*-difenoles, fenoles metoxisustituidos, diaminas, bencenotioles), iones metálicos (Mn^{2+}), compuestos organometálicos (*p. ej.*, $[W(CN)_8]^{4-}$, $[Fe(EDTA)]^{2-}$), compuestos redox de naturaleza orgánica (*p. ej.*, 2,2'-azinobis(3-etilbenzotiazolin-6-sulfonato), ABTS; 1-hidroxibenzotriazol, HBT) y el anión I^- (Yaropolov *et al.*, 1994; Xu, 1996a; Höfer y Schlosser, 1999). Además, en presencia de

mediadores redox, tanto de origen natural como sintético, la actividad catalítica de estas enzimas puede ser expandida hacia sustratos no fenólicos persistentes y difícilmente oxidables como, por ejemplo, los hidrocarburos aromáticos policíclicos (PAHs), los policlorobifenilos (PCBs), los colorantes tipo azo o los pesticidas organofosforados (Morozova *et al.*, 2007b; Cañas y Camarero, 2010) (**Figura 1.5.**).

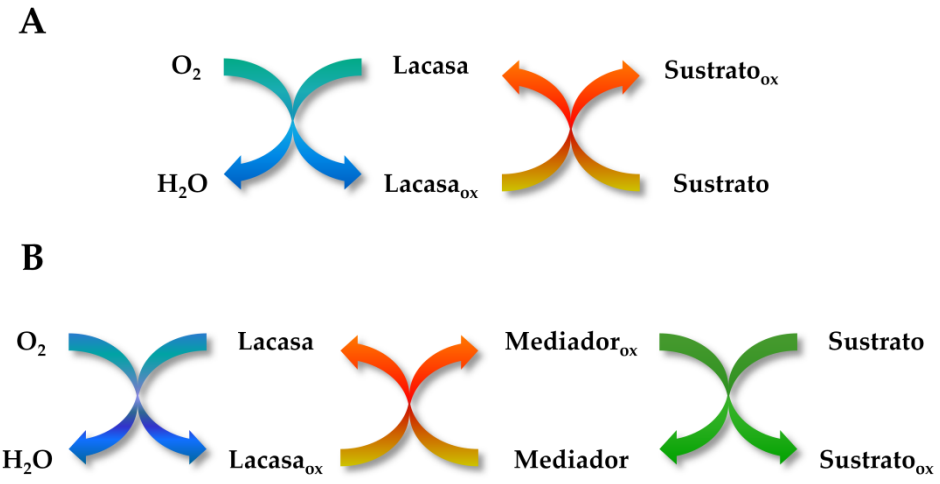

Figura 1.5. Representación esquemática de la actividad lacasa en ausencia (A) o en presencia (B) de mediadores redox.

La especificidad y afinidad de las lacasas por el sustrato reductor es dependiente del pH. Los perfiles de actividad frente al pH para sustratos fenólicos muestran forma de campana debido a dos efectos opuestos (Xu, 1997). En primer lugar, el aumento de la actividad enzimática en el intervalo de pH ácido como consecuencia del incremento de la diferencia entre el potencial redox del sustrato reductor y el Cu T1. Este aumento es debido a que el potencial redox del fenol disminuye con el pH por liberación del protón oxidativo mientras que el $E°_{T1}$ apenas varía. En segundo lugar, la inactivación a pH básico, resultado de la disminución de la concentración de protones (necesarios para la reducción del oxígeno molecular a agua) y del aumento de la presencia de iones hidroxilo. Estos últimos actúan como inhibidores de las lacasas ya que su unión al sitio T2 interrumpe la transferencia electrónica interna desde el Cu T1 al *cluster* T2/T3 y, por tanto, impide la catálisis. En cuanto a sustratos no fenólicos, sus perfiles de pH tienen forma monotónica, es decir, la actividad disminuye con el aumento del pH. La oxidación de estos sustratos no tiene protones involucrados, por lo que su potencial redox es independiente del pH y en consecuencia, la acumulación de iones hidroxilo a medida que aumenta el pH es el único factor determinante de la catálisis (Xu, 1997). Por regla general, las lacasas fúngicas tienen pHs óptimos de actividad en el intervalo ácido que varía en función del sustrato en cuestión –entre 2 y 5 para el ABTS, entre 3 y 8 para el DMP y entre 3.5 y 7 para la

siringaldazina–, careciendo de actividad catálitica a pH básico (Baldrian, 2006). Por su parte, las lacasas bacterianas presentan catálisis en un intervalo de pH más amplio, con pHs óptimos entre 4 y 8 (Singh *et al.*, 2011).

Aparte de por los iones hidroxilo, las lacasas son fuertemente inhibidas por otros pequeños aniones como son la azida, el cianuro, el tiocianuro y los haluros (F^-, Cl^-, Br^- pero no el I^-, que es sustrato de las lacasas). Al igual que los OH^-, estos aniones se unen al Cu T2 e interrumpen la transferencia electrónica interna desde el Cu T1 al *cluster* trinuclear. Otros inhibidores de las lacasas son iones metálicos (*p. ej.*, Hg^{2+}), el ácido tioglicólico, la hidroxiglicina, el ácido kójico, la deferoxamina y ácidos grasos de cadena corta, cuyas reacciones con las lacasas se cree que pueden implicar modificaciones de aminoácidos puntuales, cambios conformacionales o la quelación de los cobres catalíticos (Gianfreda *et al.*, 1999).

1.2.3. Características estructurales y mecanismo catalítico

Los cuatro átomos de cobre de la lacasa están situados en zonas muy conservadas de su estructura y se clasifican en tres clases diferentes en base a sus características espectroscópicas (Solomon *et al.*, 1996; Piontek *et al.*, 2002; Alcalde, 2007; Morozova *et al.*, 2007a; Matera *et al.*, 2008):

- El sitio de cobre tipo 1 (Cu T1) o cobre "*azul*" paramagnético presenta una intensa absorción en torno a 610 nm, lo cual confiere a estas enzimas su característico color azul en el estado basal oxidado (ε_{610} entre 4900 y 5700 $M^{-1} cm^{-1}$). Su esfera de coordinación está formada por los átomos de nitrógeno en posición δ1 (Nδ1) de dos His y el átomo de azufre de una Cys en disposición trigonal plana. En particular, la elevada absorción a 610 nm se debe a la fuerte transferencia de carga del átomo de azufre de la Cys coordinante al ion cobre. Dicha transferencia da lugar, además, a un desplazamiento hiperfino paralelo característico en el espectro de resonancia paramagnética electrónica (EPR).
- El sitio de cobre tipo 2 (Cu T2) o cobre paramagnético "*normal*" o "*no azul*" se caracteriza por una señal característica en el espectro de EPR y por la falta de absorción en la región visible del espectro. Se encuentra coordinado por los átomos de nitrógeno en posición ε2 (Nε2) de dos His y el átomo de oxígeno de una molécula de agua, dispuestos en forma trigonal plana.
- El sitio de cobre tipo 3 (Cu T3) o centro binuclear está formado por dos iones cobre. Carece de señal de EPR como consecuencia del acoplamiento antiferromagnético entre ambos cobres, unidos entre sí por una especie tipo hidroxilo que actúa como ligando puente (Bento *et al.*, 2010). Además, presenta un hombro de absorción característico en torno a 330 nm (atribuido a la transferencia de carga entre el grupo hidroxilo y los iones cobre) que desaparece tras la reducción del sitio activo. Un total de seis His y una molécula de agua

coordinan los dos Cu T3, estando cada ion cobre tetracoordinado, con los ligandos en disposición tetraédrica distorsionada. Cinco de las His se unen a los Cu mediante sus átomos Nε2 y una mediante el Nδ1. La molécula de agua está asimétricamente unida entre los dos cobres T3.

Las lacasas son proteínas globulares cuya estructura está organizada en tres dominios de tipo cupredoxina (**Figura 1.6.**). Cada uno de estos dominios tiene una arquitectura tipo barril-β, muy relacionada con la estructura de pequeñas proteínas de cobre azul (*p. ej.*, azurina y plastocianina) y común a todas las oxidasas multicobre, lo que sugiere que estas proteínas tienen el mismo ancestro (Rydén y Hunt, 1993). El Cu T1 se encuentra en el dominio 3, mientras que el cluster trinuclear formado por los centros T2 y T3 (situado aproximadamente a 12 Å del Cu T1) está embebido entre los dominios 1 y 3 con ligandos en ambos. El sitio de unión del sustrato está formado por residuos aminoacídicos pertenecientes a los dominios 2 y 3 (Morozova *et al.*, 2007a). Toda la estructura se encuentra estabilizada por dos o tres puentes disulfuro entre los dominios (*p. ej.*, dos en el caso de las lacasas de los basidiomicetos *Cerrena maxima*, *Coprinus cinereus*, *Trametes trogii* y *Trametes versicolor*, y tres en el de las de los ascomicetos *Melanocarpus albomyces* y *Thielavia arenaria*) (Ducros *et al.*, 1998; Hakulinen *et al.*, 2002; Piontek *et al.*, 2002; Lyashenko *et al.*, 2006; Matera *et al.*, 2008; Kallio *et al.*, 2011).

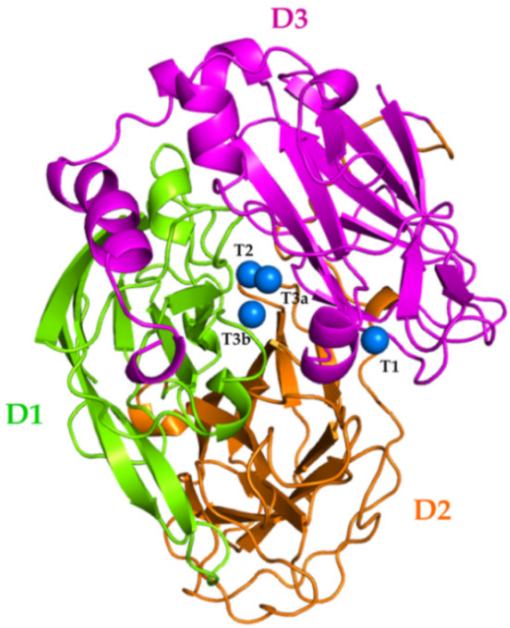

Figura 1.6. Modelo tridimensional de la lacasa del basidiomiceto PM1 en base a la estructura cristalográfica de la lacasa de *Trametes trogii* (PDB: 2HRG; 97% de identidad de secuencia con la lacasa PM1). Se muestran los tres dominios cupredoxina (D1, D2 y D3) y los cuatro cobres catalíticos.

A pesar de la numerosa bibliografía existente sobre oxidasas azules y más concretamente sobre lacasas, los mecanismo de transferencia electrónica y de reducción del oxígeno molecular siguen sin estar esclarecidos. No obstante, hay varios hechos que son ampliamente aceptados (Alcalde, 2007):

i) La oxidación mono-electrónica del sustrato reductor tiene lugar en el sitio T1. El radical libre catiónico generado puede llevar a cabo reacciones de oxidación mediadas por la lacasa (*p. ej.*, oxidación de fenoles a quinonas) o reacciones de polimerización.

ii) La reducción del oxígeno molecular a agua requiere la mono-oxidación de cuatro moléculas de sustrato reductor. En consecuencia, la enzima actúa como una batería, acumulando electrones de cada reacción de mono-oxidación hasta tener los cuatro necesarios para reducir una molécula de oxígeno a dos moléculas de agua.

iii) Cada uno de los electrones procedentes de las reacciones de mono-oxidación en el sitio T1 son transferidos al *cluster* trinuclear T2/T3, lugar donde tiene lugar la reducción del oxígeno a agua vía un intermedio tipo peróxido (Morozova *et al.*, 2007a). En base a cálculos teóricos, se ha demostrado que la vía de transferencia electrónica más favorecida es la formada por el tripéptido His-Cys-His que conecta el Cu T1 con el cluster T2/T3. Este tripéptido está altamente conservado en todas las oxidasas multicobre azul y lo componen uno de los residuos de His ligando del Cu T3a, el residuo de Cys ligando del Cu T1 y una de las His coordinantes del Cu T3b.

1.2.4. Lacasas no azules

Aunque la mayoría de las lacasas descritas presentan color azul en su estado basal, se han reportado numerosos ejemplos de lacasas con propiedades espectroscópicas distintas.

En primer lugar están las llamadas lacasas amarillas, producidas en cultivos en fase sólida con derivados de la lignina de los basidiomicetos *Panus tigrinus* cepa 8/18 (Leontievsky *et al.*, 1997a), *Phlebia radiata* cepa 79 (Leontievsky *et al.*, 1997a), *Phlebia tremellosa* cepa 77-51 (Leontievsky *et al.*, 1997a) y *Pleurotus ostreatus* cepa D1 (Pozdnyakova *et al.*, 2006a), además de las secretadas en cultivos líquidos del basidiomiceto *Agaricus bisporus* (Wood, 1980), de la producida por el ascomiceto fitopatógeno *Gaeumannomyces graminis* var. *tritici* (Edens *et al.*, 1999), así como las descritas en varias especies de líquenes (Laufer *et al.*, 2009). A pesar de que contienen cuatro átomos de cobre por molécula, sus espectros UV-visible no presentan la absorbancia característica a 610 nm sino un hombro en torno a 330 nm, debido a la absorción del sitio de Cu T3 y que explica su color amarillo. En cuanto a sus propiedades catalíticas, tienen valores de actividad frente a sustratos típicos similares a los de las lacasas azules, pero a diferencia de ellas, en la mayoría de los casos son capaces de oxidar compuestos no fenólicos derivados de la lignina en ausencia de mediadores (Leontievsky *et al.*, 1997b; Pozdnyakova *et*

al., 2006a,b). Se ha sugerido que las lacasas amarillas contienen pequeños compuestos aromáticos procedentes de la degradación de la lignina unidos al sitio T1, lo que daría lugar a la reducción del Cu T1 y por ende, a la falta de absorbancia a 610 nm. Tal efecto también se ha especulado que puede ser debido a cambios conformacionales de los aminoácidos de la cadena polipeptídica ocasionados por la unión de los compuestos ligninolíticos al sitio T1 (Leontievsky *et al.*, 1997b). La reducción de los iones cobre explicaría la ausencia de color azul de la enzima en estado basal así como los cambios en los espectros de EPR y de dicroísmo circular observados con respecto a los de las lacasas azules. Por otro lado, se piensa que las moléculas procedentes de la descomposición de la lignina asociadas al Cu T1 actúan como mediadores endógenos, permitiendo la oxidación de compuestos de alto potencial redox (unidades no fenólicas de la lignina, colorantes recalcitrantes, xenobióticos) que no son transformados por las lacasas azules en ausencia de mediadores (Leontievsky *et al.*, 1997b).

También se han descrito lacasas que además de no tener el pico de absorción a 610 nm, presentan una amplia banda en torno a 400 nm. Son las llamadas lacasas blancas, grupo en el que se incluyen la lacasa POXA1 de *P. ostreatus* (Palmieri *et al.*, 1997), la lacasa dimérica de *Phellinus ribis* (Min *et al.*, 2001) y una lacasa producida por la cepa BP-11-2 de *P. radiata* (Kaneko *et al.*, 2009). Estas lacasas contienen, además de un ion cobre, dos iones zinc y uno de hierro (POXA1 de *P. ostreatus*) o de manganeso (lacasa de *P. ribis*) o dos iones hierro y uno de zinc (lacasa de *P. radiata* cepa BP-11-2). Dentro de este grupo también puede incluirse la lacasa producida por *Marasmius* sp., que presenta una banda a 420 nm y un único ion cobre por molécula de enzima (sin ningún otro cofactor metálico) (Schückel *et al.*, 2011). Todas ellas tienen actividad catalítica con sustratos típicos de las lacasas azules y utilizan el oxígeno molecular como sustrato oxidativo.

Finalmente, se han descubierto otras lacasas que por sus características no pueden clasificarse en ninguno de los dos grupos anteriores. Se trata de la lacasa del basidiomiceto *T. hirsuta* cepa lg-9 (Haibo *et al.*, 2009), las tres isoformas de la lacasa del también basidiomiceto *Stechherinum ochraceum* cepa 1833 (Chernykh *et al.*, 2008) y la del ascomiceto fitopatógeno *Sclerotinia sclerotiorum* (Moț *et al.*, 2012). La lacasa de *T. hirsuta* lg-9 no presenta absorción a 610 nm pero sí la banda a 400 nm, típica de las lacasas blancas. Sin embargo, no contiene uno sino tres iones cobre más uno de manganeso. Además, es incapaz de oxidar el compuesto no fenólico alcohol veratrílico en ausencia de mediadores, lo que la diferencia de las lacasas amarillas. Por su parte, las tres isoformas de la lacasa de *S. ochraceum* se caracterizan por coeficientes de extinción molar a 610 nm más altos ($\geq$ 7200 M^{-1} cm^{-1}) y hombros de absorción a 330 nm más bajos que el resto de lacasas, probablemente debidos a ligeros cambios en las geometrías de coordinación del Cu T1 y de los Cu T3. Por último, la lacasa de *S. sclerotiorum* carece de absorción a 610 nm y presenta el hombro a 330 nm, propiedades características de las lacasas amarillas. Sin embargo, y a diferencia de ellas, su sitio T1 es detectable en el espectro de EPR.

Según la clasificación de la Comisión de Enzimas (EC, *Enzyme Commission*), las lacasas (EC 1.10.3.2, bencenodiol:oxígeno oxidorreductasas) pueden llevar a cabo la oxidación de *o*- y *p*-difenoles, fenoles metoxi-sustituidos, diaminas aromáticas y una amplia gama de compuestos, pero son incapaces de oxidar la tirosina, lo que las distingue de las tirosinasas (EC 1.14.18.1, L-tirosina, L-dopa:oxígeno oxidorreductasas). Si esta clasificación prevalece sobre las características estructurales y espectroscópicas, entonces tanto las lacasas amarillas como blancas son verdaderas lacasas. No obstante, muchos autores no las consideran como tales, argumentando que para que una enzima sea lacasa debe contener los cuatro átomos de cobre típicos de las oxidasas multicobre y la organización estructural característica descrita en el **Apartado 1.2.3**, pág. 32.

1.2.5. Lacasas y potencial redox

En base a un amplio conjunto de estudios comparativos que incluyen alineamiento de secuencias y análisis de estructuras cristalinas, se ha comprobado que todas las oxidasas multicobre presentan un sitio T1 con características muy conservadas, aunque con sutiles diferencias en su esfera de coordinación. El sitio T1 de la ascorbato oxidasa de *Cucurbita pepo* y de las lacasas bacterianas y de plantas está formado por dos residuos de His, un residuo de Cys y un residuo de Met, el cual actúa como ligando axial (situado a 2.90 Å del Cu T1 en la ascorbato oxidasa de *C. pepo* y a 3.27 Å en la lacasa CotA de *Bacillus subtilis*) (Messerschmidt *et al.*, 1992; Enguita *et al.*, 2003). Estos cuatro ligandos se unen al Cu T1 en una disposición tetragonal distorsionada (Xu *et al.*, 1999). Por su parte, las lacasas fúngicas tienen un residuo de Leu o de Phe en la posición correspondiente al ligando axial (**Tabla 1.4.**). Al contrario de lo que sucede con la Met axial de las lacasas bacterianas y de plantas, se ha comprobado que ni la Leu ni la Phe participan en la coordinación directa del Cu T1 de las lacasas fúngicas (Xu *et al.*, 1999). Estos ligandos se encuentran a mayor distancia del sitio T1 (Leu a 3.50 Å del Cu T1 en la lacasa de *Coprinus cinereus* y Phe a 3.60 Å del Cu T1 en la de *Trametes versicolor*), haciendo que la geometría de este centro de cobre sea triangular plana (Ducros *et al.*, 1998; Piontek *et al.*, 2002).

El potencial redox estándar del sitio T1, $E°_{T1}$, está determinado por la energía requerida por el Cu T1 para arrancar un electrón del sustrato reductor. Diversos estudios han sugerido que el valor del $E°_{T1}$ depende de la naturaleza de los ligandos del sitio T1. Así, ligandos axiales fuertes donan carga al átomo de cobre ayudando a estabilizarlo y reduciendo el $E°_{T1}$. El efecto contrario ocurre en presencia de ligandos axiales débiles (Leu y Phe), que tienden a desestabilizar el ion de cobre y, por tanto, aumentar el $E°_{T1}$ (Xu *et al.*, 1998). Aunque estudios de mutagénesis dirigida en los que la sustitución de la Met axial por una Leu en la oxidasa monocobre azurina y en la lacasa CotA de *B. subtilis* incrementaron el $E°_{T1}$ en 100 mV (Farver *et al.*, 1993; Durao *et al.*, 2006), experimentos similares realizados en lacasas fúngicas no tuvieron el mismo efecto (Xu *et*

Tabla 1.4. Potenciales redox y alineamiento de la secuencia del sitio T1 de lacasas producidas por diferentes organismos. En cursiva, ligandos de los Cu T3; subrayados, ligandos del Cu T1 y en negrita el ligando axial.

Lacasa	Organismo	Número de acceso en GenBank/PDB	$E°_{T1}$, mV (*vs.* ENH)	Alineamiento	Referencia
ALTO POTENCIAL REDOX					
Trametes trogii	Basidiomiceto	2HRG	+790	^{449}*H* C *H* I D F H L E A G **F**^{460}	Garzillo *et al.*, 2001
Trametes ochracea	Basidiomiceto	2HZH	+790	^{452}*H* C *H* I D F H L E A G **F**^{463}	Shleev *et al.*, 2004
Trametes versicolor	Basidiomiceto	1GYC	+785	^{452}*H* C *H* I D F H L E A G **F**^{463}	Reinhammar, 1972
Trametes hirsuta	Basidiomiceto	AAA33103.1	+780	^{452}*H* C *H* I D F H L D A G **F**^{463}	Shleev *et al.*, 2004
Botrytis cinerea	Ascomiceto	CCD45861.1	+780	^{508}*H* C *H* I A W H A S E G **L**^{519}	Li *et al.*, 1999
Trametes villosa	Basidiomiceto	AAC41686.1	+780	^{452}*H* C *H* I D F H L E A G **F**^{463}	Li *et al.*, 1999
Cerrena maxima	Basidiomiceto	D0VWU3.1	+750	^{452}*H* C *H* I D F H L E G G **F**^{463}	Shleev *et al.*, 2004
Pycnoporus cinnabarinus	Basidiomiceto	AAC39469.1	+750	^{450}*H* C *H* I D F H L E A G **F**^{461}	Li *et al.*, 1999
Trametes pubescens LAC1	Basidiomiceto	AAM18408.1	+746	^{457}*H* C *H* I D F H L E A G **F**^{468}	Shleev *et al.*, 2007
Pleurotus ostreatus POXC	Basidiomiceto	1587216	+740	^{460}*H* C *H* I D W H L E I G **L**^{471}	Garzillo *et al.*, 2001
Trametes pubescens LAC2	Basidiomiceto	AAM18407.1	+738	^{452}*H* C *H* I D F H L E A G **F**^{463}	Shleev *et al.*, 2007
Trametes sp. C30 LAC1	Basidiomiceto	AAF06967.1	+730	^{449}*H* C *H* I D F H L E A G **F**^{460}	Klonowska *et al.*, 2002
MEDIO POTENCIAL REDOX					
Rhizoctonia solani	Basidiomiceto	S68120	+710	^{459}*H* C *H* I D W H L E A G **L**^{470}	Xu *et al.*, 1998
Pleurotus ostreatus POXA1b	Basidiomiceto	CAA06292.1	+650	^{450}*H* C *H* I D W H L D L G **F**^{461}	Garzillo *et al.*, 2001
Trametes sp. C30 LAC2	Basidiomiceto	AAM66348.1	+560	^{452}*H* C *H* I D F H L E A G **F**^{463}	Klonowska *et al.*, 2002
Coprinus cinereus	Basidiomiceto	1A65	+550	^{451}*H* C *H* I E F H L M N G **L**^{462}	Schneider *et al.*, 1999
Trichophyton rubrum LKY-7	Ascomiceto	EGD86557.1	+540	^{530}*H* C *H* I A W H S S Q G **L**^{541}	Jung *et al.*, 2002
Trametes sp. C30 LAC3	Basidiomiceto	AAR00925.1	+530	^{452}*H* C *H* I D F H L D A G **F**^{463}	Klonowska *et al.*, 2005
Scytalidium thermophilum	Ascomiceto	n.d.	+510	^{506}*H* C H I A W H V S G G **L**^{517}	Xu *et al.*, 1998
Melanocarpus albomyces	Ascomiceto	1GW0	+470	^{502}*H* C *H* I A W H V S G G **L**^{513}	Andberg *et al.*, 2009
Myceliophthora thermophila	Ascomiceto	ADA41449.1	+470	^{502}*H* C *H* I A W H V S G G **L**^{513}	Xu *et al.*, 1998
BAJO POTENCIAL REDOX					
CotA de *Bacillus subtilis*	Bacteria	1GSK_A	+455	^{491}*H* C *H* I L E H E D Y D **M**^{502}	Melo *et al.*, 2007
Rhus vernicifera	Planta	BAB63411.2	+434	^{495}*H* C *H* F E R H T T E G **M**^{506}	Reinhammar, 1972

al., 1998). Por otro lado, el análisis comparativo de las estructuras cristalográficas de las lacasas de *T. versicolor* ($E°_{T1}$ = +785 mV *vs.* ENH) y *C. cinereus* ($E°_{T1}$ = +550 mV *vs.* ENH) sugiere que la distancia entre el Cu T1 y los átomos de nitrógeno que lo coordinan es otro de los factores involucrados en la modulación del potencial redox (Piontek *et al.*, 2002). En conclusión, el valor del $E°_{T1}$ de las lacasas no está determinado por una única característica estructural, sino que es el resultado de la combinación de diversos factores como las interacciones Cu-ligando, las interacciones electrostáticas intramoleculares, los efectos de desolvatación en torno al sitio T1 y las restricciones en el plegamiento proteico (Li *et al.*, 2004).

Desde un punto de vista electroquímico y en base al análisis de sus estructuras primarias, las lacasas se clasifican en tres grupos atendiendo al valor del potencial redox del sitio T1: lacasas de bajo, medio y alto potencial redox (Christenson *et al.*, 2004) (**Tabla 1.4.**). Las lacasas bacterianas y de plantas, con un fuerte ligando axial (Met), constituyen el grupo de lacasas de bajo potencial redox, con $E°_{T1}$ en torno a +450 mV *vs.* ENH. Por su parte, las lacasas fúngicas pueden ser de medio o alto potencial redox. Así, el grupo de las lacasas de medio potencial redox incluye lacasas de ascomicetos y basidiomicetos con $E°_{T1}$ comprendidos entre +470 y +710 mV *vs.* ENH y con un residuo de Leu en la posición axial salvo las lacasas POXA1b de *Pleurotus ostreatus* y las LAC2 y LAC3 de *Trametes* sp. C30 que tienen una Phe. En cuanto a las lacasas de alto potencial redox, son producidas por basidiomicetos (salvo la lacasa del ascomiceto *Botrytis cinerea*) y tienen $E°_{T1}$ en el intervalo de +730 a +790 mV *vs.* ENH. Todas ellas presentan una Phe en la posición axial, a excepción de las lacasas de *B. cinerea* y *P. ostreatus* (POXC), que tienen una Leu.

1.2.6. Expresión de lacasas recombinantes

La aplicación biotecnológica de lacasas requiere de la producción a nivel industrial de enzimas estables y activas. Sin embargo, el logro de tal objetivo está impedido de manera general por los bajos niveles de expresión en los microorganismos nativos así como por sus condiciones de crecimiento. Este problema se ha abordado desde dos vertientes distintas: i) mediante la optimización de diversos componentes del medio de cultivo (iones metálicos, compuestos aromáticos derivados de la lignina y fuentes de nitrógeno y de carbono) con el fin de aumentar los niveles de expresión homóloga (Collins y Dobson, 1997; Lee *et al.*, 1999; Hong *et al.*, 2002; Terron *et al.*, 2004); y ii) a través de su expresión heteróloga, combinando el empleo de fuertes promotores, de genes multicopia y de péptidos señales capaces de dirigir la secreción de la lacasa al medio extracelular, así como a través de herramientas de evolución molecular dirigida (Piscitelli *et al.*, 2010).

Y es que, con excepción de la sobreexpresión homóloga de la lacasa de *Pycnoporus cinnabarinus* que dio lugar a niveles de lacasa secretada de 1.2 g/L (Alves *et al.*, 2004), donde se

ha llevado a cabo mayor esfuerzo ha sido en el desarrollo de sistemas de expresión heteróloga (Kunamneni *et al.*, 2008a). De esta manera, se ha publicado la expresión heteróloga de lacasas de orígenes muy diversos en diferentes especies bacterianas (*E. coli* y *Streptomyces lividans*), en plantas (*Arabidopsis thaliana, Lycopersicon esculentum*, *Nicotiana tabacum*, *Oryza sativa* y *Zea mays*), en levaduras (*Kluyveromyces lactis*, *P. pastoris*, *Pichia methanolica*, *S.cerevisiae* y *Yarrowia lipolytica*) y en hongos filamentosos (*Aspergillus niger*, *Aspergillus nidulans, Aspergillus oryzae*, *Penicillium canescens* y *Trichoderma reesei*) (Piscitelli *et al.*, 2010).

Las lacasas fúngicas son las más interesantes desde el punto de vista industrial debido a que sus mayores potenciales redox les permiten la oxidación de un amplio espectro de moléculas. La expresión heteróloga de lacasas fúngicas se ha conseguido en levaduras (**Tabla 1.5.**), en hongos filamentosos y en plantas (**Tabla 1.6.**). Además, recientemente se ha expresado funcionalmente en *E. coli* la lacasa del hongo ligninolítico *Cyathus bulleri*, convirtiéndose en la primera lacasa fúngica expresada en un hospedador bacteriano (Salony *et al.*, 2008) (**Tabla 1.6.**). En muchos casos, la expresión de lacasa fue posible gracias a la sustitución del péptido señal nativo por la secuencia señal de proteínas que son secretadas en grandes cantidades por el microorganismo hospedador. Así, se ha conseguido la producción heteróloga de lacasas empleando el péptido señal del factor α o de la invertasa de *S. cerevisiae*, de la proteasa alcalina XPR2 de *Y. lipolytica*, de la glucoamilasa de *A. niger*, de la β-galactosidasa de *P. canescens*, de la glutelina B1 de *O. sativa* y de la α-amilasa de *Hordeum vulgare*, entre otros (**Tablas 1.5.** y **1.6.**).

El empleo de hongos filamentosos como sistemas de expresión ha dado lugar a los mayores niveles de producción heteróloga de lacasa hasta la fecha. *T. reesei* secreta 920 mg/L de la lacasa de *Melanocarpus albomyces* y entre 800 y 1000 mg/L de la de *T. versicolor*, mientras que *A. niger* produce 840 mg/L de la lacasa LAC3 de *Trametes* sp. C30 (**Tabla 1.6.**). Sin embargo, la optimización de la expresión génica mediante distintas técnicas mutagénicas (especialmente la evolución dirigida) es difícil de realizar utilizando dichos microorganismos (Robert *et al.*, 2011). Por este motivo, los pasos de clonaje y de expresión de lacasas se llevan a cabo a menudo en levaduras, puesto que no producen lacasas endógenas y las lacasas recombinantes son secretadas directamente al medio extracelular, facilitando la detección de actividad. Las levaduras que han permitido la producción exitosa de un mayor número de lacasas son *S. cerevisiae* y *P. pastoris*, gracias a que cuentan con una amplia variedad de técnicas de biología molecular (plásmidos replicativos, promotores inducibles o constitutivos y sencillos protocolos de transformación) y a que son fácilmente cultivables (**Tabla 1.5.**).

Tabla 1.5. Lacasas fúngicas expresadas en levaduras (*Kluyveromyces lactis*, *Pichia pastoris*, *Pichia methanolica*, *Saccharomyces cerevisiae* y *Yarrowia lipolytica*). Entre paréntesis se indica la isoenzima expresada.

Hospedador	Hongo de origen	Péptido señal (PS) empleado	Niveles de expresión*	Referencia
K. lactis	*Pleurotus ostreatus* (POXA1b)[b]	PS nativo	2030 U/L, 1.6 mg/L	Piscitelli *et al.*, 2005
K. lactis	*Pleurotus ostreatus* (POXC)[b]	PS nativo	100 U/L, 1.9 mg/L	Piscitelli *et al.*, 2005
P. pastoris	*Botrytis aclada*[a]	PS nativo	53300 U/L[1], 517 mg/L[1]	Kittl *et al.*, 2012a
P. pastoris	*Botrytis aclada*[a]	PS nativo	51000 U/L, 495 mg/L[2]	Kittl *et al.*, 2012b
P. pastoris	*Pleurotus sajor-caju*[b]	PS nativo	10200 U/L, 4.9 mg/L	Soden *et al.*, 2002
P. pastoris	*Pycnoporus cinnabarinus*[b]	PS nativo / PS del factor α de *S. cerevisiae*	8 mg/L	Otterbein *et al.*, 2000
P. pastoris	*Pycnoporus coccineus*[b]	PS nativo / PS del factor α de *S. cerevisiae*	Fase sólida	Hoshida *et al.*, 2001
P. pastoris	*Rigidoporus microporus*[b]	PS nativo	9030 U/L	Liu *et al.*, 2003
P. pastoris	*Trametes* sp. 420[b]	PS del factor α de *S. cerevisiae*	239000 U/L, 136 mg/L	Cui *et al.*, 2007
P. pastoris	*Trametes* sp. AH28-2[b]	PS del factor α de *S. cerevisiae*	32000 U/L, 31.6 mg/L	Li *et al.*, 2007
P. pastoris	*Trametes trogii*[b]	PS nativo	2520 U/L, 17 mg/L	Colao *et al.*, 2006
P. pastoris	*Trametes versicolor*[b]	PS nativo	140000 U/L	Hong *et al.*, 2002
P. methanolica	*Trametes versicolor*[b]	PS del factor α de *S. cerevisiae*	12600 U/L	Guo *et al.*, 2006
S. cerevisiae	*Melanocarpus albomyces*[a]	PS del factor α de *S. cerevisiae*	270 U/L, 7.4 mg/L	Andberg *et al.*, 2009
S. cerevisiae	*Myceliophthora thermophila*[a]	PS del factor α de *S. cerevisiae*	18 mg/L	Bulter *et al.*, 2003a
S. cerevisiae	*Pleurotus eryngii*[b]	PS nativo	146 U/L	Bleve *et al.*, 2008
S. cerevisiae	*Pleurotus ostreatus* (POXA1b)[b]	PS nativo	200 U/L	Piscitelli *et al.*, 2005
S. cerevisiae	*Pycnoporus cinnabarinus*[b]	PS del factor α de *S. cerevisiae*	300 U/L, 2 mg/L	Camarero *et al.*, 2012
S. cerevisiae	*Pycnoporus coccineus*[b]	PS nativo	Fase sólida	Hoshida *et al.*, 2001
S. cerevisiae	*Trametes* sp. C30[b] (LAC3)	PS de la invertasa de *S. cerevisiae*	2 mg/L	Klonowska *et al.*, 2005
S. cerevisiae	*Trametes hirsuta*[b]	PS nativo	Fase sólida	Kojima *et al.*, 1990
Y. lipolytica	*Pycnoporus cinnabarinus*[b]	PS de la proteasa alcalina XPR2 de *Y. lipolytica*	1026 U/L, 19.8 mg/L	Madzak *et al.*, 2005
Y. lipolytica	*Trametes versicolor*[b] (lacasa IIIb)	PS nativo	230 U/L, 2.5 mg/L	Jolivalt *et al.*, 2005
Y. lipolytica	*Trametes versicolor*[b] (lcc1)	PS nativo	250 U/L[3] -1000 U/L[4]	Theerachat *et al.*, 2012

a: Ascomiceto. b: Basidiomiceto. *Actividad medida con ABTS en todos los casos, a excepción de la lacasa LAC3 de *Trametes* sp. C30 expresada en *S. cerevisiae*, donde la actividad se determinó con siringaldazina; la expresión de la lacasa de *P. coccineus* en *P. pastoris* y *S. cerevisiae* y de *T. hirsuta* en *S. cerevisiae* se confirmó por actividad en placas de agar con guaiacol. [1]Expresión bajo el control del promotor de la gliceraldehído-3-fosfato deshidrogenasa. [2]Expresión bajo el control del promotor de la alcohol oxidasa 1. [3]Niveles de expresión conseguidos por integración de una única copia del gen. [4]Niveles de expresión conseguidos por integración de múltiples copias del gen.

Tabla 1.6. Lacasas fúngicas expresadas en hongos filamentosos (*Aspergillus niger*, *Aspergillus oryzae*, *Penicillium canescens* y *Trichoderma reesei*), en plantas (*Nicotiana tabacum*, *Oryza sativa* y *Zea mays*) y en bacterias (*Escherichia coli*). Entre paréntesis se indica la isoenzima expresada.

Hospedador	Hongo de origen	Péptido señal (PS) empleado	Niveles de expresión*	Referencia
A. niger	*Pycnoporus cinnabarinus*[b]	PS de la glucoamilasa de *A. niger*	70 mg/L	Record *et al.*, 2002
A. niger	*Trametes* sp. C30[b] (LAC3)	PS de la GAPDH de *A. niger*	840 mg/L	Mekmouche *et al.*, 2012
A. niger	*Trametes versicolor*[b]	PS nativo	2700 U/L	Bohlin *et al.*, 2006
A. oryzae	*Coprinus cinereus*[b]	PS nativo	135 mg/L	Yaver *et al.*, 1999
A. oryzae	*Myceliophthora thermophila*[a]	PS nativo	850 U/L, 19 mg/L	Berka *et al.*, 1997
A. oryzae	*Rhizoctonia solani*[b]	PS nativo	n.d.	Wahleithner *et al.*, 1996
A. oryzae	*Pycnoporus coccineus*[b]	PS nativo	3000 U/L	Hoshida *et al.*, 2005
P. canescens	*Trametes hirsuta*[b]	PS de la β-galactosidasa de *P. canescens*	3000 U/L	Abyanova *et al.*, 2010
T. reesei	*Melanocarpus albomyces*[a]	PS nativo	46800 U/L, 920 mg/L	Kiiskinen *et al.*, 2004
T. reesei	*Phlebia radiata*[b]	PS nativo	462 U/L, 19.5 mg/L	Saloheimo y Niku-Paavola, 1991
T. reesei	*Trametes versicolor*[b]	PS de la celobiohidrolasa I de *T. reesei*	800-1000 mg/L	Baker y White, 2001
N. tabacum	*Trametes versicolor*[b]	PS nativo	n.d.	Sonoki *et al.*, 2005
O. sativa	*Melanocarpus albomyces*[a]	PS de la glutelina B1 de *O. sativa*	13 ppm	de Wilde *et al.*, 2008
O. sativa	*Pycnoporus cinnabarinus*[b]	PS de la glutelina B1 de *O. sativa*	39 ppm	de Wilde *et al.*, 2008
Z. mays	*Trametes versicolor*[b]	PS de la α-amilasa de *Hordeum vulgare*	>50 ppm	Bailey *et al.*, 2004
E. coli	*Cyathus bulleri*[b]	PS nativo	n.d.	Salony *et al.*, 2008

a: Ascomiceto. b: Basidiomiceto. GAPDH: gliceraldehído-3-fosfato deshidrogenasa. *Actividad medida con ABTS en todos los casos, a excepción de las lacasas de *M. thermophila* y *P. coccineus* expresadas en *A. oryzae*, donde la actividad se cuantificó con siringaldazina y N,N-dimetil-1,4-fenilendiamina, respectivamente, y la lacasa de *T. hirsuta* expresada en *P. canescens*, donde la actividad se determinó con catecol. n.d.: no determinado.

1.2.7. Aplicaciones industriales y biotecnológicas

Debido a sus escasos requerimientos para llevar a cabo la catálisis (sólo necesitan el oxígeno del aire como aceptor de electrones y liberan agua como único subproducto) y a su capacidad para oxidar un amplio abanico de sustratos, las lacasas encuentran potenciales aplicaciones en diversos sectores industriales y biotecnológicos. Los más destacados son:

- La industria alimentaria: en el procesamiento de bebidas (vino, zumo de frutas y cerveza), en la determinación de ácido ascórbico y en la gelificación de la pectina de la remolacha azucarera (Osma *et al.*, 2010).
- La industria papelera: en el blanqueo libre de cloro de pasta de papel y en el tratamiento de efluentes (Couto y Herrera, 2006).
- La industria textil: en la modificación de fibras, en el blanqueamiento de tejidos y en la degradación de colorantes presentes en aguas residuales (Couto y Herrera, 2006).
- La industria de muebles y de la construcción: en el entrecruzamiento de materiales basados en la lignina para producir tableros de fibra de densidad media (Alcalde, 2007).
- La industria de pinturas: empleo del sistema lacasa-mediador para el secado de resinas alquídicas, ampliamente utilizadas en pinturas y recubrimientos (Greimel *et al.*, 2012).
- La industria química sintética: en el acoplamiento oxidativo de intermedios radicales para dar lugar a compuestos antitumorales (*p. ej.*, actinocina o vinblastina) y derivados de ciclosporina (*p. ej.*, ciclosporina A), de hormonas (*p. ej.*, β-estradiol) y de fitoalexinas (*p. ej.*, resveratrol) (Kunamneni *et al.*, 2008a).
- La producción de bioetanol: para eliminar los compuestos fenólicos que inhiben la fermentación de los azúcares presentes en el hidrolizado de materiales lignocelulósicos (Alcalde, 2007).
- Biorremediación de suelos: degradación de 2,4,6-trinitrotolueno (TNT) y de PAHs (Couto y Herrera, 2006).
- La industria cosmética: en la preparación de tintes para el cabello y de productos para aclarar la piel (Couto y Herrera, 2006).
- Biomedicina: inmovilización de lacasas en tiras o vendas para su uso en el diagnóstico de infecciones fúngicas (Schneider *et al.*, 2012).
- Nanobiotecnología: en el diseño de biopilas de combustible y de biosensores para la detección de diferentes compuestos (Kunamneni *et al.*, 2008b).

En la actualidad se comercializan diversos preparados de lacasas (que en algunos casos incluyen mediadores redox en la composición), con aplicaciones que van desde el tratamiento de corchos en la industria alimentaria al blanqueo o al acabado de las telas vaqueras en la industria textil (**Tabla 1.7.**).

Tabla 1.7. Preparados comerciales que contienen lacasas.

Industria	Aplicación	Marca comercial	Empresa
ALIMENTARIA	Realce del color (té, etc.)	Laccase M120	Amano Enzyme Inc. (Japón)
	Tratamiento de corchos	Suberase	Novozymes (Dinamarca)
PAPELERA	Deslignificación de la pasta de papel	Novozym 51003	Novozymes (Dinamarca)
TEXTIL	Blanqueo de la tela vaquera	Americos Laccase P	Americos Chemicals Pvt. Ltd. (India)
		Bleach Cut 3-S	Season Chemicals & Dyestuffs (China)
		DeniLite	Novozymes (Dinamarca)
		Primagreen Ecofade LT100	DuPont Industrial Biosciences(EE.UU.)
	Acabado de la tela vaquera	Cololacc BB	Colotex Bio-technology Co. Ltd. (China)
		Ecostone LCC10	AB Enzymes GmbH (Alemania)
		IndiStar	DuPont Industrial Biosciences(EE.UU.)
		Novoprime Base 268	Novozymes (Dinamarca)
		ZyLite	Zytex Pvt. Ltd. (India)

1.2.8. Lacasas en biopilas de combustible y biosensores enzimáticos

Una pila de combustible es un dispositivo electroquímico que convierte la energía química contenida en un combustible (*p. ej.,* hidrógeno o metano) en energía eléctrica. Las pilas de combustible se componen de dos electrodos: un ánodo (donde tiene lugar la reacción de oxidación del combustible) y un cátodo (en el que ocurre la reacción de reducción, normalmente, de oxígeno a agua). Para llevar a cabo ese proceso de manera eficaz es necesario implementar catalizadores en los electrodos de la pila, siendo el más habitual el platino. Alternativamente, se pueden emplear catalizadores enzimáticos, bien en forma de microorganismos o de enzimas aisladas (Kim *et al.*, 2006). La combinación de las pilas de combustible con estos elementos biológicos da lugar a las llamadas biopilas de combustible (Palmore y Whitesides, 1994).

Actualmente, una parte muy importante de los estudios están enfocados en el desarrollo de biopilas de combustible basadas en enzimas (**Figura 1.7.**). En este tipo de biopilas, una enzima capaz de oxidar el combustible (típicamente azúcares como la glucosa) se inmoviliza en el ánodo de manera que su centro redox quede conectado al electrodo. El proceso de oxidación da lugar a

electrones y protones. Los electrones fluyen a través del circuito eléctrico hasta el cátodo, donde otra enzima allí inmovilizada y conectada se encarga de reducir el agente oxidante (normalmente oxígeno o peróxidos) a agua utilizando los electrones y protones procedentes del ánodo. Ejemplos típicos de enzimas que se han inmovilizado hasta la fecha en el compartimento anódico de biopilas de combustible son la glucosa oxidasa (Chen *et al.*, 2001; Katz *et al.*, 2001; Pizzariello *et al.*, 2002; Katz y Willner, 2003; Mano *et al.*, 2003), la celobiosa deshidrogenasa (Stoica *et al.*, 2009; Coman *et al.*, 2008; Coman *et al.*, 2010; Falk *et al.*, 2012), la glucosa deshidrogenasa (Okuda-Shimazaki *et al.*, 2008; Zafar *et al.*, 2012) y la lactato deshidrogenasa (Leung y Lai, 2011). Por su parte, en el cátodo de biopilas de combustible se han empleado lacasas (Chen *et al.*, 2001; Coman *et al.*, 2008; Stoica *et al.*, 2009), peroxidasas (Pizzariello *et al.*, 2002), bilirrubina oxidasas (Mano *et al.*, 2003; Coman *et al.*, 2010; Falk *et al.*, 2012), glutamato deshidrogenasas (Leung y Lai, 2011) y el citocromo c unido a la citocromo c oxidasa (Katz *et al.*, 2001; Katz y Willner, 2003).

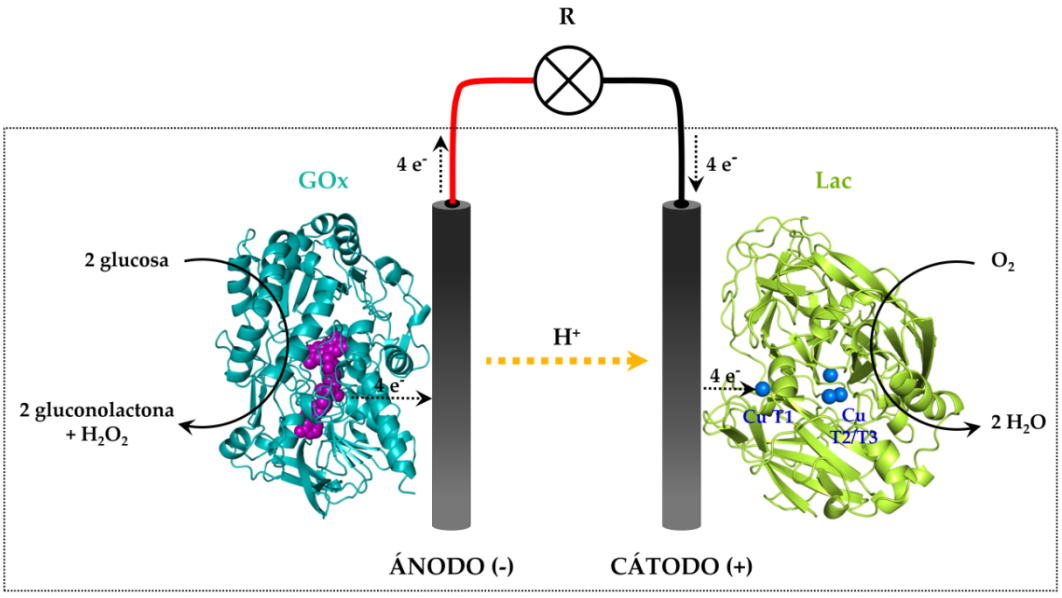

Figura 1.7. Esquema de una biopila de combustible enzimática con transferencia electrónica directa. Una glucosa oxidasa (GOx) actúa como biocatalizador anódico y una lacasa (Lac) como catalizador catódico (Chen *et al.*, 2001).

Por su parte, un biosensor se define como un dispositivo capaz de proveer información analítica cuantitativa específica utilizando un elemento de reconocimiento biológico, el cual está en contacto directo con un transductor (IUPAC, 1997). El transductor se encarga, a su vez, de convertir la respuesta biológica resultante de la interacción del elemento de biorreconocimiento con el analito de interés en una señal fácilmente cuantificable. Los biosensores se clasifican en varios tipos en función tanto del tipo de transductor como del elemento de bio-reconocimiento.

En base al elemento de transducción, los biosensores pueden ser electroquímicos, ópticos, piezoeléctricos o térmicos. Por otro lado, de acuerdo con el elemento de reconocimiento, los biosensores se clasifican en sensores inmunoquímicos, sensores basados en receptores no enzimáticos, sensores conteniendo células enteras y sensores enzimáticos (Rodriguez-Mozaz *et al.*, 2006).

Uno de los factores críticos en el desarrollo de biopilas de combustible y biosensores enzimáticos es conseguir una conducción eléctrica eficiente entre el biocatalizador y los electrodos. El proceso de transferencia electrónica directa (TED) entre una enzima y un electrodo se ha observado para un número reducido de enzimas, entre las que se encuentran las lacasas (Shleev *et al.*, 2005a). Para que haya TED es necesario que el centro activo de la enzima esté en contacto directo con la superficie del electrodo. Se ha propuesto que la distancia crítica entre el electrodo y el *cluster* trinuclear de las lacasas para una efectiva reducción electroquímica del oxígeno es de 20 Å (Iaropolov *et al.*, 1981). Distancias mayores a ésta disminuirían la reacción, cuya velocidad viene determinada por el flujo de electrones; mientras que distancias menores harían la conducción eléctrica tan eficiente que la cinética de la reacción se convertiría en el paso limitante.

Las lacasas de alto potencial redox resultan de especial interés para el desarrollo de biopilas de combustible gracias a: i) su capacidad de trabajar en régimen de TED, evitando así el uso de mediadores redox que conllevan una reducción del potencial efectivo del electrodo; y ii) su elevado potencial redox, lo que permite el desarrollo de pilas con mayor voltaje y, por tanto, que producen mayor cantidad de energía eléctrica. Por ejemplo, se han desarrollado biopilas de combustible glucosa/O_2 en miniatura operativas a pH ácido y a un potencial de hasta 0.88 V empleando la lacasa de *T. hirsuta* ($E°_{T1}$ = +780 mV *vs.* ENH) como biocatalizador catódico (Soukharev *et al.*, 2004).

El desarrollo de dispositivos a escala nanométrica que puedan ser implantados y que sean capaces de funcionar en fluidos fisiológicos (*p. ej.*, sangre, plasma, saliva o lágrimas) con el objetivo de detectar la concentración de diferentes metabolitos (*p. ej.*, glucosa, insulina u oxígeno) constituye una de las líneas de estudio más prometedoras dentro de la Biotecnología y de la Bioelectroquímica (Heller, 2004). Estos dispositivos están formados por un biosensor capaz de detectar analitos *in vivo*, un sistema transductor-transmisor que transforme la señal química en una fácilmente medible y transmisible al exterior, y una biopila de combustible que genere la potencia suficiente como para que el dispositivo funcione (**Figura 1.8.**). Para ello, es requisito imprescindible que todos los elementos del dispositivo, incluidos los biocatalizadores, sean químicamente estables y activos en condiciones fisiológicas, es decir, pH por encima de la neutralidad (7.4) y concentraciones de cloruro superiores a 100 mM (Calabrese Barton *et al.*, 2004).

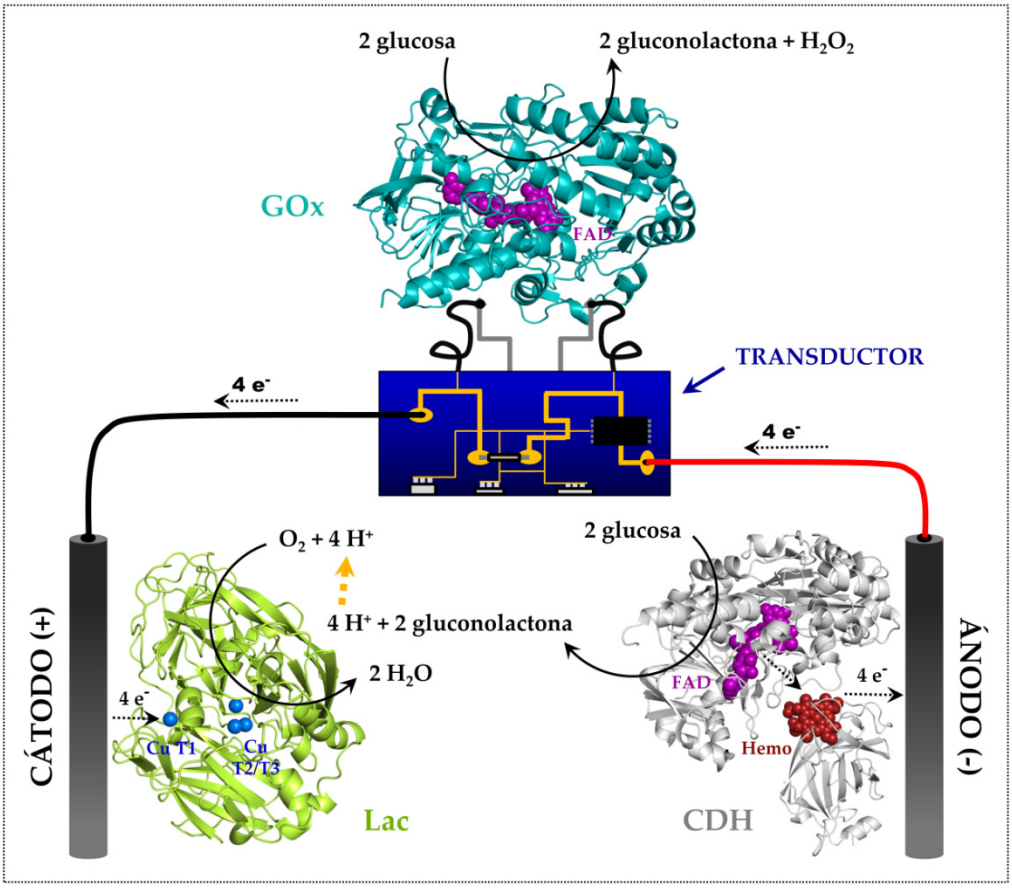

Figura 1.8. Representación esquemática de un dispositivo autónomo con aplicaciones biomédicas. Se compone de: i) un biosensor basado en la detección de glucosa por una glucosa oxidasa (GOx); ii) un transductor; y iii) una biopila de combustible con una celobiosa deshidrogenasa (CDH) como biocatalizador anódico y una lacasa (Lac) como catalizador catódico.

Desafortunadamente, las lacasas de alto potencial redox no son activas a ese pH y son fuertemente inhibidas por los iones cloruro, propiedades que limitan de manera significativa su aplicación en dispositivos operativos en condiciones fisiológicas. En los últimos años, se han desarrollado biopilas de combustible operativas en suero humano (Gao *et al.*, 2007; Coman *et al.*, 2010) y líquido lacrimal humano (Falk *et al.*, 2012) utilizando bilirrubina oxidasas fúngicas como biocatalizadores catódicos. Estas enzimas presentan peores prestaciones que las lacasas en lo referente a sus potenciales redox y limitan la generación de un voltaje suficiente para alimentar el dispositivo, pero con la ventaja de que son activas a pH neutro y menos sensibles a la presencia de cloruros (Coman *et al.*, 2010).

Aparte de sus potenciales aplicaciones en biopilas de combustible, las lacasas fúngicas se han empleado en el desarrollo de biosensores para, entre otros, los siguientes fines:

- La determinación de polifenoles presentes en zumos de frutas (Cliffe *et al.*, 1994), en vinos (Júnior y Rebelo, 2008; Di Fusco *et al.*, 2010), en tés (Ghindilis *et al.*, 1992) o en las aguas residuales de diferentes industrias (Oktem *et al.*, 2012).
- La medida del nivel de contaminación por hongos en mostos de uva (Zouari *et al.*, 1988).
- La detección de inhibidores de la actividad lacasa, como los aniones azida, cianuro o fluoruro. En este caso, el biosensor actúa como un dispositivo de alarma o "canario electroquímico" para detectar y monitorizar la presencia de compuestos tóxicos (Trudeau *et al.*, 1997; Leech y Daigle, 1998; Liu y Dong, 2008).
- La medida de la concentración de oxígeno en disolución (Gardiol *et al.*, 1996).
- La cuantificación de insulina (inmunosensor de insulina) (Milligan y Ghindilis, 2002).

1.2.9. La lacasa PM1

El basidiomiceto PM1 (CECT 2971), aislado de las aguas residuales de la Empresa Nacional de Celulosa (Miranda de Ebro, España), se clasificó dentro de los hongos de la podredumbre blanca al ser capaz de modificar el *kraft* de lignina en la misma extensión que los también basidiomicetos *T. versicolor* y *P. chrysosporium* (Coll *et al.*, 1993a).

El basidiomiceto PM1 secreta al medio extracelular una lacasa codificada por el gen *lac1*, objeto de esta Tesis Doctoral. Este gen tiene un marco abierto de lectura de 1551 nucleótidos que se transcriben y traducen en una proteína de 517 aminoácidos, de los cuales los 21 primeros constituyen el péptido señal (Coll *et al.*, 1993b). La lacasa PM1 es una glicoproteína monomérica con una masa molecular de 64 kDa y un contenido en carbohidratos del 6.5%. Su pI es 3.6, es estable en el intervalo de pH de 3.0 a 9.0 y su pH óptimo de actividad es 4.5 (Coll *et al.*, 1993a). Es una lacasa altamente termoestable, reteniendo la actividad tras una hora de incubación a 60°C y presentando una inusual activación térmica en el intervalo de 37 a 80°C. Su contenido en cobre es de cuatro átomos por molécula de enzima, distribuidos en un cobre de tipo 1, uno de tipo 2 y dos de tipo 3 en base a las características de su espectro UV-visible (Coll *et al.*, 1993a). Además, su secuencia de aminoácidos comparte una elevada identidad con las de las lacasas de alto potencial redox producidas por los basidiomicetos *Trametes* sp. C30 (99% de identidad de secuencia), *T. trogii* (97%), *T. versicolor* (80%), *T. hirsuta* (78%), *Cerrena maxima* (77%) y *Pycnoporus cinnabarinus* (77%). Esto último sugiere que la lacasa PM1 es también de alto potencial redox lo que, combinado con su activación térmica, y sus elevadas estabilidades frente a la temperatura y al pH, la convierten en un excelente punto de partida para llevar a cabos estudios de evolución molecular dirigida hacia diferentes fines.

1.3. OBJETIVOS

La lacasa PM1 es una enzima altamente estable, presentando además un elevado potencial redox en el sitio T1 lo cual es de gran interés para diversas aplicaciones biotecnológicas que incluyen el diseño de bionanodispositivos funcionales en fluidos fisiológicos. La ingeniería de esta enzima mediante herramientas de evolución molecular dirigida para adaptarla a ambientes extremos como la sangre humana (pH 7.4, concentraciones de NaCl cercanas a 150 mM), se planteó a través de la consecución de dos objetivos fundamentales:

i) La obtención y mejora mediante evolución dirigida de un sistema de expresión funcional en *S. cerevisiae* robusto y fiable.

ii) El diseño de una estrategia evolutiva adecuada para superar la inherente inhibición por cloruros e hidroxilos presentes en la sangre de humanos.

Para el desarrollo de estos dos objetivos se abordaron de manera secuencial las siguientes tareas:

1. El incremento de los niveles de expresión funcional de la lacasa en *S. cerevisiae* mediante ciclos iterativos de evolución dirigida. Para este fin se diseñó un gen de fusión formado por el prepro-líder del factor α y la lacasa madura que se sometió a evolución conjunta empleando una estrategia "*uphill walk*" combinada con experimentos de mutagénesis dirigida.

2. La caracterización bioquímica y espectro-electroquímica de la mejor variante del proceso evolutivo (mutante OB-1).

3. La evolución dirigida del mutante OB-1 con el fin de hacerlo tolerante a la sangre humana. Para ello, se diseñó un sistema de HTS basado en la simulación de la composición bioquímica de la sangre al tiempo que se incrementó la presión selectiva generación tras generación.

4. La caracterización bioquímica y espectro-electroquímica de la mejor variante obtenida en este proceso (mutante ChU-B) así como su clonaje en *P. pastoris* y producción en biorreactor.

2. PUBLICACIONES

CAPÍTULO 1

Laboratory evolution of high-redox potential laccases

Diana Maté, Carlos García-Burgos, Eva García-Ruiz,
Antonio O. Ballesteros, Susana Camarero and Miguel Alcalde

Published in *Chemistry & Biology*, 2010, vol. 17, pp. 1030-1041.

2.1.1. SUMMARY

Thermostable laccases with a high redox potential have been engineered through a strategy that combines directed evolution with rational approaches. The original laccase signal sequence was replaced by the α-factor prepro-leader, and the corresponding fusion gene was targeted for joint laboratory evolution with the aim of improving kinetics and secretion by *Saccharomyces cerevisiae*, whilst retaining high thermostability. After eight rounds of molecular evolution, the total laccase activity was enhanced 34,000-fold culminating in the OB-1 mutant as the last variant of the evolution process, a highly active and stable enzyme in terms of temperature, pH range and organic co-solvents. Mutations in the hydrophobic core of the evolved α-factor prepro-leader enhanced functional expression, whereas some mutations in the mature protein improved its catalytic capacities by altering the interactions with the surrounding residues.

2.1.2. INTRODUCTION

Laccases (EC 1.10.3.2) belong to the group of blue multicopper oxidases along with ceruloplasmin, ascorbate oxidase and bilirubin oxidase, among others. Laccase is one of the oldest enzymes reported and it is currently arousing great interest in the scientific community due to its very basic requirements (it just needs air to work and its only released by-product is water) and huge catalytic capabilities, making it one of the "greenest" enzymes of the 21st century (Alcalde *et al.*, 2006a; Riva, 2006; Rodgers *et al.*, 2010).

In a well conserved and better fitting laccase scaffold, the characteristic paramagnetic blue copper at the T1 site is responsible for sequestering one electron from the reducing substrate and transferring it to the trinuclear T2/T3 copper cluster, where molecular oxygen binds (Solomon *et al.*, 1996; Giardina *et al.*, 2010). As a generalist biocatalyst, laccase is capable of oxidizing dozens of different compounds (phenols, polyphenols, benzenethiols, polyamines,

hydroxyindols, aryl diamines, Mn^{2+}, $Fe(EDTA)^{2-}$), and its substrate promiscuity can be even further expanded by the use of redox mediators (diffusible electron carriers from natural or synthetic sources) (Call and Mucke, 1997; Gianfreda *et al.*, 1999; Kunamneni *et al.*, 2008a; Cañas and Camarero, 2010). Laccases are commonly classified as low-, medium- and High-Redox Potential Laccases (HRPLs) according to their redox potential at the T1 site (ranging from +430 mV in bacterial and plant laccases to +790 mV in some fungal laccases), and the later are by far the most important from a biotechnological point of view (Alcalde, 2007; Rodgers *et al.*, 2010). HRPLs are typically secreted by ligninolytic basidiomycetes, the so-called white-rot fungi, displaying a high catalytic rate along with the capacity to oxidize compounds with higher redox potential that cannot be transformed by their medium and low redox potential laccase counterparts (Shleev *et al.*, 2005b).

However, the engineering of HRPLs for practical uses has hardly been addressed because of the lack of suitable expression systems to improve them through directed evolution. Although *E. coli* is the preferred host organism for *in vitro* evolution experiments, the differences between the eukaryotic expression system for HRPLs and that of bacteria (codon usage, missing chaperones and posttranslational modifications such as glycosylation or the formation of disulfide bridges) are hurdles that are not easily overcome. Accordingly, all attempts to functionally express fungal laccases in bacteria have so far ended up in misfolding and the formation of inclusion bodies (Kunamneni *et al.*, 2008b). However, the secretory machinery of *Saccharomyces cerevisiae* permits posttranslational modifications and it is also an excellent host to carry out laboratory evolution experiments (Alcalde, 2010). Indeed, the high level of homologous recombination enables scientists to produce *in vivo* shuffled mutant libraries or to develop new tools to generate diversity (Cherry *et al.*, 1999; Bulter *et al.*, 2003a; Okkels, 2004; Alcalde *et al.*, 2006b; Zumárraga *et al.*, 2008a). In this context, we have already used directed evolution to improve the functional expression of the medium redox potential laccase from the ascomycete *Myceliophthora thermophila* in *S. cerevisiae*, to confer organic co-solvent tolerance, as well as to perform semirational studies (Bulter *et al.*, 2003; Zumárraga *et al.*, 2007a,b). Unfortunately, the past success with this medium redox potential laccase cannot be easily translated to its HRPL counterparts, since the differences between the basidiomycete processing mechanism of HRPLs and that of the ascomycete *S. cerevisiae* impair functional expression at the levels required for directed evolution, as can be deduced from recent studies (Festa *et al.*, 2008; Cusano *et al.*, 2009; Miele *et al.*, 2010b).

Here, for the first time we describe the directed evolution of a high redox potential laccase functionally expressed in *S. cerevisiae* enhancing its activity and thermostability. Our starting point was the basidiomycete PM1 HRPL, which exhibits remarkable stability and activity, including thermal activation (Coll *et al.*, 1993a). After replacing the native signal sequence with the α-factor prepro-leader to regulate heterologous protein trafficking, the fusion protein was

subjected to eight rounds of laboratory evolution in combination with rational approaches. The last mutant in this process constitutes a valuable point of departure for further directed evolution experiments to tailor custom-made HRPLs with improved properties.

2.1.3. RESULTS AND DISCUSSION

2.1.3.1. Point of departure for evolution: the construction of α-PM1

Our starting point was the HRPL from basidiomycete PM1 (CECT 2971). In addition to its high redox potential (above +700 mV *vs.* NHE), PM1 laccase is highly stable in the pH interval of 3 to 9 and at high temperature (with optimal thermoactivity at 80°C) (Coll *et al.*, 1993a,b). These features are highly desirable not only for practical use, but also to perform directed evolution experiments. Bearing in mind that the accumulation of beneficial mutations over several rounds of laboratory evolution generally destabilizes the protein scaffold, the better the stability of the starting enzyme the greater the likelihood of achieving the desired improvements without jeopardizing the proteins function (Bloom and Arnold, 2009). In the first place, the PM1 cDNA with the native signal leader was cloned into the corresponding shuttle vector, although no detectable levels of functional expression were found in *S. cerevisiae*. To enhance its expression to values that can be detected in the screening assays, the PM1 native signal sequence was replaced by different leader peptides commonly used to express heterologous proteins in yeast (see **Supplemental Experimental Procedures**, p. 72). The best result was obtained with the α-PM1 construction (**Figure 2.1.S1.**, p. 81) constituted by the prepro-leader of the yeast α-factor mating pheromone (Shuster, 1991) coupled to the mature PM1, which gave rise to very low but detectable levels of expression (~35 mU/L). The coefficients of variance (CV) for the screening assays were adjusted throughout the evolution process (achieving CVs below 11% from the third cycle of evolution onward) and the microfermentation conditions were optimized (copper uptake, medium composition, oxygen availability, and temperature) (see **Supplemental Experimental Procedures**, p. 75).

2.1.3.2. Laboratory evolution of α-PM1

A directed evolution strategy was elaborated according to the following rules: (1) to better fulfill the requirements of the host´s secretory pathway for functional laccase expression, the whole fusion gene was targeted for random mutagenesis and/or recombination, thereby jointly evolving both the α-factor prepro-leader and the foreign laccase gene to adjust both elements for successful exportation by *S. cerevisiae;* (2) to ensure the improvement in activity was not substrate dependent, screening assays based on the oxidation of phenolic (DMP) and non-phenolic (ABTS) compounds were validated and employed during the molecular evolution; (3)

to guarantee the overall thermostability of the ultimate mutant, the drops in stability produced by the accumulation of mutations during evolution were detected and recovered by rational approaches coupled with the screening of mutant libraries for thermostability; and (4) mutations representing significant improvements during the first rounds of *in vitro* evolution but that were not eventually selected after recombination and screening, were recovered individually, analyzed and introduced into the last variants by site-directed mutagenesis. In addition, new mutations identified in a parallel directed evolution experiment that we performed with other highly related HRPL (the laccase from *Pycnoporus cinnabarinus* with 77% identity to the PM1 laccase) were individually tested in the α-PM1 mutants.

The generation of diversity was emulated by taking advantage of the eukaryotic machinery of *S. cerevisiae*. From our previous experience, the *in vivo* recombination of mutagenic libraries can confer significant advantages when compared with *in vitro* recombination protocols, particularly in terms of cloning simplicity and the quality of the libraries generated (Alcalde, 2010). The high level of homologous recombination of *S. cerevisiae* allowed us to repair the mutagenized products within the linear vector *in vivo* by engineering specifically overlapping regions without altering the open reading frame. Mutagenic libraries were recombined by *in vivo* DNA shuffling and/or by *in vivo* assembly of mutant libraries with different mutational spectra (IvAM) (Okkels, 2004; Zumárraga *et al.*, 2008a). To enhance the number of crossover events among the inserts without compromising the transformation efficiency, several overlapping regions with lower homology to the linear vector were tested. The mutational rate was tuned so that ~1-3 amino acid changes per fusion protein were introduced on average for each cycle of evolution (Tracewell and Arnold, 2009).

Over 50,000 clones were explored in eight rounds of directed evolution and site directed mutagenesis, culminating in the selection of the ultimate variant, the OB-1 mutant, with a 34,000-fold total activity improvement (TAI) over α-PM1 (the TAI value represents the joint enhancement of specific activity and secretion; **Figure 2.1.1.**). Regardless of the enzyme and the attribute subjected to *in vitro* evolution, it is rare to achieve such a strong improvement. It seems plausible that by jointly evolving the α-factor prepro-leader along with the mature PM1 for secretion in yeast, a synergic effect between both polypeptides has occurred, eventually improving the exportation of α-PM1 in the eukaryotic host. During the artificial evolution pathway (**Figure 2.1.1.**), 26 mutants with improvements ranging from 1.3- to 12-fold against the best corresponding parental type were characterized in each cycle and further recombined. In general terms, up to 28 different positions were mutated (nine of them synonymous mutations) throughout the α-PM1 fusion gene (**Table 2.1.S1.**, p. 86). From these, nine mutations were found in the α-factor prepro-leader and the remaining 19 in the laccase gene.

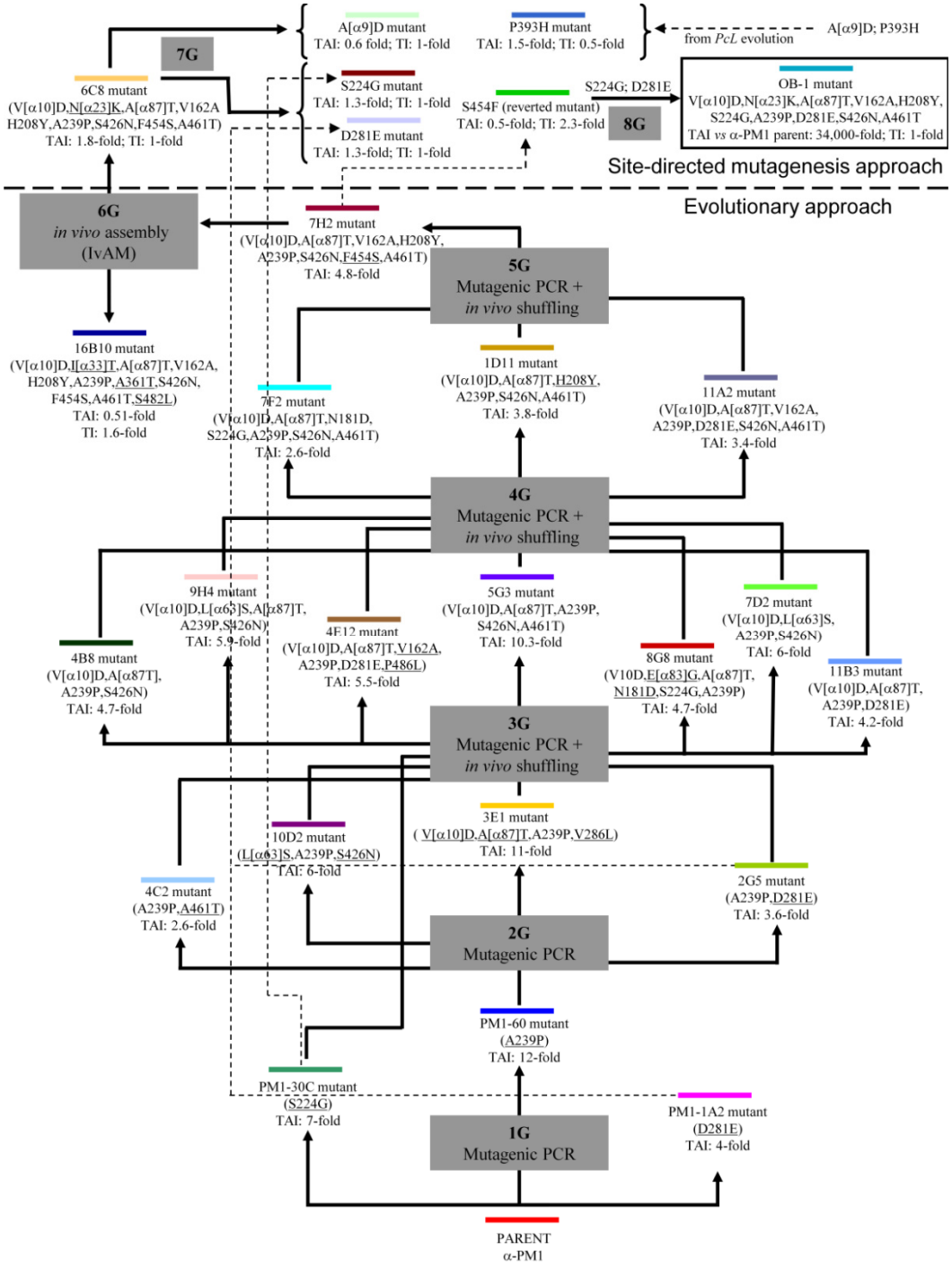

Figure 2.1.1. Artificial evolution pathway for α-PM1 laccase. A combination of evolutionary approaches (random mutagenesis, *in vivo* DNA shuffling, and IvAM) and rational strategies (site-directed mutagenesis for both beneficial mutational recovery and mutational exchange with related evolved HRPL) was used during the evolution of the α-PM1 fusion gene. The new point mutations are underlined. The point of

departure for mutations incorporated in the seventh round by site-directed mutagenesis are indicated by the dashed arrows. TAI (total activity improvement): this value indicates the improvement in laccase activity detected in *S. cerevisiae* microcultures for each mutant selected when compared with the best parental type of the corresponding generation. Measurements were made in quintuplet from supernatants of independent cultures grown in 96-well plates, using 3 mM ABTS as the substrate (see the **Supplemental Experimental Procedures**, p. 75, for further details). The OB-1 mutant had an accumulated TAI value of 34,000-fold that of the original parental α-PM1 type. The breakdown of the TAI into specific activity and level of expression is represented in **Table 2.1.1.**, p. 62. TI: thermostability improvement versus parental type of the corresponding generation. PcL: Laccase from *Pycnoporus cinnabarinus* (see section **Mutational exchange with a related evolved HRPL**, p. 60; **Figures 2.1.S2.** and **S3**, pp. 82 and 83, respectively; and **Table 2.1.S1.**, p. 86).

The first two rounds of evolution involved error-prone PCR at different mutational rates and with DNA polymerases that had distinct mutational bias (**Figure 2.1.1.** and **Table 2.1.S1.**, p. 86). To speed up the evolution process, from the second round onward, a protocol was used that combined the construction of mutant libraries from each parental type by *in vivo* DNA shuffling. This strategy produced complex crossover events for each offspring along with the introduction of new point mutations (**Figure 2.1.2.**). The best variant from the fifth cycle, mutant 7H2, had ~24,300-fold improved activity over α-PM1, with a total laccase activity of 1000 U/L. The preliminary characterization of 7H2 demonstrated a strong reduction in its thermostability with a decrease in the T_{50} of ~5°C with respect to its corresponding parental, 1D11 and 11A2 mutants (from 73°C to 68°C, **Figure 2.1.3B**), which was coupled to a significant drop during its long-term storage (loosing ~30% of its activity after 14 days at 4°C). The accumulation of beneficial but destabilizing mutations during evolution is a well-known phenomenon (Bloom *et al.*, 2006; Bloom and Arnold, 2009; García-Ruiz *et al.*, 2010 and references therein). To overcome this shortcoming and to recover the stability while tolerating the introduction of a new set of beneficial mutations, a thermostability screening assay was incorporated in the sixth round on the basis of the determination of the T_{50} (defined as the temperature at which the enzyme retains 50% of its activity after a 10 min incubation) (Bommarius *et al.*, 2006; García-Ruiz *et al.*, 2010). On this occasion, the library was constructed by IvAM, mixing different mutational profiles and biases (Zumárraga *et al.*, 2008a). The best thermostable variant, 16B10, recovered part of its thermostability with an improvement in its T_{50} of 3°C (**Figure 2.1.3B**), albeit at expense of its activity, which halved from 1000 to 510 U/L (**Figure 2.1.1.** and **Table 2.1.S1.**, p. 86). On the other hand, the variant with the best activity in this cycle, 6C8, still improved the total activity values to ~2000 U/L while maintaining similar stability to 7H2. At this point, we reached a crossroads where we could either continue evolving thermostability from 16B10 while endangering its activity, or use the 6C8 mutant as the parent and try to resolve the stability issue "rationally". Rather than facing the well-known trade-off that usually arises between activity and stability for many single point mutations (Romero and Arnold, 2009), we

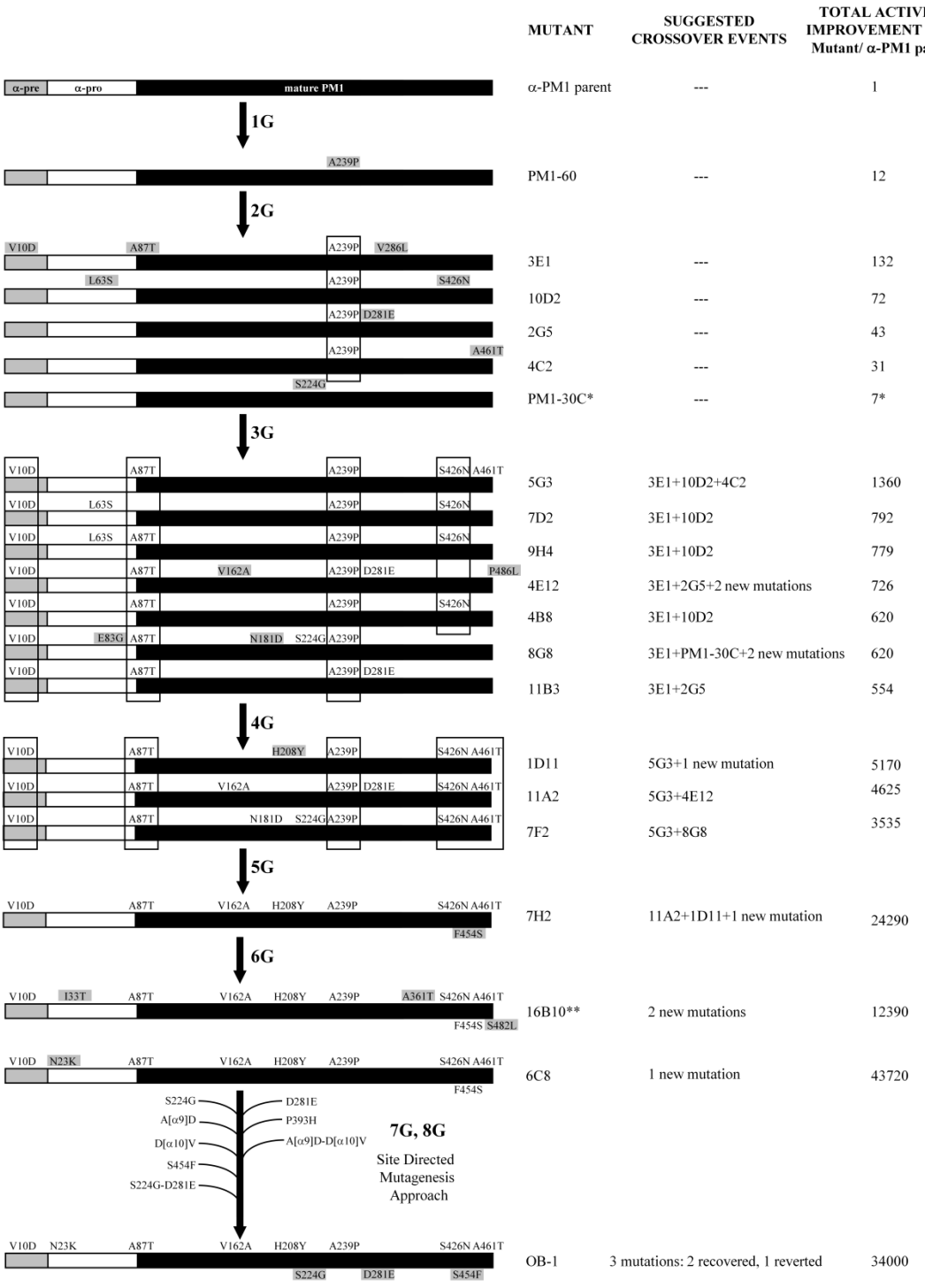

Figure 2.1.2. Suggested crossovers events during the directed evolution of α-PM1 laccase. The α-factor pre-leader is represented in grey, the α-factor pro-leader in white, and the mature PM1 in black. New point mutations are highlighted in grey. With single asterisk is highlighted PM1-30C, the second best

mutant from first generation which was recovered for backcrossing in the third round. With double asterisk is highlighted 16B10 mutant, the best thermostability mutant of the sixth round. TAI values are in reference to the original parental α-PM1 expressed in *S. cerevisiae*. See also **Tables 2.1.S1** and **S2** (pp. 86 and 87, respectively).

went back to analyze the unstable 7H2. This mutant came from a crossover event between 1D11 and 11A2, which allowed us to join the V(α10)D, A(α87)T and V162A mutations in the 11A2 mutant with H208Y, A239P, S426N and A461T in the 1D11 mutant (**Figure 2.1.2.** and **Table 2.1.S1.**, p. 86). Moreover, 7H2 incorporated one synonymous mutation plus mutation F454S, generated by random mutagenesis in combination with *in vivo* DNA shuffling. We mapped this mutation in a 3D-structure model based on the crystal structure of the *Trametes trogii* laccase (97% identity, Matera *et al.*, 2008). Phe454 is located in an alpha helix close to the T1 Cu site, the place where the reducing substrate binds. In fact, Phe454 lies next to one of the coordinating ligands of the T1 Cu, the His455 which seems to be involved in binding the reducing substrate enabling the entrance of electrons to the T1 Cu (Bertrand *et al.*, 2002; Matera *et al.*, 2008). Inspection of the protein model suggests that the F454S mutation allows an additional hydrogen bond to form with Ala161 (**Figure 2.1.3A**). It seems plausible that this new hydrogen bond might provoke the movement of the helicoidal segment where His455 is found, amplifying the distance between the coordinating ligand and the T1 Cu. This effect would increase the catalytic rate, but it would dramatically affect the stability of the variant. Therefore, we decided to reverse the F454S mutation in the 6C8 mutant by site-directed mutagenesis. The resulting S454F reverted variant completely recovered its stability with a T_{50} identical to the parents from the fourth round and beyond (**Figure 2.1.3C**). Notably, while the reverted mutant decreased its activity by half (900 U/L), it displayed a similar activity to that reported for 7H2 and it was again very thermostable. The synergistic effect of recombining 1D11 and 11A2, along with the new beneficial mutation that appeared in 6C8 (N[α23]K) overcame the loss of the beneficial but destabilizing F454S mutation in terms of the overall improvement in activity.

2.1.3.3. Recovery of beneficial mutations

During the engineering of the HRPL in *S. cerevisiae*, some of the mutations discovered in the early stages of evolution that affected activity were eventually discarded by the *S. cerevisiae* recombination apparatus, despite their potential benefits. In the eukaryotic host, the likelihood of a crossover event occurring between two mutations is directly proportional to the number of nucleotides separating those mutations. Thus, it is not surprising that some beneficial mutations were not eventually incorporated in a scaffold that already contained the mutation A239P, such as S224G or D281E (**Figure 2.1.2.**). We thought that it would be interesting to rescue these mutations and test them individually in the 6C8 variant. Mutation S224G was the only mutation

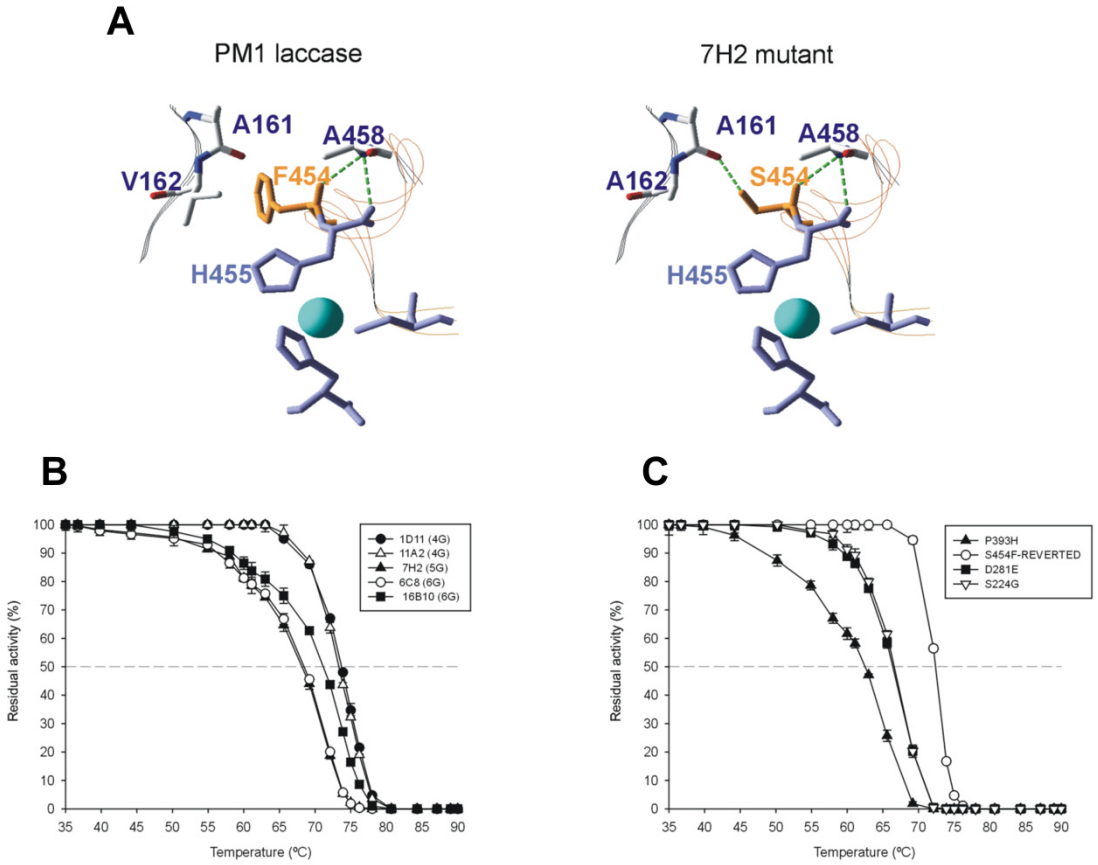

Figure 2.1.3. Rational approach to thermostability. (**A**) Detail of a 3D laccase model showing the location of residue 454 in the vicinity of the T1 Cu site for the parental PM1 and 7H2 mutant. S454 establishes two H-bonds with A458 and after mutation, an additional bond with A161 is formed. Blue sphere, T1 copper. Thermostability of evolved HRPLs: (**B**) T_{50} of mutants from fourth, fifth and sixth generations. Black circles, 1D11 mutant (4th G); white triangles, 11A2 mutant (4th G); black triangles, 7H2 mutant (5th G); white circles, 6C8 mutant (6th G); black squares, 16B10 mutant (6th G). (**C**) T_{50} of mutants constructed by site-directed mutagenesis using the 6C8 mutant as the template. Black triangles, P393H mutant; black squares, D281E mutant; white inverted triangle, S224G mutant; white circles, S454F reverted mutant. Each point, including the standard deviation, is for three independent experiments.

harbored by the PM1-30C mutant (from the first generation) producing a seven-fold improvement in activity (**Figure 2.1.1.**) This variant was again used as a parent in the third round for backcrossing, and S224G was incorporated into the offspring. Unfortunately, as a result of the aforementioned crossover between 1D11 and 11A2 in the fifth round, S224G was finally lost. Likewise, the D281E mutation appeared separately in different points in evolution (in the PM1-1A2 and 2G5 mutants from first and second round of evolution with improvements of 4- and 3.6-fold, respectively). Once again, the recombination event between 1D11 and 11A2 ruled out D281E from the laccase gene. Both these mutations were studied individually by site-

directed mutagenesis in the seventh round and, in both cases, the total activity was enhanced without compromising thermostability (**Figures 2.1.1.** and **2.1.3C**). Accordingly, S224G and D281E were both incorporated into the reverted variant in the last cycle giving rise to the OB-1 mutant.

2.1.3.4. Mutational exchange with a related evolved HRPL

In a parallel effort, we were also involved in the directed evolution of another HRPL from *Pycnoporus cinnabarinus* (Camarero *et al.*, 2010), which shares 77% identity with the PM1 laccase. Mimicking the same approach as that followed with the PM1 laccase, the native signal sequence of *P. cinnabarinus* laccase was also replaced by the α-factor prepro-leader, and the corresponding fusion protein was subjected to several rounds of random mutagenesis and recombination (**Figure 2.1.S2**, p. 82). One of the best mutations found during the evolution of *P. cinnabarinus laccase* (P394H) lies in the vicinity of the T1 Cu. The replacement of Pro by His at position 394 promotes a new hydrogen bond with Asn208 that is close to His395, one of the ligands of T1 Cu (Camarero *et al.*, 2010). The sequence alignment of PM1 with *P. cinnabarinus* laccase indicates that P394 belongs to a highly conserved region in HRPLs (**Figure 2.1.S3.**, p. 83). Accordingly, the P394H mutation (P393H using the PM1 numbering) was introduced into 6C8 during the seventh cycle improving its activity to ~3000 U/L but with a significant fall in thermostability (the T_{50} dropped 2°C, **Figure 2.1.3C**). We truly do not know whether the loss in thermostability upon mutation was a common side-effect in both laccases or if it only occurred in the evolved 6C8. In fact, an analysis of thermostability could not be performed in the *P. cinnabarinus* laccase because P394H was introduced in the first round of evolution, when the expression levels were virtually undetectable (**Figure 2.1.S2.**, p. 82). Taking into account that our main goal was to tailor a highly active and stable HRPL, and despite the improvement in activity, P393H was not eventually incorporated into the last variant, the OB-1 mutant.

2.1.3.5. Directed evolution of the α-factor prepro-leader

The α-factor prepro-leader encodes an 83 amino acid polypeptide of which the first 19 residues constitute the pre-leader that direct the nascent polypeptide to the endoplasmic reticulum (ER). Upon extrusion into the ER, the pre-leader is cleaved by a signal peptidase leaving a proprotein. At this point, N-linked glycosylation of three asparagine residues in the pro-leader facilitates ER to Golgi transit, and in the Golgi compartment, the proleader may act as chaperone until it is processed by the *KEX1*, *KEX2* and *STE13* proteases (Shuster, 1991; Romanos *et al.*, 1992). In addition, the pro-leader is thought to be involved in vacuolar targeting, which is detrimental to heterologous secretion (Rakestraw *et al.*, 2009). Up to nine mutations (3 synonymous) were introduced into the α-factor prepro-leader during α-PM1 laboratory

evolution although only V[α10]D, N[α23]K, A[α87]T and the synonymous G[α62]G were conserved in the ultimate OB-1 variant. V[α10]D was located in the hydrophobic domain of the pre-leader and, interestingly, one of the best mutations found during the evolution of the *P. cinnabarinus* laccase fused with the α-factor prepro-leader was also discovered in this domain (mutation A[α9]D, **Figure 2.1.S2.**, p. 82). It has been reported that mutations in the pre-region can affect ER targeting and secretion (Romanos *et al.*, 1992). The role of these two consecutive mutations in laccase trafficking was tested in single, double and reverted mutants constructed in the 6C8 template during the seventh round (**Table 2.1.S2.**, p. 87). The experimental data indicated that individually, A[α9]D and V[α10]D exerted a 2.2-fold improvement in secretion but when they were combined, the hydrophobicity of this domain was drastically diminished. It is well known that most alterations that reduce the translocation efficiency are related with an overall decrease in the hydrophobicity of this domain (Romanos *et al.*, 1992). We assume that the individual changes of charged carboxylic residues at positions 9 or 10 of the α-factor pre-leader may positively affect the interaction between the signal peptide and the signal recognition particle involved in orienting and inserting the polypeptide laccase chain into the membrane bilayer of the ER (Boyd and Beckwith, 1990; Nothwehr and Gordon, 1990). The mutation N[α23]K was situated at the first of the three sites for Asn-linked glycosylation in the proleader (Romanos *et al.*, 1992). Although not absolutely essential for secretion, such glycosylation might facilitate ER to Golgi transport (Rakestraw *et al.*, 2009). However, our results did not support this hypothesis since removal of the glycosylation site in the sixth round (giving rise to 6C8) improved secretion. Finally, the A[α87]T mutation was found in the processing site of *STE13*, a dipeptidyl aminopeptidase that removes the spacer residues $(Glu/Asp\text{-}Ala)_2$ at the amino terminus between the α-factor proleader and the mature PM1. After mutation, the spacer residues provide an even more hydrophilic environment at the adjacent *KEX2* cleavage site (Lys-Arg), which might affect the secretion of mature laccase (Brake, 1990).

2.1.3.6. Characterization of the OB-1 mutant

The last mutant obtained, the OB-1 variant, was purified to homogeneity and characterized biochemically (**Table 2.1.1.**; **Figures 2.1.4.** and **2.1.S4.**, p. 84). The specific activity of the OB-1 mutant was 400 U/mg and it was secreted with levels of ~8 mg/L. The molecular mass of OB-1 was estimated by MALDI-TOF mass spectrometry as 60,310 Da, 3,690 Da below the molecular weight reported for the native laccase expressed by the basidiomycete PM1 (Coll *et al.*, 1993a) (**Figure 2.1.S4.**). The molecular mass determined from the amino acid composition of OB-1 was 53,284 Da and the contribution of glycosylation deduced from the deglycosylation pattern was ~10% (**Figure 2.1.S4.**). Our results in *S. cerevisiae* from the directed evolution of laccases from *P. cinnabarinus* (PcL) (Camarero *et al.*, 2010) and *M. thermophila* (MtL) (Bulter *et al.*, 2003a;

Table 2.1.1. Comparison of the kinetic parameters of PM1 mutants expressed in *S. cerevisiae* and of the highly related *Trametes* sp. C30 and *Trametes trogii* laccases.

HRPL	Generation	Substrate	K_m (mM)	k_{cat} (s^{-1})	k_{cat}/K_m ($mM^{-1}s^{-1}$)	TAI[c] (fold increase)		Improvement *vs.* 3E1 mutant[d]	
						vs. α-PM1	*vs.* 3E1 mutant	k_{cat}	Expression
3E1 mutant	2	ABTS	0.009 ± 0.002	15.7 ± 0.8	1744	132	1	1	1
		DMP	0.068 ± 0.005	7.7 ± 0.1	113				
		Guaiacol	0.95 ± 0.07	3.31 ± 0.05	3.5				
5G3 mutant	3	ABTS	0.020 ± 0.006	54 ± 5	2700	1360	10	3.4	3
		DMP	0.087 ± 0.009	20.6 ± 0.5	237				
		Guaiacol	2.09 ± 0.08	8.43 ± 0.08	4.0				
1D11 mutant	4	ABTS	0.013 ± 0.002	105 ± 4	8077	5170	39	6.7	6
		DMP	0.106 ± 0.006	40.9 ± 0.6	386				
		Guaiacol	2.10 ± 0.08	18.5 ± 0.2	8.8				
OB-1 mutant	8	ABTS	0.0063 ± 0.0009	200 ± 7	31746	34000	255	12.7	20
		DMP	0.14 ± 0.02	134 ± 5	957				
		Guaiacol	4.6 ± 0.1	90 ± 1	20				
T. trogii LccI[a]	---	ABTS	0.0083 ± 0.0003	98	11807	—	—	—	—
		DMP	0.195 ± 0.0001	51	262				
		Guaiacol	3.073 ± 0.088	6.5	2.1				
T. sp. C30 Lac1[b]	---	ABTS	0.0107	56	5234	—	—	—	—
		DMP	n.r.	n.r.	n.r.				
		Guaiacol	n.r.	n.r.	n.r.				

[a]Data from Colao *et al.* 2006. [b]Data from Klonowska *et al.,* 2002. [3]TAI: total activity improvement with respect to the α-PM1 parental type and the 3E1 mutant from the second generation. The TAI was measured using 3 mM ABTS as the substrate in supernatants of cultures grown in 96-well plates. The numbers are the averages of five measurements. [d]Dissection of the TAI for activity (k_{cat}) and expression in reference to the 3E1 mutant (second generation). The improvement in expression is defined as the ratio of the total increase in activity and k_{cat} with ABTS as the substrate. n.r.: not reported.

Zumárraga *et al.*, 2007a) were quite different, and unlike the OB-1 variant, the PcL and MtL mutants were hyperglycosylated with sugar moieties contributing around 50% of their molecular weight. Because complex outer chain carbohydrate addition occurs in the Golgi apparatus, incorporating mannose moieties, hyperglycosylation can be considered to be a consequence of longer residence times in this cellular compartment. We assumed that the evolved mutant is readily secreted by *S. cerevisiae* while other heterologous laccases experience serious difficulties in exiting the Golgi. The pH profiles of relative activities versus phenolic and non-phenolic compounds were not significantly altered during evolution, with OB-1 and the former evolved variants displaying similar optimal pH values (~4.0 and 3.0 for DMP and ABTS, respectively; **Figures 2.1.4A** and **B**). Unfortunately, the very low expression levels of the parental α-PM1 (0.035 ABTS-U/L) did not enable us to purify it in sufficient quantity to be able to characterize it kinetically and compare it with the evolved mutants. However, the total activity improvements (TAI) obtained in the evolution process were determined as the improvement in specific activity and expression. To this end, several variants from the second round of evolution onward were produced and characterized kinetically using classic laccase substrates (**Table 2.1.1.**). The improvement in activity was not dependent on the substrate, since the catalytic efficiencies were enhanced in each round of evolution regardless of the substrate tested. The last mutant, OB-1, displayed a 13-fold increase in k_{cat} together with 20-fold increase in functional expression when compared to the best variant from the second generation, the 3E1 mutant, which correspondingly had a 132-fold TAI when compared with the original parental type α-PM1. Similarly, the catalytic efficiency of OB-1 was up to six-fold better than that reported for the highly related *Trametes* sp. C30 and *Trametes trogii* laccases, which are 99% and 97% identical to the PM1 laccase, respectively (Klonowska *et al.*, 2002; Colao *et al.*, 2006). Notably, after eight rounds of evolution the thermostability of OB-1 mutant was 100% conserved, with a T_{50} value of ~73°C. PM1 laccase belongs to the group of HRPLs isolated from the western Mediterranean area, together with *T. trogii* laccase, *Trametes* sp. C30 laccase or *Coriolopsis gallica* laccase. All these HRPLs share a high degree of sequence identity (above 97%) and similar biochemical features, including in all cases strong thermostability (Colao *et al.*, 2003; Hildén *et al.*, 2009). To additionally evaluate the thermostability of our evolved laccase, it was compared with a battery of HRPLs from different sources (**Figure 2.1.4C**). The T_{50} of OB-1 mutant was higher than that of HRPLs from *Trametes hirsuta, P. cinnabarinus,* or *Pleurotus ostreatus* and similar to the T_{50} of laccases from *C. gallica* and *T. versicolor*. The stability of OB-1 was further evaluated in the presence of high concentrations of organic cosolvents with different polarities and chemical nature (**Figure 2.1.4D**). As expected from a highly thermostable enzyme (Zumárraga *et al.*, 2007a), the evolved PM1 laccase was quite tolerant to the presence of cosolvents (retaining 30%-90% of its activity after 4 h at solvent concentrations as high as 50% (v/v)). The stability of the evolved laccase at different pHs was also evaluated, keeping ~90% of its activity in the pH range of 3.0-9.0 after 4 h of incubation (**Figure 2.1.4E**).

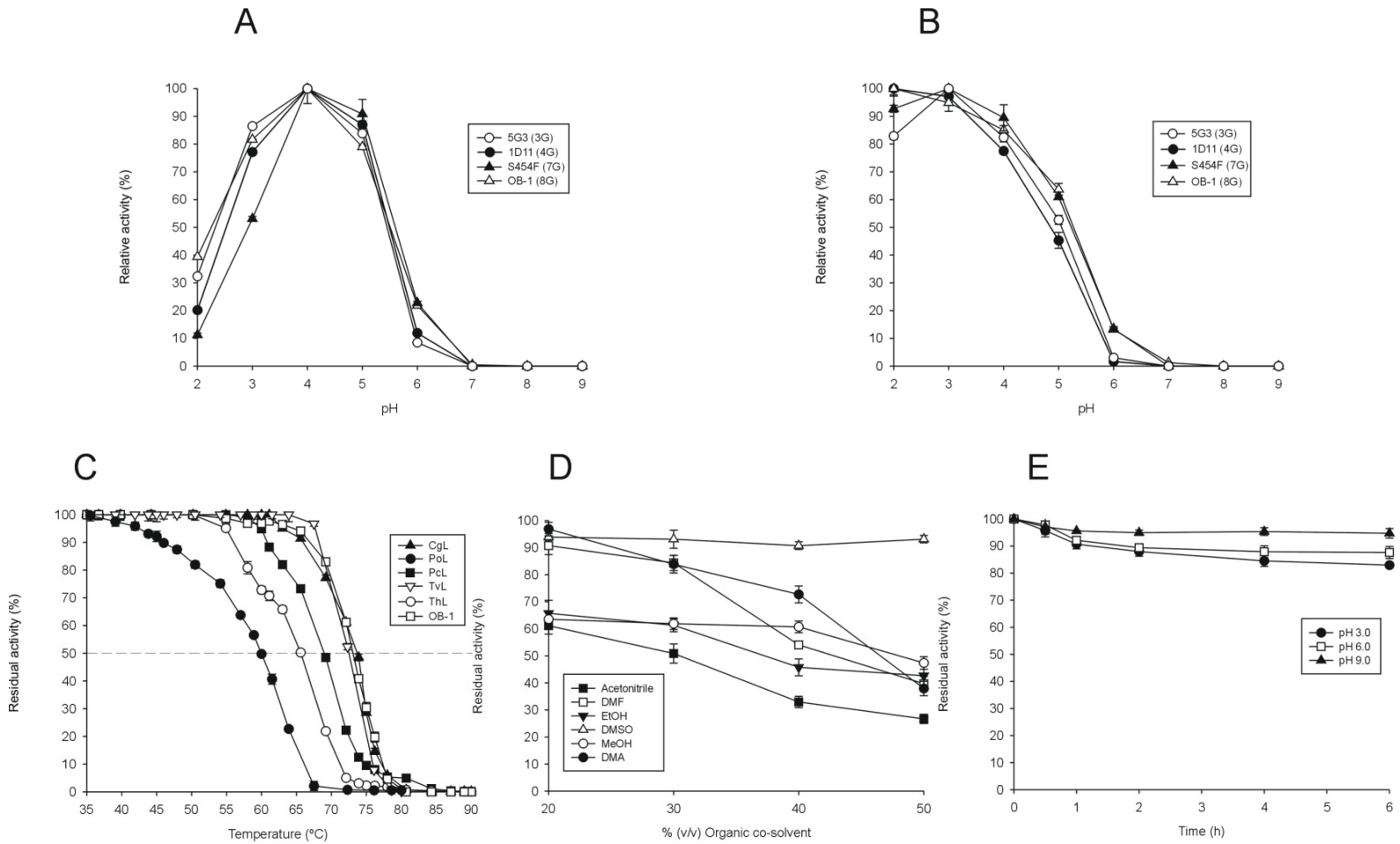

Figure 2.1.4. Biochemical characterization of OB-1 mutant. (**A** and **B**) pH activity profiles of mutant laccases. White circles, 5G3 mutant (3th G); black circles, 1D11 mutant (4th G); black triangles, S454F mutant (7th G); white triangles, OB-1 mutant (8th G). Activities were measured in 100 mM Britton and Robinson buffer at different pHs with 3 mM DMP (**A**) or ABTS (**B**) as the substrates. Laccase activity was normalized to the optimum activity value and each point, including the standard deviation, in three independent experiments. (**C**) T_{50} of the OB-1 mutant and other related HRPLs. Black triangle, *Coriolopsis gallica* laccase; black circles, *Pleurotus ostreatus* laccase; black

squares, *Pycnoporus cinnabarinus* laccase; white inverted triangles, *Trametes versicolor* laccase; white circles, *Trametes hirsuta* laccase; white squares, the OB-1 mutant. Each point, including the standard deviation, is from three independent experiments. (**D**) Stability of OB-1 in the presence of increasing concentrations (v/v) of several organic co-solvents. The experiments were performed in screw-cap vials containing the OB-1 variant in a co-solvent/100 mM Britton and Robison buffer (pH 6.0) mixture. After 4 h, aliquots were removed and assayed for activity with 3 mM ABTS in 100 mM sodium acetate buffer (pH 4.0). Black squares, acetonitrile; black inverted triangles, ethanol; white squares, dimethyl formamide; white circles; methanol; black circles, dimethyl acetamide; white triangles, dimethyl sulfoxide. Residual activity was expressed as the percentage of the original activity at the corresponding concentration of organic cosolvent. Each point, including the standard deviation, is from three independent experiments. (**E**) The pH stability of the OB-1 mutant at pH 3.0, 6.0 and 9.0. Enzyme samples were incubated in 10 mM Britton and Robinson buffer at different pH values, and residual activity was measured in 3 mM ABTS in 100 mM sodium acetate buffer (pH 4.0). Black circles, pH 3.0; white squares, pH 6.0; black triangles, pH 9.0. Each point, including the standard deviation, comes from three independent experiments. See also **Figure 2.1.S4.**, p. 84.

The ultimate OB-1 variant accumulated 15 mutations: five in the α-factor prepro-leader (two silent) and ten in the mature protein (three silent). Three of the five synonymous mutations favored codon usage (**Table 2.1.S1.**, p. 86), which may be a factor that potentially favors the yield of secretion by affecting the elongation rate (Romanos *et al.*, 1992). In general terms, strongly expressed genes show a bias towards a specific subset of codons (Dix and Thompson, 1989) and, thus, codon optimization may be important for the expression of laccases in yeast. Hence, the protein abundance may be modulated by the differential usage of synonymous codons, which is closed related to the levels of the corresponding tRNAs in the eukaryotic apparatus. Very recently, it was reported that translation efficiency can be also regulated by the folding energy of the mRNA transcript, which may affect ribosome binding and the translation initiation (Tuller *et al.*, 2010).

Beneficial mutations in the mature laccase basically mapped to rather accessible residues, some located far from the catalytic coppers whereas others were in the vicinity of the catalytic sites (**Figure 2.1.5.** and **Table 2.1.2.**, and **Figure 2.1.S5.**, p. 85, summarize the features of these changes in the laccase structure). In particular, the V162A, S426N and A461T mutation are in the T1 Cu neighborhood. Val162 is one of the hydrophobic residues in the loop that delimits the cavity of the substrate pocket at the T1 site (Bertrand *et al.*, 2002). The change from Val to Ala at this position represents the substitution of a hydrophobic residue by another somewhat smaller hydrophobic one, which may favor substrate binding (**Figures 2.1.5A** and **B**). Ser426 is H-bonded to Gly428 but after mutation the H-bond no longer exists. The inspection of the protein model suggests that the resulting Asn426 may establish a new H-bond with the adjacent Thr427 residue. In turn, the latter is double bonded to the T1 Cu ligand His394, such that this change might affect the position of His394 relative to the T1 site (**Figures 2.1.5A** and **B**). Ala461 is

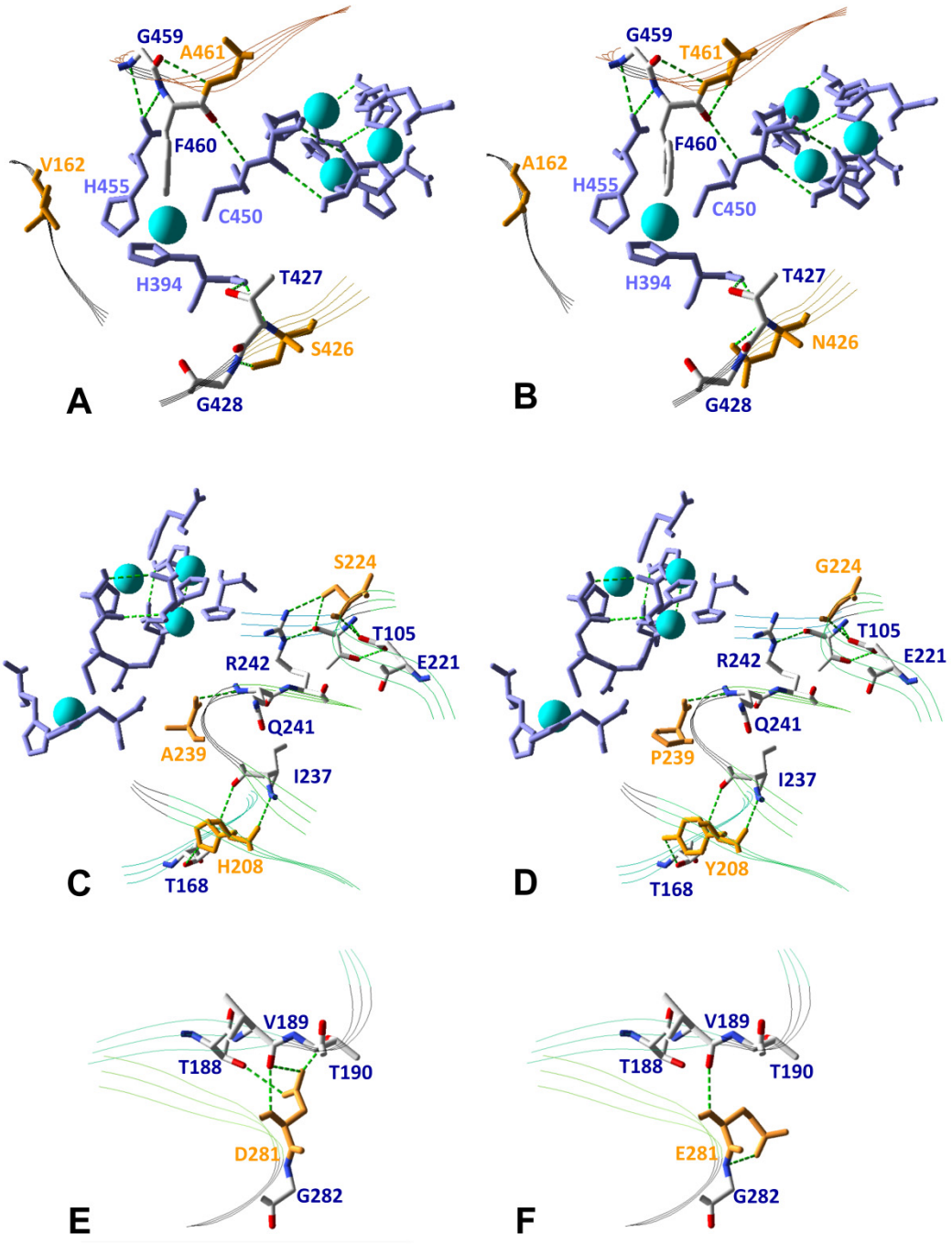

Figure 2.1.5. Mutations in evolved laccase. Details of the seven mutations (in orange) in the OB-1 variant (**B**, **D** and **F**) compared with the corresponding residues in the native PM1 laccase (**A**, **C** and **E**). Ligands of T1 Cu and the T2/T3 trinuclear Cu cluster are shown in light blue. Blue spheres represent Cu atoms. H-bonds involving the mutated residues (before and after mutation) are shown as green dashes. See also **Figure 2.1.S5.**, p. 85.

adjacent to Phe460 (the position for the fourth axial ligand in plant and bacterial laccases) (Alcalde, 2007), the latter establishing hydrogen bonds with the T1 Cu ligands, His455 and Cys450. TheA461T mutation seems to render a new H-bond with Phe460, which might change the local geometry of the T1 site (Xu *et al.*, 1998) (**Figures 2.1.5A** and **B**).

Most of the remaining beneficial mutations (H208Y, S224G, A239P and D281E) were mapped far from the catalytic coppers, appearing in coils or secondary motifs whose role in the laccase function remains uncertain (**Table 2.1.2.** and **Figures 2.1.5C-F**). It is highly unlikely that such mutations could have been anticipated by rational design; however, the use of directed evolution has unmasked a functional relevance to these previously unknown regions of laccases. For instance, Asp281 is located in a distal loop of the D2 domain that is almost completely exposed at the protein surface (at ~40 Å from the T1 Cu site). Our protein model suggests that the replacement of Asp by Glu at position 281 breaks two H-bonds with Thr188 and Thr190 in a neighbouring loop, and may produce a new H-bond with Gly282 of the same motif, which might increase the flexibility of this zone (**Figures 2.1.5E** and **F**). That the above mentioned mutations improve folding and maturation in *S. cerevisiae* cannot be ruled out, in addition to their possible contribution to the final robustness of the protein.

2.1.4. SIGNIFICANCE

HRPLs are a clear example of generalist biocatalysts that make a virtue of their substrate promiscuity. Fuelled by molecular oxygen, they transform hundreds of substrates of different nature and complexity, ranging from xenobiotic (*e.g.*, pesticides, industrial dyes and PAHs) to biopolymers (lignin and starch). Hence, HRPLs have potential applications in bioremediation, finishing of textiles, pulp-paper biobleaching, biofuels, organic synthesis and many other processes (Bragd *et al.*, 2004; Xu, 2005; Kunamneni *et al.*, 2008a; Widsten and Kandelbauer, 2008). In addition, HRPLs are among the few enzymes capable of accepting electrons in a direct manner from a cathodic compartment, thus being essential for bioelectrochemists in the engineering of nanobiodevices and generating special interest for the engineering of 3D-bionanosensors and biofuel cells (Shleev *et al.*, 2005a). Unfortunately, their practical design by directed evolution has hitherto been hampered by the lack of appropriate approaches to circumvent the complex problems of their functional expression (Roodveldt *et al.*, 2005). Indeed, there are only a few preliminary studies along these lines because of their poor exocytosis by yeast (Festa *et al.*, 2008; Cusano *et al.*, 2009; Miele *et al.*, 2010b). Our tailor-made HRPL is readily exportable in soluble, active and stable forms, opening a new array of possibilities for further protein engineering. The meticulous experimental design employed, involving directed evolution and site-directed mutagenesis, has been crucial to tailor a highly active and thermostable biocatalyst that can now be adapted to face new challenges. Likewise, the joint

Table 2.1.2. Mutations in mature OB-1 variant.

Mutation	Domain	Secondary structure motif	Relative position	Distance to the T1 site (Å)	Distance to the T2/T3 cluster (Å)	Interaction by hydrogen bonds with surrounding residues[a]	
						Before mutation	After mutation
V162A	D2	Coil	Surface	9.62	21.29	—	—
H208Y	D2	Beta sheet	Near D206 (that binds phenols in Cu T1 site)	14.74	19.33	I237, T168	I237, T168
S224G	D3	Coil	Surface	21.22	9.96	T105, E221, R242	E221
A239P	D2	Coil	Surface	8.57	11.65	Q241	Q241
D281E	D2	Coil	Surface	39.95	35.33	T188, V189, T190	V189, **G282**
S426N	D3	Beta sheet	Surface. At the vicinity of Cu T1, beside T427 (bonded to H394)	8.23	16.40	G428	**T427**
A461T	D3	Beta sheet	At the vicinity of Cu T1, beside F460 (position of 4th axial ligand)	8.86	10.93	G459	G459, **F460**

[a]Underlined, interrupted bonds after mutation; in bold, new formed bonds after mutation.

evolution of a "foreign" HRPL gene with the α-factor prepro-leader provides a suitable mean to improve these capacities from undetectable levels of expression. This approach could now be translated to other related HRPLs, supporting the general idea of using the directed evolution of the α-factor prepro-leader as a common scaffold for the expression of different protein systems (Rakestraw *et al.*, 2009).

2.1.5. EXPERIMENTAL PROCEDURES

2.1.5.1. Laboratory evolution: general aspects

The original parental type α-PM1 fusion gene was constructed as described in the **Supplemental Experimental Procedures**, p. 72. For each generation, PCR fragments were cleaned, concentrated and loaded onto a low melting point preparative agarose gel, then purified using the Zymoclean Gel DNA Recovery kit (Zymo Research). PCR products were cloned under the control of the GAL1 promoter of the pJRoC30 expression shuttle vector, replacing the native gene in pJRoC30. To remove the native gene, the pJRoC30 plasmid was linearized with *Xho*I and *Bam*HI and the linear plasmid was concentrated and purified as described above for the PCR fragments.

2.1.5.2. First generation

Three independent libraries were prepared with distinct DNA polymerases and under different mutational rates. The first mutagenic library (~15,000 mutants) was constructed with the Genemorph I kit (Stratagene) adjusting the mutation rate to 1.1-3.5 mutations per kb. The second and third mutagenic libraries (~15,000 mutants each), were constructed with the Genemorph II kit (Stratagene) adjusting the mutation rate to 0-4.5 and 4.5-9 mutations per kb, respectively. Error prone-PCR was carried out on a gradient thermocycler (Mycycler, BioRad, US) using the following parameters: 95°C for 2 min (1 cycle); 94°C for 0.45 min, 53°C for 0.45 min, 74°C for 3 min (28 cycles); and 74°C for 10 min (1 cycle). The primers used for amplification were: RMLN sense (5'-CCTCTATACTTTAACGTCAAGG-3', which binds to bp 420-441 of pJRoC30-αPM1) and RMLC antisense (5'-GGGAGGGCGTGAATGTAAGC-3', which binds to bp 2288-2307 of pJRoC30-αPM1). To promote *in vivo* ligation, overhangs of 40 and 66 bp homologous to the linear vector were designed. The PCR products (400 ng) were mixed with the linearized vector (100 ng) and transformed into competent cells using the yeast transformation kit (Sigma). Transformed cells were plated in SC drop-out plates and incubated for 3 days at 30°C. Colonies containing the whole autonomously replicating vector were picked and subjected to the screening assays, as well as to additional re-screenings as described in the **Supplemental Experimental Procedures**, p. 75. From the first to the fifth round of evolution the

libraries were explored for improvements in activity and from the sixth round onward, a thermostability assay was incorporated.

2.1.5.3. Second generation

The second round was performed by mutagenic PCR construction, with Mutazyme I DNA polymerase and using the PM1-60 mutant as the parental type. The mutational rate was adjusted to 2.1-3.5 mutations per kb and the mutagenic library (~1000 mutants) was prepared as described above for the first round.

2.1.5.4. Third generation

The best variants from the second round (3E1, 10D2, 2G5 and 4C2) were submitted to *Taq*/$MnCl_2$ amplification and recombined by *in vivo* DNA shuffling (~1,000 clones). The PM1-30C mutant from the first round was also included as a parental type for backcrossing. The *Taq*/$MnCl_2$ amplifications were prepared in a final volume of 50 µL containing 90 nM RMLN, 90 nM RMLC, 0.1 ng/µL mutant template, 0.3 mM dNTPs (0.075 mM each), 3% DMSO, 1.5 mM $MgCl_2$, and 0.05 U/µL *Taq* polymerase. Different concentrations of $MnCl_2$ were tested to estimate the appropriate mutation rate before adopting 0.01 mM as the final concentration, and PCR was carried out as in the former generations. Several overlapping areas, ranging from 5 to 70 bp in size, were designed to enhance the number of crossover events without compromising the transformation efficiency. Mutated PCR products were mixed in equimolar amounts and transformed along with the linearized vector into yeast (ratio PCR products:vector, 4:1).

2.1.5.5. Fourth generation

The best variants of the third round (5G3, 7D2, 9H4, 4E12, 4B8, 8G8 and 11B3) were submitted to *Taq*/$MnCl_2$ amplification and recombined by *in vivo* DNA shuffling (~1,000 clones) as described for the third generation.

2.1.5.6. Fifth generation

The best variants of the fourth round (1D11, 11A2 and 7F2) were subjected to *Taq*/$MnCl_2$ amplification and recombined by *in vivo* DNA shuffling (~1,000 clones) as described for the fourth generation.

2.1.5.7. Sixth generation

A library of ~1,300 clones was built by *in vivo* assembly of mutant libraries constructed with different mutational spectra (IvAM) (Zumárraga *et al.*, 2008a). The 7H2 mutant was used as the parental type, and *Taq*/$MnCl_2$ and Mutazyme libraries were mixed in equimolar amounts, and transformed into competent *S. cerevisiae* cells along with the linearized vector as described above (ratio library:vector, 8:1). A thermostability screening assay was incorporated from this generation onward (see p. 76).

2.1.5.8. Site-directed mutagenesis

The seventh and eight generations were produced by site-directed mutagenesis by using *In Vivo* Overlap Extension (IVOE) (Alcalde, 2010) (details in **Supplemental Experimental Procedures**, p. 73).

2.1.5.9. High-throughput screening

Activity and thermostability screening assays were performed in solid and liquid format (in 96-well plates) as indicated the **Supplemental Experimental Procedures**, p. 75. Selected mutants were produced and purified as described in the **Supplemental Experimental Procedures**, p. 78.

2.1.6. SUPPLEMENTAL EXPERIMENTAL PROCEDURES

2.1.6.1. Reagents and enzymes

The pUEX1 vector containing the native PM1 cDNA was kindly donated by Prof. R. Santamaría (Universidad de Salamanca). The laccase from *Trametes versicolor*, the laccases from *Pycnoporus cinnabarinus* and *Trametes hirsuta*, and the laccases from *Coriolopsis gallica* and *Pleurotus ostreatus*, were kindly donated, by Novozymes (Davis, CA, USA), Prof. E. Record (University of Marseille, France), Prof. A. Yaropolov (Institute of Biochemistry, Moscow, Russia) and Prof. R. Vázquez-Duhalt (UNAM, Cuernavaca, Mexico), respectively. ABTS (2,2´-azino-bis(3-ethylbenzothiazoline-6-sulfonic acid)), DMP (2,6-dimethoxyphenol), *Taq* polymerase and the *S. cerevisiae* transformation kit were purchased from Sigma-Aldrich (Madrid, Spain). The *E. coli* XL2-Blue ultracompetent cells, and the Genemorph I and II Random mutagenesis kits were from Stratagene (La Jolla, CA, USA). The protease-deficient *S. cerevisiae* strain BJ5465 was from LGCPromochem (Barcelona, Spain). The uracil independent and ampicillin resistance shuttle vector pJRoC30 was obtained from the California Institute of

Technology (Caltech, CA, USA), while the pGAPZα vector containing α-factor prepro-leader was from Invitrogen, USA. The Zymoprep Yeast Plasmid Miniprep kit, Zymoclean Gel DNA Recovery kit, and the DNA Clean and Concentrator-5 kit were all from Zymo Research (Irvine, CA). The NucleoSpin Plasmid kit was purchased from Macherey-Nagel (Düren, Germany) and the restriction enzymes *Bam*HI and *Xho*I were from New England Biolabs (Hertfordshire, UK). All chemicals were of reagent-grade purity.

2.1.6.2. Culture media

Minimal medium contained 100 mL 6.7% sterile yeast nitrogen base, 100 mL 19.2 g/L sterile yeast synthetic drop-out medium supplement without uracil, 100 mL sterile 20% raffinose, 700 mL *sdd*H_2O and 1 mL 25 g/L chloramphenicol. YP medium contained 10 g yeast extract, 20 g peptone and *dd*H_2O to 650 mL. Expression medium contained 720 mL YP, 67 ml 1 M potassium phosphate buffer pH 6.0, 111 mL 20% galactose, 2mM $CuSO_4$, 25 g/L ethanol, 1 ml 25 g/L chloramphenicol and *dd*H_2O to 1000 mL. YPD solution contained 10 g yeast extract, 20 g peptone, 100 mL 20% sterile glucose, 1 ml 25 g/L chloramphenicol and *dd*H_2O to 1000 mL. Synthetic complete (SC) drop-out plates contained 100 mL 6.7 % sterile yeast nitrogen base, 100 mL 19.2 g/L sterile yeast synthetic drop-out medium supplement without uracil, 20 g bacto agar, 100 mL 20% sterile glucose, 1 mL 25 g/L chloramphenicol and *dd*H_2O to 1000 mL.

2.1.6.3. Construction of α-PM1

The cDNA from PM1 including the native signal leader was cloned into the pJRoC30 shuttle vector in *S. cerevisiae*. The pUEX1 vector containing the PM1 cDNA was used as a template to amplify PM1 including its 21 amino acid signal peptide. The primers used for amplification were: F3PM1 (5'-CTCTATACTTTAACGTCAAGGAGAAAAAACTATAGGATCCCCAACatggccaagttccaatctctcc-3′) and R3PM1 (5'-GACATAACTAATTACATGATGCGGCCCTCTAGATGCATGCTCGAGCtcactggtcgtcaggcgagagc3′-), the capital letters indicate the overhangs that specifically annealed *in vivo* in *S. cerevisiae* cells with pJRoC30 linearized with *Bam*HI and *Xho*I. The corresponding pJRoC30-PM1 construct did not give rise to functional expression levels in *S. cerevisiae*. Accordingly, the native signal sequence of PM1 was replaced by the signal leaders from the evolved MtLT2 (Bulter *et al.*, 2003), the glucose oxidase from *Aspergillus niger* (Frederick *et al.*, 1990) and the α-factor from *S. cerevisiae* (Brake *et al.*, 1984), only the latter giving rise to detectable levels of PM1 secretion in *S. cerevisiae* (below 35 mU/L). The α-PM1 construct was generated by amplifying the native PM1 gene excluding the signal leader with the primers PM1Eco-F (5′-gcGAATTCagcattgggccagtc-3′) and PM1-R (5′-atGGCGGCCGC**tta**ctggtcgtcaggcgagagc-3′), which included targets for *Eco*RI

and *Not*I (in capital letters) as well as the optimized stop codon (in bold and underlined) for *Pichia pastoris*. The pGAPZα vector (Invitrogen) containing the α-factor prepro-leader was linearized with *Eco*RI and *Not*I and the corresponding amplified fragment was digested with *Eco*RI and *Not*I, then cloned into the linearized pGAPZα to give rise to the pGAPZα-PM1 construct. This pGAPZα-PM1 was used to amplify the α-PM1 fusion gene with the following primers: α-F (5′-ATAGGATCCatgagatttccttcaatttttactgctgtt-3′) which included the *Bam*HI target (in capital letters) and PM1-R (5'-tcaatgtccgcgttcgcaggga-3′). The fragment obtained was digested with *Not*I. The episomal shuttle vector pJRoC30 was digested with *Bam*HI and further amplified with Klenow for blunt end cloning. Finally the plasmid was digested with *Not*I, dephosphorylated and ligated with α-PM1 to generate pJRoC30-αPM1.

Two separate PCR reactions were carried out simultaneously to amplify the two DNA fragments that overlapped at specific positions corresponding to the regions targeted for site-directed mutagenesis of the parental sequence. PCR reactions were performed in a final volume of 50 µL containing 0.25 µM of each primer, 100 ng of template, dNTPs (0.25 mM each), 3% dimethyl sulfoxide (DMSO) and 2.5 Units of Pfu-Ultra DNA polymerase. The PCR conditions were as follows: 95°C for 2 min (1 cycle); 94°C for 0.45 min, 55°C for 0.45 min, 74°C for 2 min (28 cycles); and 74°C for 10 min (1 cycle). The PCR fragments were loaded on low-melting-point preparative agarose gels and purified using the Zymoclean Gel DNA Recovery kit. The pJRoC30 plasmid was linearized with *Xho*I and *Bam*HI and the linearized vector was purified as described above for the PCR fragments. The PCR fragments (400 ng each) were mixed with the linearized vector (100 ng, 8:1 ratio PCR-product:vector) and transformed into competent yeast cells as described previously. On average, 50 individual clones were analyzed per mutation. The selected plasmids were isolated and sequenced to verify the site-directed mutagenesis.

2.1.6.4. Site-directed mutagenesis approach

The seventh and eight generations were produced by site-directed mutagenesis by using *In Vivo* Overlap Extension (IVOE) (Alcalde, 2010).

Seventh generation

The following individual mutants were constructed using the 6C8 mutant as the parental template:

S454F reverted mutant. The primers for PCR 1 were: RMLN and DEL-REV (5′-cgtgaacccagcctcaaggtgGAAgtcgatgtggcagtggagg-3′ that binds to bp 5′-2083-2125-3′ of pJRoC30-αPM1). The primers for PCR 2 were: DEL-FOR (5′-cctccactgccacatcgacTTCcaccttgaggctgggttcacg-3′ that binds to bp 5′-2083-2125-3′ of pJRoC30-αPM1) and RMLC.

S224G mutant. The primers for PCR 1 were: RMLN and 5-S315G-REV (5′-gtctggggcttgagattcacGCCgtccgcctcgatgacg-3′ that binds to bp 5′-1396-1434-3′ of pJRoC30-αPM1). The primers for PCR 2 were: 5-S315G-FOR (5′-cgtcatcgaggcggacGGCgtgaatctcaagccccagac-3′ that binds to bp 5′-1396-1434-3′ of pJRoC30-αPM1) and RMLC.

D281E mutant. The primers for PCR 1 were: RMLN and 4-D372E-REV (5′-gctcaacgggcgcagcaccTTCgtagcgaaggatggc-3′ that binds to bp 5′-1568-1604-3′ of pJRoC30-αPM1). The primers for PCR 2 were: 4-D372E-FOR (5′- gccatccttcgctacGAAggtgctgcgcccgttgagc-3′ that binds to bp 5′-1568-1604-3′ of pJRoC30-αPM1) and RMLC.

P393H mutant. The primers for PCR 1 were: RMLN and 3CP484HREV (5′-gcaagtggaaggggtgGTGgaagccgggggcggcggagg-3′ that binds to bp 5′-1899-1937-3′ of pJRoC30-αPM1). The primers for PCR 2 were: 3CP484HFOR (5′-cctccgccgcccccggcttcCACcacccttccacttgc-3′ that binds to bp 5′-1899-1937-3′ of pJRoC30-αPM1) and RMLC.

A[α9]D mutant. The primers for PCR 1 were: RMLN-2 (5′-ggtaattaatcagcgaagc-3′ that binds to bp 5′-5-24-3′of pJRoC30-α) and 1C-REVDI (5′-gaggatgctgcgaataaATCatcagtaaaaattgaagg-3′ that binds to bp 5′-479-516-3′of pJRoC30-αPM1). The primers for PCR 2 were: 1C-FORDI (5′-ccttcaatttttactgatGATttattcgcagcatcctc-3′ that binds to bp 5′-479-516-3′ of pJRoC30-αPM1) and RMLC.

A[α9]D-D[α10]V double mutant. The primers for PCR 1 were: RMLN-2 and 1C-PREALREV (5′-gaggatgctgcgaaAACATCatcagtaaaaattgaagg-3′ that binds to bp 5′-479-516-3′of pJRoC30-αPM1). The primers for PCR 2 were: 1C-PREALFOR (5′-ccttcaatttttactGATGTTttattcgcagcatcctc-3′ that binds to bp 5′-479-516-3′ of pJRoC30-αPM1) and RMLC.

D[α10]V reverted mutant. The primers for PCR 1 were: RMLN-2 and 1C-PREALDOBREV (5′-gaggatgctgcgaaAACatcatcagtaaaaattgaagg-3′ that binds to bp 5′-479-516-3′of pJRoC30-αPM1). The primers for PCR 2 were: 1C-PREALDOBFOR (5′-ccttcaatttttactgatGTTttattcgcagcatcctc-3′ that binds to bp 5′-479-516-3′ of pJRoC30-αPM1) and RMLC.

Eight generation

The OB-1 mutant was engineered by introducing S224G and D281E mutations in the S454F reverted mutant from the 7th round. The primers for PCR1 were: RMLN and 5-S315G-REV. Primers for PCR 2 were: 5-S315G-FOR and 4-D372E-REV. The primers for PCR 3 were: 4-D372E-FOR and RMLC.

All the codons submitted to site-directed mutagenesis are underlined.

2.1.6.5. High-throughput screening assays: general aspects

In the first cycles of evolution, and because of the low secretion levels, pre-screenings in solid format were combined together with subsequent screenings in liquid format with longer inductions times (up to five days). From the 3rd cycle onwards the expression was sufficiently strong as to reduce the protein induction to 24 h. It is worth noting that in the first cycles, the screening had to be performed in an end-point mode obtaining reliable responses after incubating the supernatants for 24 h in the presence of the substrates. In the last cycles, the improvements were assessed in a few seconds in kinetic mode, mainly as consequence of the higher expression/activities obtained.

Pre-screening in solid format

In the first generation, pre-screening for the expression and detection of laccase activity against ABTS was carried out in solid format on SC-drop out plates. The transformants were plated and those colonies that developed a green halo were examined in the standard liquid screen described below. The SC drop-out plates for the pre-screening were prepared as described above but also including the following additional ingredients (final concentrations): $CuSO_4$ 10μM, ABTS 200 μM, potassium phosphate buffer (pH 6.0) 60 mM, and galactose 2 g/L in place of glucose.

High-throughput screening assays for laccase activity

Individual clones were picked and cultured in 96-well plates (Sero-well, Staffordshire, UK) containing 50 μL of minimal medium per well. In each plate, column number 6 was inoculated with the parental type, and one well (H1-control) was not inoculated. Plates were sealed to prevent evaporation and incubated at 30°C, 225 rpm and 80% relative humidity in a humid shaker (Minitron-INFORS, Biogen, Spain). After 48 h, 160 μL of expression medium was added to each well and the plates were incubated for 24 h. The plates (master plates) were centrifuged (Eppendorf 5810R centrifuge, Germany) for 5 min at 3000 x g at 4°C, and 20 μL of supernatant were transferred from the master plate with the help of a robot onto two replica plates (Liquid Handler Quadra 96-320, Tomtec, Hamden, CT, USA). The first replica plate was filled with 180 μL of 100 mM sodium acetate buffer (pH 5.0) containing 3 mM ABTS and the second replica was filled with 180 μL of 100 mM sodium acetate buffer (pH 5.0) containing 3 mM DMP. The plates were stirred briefly and the absorption at 418 nm ($\varepsilon_{ABTS^{\bullet+}}$=36,000 M^{-1} cm^{-1}) and at 469 nm (ε_{DMP} = 27,500 M^{-1} cm^{-1}) was recorded in a plate reader (SpectraMax Plus 384, Molecular Devices, Sunnyvale, CA). The plates were incubated at room temperature until the color developed, and the absorption was measured again. Relative activities were calculated from the difference between the absorption after incubation and that of the initial measurement normalized against the parental type and used as reference in the corresponding plate (the reference parental types

were as follows: 1G, α-PM1; 2G, PM1-60; 3G, 3E1; 4G, 5G3; 5G, 1D11; 6G, 7H2; 7G, 6C8; 8G, S454F reverted mutant).

High-throughput screening assays for thermostability

From the 6th generation onwards a thermostability assay was incorporated according to (García-Ruiz *et al.*, 2010) with minor modifications. 20 μL of supernatant were transferred from the master plate with the help of the robot onto the replica plate. Subsequently, 180 μL of stability buffer (10 mM Britton and Robinson buffer pH 6.0) were added to each replica they were stirred briefly. The replica plate was duplicated with the help of the robot by transferring 50 μL of mixture to a thermocycler plate (Multiply PCR plate without skirt, neutral, Sarstedt, Germany) and 20 μL to the initial activity plate. Thermocycler plates were sealed with thermoresistant film (Deltalab, Spain) and incubated at the corresponding temperature using a thermocycler (MyCycler, Biorad, USA). The incubation took place over 10 min so that the activity assessed was reduced to 2/3 of the initial activity. Afterwards, the thermocycler plates were placed on ice for 10 min and further incubated for 5 min at room temperature. Then, 20 μL of the supernatants were transferred from both the thermocycler and initial activity plates to new plates to estimate the initial and residual activities values by adding ABTS buffer. The plates were briefly stirred and the absorption at 418 nm ($\varepsilon_{ABTS^{\bullet+}}$=36,000 M^{-1} cm^{-1}) was recorded in a plate reader (SpectraMax Plus 384, Molecular Devices, Sunnyvale, CA). The plates were incubated at room temperature until a green color developed and the absorption was measured again. The same experiment was performed for both the initial activity plate and the residual activity plate. The relative activities were calculated from the difference between the absorption after incubation and that of the initial measurement normalized against the parental type in the corresponding plate. Thermostability values were taken as the ratio between the residual and initial activities.

Re-screening

To rule out false positives, two consecutive rescreenings were carried out according to a previously reported protocol with some modifications. A third re-screening was incorporated to calculate the T_{50} of selected mutants in the thermostability assay.

First re-screening: Aliquots of 5 μL of the best clones were removed from the master plates to inoculate 50 μL of minimal media in new 96-well plates. Columns 1 and 12 (rows A and H) were not used to prevent the appearance of false positives. After a 24 h incubation at 30°C and 225 rpm, 5 μL were transferred to the adjacent wells and further incubated for 24 h. Finally, 160 μL of expression medium were added and the plates were incubated for 24 h. Accordingly, each mutant was grown in 4 wells. The parental types were subjected to the same procedure (lane D,

wells 7-11) and the plates were assessed using the same protocols for the screenings described above.

Second re-screening: An aliquot from the wells with the best clones of the first rescreening was inoculated in 3 mL of YPD and incubated at 30°C and 225 rpm for 24 h. The plasmids from these cultures were extracted (Zymoprep Yeast Plasmid Miniprep kit, Zymo Research). As the product of the zymoprep was very impure and the concentration of DNA extracted was very low, the shuttle vectors were transformed into ultracompetent *E. coli* cells (XL2-Blue, Stratagene) and plated onto LB/amp plates. Single colonies were picked and used to inoculate 5 mL LB/amp medium and they were grown overnight at 37°C and 225 rpm. The plasmids were then extracted (NucleoSpin Plasmid kit, Macherey-Nagel, Germany) and *S. cerevisiae* was transformed with plasmids from the best mutants as well as with the parental type. Five colonies for each mutant were picked and rescreened as described above.

Third re-screening for thermostability (T_{50} determination): Fresh transformants of selected mutants and of the parental types were cultivated (10 mL) in a 100 mL flask for HRPL production. The supernatants were subjected to a thermostability assay to accurately estimate their T_{50} using 96/384 well gradient thermocyclers. Appropriate dilutions of supernatants were prepared with the help of the robot such that 20 µL aliquots gave rise to a linear response in kinetic mode, and 50 µL (from both selected mutants and the parental types) were used for each point in the gradient scale. A temperature gradient profile ranging from 35 to 90°C was established. After a 10 min incubation, samples were chilled on ice for 10 min and further incubated at room temperature for 5 min. Finally, 20 µL were removed and subjected to the same ABTS-based colorimetric assay described above for the screening. Thermostability values were deduced from the ratio between the residual activities incubated at different temperatures and the initial activity at room temperature.

2.1.6.6. Estimation of total activity improvement (TAI)

Five colonies of the best mutants in each generation were picked and cultured in 96-well plates containing 50 µL of minimal medium per well. The plates were sealed to prevent evaporation and incubated at 30°C, 225 rpm and 80% relative humidity in a humid shaker. After 48 h, 160 µL of expression medium were added to each well and the plates were incubated for 24 h. The plates were centrifuged for 5 min at 3000 x g at 4°C, and 20 µL of supernatant were transferred from the plate with the help of a robot onto one replica plate (from the 4th round onwards supernatants were diluted 1:10 to facilitate measurement in end-point mode). The replica plate was filled with 180 µL of 100 mM sodium acetate buffer (pH 5.0) containing 3 mM ABTS, the plates were stirred briefly and the absorption at 418 nm ($\varepsilon_{ABTS^{\bullet+}}$=36,000 M^{-1} cm^{-1}) was

recorded. The plates were incubated at room temperature until the color developed and the absorption was measured again.

The TAI value in each generation, when compared to the best corresponding parental type (used as reference), was calculated from the difference between the absorption after incubation and that of the initial measurement normalized against the reference. The parental types used as the reference in each generation were as follows: 1G, α-PM1; 2G, PM1-60; 3G, 3E1; 4G, 5G3; 5G, 1D11; 6G, 7H2; 7G, 6C8; 8G, S454F reverted mutant. The TAI value with respect to the original α-PM1 was the result of multiplying the TAI of the corresponding mutant by the TAI values of the references from previous generations.

2.1.6.7. Production and purification of laccase

Production of laccase in S. cerevisiae

A single colony from the *S. cerevisiae* clone containing the parental or mutant laccase gene was picked from a SC drop-out plate, inoculated in 10 mL of minimal medium and incubated for 48 h at 30°C and 225 rpm (Micromagmix shaker, Ovan, Spain). An aliquot of cells was removed and inoculated into a final volume of 50 mL of minimal medium in a 500 mL flask (optical density, OD_{600}=0.25). Incubation proceeded until two growth phases were completed (6 to 8 h) and then, 450 mL of expression medium was inoculated with the 50 mL preculture in a 2 L baffled flask (OD_{600}=0.1). After incubating for 92-96 h at 30°C and 225 rpm (maximal laccase activity; OD_{600}=28-30), the cells were separated by centrifugation for 15 min at 6000 rpm and 4°C (Avantin J-E Centrifuge, Beckman Coulter, Fullerton, CA) and the supernatant was double-filtered (through both a glass and then nitrocellulose membrane of 0.45 μm pore size).

Purification

Laccases were purified by fast protein liquid chromatography (FPLC) equipment (LCC-500CI, Amersham Bioscience, Barcelona, Spain) and high performance liquid chromatography (HPLC) equipment (Waters 600E System with a PDA detector Varian, USA). The crude extract was first submitted to a fractional precipitation with ammonium sulphate at 55% (first cut) and the pellet was then removed before the supernatant was subjected to 75% ammonium sulphate precipitation (second cut). The final pellet was recovered in 20 mM piperazine buffer pH 5.5 (buffer P) and the sample was filtered and loaded onto the FPLC coupled with a strong anionic exchange column (HiTrap QFF, Amersham Bioscience) pre-equilibrated with buffer P. The proteins were eluted with a linear gradient from 0 to 1 M of NaCl in two phases at a flow rate of 1 mL/min: from 0 to 50% over 40 min and from 50 to 100% over 10 min. Fractions with laccase activity were pooled, concentrated, dialyzed against buffer P and further purified by HPLC-PDA coupled with a 10 μm high resolution anion exchange Biosuite Q (Waters, MA, USA) pre-

equilibrated with buffer P. The proteins were eluted with a linear gradient from 0 to 1 M of NaCl at a flow rate of 1 mL/min in two phases: from 0 to 8% in 60 min and from 8 to 100% in 10 min. The fractions with laccase activity were pooled, dialyzed against 10 mM Britton and Robinson buffer pH 6.0, concentrated and stored at -20°C. Throughout the purification protocol the fractions were analyzed by SDS-polyacrylamide gel electrophoresis (SDS-PAGE) on 12% gels in which the proteins were stained with Coomassie Brilliant Blue G-250 (Protoblue Safe, National Diagnostics, GA, USA). All protein concentrations were determined using the Bio-Rad protein reagent (Bio-Rad Laboratories, Hercules, USA) and bovine serum albumin as a standard.

2.1.6.8. MALDI-TOF analysis

The MALDI experiments were performed on an Autoflex III MALDI-TOF-TOF instrument (Bruker Daltonics, Bremen, Germany) with a smartbeam laser. The spectra were acquired using a laser power just above the ionization threshold. Samples were analysed in the positive ion detection and delayed extraction linear mode. Typically, 1,000 laser shots were summed into a single mass spectrum. External calibration was performed, using the BSA from Bruker, covering the range from 30,000 to 70,000 Da. The 2,5-dihydroxyacetophenone (DHAP) matrix solution was prepared by dissolving 7.6 mg (50 μmol) in 375 μL ethanol followed by the addition of 125 μL of 80 mM diammonium hydrogen citrate aqueous solution. For sample preparation, 2.0 μL of purified enzyme were diluted with 2.0 μL of 2% trifluoroacetic acid aqueous solution and 2.0 μL of matrix solution. A volume of 1.0 μL of this mixture was spotted onto the stainless steel target and allowed to dry at room temperature.

2.1.6.9. N-terminal analysis

The N-terminal region of OB-1 was sequenced on a 494 Procise Sequencing System (Applied Biosystems, CA, USA) using 50-100 pmol of purified laccase solved in *sdd* water.

2.1.6.10. Determination of thermostability

The thermostability of the different laccase samples was estimated by assessing their T_{50} values using 96/384 well gradient thermocyclers. Appropriate laccase dilutions were prepared with the help of the robot in such a way that 20 μL aliquots gave rise to a linear response in the kinetic mode. Then, 50 μL was used for each point in the gradient scale and a temperature gradient profile ranging from 35 to 90°C was established as follows (in °C): 35.0, 36.7, 39.8, 44.2, 50.2, 54.9, 58.0, 60.0, 61.1, 63.0, 65.6, 69.2, 72.1, 73.9, 75.0, 76.2, 78.0, 80.7, 84.3, 87.1, 89.0 and 90.0 After a 10 min incubation, samples were chilled out on ice for 10 min and further incubated at room temperature for 5 min. Afterwards, 20 μL of samples were subjected to the same ABTS-

based colorimetric assay described above for the screening. The thermostability values were deduced from the ratio between the residual activities incubated at different temperature points and the initial activity at room temperature.

2.1.6.11. DNA sequencing

Plasmids containing variants HRPLs were sequenced using a BigDye Terminator v 3.1 Cycle Sequencing Kit. The primers were designed with Fast-PCR software (University of Helsinki, Finland) and were as follows: RMLN; PM1FS (5′-ACGACTTCCAGGTCCCTGACCAAGC-3′, which binds to bp 5′-1026-1050-3′ of pJRoC30-αPM1); PM1RS (5′-TCAATGTCCGCGTTCGCAGGGA-3′, which binds to bp 5′-1860-1881-3′ of pJRoC30-αPM1) and RMLC.

2.1.6.12. Protein modelling

We carried out a search of the Protein Data Bank for proteins with known structural homology to the PM1 laccase. The most similar protein to PM1 was a laccase from *Trametes trogii*, the crystal structure of which was solved at a resolution of 1.58 Å and that has 97% sequence identity (PDB id: 2HRG) (Matera *et al.*, 2008). A model from the Swiss-Model protein automated modeling server was generated (http://swissmodel.expasy.org/) and analyzed with DeepView/Swiss-Pdb Viewer and PyMol Viewer.

2.1.7. SUPPLEMENTAL FIGURES AND TABLES

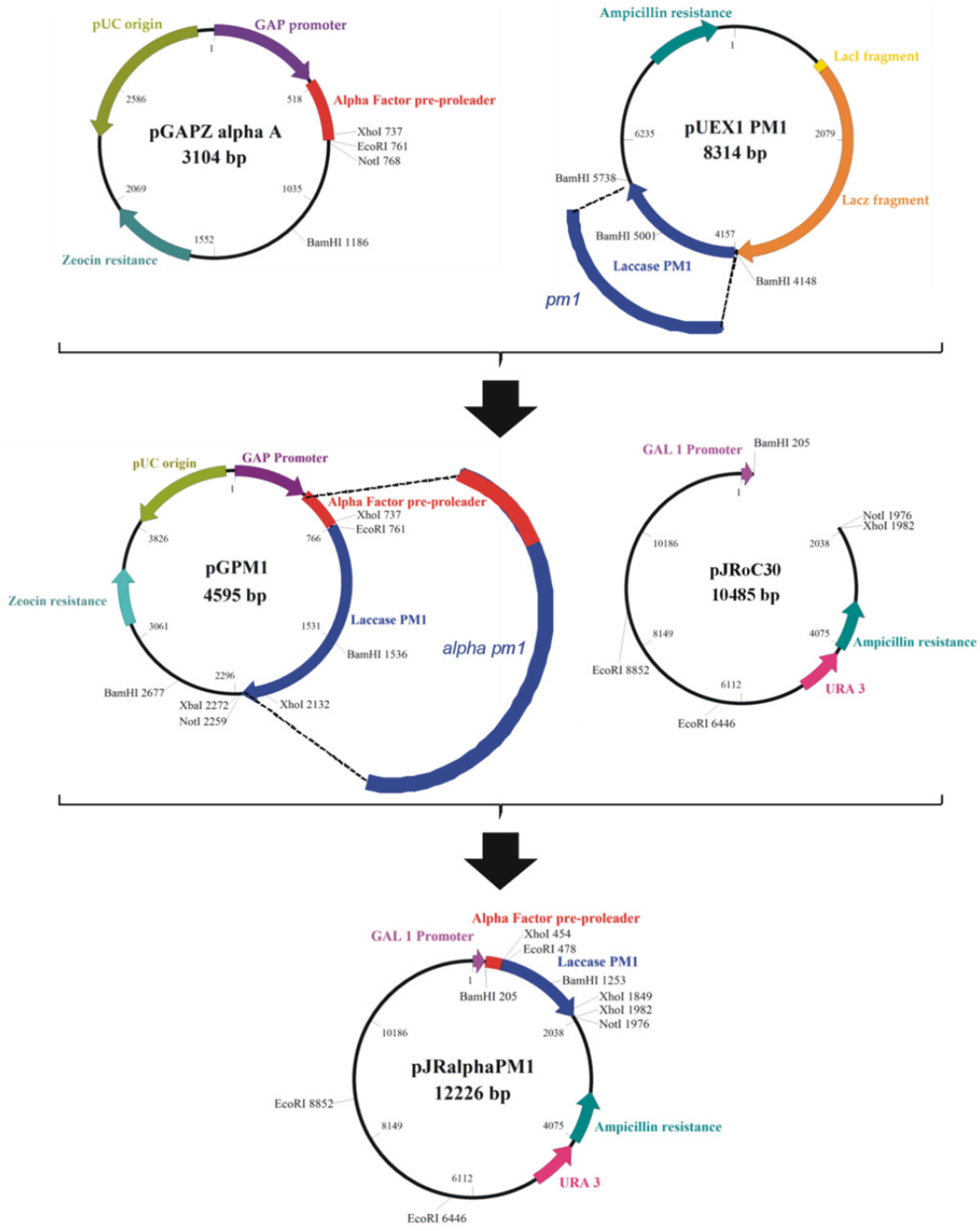

Figure 2.1.S1. Cloning strategy for the construction of α-PM1. Additional information in the **Supplemental Experimental Procedures**, p. 72.

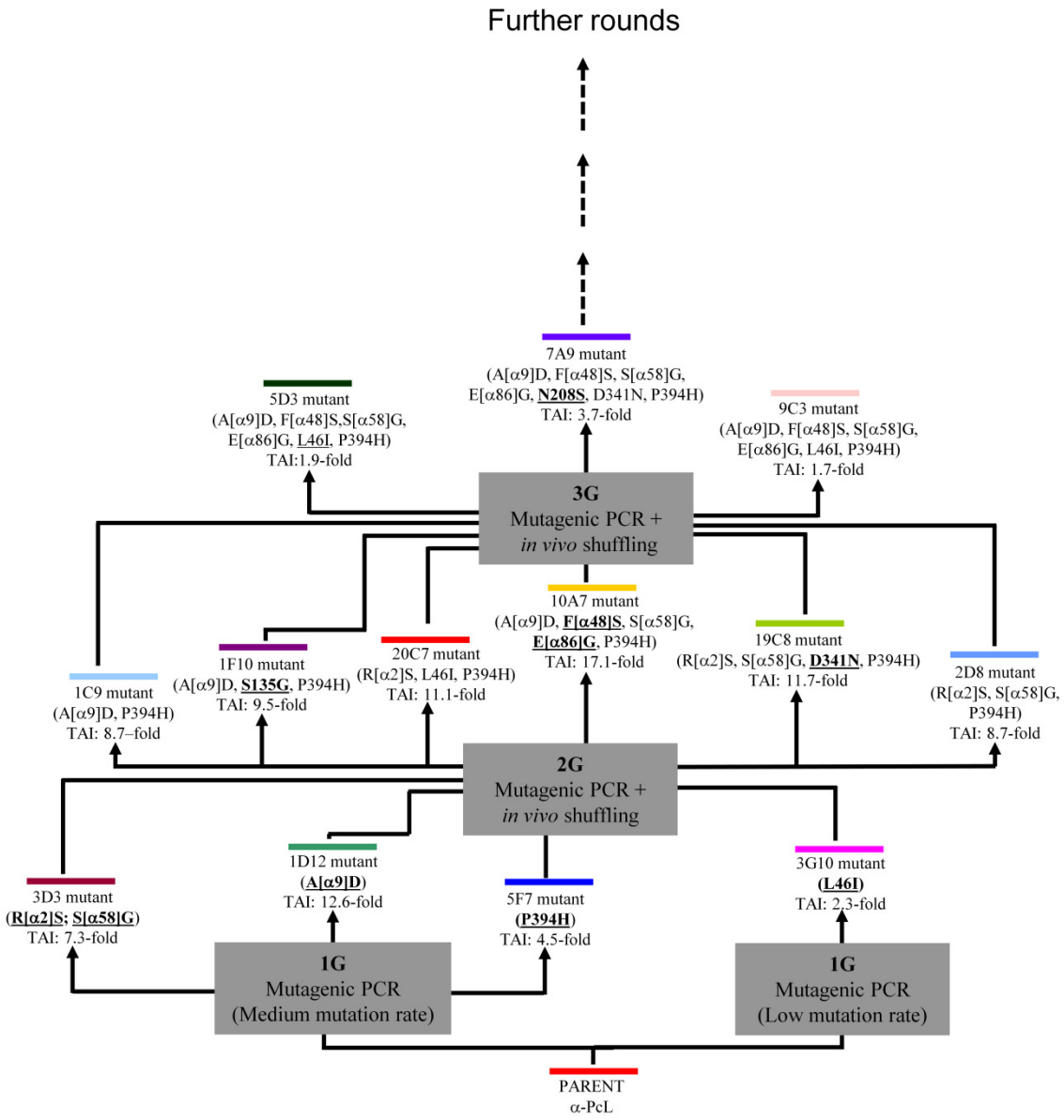

Figure 2.1.S2. Artificial evolution pathway for α-PcL, related to **Figure 2.1.1.**, p. 55. The figure depicts the three first generations of directed evolution of *Pycnoporus cinnabarinus* laccase (Camarero *et al.*, 2010). New point mutations are underlined. TAI: total activity improvement *vs.* best parental type from the previous generation.

HRPL	IDENTITY			
PM1		400	IEISLPATSAAPGFPHPFHLHGHTFAVVRSAGSSTYNYANPVYRDVVSTGSP--GDNVTIRFRTDNPGPWFLHCHIDFHL	477
*T.*sp.C30	99%	400	IEISLPATSAAPGFPHPFHLHGHTFAVVRSAGSSTYNYANPVYRDVVSTGSP--GDNVTIRFRTDNPGPWFLHCHIDFHL	477
T.trogii	97%	379	IEISLPATAAAPGFPHPFHLHGHTFAVVRSAGSSTYNYENPVYRDVVSTGSP--GDNVTIRFRTDNPGPWFLHCHIDFHL	456
C.gallica	96%	400	IEISLPATTAAPGFPHPFHLHGHAFAVVRSAGSSTYNYENPVYRDVVSTGSP--GDNVTIRFRTDNPGPWFLHCHIDFHL	477
C.rigida	90%	379	IEISLPATAAAPGFPHPFHLHGHTFAVVRSSGQQTYNYANPVYRDVVSTGSP--GDNVTIRFRTDNPGPWFLHCHIDFHL	456
*T.*sp.AH28-2	81%	401	IEISFPATAAAPGAPHPFHLHGHAFAVVRSAGSTVYNYDNPIFRDVVSTGTPAAGDNVTIRFRTDNPGPWFLHCHIDFHL	480
T.versicolor	80%	401	IEISFPATAAAPGAPHPFHLHGHAFAVVRSAGSTVYNYDNPIFRDVVSTGTPAAGDNVTIRFRTDNPGPWFLHCHIDFHL	480
T.pubescens	80%	401	IEISFPATTAAPGAPHPFHLHGHAFAVVRSAGSTVYNYDNPIFRDVVSTGTPAAGDNVTIRFRTDNPGPWFLHCHIDFHL	480
T.hirsuta	78%	401	IEISFPATAAAPGAPHPFHLHGHTFAVVRSAGSTVYNYDNPIFRDVVSTGTPAAGDNVTIRFDTNNPGPWFLHCHIDFHL	480
*T.*sp.I-62	78%	401	IEISFPATAAAPGVPHPFHLHGHTFAVVRSAGSTEYNYDNPIFRDVVSTGTPAAGDNVTIRFQTNNPGPWFLHCHIDFHL	480
P.coccineus	78%	401	IEISFPATANAPGAPHPFHLHGHTFAVVRSAGSSEYNYDNPIFRDVVSTGTP--GDNVTIRFQTNNPGPWFLHCHIDFHL	478
P.sanguineus	77%	401	IEISFPATANAPGAPHPFHLHGHTFAVVRSAGSSEYNYDNPIFRDVVSTGTP--GDNVTIRFETNNPGPWFLHCHIDFHL	478
P.cinnabarinus	77%	401	IEISFPATANAPGFPHPFHLHGHAFAVVRSAGSSVYNYDNPIFRDVVSTGQP--GDNVTIRFETNNPGPWFLHCHIDFHL	478
L.tigrinus	76%	379	IEITFPATTAAPGAPHPFHLHGHVFAVVRSAGSTSYNYDDPVWRDVVSTGTPQAGDNVTIRFQTDNPGPWFLHCHIDFHL	458

Figure 2.1.S3. Partial alignment of the PM1 amino acid sequence and that of other highly related HRPLs. The numbering includes the leader signal sequences, P393 highlighted in grey (following PM1 mature protein numbering). The sequences were aligned in the NCBI-blast server, with the cobalt (constraint-based multiple alignment tool) algorithm. PM1, laccase from basidiomycete PM1 (CAA78144.1); *T.* sp. C30, laccase from *Trametes* sp. C30 LAC1 (AAF06967.1); *T. trogii*, laccase from *Trametes trogii* (2HRG); *C. gallica*, laccase from *Coriolopsis gallica* (ABD93940.1); *C. rigida*, laccase from *Coriolopsis rigida* (ACU29545.1); *T.* sp. AH28-2, laccase A from *Trametes* sp. AH28-2 (AAW28933.1); *T. versicolor*, laccase III from *Trametes versicolor* (AAL93622.1); *T. pubescens*, laccase 2 from *Trametes pubescens* (AAM18407.1); *T. hirsuta*, laccase from *Trametes hirsuta* (ACC43989.1); *T.* sp. I-62, laccase from *Trametes* sp. I-62 (AAQ12269.1); *P. coccineus*, laccase from *Pycnoporus coccineus* (BAB69775.1); *P. sanguineus*, laccase from *Pycnoporus sanguineus* (ACN69056.1); *P. cinnabarinus*, laccase from *Pycnoporus cinnabarinus* (AAF13052.1); *L. tigrinus*, laccase from *Lentinus triginus* (2QT6).

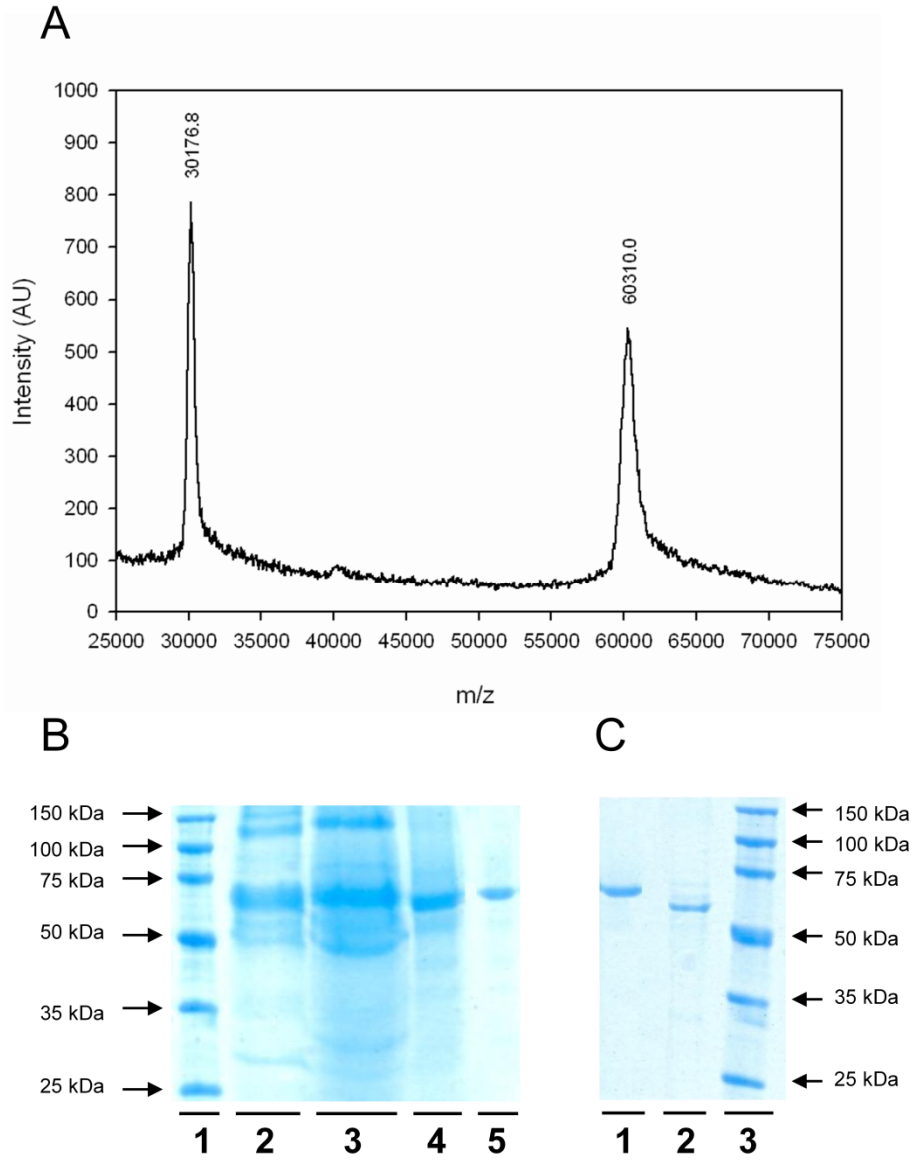

Figure 2.1.S4. Characterization of OB-1, related to **Figure 2.1.4.**, p. 64. (**A**) MALDI-TOF mass spectra of OB-1 mutant (**B**) SDS-PAGE of purified OB-1 mutant. Lanes: 1, protein ladder; 2, Culture filtrate; 3, $(NH_4)_2SO_4$ fractional precipitation; 4, Anion exchange (HiTrap QFF); 5, High resolution anion exchange (Biosuite Q). (**C**) N-deglycosylation of OB-1. Lanes: 1, OB-1; 2, deglycosylated OB-1; 3, protein ladder. The purified enzyme was deglycosylated using the N-glycosidase PNGaseF. Samples were resolved on 12% SDS-polyacrylamide gel and stained with Coomassie Brilliant Blue G-250.

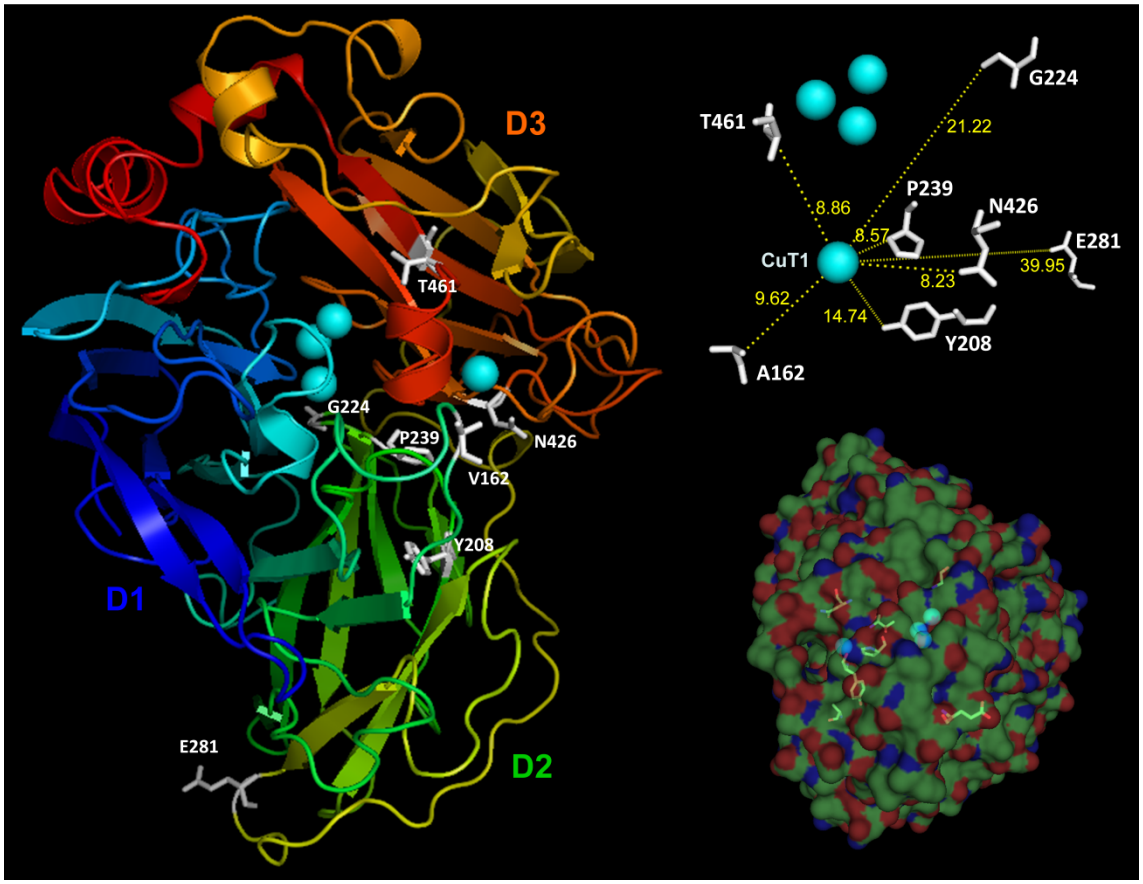

Figure 2.1.S5. General structure of the OB-1 evolved laccase, related to **Figure 2.1.5.**, p. 66. The three cupredoxine-like domains (D1, D2 and D3) are represented in different colours, the copper atoms as blue spheres and the amino acid substitutions are highlighted as white sticks. The distances of the mutated residues to the Cu T1 (represented by yellow dashed lines) and protein surface (colored by element) are also shown.

Table 2.1.S1. Mutations introduced in the directed evolution of α-PM1, related to **Figures 2.1.1.** and **2.1.2.**, pp. 55 and 57, respectively. +, accumulated mutation; •, new mutation. In shadow are shown synonymous mutations; subscript indicates codon usage in *S. cerevisiae*. n.d.: not determined.

Generation		1G			2G				3G							4G			5G	6G		8G
Mutation		PM1-60	PM1-30C	PM1-1A2	3E1	10D2	2G5	4C2	5G3	7D2	9H4	4E12	4B8	8G8	11B3	1D11	11A2	7F2	7H2	6C8	16B10	OB-1*
Amino acid	Codon																					
V(α10)D	G**T**T(29)G**A**T				•				+	+	+	+	+	+	+	+	+	+	+	+	+	+
N(α23)K	AA**C**(69)AA**A**																			•		+
I(α33)T	A**T**T(98)A**C**T																				•	
L(α53)L	$_{27}$**T**TG(157)**C**TG$_{10}$															•						
G(α62)G	$_{6}$GG**G**(186)GG**A**$_{11}$																			•		+
L(α63)S	T**T**A(188)T**C**A					•				+	+											
E(α 83)G	G**A**G(248)G**G**G													•								
A(α87)T	**G**CT(259)**A**CT				•				+		+	+	+	+	+	+	+	+	+	+	+	+
E(α90)E	$_{45}$GA**A**(270)GA**G**$_{1}$																•		+	+	+	+
Q70Q	$_{27}$CA**A**(483)CA**G**$_{12}$				•				+			+	+	+	+	+	+	+	+	+	+	+
V162A	G**T**C(758)G**C**C											•					+		+	+	+	+
A167A	$_{6}$G**C**G(774)G**C**T$_{21}$				•							+	+	+			+	+	+	+	+	+
N181D	**A**AC(814)**G**AC													•				+				
A185A	$_{21}$G**C**T(828)G**C**C$_{13}$																				•	
H208Y	**C**AC(895)**T**AC															•			+	+	+	+
S224G	**A**GC(943)**G**GC		•											+				+				+
A239P	**G**CT(988)**C**CT	•			+	+	+	+	+	+	+	+	+	+	+	+	+	+	+	+	+	+
D281E	GA**C**(1116)GA**A**			•			•					+			+		+					+
V286L	**G**TT(1129)**C**TT				•																	
A361T	**G**CG(1354)**A**CG																				•	
P395P	$_{7}$CC**C**(1458)CC**T**$_{13}$																				•	
S426N	A**G**C(1550)A**A**C					•			+	+	+		+			+	+	+	+	+	+	+
C450C	$_{5}$TG**C**(1623)TG**T**$_{8}$													•								
F454S	T**T**C(1634)T**C**C																		•	+	+	
L456L	$_{5}$CT**C**(1641)CT**T**$_{12}$																		•	+	+	+
A461T	**G**CG(1654)**A**CG							•	+							+	+	+	+	+	+	+
S482L	T**C**G(1718)T**T**G																				•	
P486L	C**C**G(1730)C**T**G											•										
Total activity improvement (fold)		12	7	4	132	72	43	31	1360	792	779	726	620	620	554	5170	4625	3535	24290	43720	12390	34000
Thermostability (fold) mutant/α-PM1 parent		n.d.	n.d.	n.d.	n.d.	n.d.	n.d.	n.d.	n.d.	n.d.	n.d.	n.d.	n.d.	n.d.	n.d.	1	1	n.d.	0.4	0.4	0.7	1

*OB-1 mutant incorporated the two recovered mutations S224G and D281E plus reverted mutation S454F introduced by site directed mutagenesis in the 7th and 8th cycles.

Table 2.1.S2. Activities improvements for mutants at position 9 and 10 of the α-factor pre-leader. The mutants were constructed using 6C8 mutant (4th G) as parental type.

	A(α9)D	**V(α10)D**	**A(α9)D V(α10)D**	**D(α9)A D(α10)V**
Total activity improvement (fold)	2.2	2.2	0.5	0.1

CAPÍTULO 2

Evolving thermostability in mutant libraries of ligninolytic oxidoreductases expressed in yeast

Eva García-Ruiz, **Diana Maté**, Antonio O. Ballesteros,
Ángel T. Martínez and Miguel Alcalde

Published in *Microbial Cell Factories*, 2010, vol. 9, issue 17.

2.2.1. SUMMARY

Background: In the picture of a laboratory evolution experiment, to improve the thermostability whilst maintaining the activity requires of suitable procedures to generate diversity in combination with robust high-throughput protocols. The current work describes how to achieve this goal by engineering ligninolytic oxidoreductases (a high-redox potential laccase -HRPL- and a versatile peroxidase, -VP-) functionally expressed in *Saccharomyces cerevisiae*.

Results: Taking advantage of the eukaryotic machinery, complex mutant libraries were constructed by different *in vivo* recombination approaches and explored for improved stabilities and activities. A reliable high-throughput assay based on the analysis of T_{50} was employed for discovering thermostable oxidases from mutant libraries in yeast. Both VP and HRPL libraries contained variants with shifts in the T_{50} values. Stabilizing mutations were found at the surface of the protein establishing new interactions with the surrounding residues.

Conclusions: The existing trade-off between activity and stability determined from many point mutations discovered by directed evolution and other protein engineering means can be circumvented combining different tools of *in vitro* evolution.

2.2.2. BACKGROUND

During the last couple of decades, thermostability has been considered by many as a key feature in terms of protein robustness, evolvability and catalytic function (Bloom *et al.*, 2004; Bloom *et al.*, 2006; Watanabe *et al.*, 2006; Bloom and Arnold, 2009). From a practical point of view, the engineering of thermo-tolerant biocatalysts is highly desirable since transformations

at high temperatures intrinsically supply a box-set of key biotechnological advantages (higher entropies -better reaction yields-, solubilisation of hydrophobic compounds or low levels of microbial side-contamination, among others). Besides, thermostable enzymes are typically tolerant to many other harsh conditions often required in industry, such as the presence of organic co-solvents, extreme pHs, high salt concentrations, high pressures, etc. (Arnold, 1990; Ogino and Ishikawa, 2001). Few exceptions aside (Suen *et al.*, 2004; Johannes *et al.*, 2005), the discovery of stabilizing mutations is not always straightforwardly accomplished without significant drops in turnover rates (Arnold and Georgiou, 2003). Most of these mutations, which establish new interactions by salt bridges, hydrogen bonds, hydrophobic contacts or even disulfide bridges, are placed either at the protein surface or in internal cores pursuing the tightly packing of the tertiary protein structure in order to prevent unfolding and denaturation under extreme environments (Reetz *et al.*, 2006). On the contrary, improvements in activity are generally accomplished by introducing beneficial but destabilizing mutations in *hot* regions for catalysis (substrate binding sites, channels of access to the active pockets) although sometimes distant mutations can also vary the catalytic function by altering the dynamics and geometry in the protein scaffold (Bloom and Arnold, 2009). There are several examples in literature about the stabilization of enzymes by directed evolution or rational design but unfortunately, main constraints still remain from the lack of appropriate methods to recreate diversity in conjunction with reliable screening strategies, especially if one wants to surpass the existing trade-off between activity and thermostability for many single residue substitutions (Lopez-Camacho *et al.*, 1996; Giver *et al.*, 1998; Arnold *et al.*, 1999; Reading and Aust, 2000; Morawski *et al.*, 2001; Sun *et al.*, 2001; Salazar *et al.*, 2003; Hao and Berry, 2004; Bommarius *et al.*, 2006; Miyazaki *et al.*, 2006; Reetz *et al.*, 2006).

Among the enzymes forming the ligninolytic system of white-rot fungi (*i.e.* involved in lignin biodegradation), high-redox potential laccases (HRPL; EC 1.10.3.2) and peroxidases, including versatile peroxidases (VP; EC 1.11.1.14) are outstanding biocatalysts finding potential applications in paper pulp bleaching and functionalization, bioremediation, organic synthesis, food and textile industries, nanobiodevice construction and more (Alcalde *et al.*, 2006a; Kunamneni *et al.*, 2008a; Martínez *et al.*, 2009). Indeed, HRPL can oxidize dozens of different compounds releasing water as the only by-product and in the presence of redox mediators (diffusible electron carriers from natural or synthetic sources) their substrates specificities are further expanded (Riva, 2006; Alcalde, 2007). On the other hand, VP (with redox potential above +1000 mV) shares the catalytic features of lignin and manganese peroxidase in terms of substrate specificity, together with the ability to oxidize phenols and dyes characteristic of low redox-potential peroxidases. Indeed, the presence of different catalytic sites in a small and compact protein structure (around 300 amino acids) makes VP an ideal platform for laboratory evolution strategies (Ruiz-Dueñas *et al.*, 1999; Martínez *et al.*, 2009; Ruiz-Dueñas *et al.*, 2009).

Here, we have employed these two enzymatic systems as departure points to improve their protein thermostability by directed evolution. VP and HRPL were functionally expressed in yeast and mutant libraries were constructed combining several methodologies of *in vitro* evolution to guarantee the library complexity, favoring the selection of optimal crossover events or the discovery of beneficial mutations. Highly functional/soluble expressed mutants were stressed under high temperatures and explored for activity and stability. The analysis of the data from screening (ratio residual activity/initial activity in combination with the T_{50} values) enabled us to discover stabilizing mutations in both systems.

2.2.3. MATERIALS AND METHODS

HRPL from basidiomycete PM1 (Coll *et al.*, 1993b) (PM1-7H2 mutant) and VP from *Pleurotus eryngii* (10C3, 6B1, 13E4, 6E7 and 11F3 mutants of the allelic variant VPL2, GenBank AF007222) were used as parent types for library construction. Both systems are from previous engineering work by several rounds of directed evolution in *S. cerevisiae* including the replacement of their original native signal sequences by the alpha factor prepro-leader (García *et al.*, 2010; Garcia-Ruiz *et al.*, 2012). ABTS (2,2´-azino-bis(3-ethylbenzothiazoline-6-sulfonic acid)), bovine haemoglobine, *Taq* polymerase and the *S. cerevisiae* transformation kit were purchased from Sigma-Aldrich (Madrid, Spain). The *E. coli* XL2-Blue ultracompetent cells and the Genemorph Random mutagenesis kit were from Stratagene (La Jolla, CA, USA). The protease-deficient *S. cerevisiae* strain BJ5465 was from LGCPromochem (Barcelona, Spain). The uracil independent and ampicillin resistance shuttle vector pJRoC30 was obtained from the California Institute of Technology (CALTECH, USA), while the Zymoprep Yeast Plasmid Miniprep kit, Zymoclean Gel DNA Recovery kit, and the DNA Clean and Concentrator-5 kit were all from Zymo Research (Irvine, CA). The NucleoSpin Plasmid kit was purchased from Macherey-Nagel (Düren, Germany) and the restriction enzymes *Bam*HI and *Xho*I were from New England Biolabs (Hertfordshire, UK). All chemicals were of reagent-grade purity.

2.2.3.1. Culture media

Minimal medium contained 100 mL 6.7% sterile yeast nitrogen base, 100 mL 19.2 g/L sterile yeast synthetic drop-out medium supplement without uracil, 100 mL sterile 20% raffinose, 700 mL *sdd*H_2O and 1 mL 25 g/L chloramphenicol. YP medium contained 10 g yeast extract, 20 g peptone and *dd*H_2O to 650 mL. Expression medium contained 720 mL YP, 67 ml 1 M potassium phosphate buffer pH 6.0, 111 mL 20% galactose, 1 ml 25 g/L chloramphenicol and *dd*H_2O to 1000 mL. For HRPL the expression medium was supplemented with 2 mM $CuSO_4$ and 25 g/L ethanol. For VP the expression medium was supplemented with 100 mg/L bovine haemoglobine. YPD solution contained 10 g yeast extract, 20 g peptone, 100 mL 20% sterile

glucose, 1 ml 25 g/L chloramphenicol and *dd*H_2O to 1000 mL. SC drop-out plates contained 100 mL 6.7 % sterile yeast nitrogen base, 100 mL 19.2 g/L sterile yeast synthetic drop-out medium supplement without uracil, 20 g bacto agar, 100 mL 20% sterile glucose, 1 mL 25 g/L chloramphenicol and *dd*H_2O to 1000 ml.

2.2.3.2. Library construction for laboratory evolution

General aspects

Unless otherwise specified, PCR fragments were cleaned, concentrated and loaded onto a low melting point preparative agarose gel and purified using the Zymoclean Gel DNA Recovery kit (Zymo Research). PCR products were cloned under the control of the GAL10 promoter of the expression shuttle vector pJRoC30, replacing the corresponding parental gene in pJRoC30. To remove the parental gene, the pJRoC30 plasmid was linearized (with *Xho*I and *Bam*HI for HRPL- and VP-libraries). Linearized vector was concentrated and purified as described above for the PCR fragments.

Mutagenic *StEP* (*Staggered Extension Process*) followed by *in vivo* DNA shuffling and *IvAM* (*In vivo A*ssembly of *M*utant libraries with different mutational spectra) were used to create the VP and HRPL libraries, respectively, as described below.

VP library: mutagenic StEP + in vivo DNA shuffling

10C3, 6B1, 13E4, 6E7 and 11F3 VP-mutants were used as parental types. StEP was performed as reported elsewhere (Zhao *et al*., 1998) with some modifications. In order to favor random mutagenesis during StEP, *Taq* DNA polymerase was employed for the PCR reaction along with low concentration of templates to promote the introduction of point mutations during the amplification. The primers used were: RMLN-sense (5′-CCTCTAATACTTTAACGTCAAGG-3′) and RMLC-antisense (5′-GGGAGGGCGTGAATGTAAGC-3′). For the *in vivo* ligation, overhangs of 40 bp and 66 bp that were homologous to linearized vector were designed. PCR reactions were performed in a final volume of 50 µL containing 90 nM RMLN, 90 nM RMLC, 0.3 mM dNTPs, 3% dimethylsulfoxide (DMSO), 0.05 U/µL of *Taq* polymerase (Sigma), 1.5 mM $MgCl_2$ and 0.1 ng/ µL of 10C3, 6B1, 13E4, 6E7 and 11F3 DNA-template mixture. StEP was carried out using a gradient thermocycler (Mycycler, Biorad, USA). The thermal cycling parameters were as follows: 95°C for 5 min (1 cycle); and 94°C for 30 s, 55°C for 20 s (90 cycles). Purified PCR products were further recombined by *in vivo* DNA shufflling (Okkels, 2003). PCR mutated/recombined products were mixed equimolarly (160 ng of each product) and transformed along with linearized vector (ratio PCR product:vector, 4:1) into competent cells using the yeast transformation kit (Sigma). A mutant library of ~2000 clones was explored.

HRPL library: IvAM

IvAM (~1300 clones) was performed as reported elsewhere (Zumárraga *et al.*, 2008a) with some modifications. HRPL PM1-7H2 mutant was used as parent type. Mutagenic PCR was carried out using the following thermal cycling parameters: 95°C for 2 min (1 cycle); 94°C for 0.45 min, 53°C for 0.45 min, 74°C for 3 min (28 cycles); and 74°C for 10 min (1 cycle). For the *Taq* library the concentrations of each ingredient in 50 μL final volume were as follows: 90 nM RMLN, 90 nM RMLC, 0.1 ng/μL HRPL template, 0.3 mM dNTPs (0.075 mM each), 3% DMSO, 1.5 mM $MgCl_2$, 0.01 mM $MnCl_2$ and 0.05 U/μL *Taq* polymerase. For the Mutazyme library the concentrations of each reagent in 50 μL final volume were as follows: 370 nM RMLN, 370 nM RMLC, 40 ng/μL HRPL template, 0.8 mM dNTPs, 3% DMSO, and 0.05 U/μL Mutazyme DNA polymerase. *Taq*/$MnCl_2$ and Mutazyme libraries were equimolarly mixed and transformed along with linearized vector (ratio equimolar library:vector, 8:1) into competent *S. cerevisiae* cells as described above.

2.2.3.3. High-throughput thermostability assay

Individual clones were picked and cultured in 96-well plates (Sero-well, Staffordshire, UK) containing 50 μL of minimal medium per well. In each plate, column number 6 was inoculated with standard (parental HRPL or VP), and one well (H1-control) was either not inoculated for HRPL libraries or inoculated with untransformed *S. cerevisiae* cells for VP-libraries. Plates were sealed to prevent evaporation and incubated at 30°C, 225 rpm and 80% relative humidity in a humidity shaker (Minitron-INFORS, Biogen, Spain). After 48 h, 160 μL of expression medium were added to each well, and the plates were incubated for 24 h. The plates (master plates) were centrifuged (Eppendorf 5810R centrifuge, Germany) for 5 min at 3000 x *g* at 4°C and 20 μL of supernatant was transferred from the master plate with the help of a robot (Liquid Handler Quadra 96-320, Tomtec, Hamden, CT, USA) onto the replica plate. Subsequently, 180 μL of stability buffer (10 mM sodium tartrate buffer pH 5.1 for VP-library and 10 mM Britton and Robinson buffer pH 6.0 for HRPL-library) were added to each replica and briefly stirred. Replica plate was duplicated with the help of the robot by transferring 50 μL of mixture to a thermocycler plate (Multiply PCR plate without skirt, neutral, Sarstedt, Germany) and 20 μL to the initial activity plate. Thermocycler plates were sealed with thermoresistant film (Deltalab, Spain) and incubated at the corresponding temperature using a thermocycler (MyCycler, Biorad, USA). Incubation took place for 10 min (so that the assessed activity was reduced 2/3 of the initial activity). Afterwards, thermocycler plates were placed on ice for 10 min and further incubated for 5 min at room temperature. 20 μL of supernatants were transferred from both thermocycler and initial activity plates to new plates to estimate the initial activities and residual activities values by adding ABTS containing specific buffers. For VP-libraries 180 μL of 100 mM sodium tartrate buffer pH 3.5 containing 2 mM ABTS and 0.1 mM H_2O_2 were added to

each plate. For HRPL-libraries 180 μL of 100 mM sodium acetate buffer pH 5.0 containing 3 mM ABTS were added. Plates were stirred briefly and the absorption at 418 nm ($\varepsilon_{ABTS^{\bullet+}}$=36,000 M^{-1} cm^{-1}) was recorded in the plate reader (SpectraMax Plus 384, Molecular Devices, Sunnyvale, CA). The plates were incubated at room temperature until a green color developed, and the absorption was measured again. The same experiment was performed for both the initial activity plate and residual activity plate. Relative activities were calculated from the difference between the absorption after incubation and that of the initial measurement normalized against the parental type in the corresponding plate. Thermostability values came from the ratio between residual activities and initial activities values. To rule out false positives, two consecutive re-screenings were carried out according to the protocol previously reported (Zumárraga *et al.*, 2008b) with some modifications. A third rescreening was incorporated to calculate the T_{50} of selected mutants.

First re-screening

Aliquots of 5 μL of the best clones were removed from master plates to inoculate 50 μL of minimal medium in new 96-well plates. Columns 1 and 12 (rows A and H) were not used to prevent the appearance of false positives. After 24 h of incubation at 30°C and 225 rpm, 5 μL were transferred to the adjacent wells and further incubated for 24 h. Finally, 160 μL of expression medium were added and plates were incubated for 24 h. Accordingly, every single mutant was grown in 4 wells. Parent types were subjected to the same procedure (lane D, wells 7-11). Plates were assessed using the same protocol of the screening described above but including not only an endpoint assay but also a kinetic assay. In the ABTS kinetic assay, linear absorption increases over a wide range of enzyme concentration (1-20 mU/mL) allowing the estimation of initial rates.

Second re-screening

An aliquot from the wells with the best clones of first rescreening was inoculated in 3 mL of YPD and incubated at 30°C and 225 rpm for 24 h. Plasmids from these cultures were extracted (Zymoprep Yeast Plasmid Miniprep kit, Zymo Research). As the product of the zymoprep was very impure and the concentration of extracted DNA was very low, the shuttle vectors were transformed into ultracompetent *E. coli* cells (XL2-Blue, Stratagene) and plated onto LB/amp plates. Single colonies were picked and used to inoculate 5 mL LB/amp medium and were grown overnight at 37°C and 225 rpm. Plasmids were then extracted (NucleoSpin Plasmid kit, Macherey-Nagel, Germany). *S. cerevisiae* was transformed with plasmids from the best mutants and also with parent type. Five colonies of every single mutant were picked and rescreened as described above (using both end-point and kinetic assays).

Third re-screening (T_{50} determination)

Fresh transformants of selected mutants and parent types were cultivated (10 mL) in 100 mL flask for VP and HRPL production. Supernatants were subjected to a thermostability assay to accurate estimate their T_{50} using 96/384 well gradient thermocyclers (Mycycler, Biorad, US). Appropriate dilutions of supernatants were prepared with the help of the robot in such a way that aliquots of 20 μL give rise to a linear response in kinetic mode. 50 μL (from both selected mutants and parent types) were used for each point in the gradient scale. A temperature gradient profile ranging from 30 to 90°C was established. After 10 min of incubation, samples were removed and chilled out on ice for 10 min. After that, samples of 20 μL were removed and incubated at room temperature for 5 min. Finally, samples were subjected to the same ABTS-based colorimetric assay described above for the screening. Thermostabilities values were deduced from the ratio between the residual activities incubated at different temperature points and the initial activity at room temperature.

2.2.3.4. Determination of thermostabilities in VP and HRPL parent types

Thermostabilities of 7H2-HRPL and 10C3-VP mutants were assessed mimicking the growth conditions established for the screening assay as described above. Two 96 well-plates containing 50 μL minimal media were inoculated with 7H2 and 10C3 respectively and cultivated until reaching functional expression following the conditions used for the assay. Afterwards, supernantants of 7H2 and 10C3 were pooled and employed to estimate their respective thermostabilities with the gradient thermocycler. The gradient of temperature was set at the following points (in °C): 30.0, 31.7, 34.8, 39.3, 45.3, 49.9, 53.0, 55.0, 56.8, 59.9, 64.3, 70.3, 75.0, 78.1 and 80 for the VP mutant and 35.0, 36.7, 39.8, 44.2, 50.2, 54.9, 58.0, 60.0, 61.1, 63.0, 65.6, 69.2, 72.1, 73.9, 75.0, 76.2, 78.0, 80.7, 84.3, 87.1, 89.0 and 90.0 for the HRPL mutant. The protocol followed the general rules described for the third re-screening.

2.2.3.5. DNA sequencing

Plasmids containing HRPL and VP variant genes were sequenced by using a BigDye Terminator v 3.1 Cycle Sequencing Kit. Primers were designed with Fast-PCR software (University of Helsinki, Finland). Primers used for VP variants were: RMLN; 3R-direct (5′-GTTCCATCATCGCGTTCG-3′); 5F-reverse (5′-GGATTCCTTTCTTCTTGG-3′) and RMLC. For HRPL primers were: RMLN; PM1FS (5′-ACGACTTCCAGGTCCCTGACCAAGC-3′); PM1RS (5′-TCAATGTCCGCGTTCGCAGGGA -3′) and RMLC.

2.2.3.6. Protein modelling

We carried out a search in the Protein Data Bank for proteins with known structural homology to laccase PM1. The most similar protein to PM1 was a laccase from *Trametes trogii* (crystal structure solved with a resolution of 1.58 Å), showing 97% sequence identity (PDB id: 2HRG) (Matera *et al.*, 2008). A model from the Swiss-Model protein automated modelling server was generated (http://swissmodel.expasy.org/) and analyzed with DeepView/Swiss-Pdb Viewer.

2.2.4. RESULTS AND DISCUSSION

2.2.4.1. Library construction

VP and HRPL variants come from laboratory evolution approaches to be functionally expressed in *Saccharomyces cerevisiae* (García *et al.*, 2010; Maté *et al.*, 2010; Garcia-Ruiz *et al.*, 2012). Therefore, the array of variants used as starting points for enhancing thermostability, in principle only were going to harbor mutations which conferred higher secretion levels and/or better kinetics. Both VP and HRPL native signal peptides were replaced by the α-factor prepro-leader to promote secretion in yeast (Shuster, 1991). Thus, the whole fusion proteins (α-VP and α-HRPL) were subjected to directed evolution in order to enhance their functional expression; *i.e.* the accumulation of neutral and beneficial mutations took place both in the α-factor prepro-leader as well as in mature protein. If high fidelity DNA recombination strategies are used, where only accumulated mutations recombine each other based on the number of crossovers generated in the protocol, it is highly likely that the discovery of thermostable variants become a complex task, since all these mutations have been unmasked from improvements in total activities; *i.e.* the sum of secretion levels plus the specific activity. Hence, we decided to tackle the library design by combining the already accumulated mutations with the generation of new ones randomly incorporated in the frame of mutagenic DNA recombination fashion approaches (**Figure 2.2.1.**).

For the VP library the well-known *Staggered Extension Process* (*StEP*) (Zhao *et al.*, 1998) was slightly modified by decreasing templates concentration with the aim of provoking amplification mistakes by the *Taq* DNA polymerase which has a high intrinsic error rate because of the lack of 3′→5′ proofreading exonuclease activity. The mutational rate was adjusted to 1-2 mutations per whole gene (Tracewell and Arnold, 2009). Afterwards, and instead of *in vitro* ligating the StEP products with the linearized plasmid to give rise to individual autonomously replicating vectors as usually proceeds, we thought that might be interesting to further recombine the pool of mutagenized/crossover containing genes in an *in*

vivo approach with the aim of expanding the library diversity. Thus, StEP products were further subjected to an *in vivo* DNA shuffling process (Cherry *et al.*, 1999; Bulter *et al.*, 2003; Okkels, 2004) taking advantage of the high level of homologous recombination of *S. cerevisiae* apparatus as described in the **Materials and Methods** section, p. 92. With this strategy, new crossover events were generated that otherwise hardly could be achieved by using conventional *in vitro* or *in vivo* recombination methods independently. In the case of HRPL library, the only starting template gene was subjected to the *in vivo* assembly of mutant libraries with different mutational spectra (IvAM) (Zumárraga *et al.*, 2008a), to guarantee the enrichment of the library in different mutational types and bias. With this simple approach, the homologous recombination, reparation and *in vivo* cloning of mutant genes along with their *in vivo* DNA shuffling in one single step were achieved.

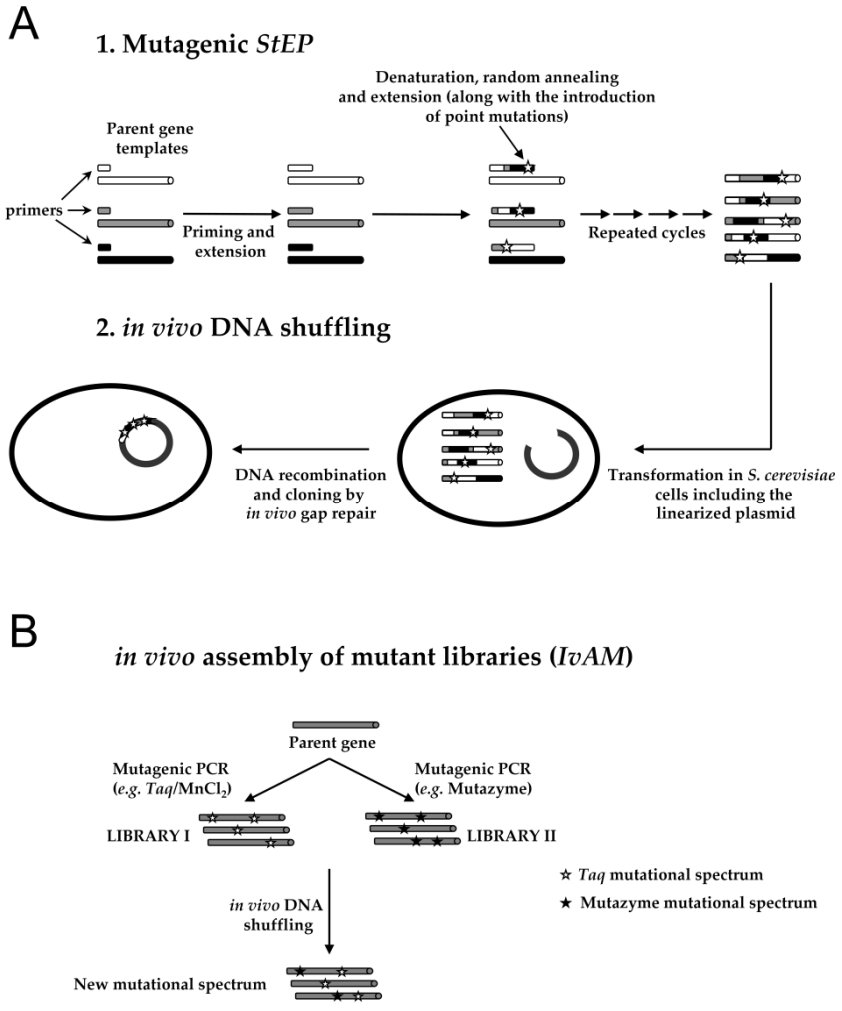

Figure 2.2.1. Schematic representation of methods employed for the construction of VP (A) and HRPL (B) mutant libraries.

2.2.4.2. High-throughput screening assay

ABTS was chosen as substrate for the screening assay since it has a reliable response, high sensitivity and hardly interferes with the main components of culture broth. Indeed, in our former works ABTS was validated in the frame of directed laccase evolution for several purposes (Bulter *et al.*, 2003; Alcalde *et al.*, 2006b; Zumárraga *et al.*, 2007a; Zumárraga *et al.*, 2008b). However, the response of this substrate against the secreted VP mutants by *S. cerevisiae* was unknown and therefore we had to validate it before starting the thermostability studies. First, the relationship between absorbance and VP concentration was evaluated. Fresh transformants containing VP-10C3 mutant (the best parent type) were inoculated in a 96-well plate, VP-10C3 was expressed and different volumes of supernatant were assessed. A linear behavior between the amount of VP and the response of the assay was found (**Figure 2.2.2A**). The coefficient of variation for the ABTS in kinetic mode was 13%, which is an acceptable value to study mutagenic libraries engineered for directed evolution experiments (Arnold and Georgiou, 2003) (**Figure 2.2.2B**).

For the thermostability assay, we first had to set the temperature under which the mutant libraries would be stressed. Accordingly, the two best parent types of both VP and HRPL libraries were tested in order to know their respective thermostabilities. Taking into account that micro-fermentation conditions (*i.e.* in 96-well plates) were far away from an ideal large-scale fermentation in terms of oxygen availability, surface stirring and length of incubation time, VP-10C3 and HRPL-7H2 mutants were produced under such a limited growth conditions and evaluated to obtain the closest real value of thermostability in the screening assay (further details in **Materials and Methods** section, p. 93). In principle, an appropriate enzyme heat treatment for the screening is generally chosen so that the residual activity is about one-third of the initial activity (Arnold and Georgiou, 2003). At 60°C and 68°C, VP-10C3 and HRPL-7H2 mutants kept *c.a.* 30% of their initial ABTS-activity values, and those temperatures were selected for the screening. At this point, it is important to highlight that both VP and HRPL libraries were functionally secreted by yeast, which made the development of the assay faster, reliable and simple since it was not necessary to include cell lysis steps, thus avoiding possible interferences with the complex lysate mixture. Besides, both VP and HRPL secretion levels were previously improved by several iterative rounds of directed evolution to provide: i) short incubations times for functional secretion (24 h) after protein induction that becomes essential for the episomal plasmid stability; and ii) a high level of activity in supernatants (getting measurements from kinetic mode in a few seconds with turnover rates ranging from 0.5 to 1 ABTS-U/mL). Taking advantage of the high level of activity in the culture broth, supernatants of respective libraries were previously diluted in suitable corresponding stability buffers to correctly assess initial and residual activities (**Figure 2.2.3.**). The final values of thermostability came from the ratio of residual activity to initial activity (RA/IA) normalized with the

corresponding parent type. The initial activity value reflected the total activity of the mutant and was highly useful to prevent the selection of mutants with improved stability by greatly reduced activity.

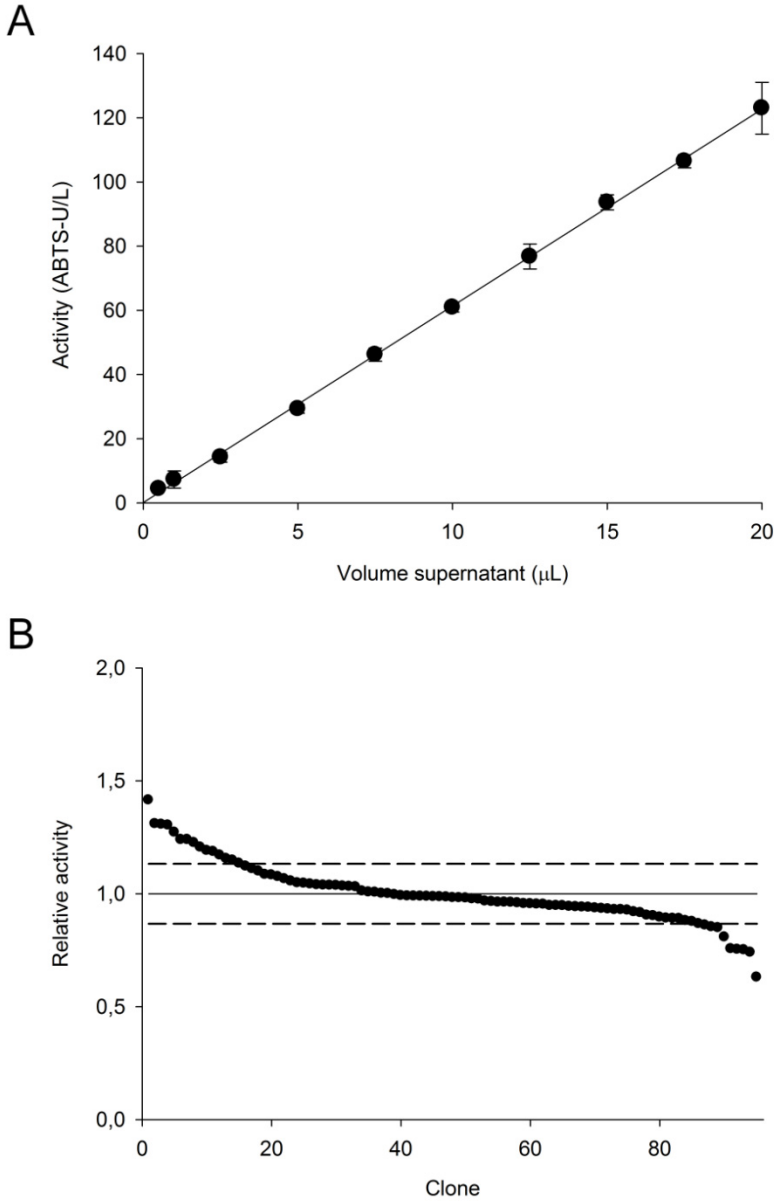

Figure 2.2.2. Validation of the colorimetric assay for the VP-library. (**A**) Linearity of the assay. Each point represents the average of eight experiments (eight wells). (**B**) Activities of VP-10C3 plotted in descending order. Dashed lines indicate the variation coefficient of the assay. *S. cerevisiae* cells were transformed with pJRoC30-VP-10C3 and plated on SC dropout plates. Individual colonies were picked and inoculated in a 96 well-plate. The activities of the clones were evaluated from fresh supernatant preparations.

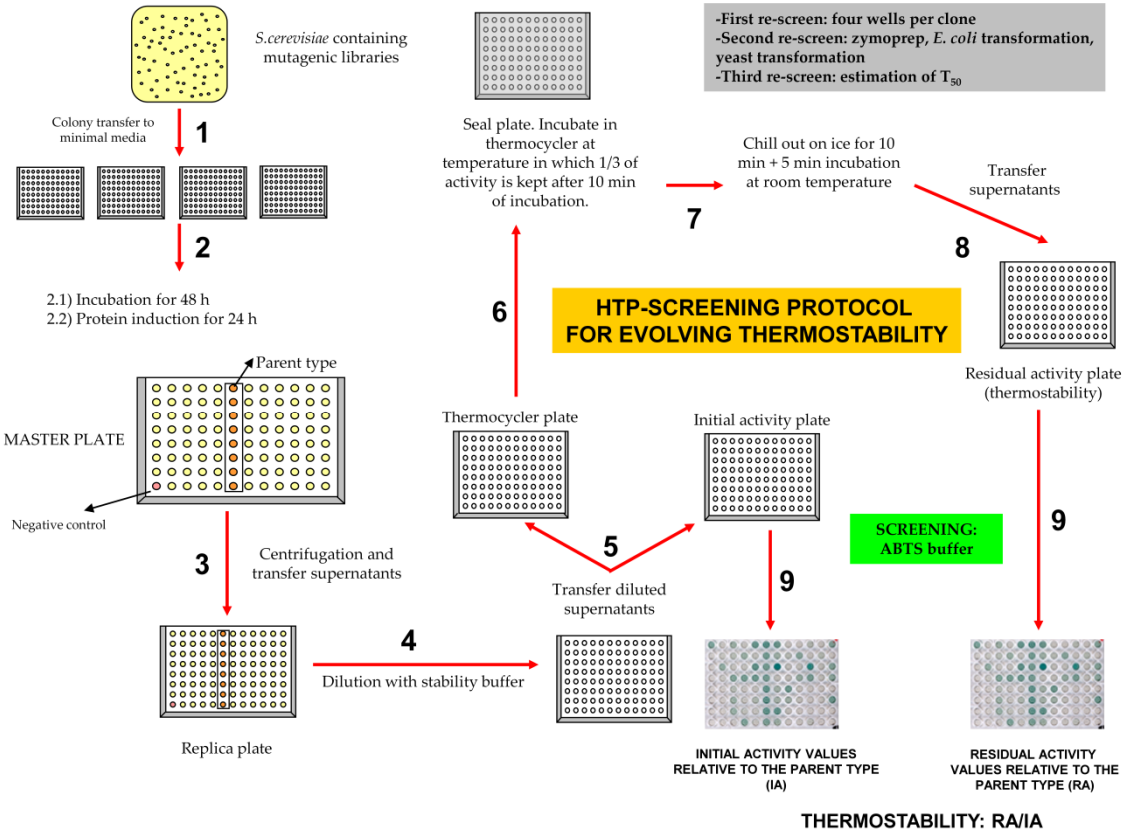

Figure 2.2.3. High-throughput protocol used for screening thermostability in VP- and HRPL-libraries. Further details in **Materials and Methods** section, p. 93.

2.2.4.3. Library analysis

Under the above premises, two libraries of ~2000 clones were independently constructed and explored for VP and HRPL (**Figure 2.2.4.**). The estimated coefficients of variance for the landscapes of initial activity and residual activity were below 12%. Three consecutive re-screens were incorporated to ensure the selection of mutant *hits* in protein function. Systematically, the best 50 clones retaining ~0.7 fold the activity of parent type and showing improvements in thermostability were selected and double rescreened from supernatants and new fresh transformants. Finally, best mutants were subjected to a third rescreen to estimate their T_{50}, *i.e.* the transition midpoint of the inactivation curve of the protein as a function of temperature, which in our case was defined as the temperature at which the enzyme loses 50% of its activity following incubation for 10 min.

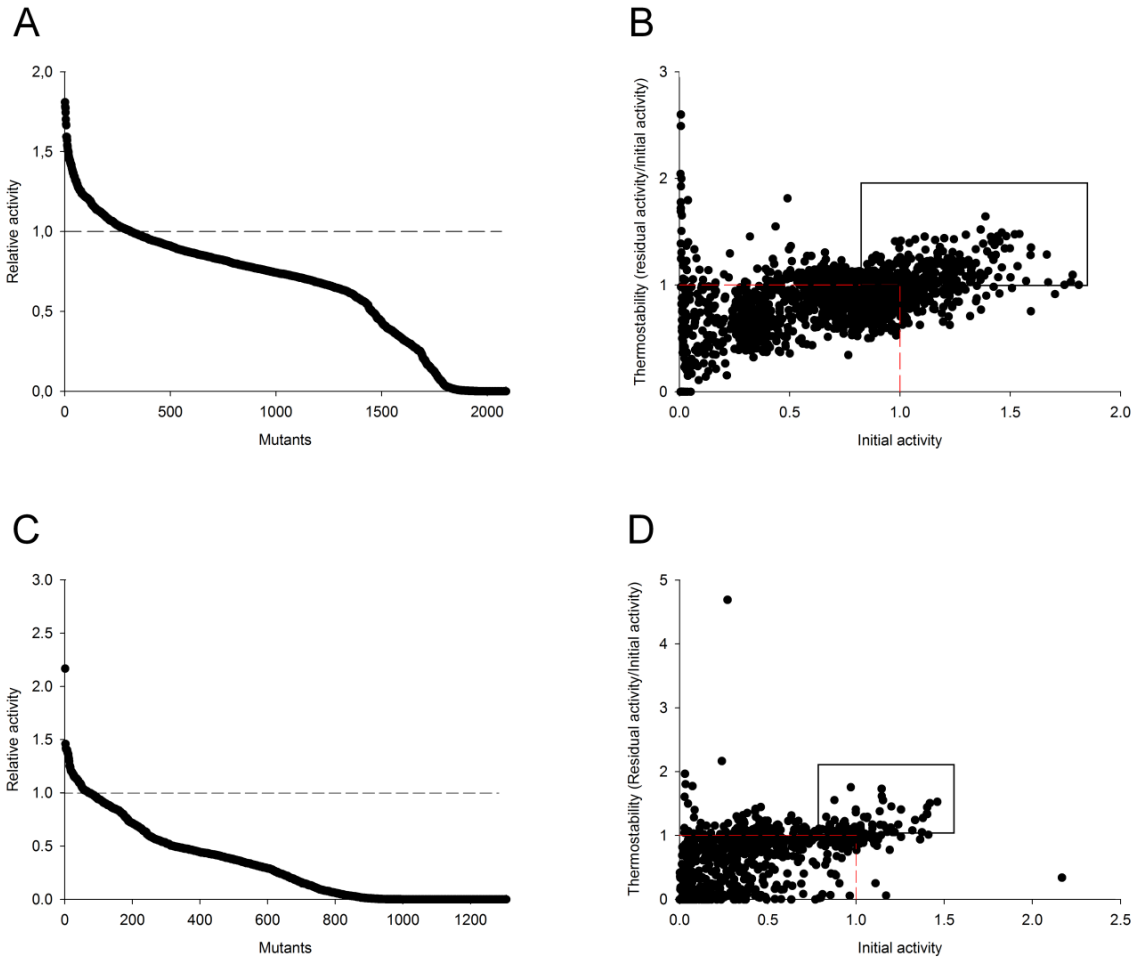

Figure 2.2.4. Directed evolution landscapes. (**A**) Activities of clones from the library of VP mutants prepared by mutagenic StEP + *in vivo* DNA shuffling, plotted in descending order. (**B**) Initial activities *vs.* thermostabilities in VP mutants. Red dashed lines represent 10C3 parent type. Mutants selected for further re-screens are squared (see **Materials and Methods** section, p. 92, for details). (**C**) Activities of clones from the library of HRPL mutants prepared by IvAM, plotted in descending order. (**D**) Initial activities *vs.* thermostabilities in HRPL mutants. Red dashed lines represent 7H2 parent type. Mutants selected for further re-screens are squared.

The best four mutants of VP library, with significant improvements in their activities and/or thermostabilities, were sequenced (**Figure 2.2.5.**). These variants shared the common feature of incorporating 4 mutations (E37K, V160A, T184M and Q202L) accumulated round after round of evolution in the same mature protein. Interestingly, the best variant of activity (R4 mutant with 3180 ± 30 ABTS-U/L) only contained the mentioned 4 mutations after 4 cycles of evolution. The remaining selected variants displayed a negative epistatic effect, *i.e.* the general combination of mutations is beneficial but at least one individual mutation is not, after incorporating new point

mutations (with improvement ranging from 1.7 to 1.1 fold *vs.* best parent type, 10C3 mutant). It is noteworthy that the best thermostable variant (24E10 mutant, with 1.23-fold better stability than 10C3) contains the same four mutations as R4 plus mutation G330R, which logically is responsible for the improvement in the thermostability. Mutation G330R shifted the T_{50} 2.2°C, from 60.5 to 62.7°C (**Figure 2.2.6A**), but decreased the activity of the variant almost 0.77 fold. Indeed, the improvement in protein stability came at the cost of reducing activity (the well-known tradeoff that usually appears between activity and stability for many single point mutations).

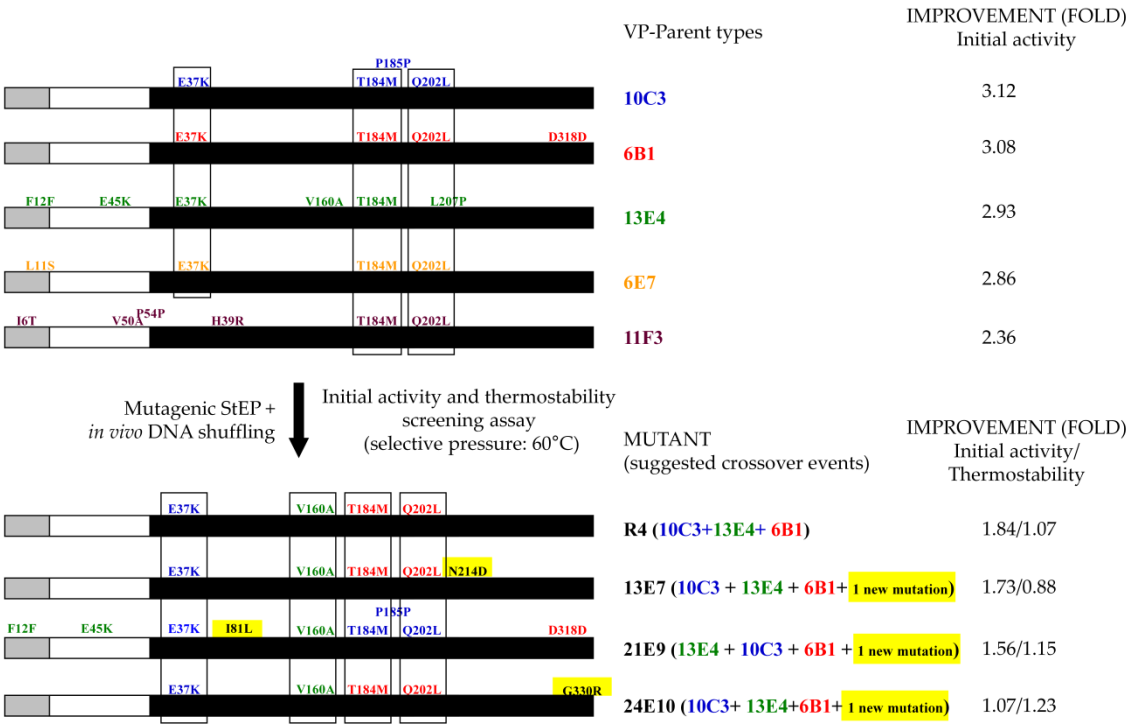

Figure 2.2.5. Improved variants screened from VP-library. The α factor pre-leader is represented in grey, the α factor pro-leader in white and the mature protein in black. Suggested recombination events are indicated in different colours. New point mutations are highlighted in yellow.

However, the recombination method designed for this experiment (mutagenic StEP + *in vivo* DNA shuffling) made possible to join the four beneficial mutations for the activity which somehow buffered the effect of incorporating the stabilizing mutation G330R, giving rise to an enzyme with similar activity to the parent types but more thermostable. Mutation G330R is placed at the C-terminal tail of VP, a controversial region that, although is not involved in VP oxidation of Mn^{2+} as initially suggested for the C-tail of *Phanerochaete chrysosporium* MnP (Ruiz-Dueñas *et al.*, 2007), presents a high mobility that prevented to fix the position of the last 12

residues when the VP crystal structure was solved (PDB entry 2BOQ). This highly-mobile region could contribute to the thermal denaturation of the protein, and it is possible to speculate that the introduction of an arginine side-chain at position 330 could stabilize the region, and the whole VP protein, by establishing some new interaction/s, whose nature cannot be determined due to the lack of valuable crystallographic data for the C-terminal tail of VP.

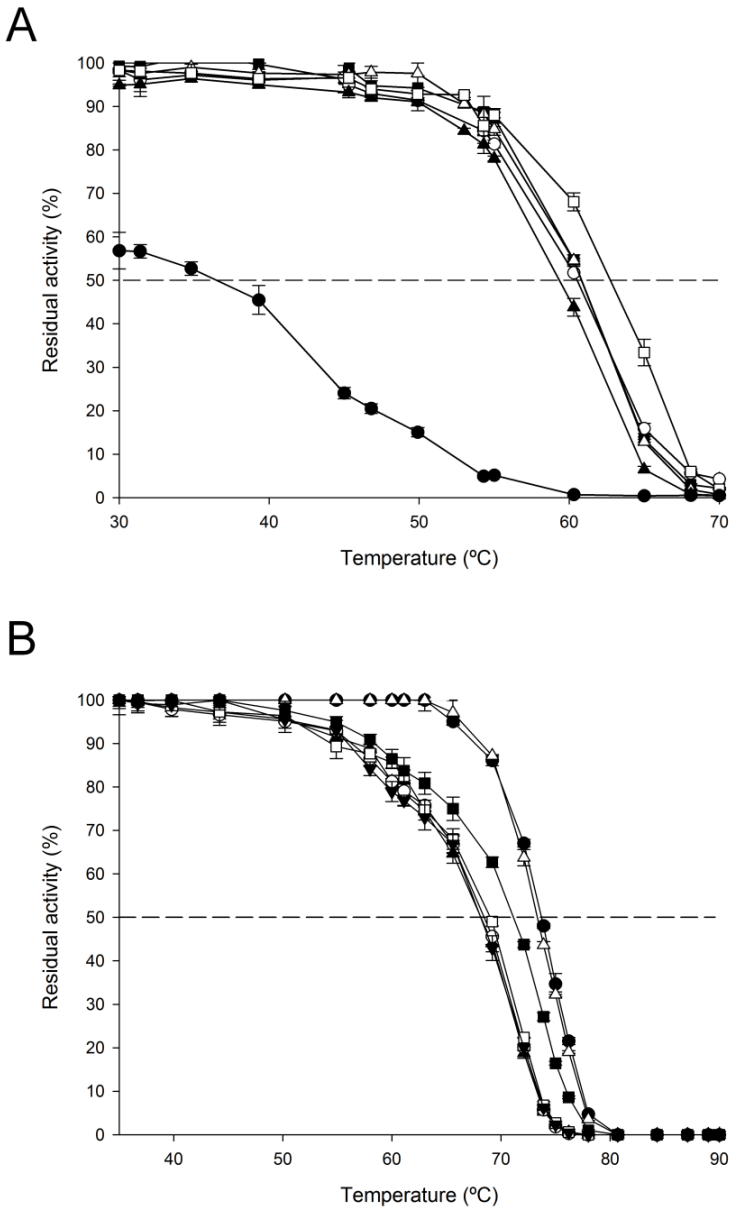

Figure 2.2.6. (**A**) T_{50} for VP parent types and different mutants of the evolutionary process. White squares, 24E10 mutant; black triangles, R4 mutant; black squares, 10C3 mutant (best parent type from 3rd generation); white circles, best parent type from 2nd generation; white triangles, best parent type from 1st

generation; black circles, native VP expressed in *E. coli* after *in vitro* refolded from inclusion bodies. (**B**) T_{50} for HRPL parent types and mutants of the *in vitro* evolution. Black circle, 1D11 mutant (4th generation); white triangle, 11A2 mutant (4th generation); black triangle, 7H2 mutant (5th generation); white circle, 6C8 mutant (6th generation); white square, 5H12 mutant (6th generation); black down triangle, 10B1 mutant (6th generation); black square, 16B10 mutant (6th generation). Each point, including the standard deviation, comes from three independent experiments.

The HRPL-library was generated by IvAM from 7H2 mutant, the best variant of the 5th round of evolution for total activity enhancement (**Figure 2.2.7.**). 7H2 was a good candidate to improve the thermostability: during the former round of evolution by mutagenic *in vivo* DNA shuffling, although its activity was improved almost 5-fold (achieving 1000 ± 24 ABTS-Units/L), its stability diminished considerably, with a decrease in the T_{50} of ~5°C *vs.* 1D11 and 11A2 parent types (**Figure 2.2.6B**). As main consequence of the drop in the T_{50}, 7H2 was unstable during long-term storage (losing about 30% of its activity after 15 days at 4°C). In the context of directed evolution experiments, this effect is not surprising and there are many examples in literature about falls in stability because of introducing beneficial but destabilizing mutations for enhanced activity (Bloom and Arnold, 2009). Taking into account that 7H2 was created from a single crossover event between 1D11 and 11A2 variants (**Figure 2.2.7.**), and that both parent types shares similar T_{50} values (73.7 and 73.3°C respectively, **Figure 2.2.6B**) it became clear that the only new mutation incorporated in 7H2 (F454S) was responsible for the dramatic drop in the T_{50}. The mutation was mapped in a model based on the *Trametes trogii* laccase (97% identity) crystal structure (Matera *et al.*, 2008). Phe454 is placed in a region close to the T1 cooper site, the place where the reducing substrate binds. The change from Phe to Ser at this position seems to disrupt several interactions with neighboring residues, which probably affects stability. Best mutants of the thermostability cycle where sequenced (**Table 2.2.1.**) and in all cases new mutations at the pre- or pro-leader were introduced benefiting the secretion levels by yeast (with improvement in total activities ranging from 1800 to 500 ABTS-U/L). The best thermostable mutant (16B10 variant) displayed 1.6-fold better stability than 7H2, shifting its T_{50} value over 3°C, but at the cost of reducing its activity by half (**Figure 2.2.6B** and **Figure 2.2.7.**). In spite of the fact that IvAM method takes advantage of mixing different mutational profiles created by polymerases with broad differences in mutational bias (**Table 2.2.1.**), the constraint of starting from only one single parent type hindered to find appropriate crossovers events (as happened in VP-libraries) that otherwise could have helped to prevent the detrimental effect on activity of introducing stabilizing mutations. 16B10 harbours 4 mutations in mature protein (two silent). Mutations A361T and S482L are placed at the surface of the protein, close to the C-end. Both mutations are at least 21 Å from the nearest catalytic copper atom (**Table 2.2.1.** and **Figure 2.2.8.**). Ala361 is located in a loop and interacts with Leu364 by a hydrogen bond. The change from Ala to Thr at position 361, kept the mentioned interaction and allowed one additional hydrogen bond with Ser372 placed in a beta-sheet. This structural reinforcement

upon mutation might confer rigidity to the protein enhancing its stability. Mutation S482L is in the neighbourhood of the disulfide bridge between Cys485 and Cys85. Ser482 is part of a α-helix and establishes a hydrogen bond with Gln479 of same motif. Inspection of the protein model suggests that the S482L mutation does not interrupt such a bond. The change of a polar amino acid by a bigger hydrophobic one might allow establishing hydrophobic interactions with surrounding residues which may further stabilize the protein structure at this region.

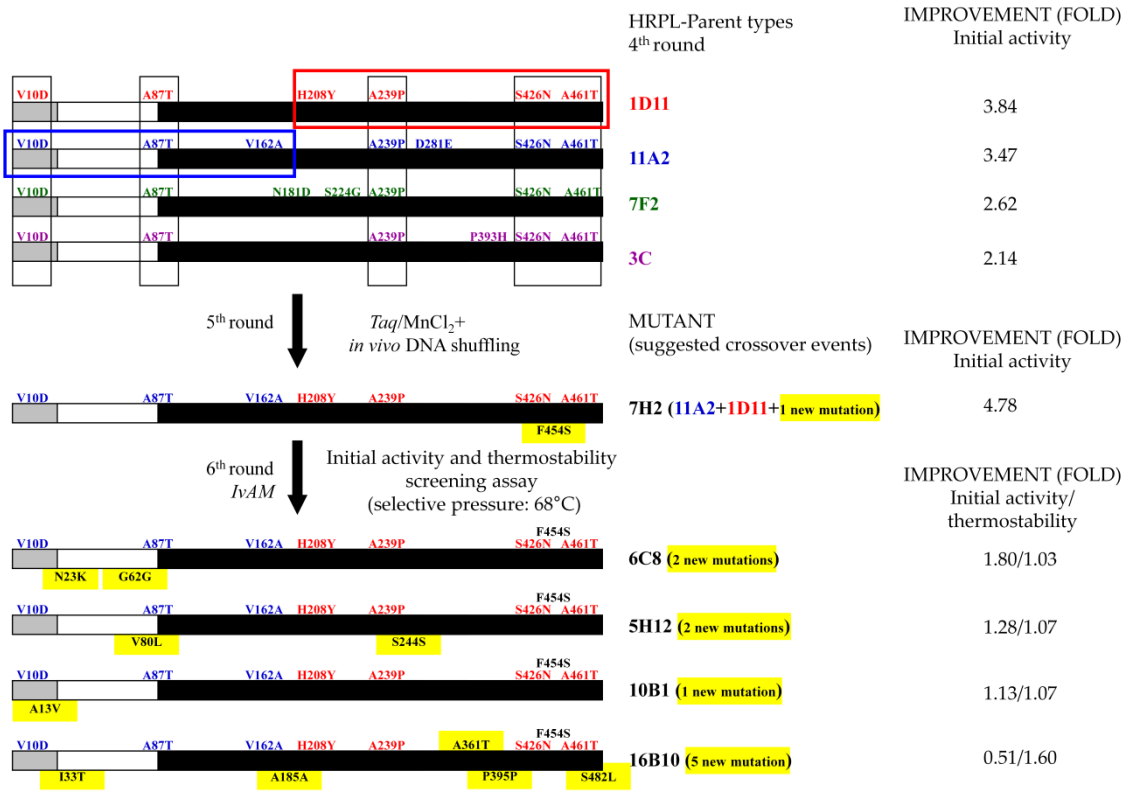

Figure 2.2.7. Improved variants screened from HRPL-library. α-factor pre-leader is represented in grey, α-factor pro-leader in white and mature protein in black. Suggested recombination events are indicated in different colours. New point mutations are highlighted in yellow. Squared in red and blue is highlighted the recombination event that took place between 11D11 and 11A2 to generate 7H2 mutant in the 4th cycle of evolution.

2.2.5. CONCLUSIONS

In summary, *S. cerevisiae* is a valuable cell factory for the directed evolution of ligninolytic enzymes for thermostability and taking together, the VP and the HRPL evolved variants share several common features. First, the thermostability improvements obtained for both VP and HRPL systems are especially significant near the enzyme inactivation temperatures: the best VP

(24E10) showed ~30% of its maximal activity at 65°C (3-fold more than the initial VP) and the best laccase (16B10) up to 40% of its maximal activity at 72°C (over 10-fold more than the corresponding parent type). Second, an apparently inherent trade-off between activity and stability appeared in both enzymes for different amino acid substitutions. Although not physically incompatible, in general protein scaffolds activity and thermostability tend to act as communicating vessels and the laboratory design of any of them usually come at the cost of its counterpart. For protein engineers, to find single mutations which improve both properties simultaneously is extremely difficult. In nature, stability is under selection just in the case that it is required for biochemical function, hence mutations which join activity and stability are rare taking into account the genetic drift and that a selective pressure towards both features at the same time is not frequently exerted. It has been reported that in principle is easier to evolve thermostability while keeping activity than vice versa, although recent research indicates that evolving activity while maintaining stability can be accomplished as well (Bloom *et al.*, 2006; Zumárraga *et al.*, 2007a). We have demonstrated that the generation of complex crossover events along with the introduction of new mutations facilitates the improvement in the stability of ligninolytic oxidoreductases buffering the drops on their activities. In the evolutionary scenario, the recombination methods described in this work for the generation of diversity along with the screening assay engineered for this specific task can be valuable tools not only to tailor thermostable ligninolytic oxidoreductases but also other enzymatic systems.

Table 2.2.1. HRPL selected mutants generated by IvAM.

Mutant	Amino acid change	Nucleotide change	Mutation type	Location	Secondary structure motif	Distance to the T1 site (Å)	Distance to the T2/T3 cluster (Å)
6C8	N23K	AA**C**69AA**A**	Tv	Pro-leader			
	G62G	$_{6}$GG**G**186GG**A**$_{11}$	Ts	Pro-leader			
5H12	V80L	**G**TA238**C**TA	Tv	Pro-leader			
	S244S	$_{8}$TC**G**1005TC**C**$_{14}$	Tv	Mature protein			
10B1	A13V	G**C**A38G**T**A	Ts	Pre-leader			
16B10	I33T	A**T**T98A**C**T	Ts	Pro-leader			
	A185A	$_{21}$GC**T**828GC**C**$_{13}$	Ts	Mature protein			
	A361T	**G**CG1354**A**CG	Ts	Mature protein	Loop	23	21
	P395P	$_{7}$CC**C**1458CC**T**$_{13}$	Ts	Mature protein			
	S482L	T**C**G1718T**T**G	Ts	Mature protein	Sheet	34	24

Synonymous mutations are underlined; nucleotide change is highlighted in bold; subscript numbers on codons indicate codon usage in *S. cerevisiae*. Tv: transversions. Ts: transitions.

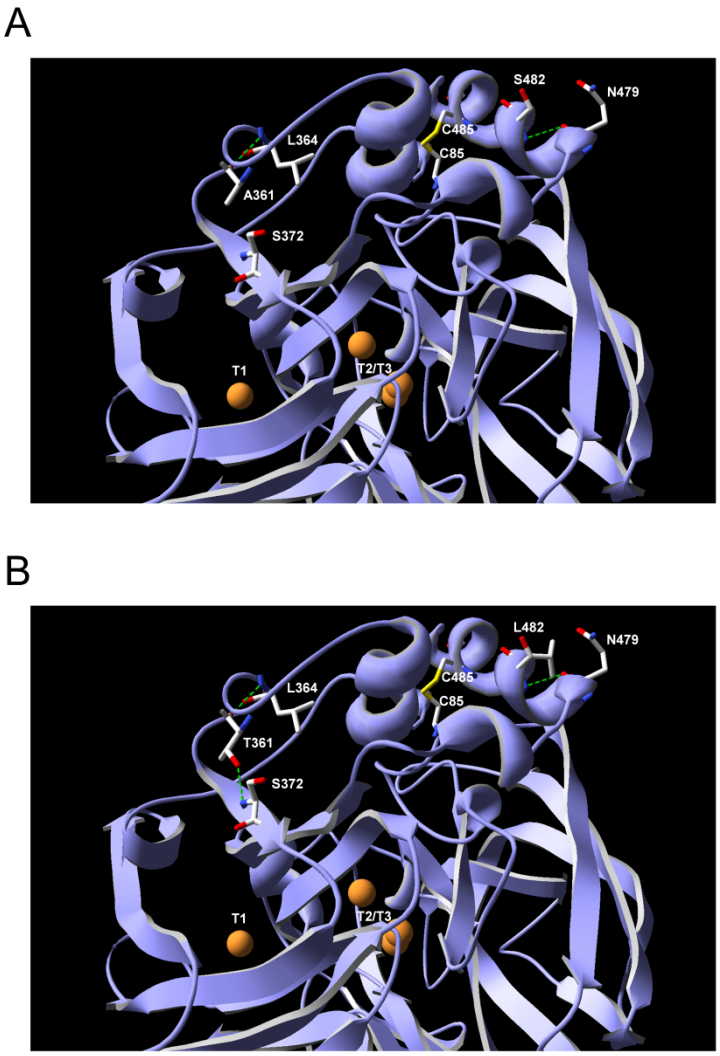

Figure 2.2.8. Location and surroundings of stabilizing mutations in HRPL. (**A**) Parent type. (**B**) 16B10 variant. The orange spheres represent Cu atoms.

CAPÍTULO 3

Directed evolution of fungal laccases

Diana Maté, Eva García-Ruiz, Susana Camarero and Miguel Alcalde

Published in *Current Genomics*, 2011, vol. 12, pp. 113-122.

2.3.1. SUMMARY

Fungal laccases are generalist biocatalysts with potential applications that range from bioremediation to novel green processes. Fuelled by molecular oxygen, these enzymes can act on dozens of molecules of different chemical nature, and with the help of redox mediators, their spectrum of oxidizable substrates is further pushed towards xenobiotic compounds (pesticides, industrial dyes, PAHs), biopolymers (lignin, starch, cellulose) and other complex molecules. In recent years, extraordinary efforts have been made to engineer fungal laccases by directed evolution and semi-rational approaches to improve their functional expression or stability. All these studies have taken advantage of *Saccharomyces cerevisiae* as a heterologous host, not only to secrete the enzyme but also, to emulate the introduction of genetic diversity through *in vivo* DNA recombination. Here, we discuss all these endeavours to convert fungal laccases into valuable biomolecular platforms on which new functions can be tailored by directed evolution.

2.3.2. LACCASES: GENERAL FEATURES

Laccases (EC 1.10.3.2) are typically extracellular monomeric glycoproteins that belong to the blue multicopper oxidase family (together with ascorbate oxidase, bilirubin oxidase and ceruloplasmin, among others) (Gianfreda *et al.*, 1999; Alcalde, 2007; Rodgers *et al.*, 2010). Laccases are considered to be ideal "*green catalysts*" since they are capable of oxidizing a wide variety of compounds in a straightforward manner, using O_2 from the air and releasing H_2O as the only by-product (Alcalde *et al.*, 2006a; Kunamneni *et al.*, 2007; Giardina *et al.*, 2010). These enzymes harbour one paramagnetic T1 copper (producing the beautiful characteristic blue-greenish colour in the oxidized resting state) where the oxidation of the reducing substrate takes place, and a trinuclear T2/T3 copper cluster where one molecule of oxygen is reduced to two molecules of water. The reaction mechanism acts like a battery, storing electrons from the monovalent oxidation reactions of the four reducing substrates required to reduce one molecule of oxygen to two molecules of water (Solomon *et al.*, 1996; Mayer and Staples, 2002; Claus, 2004;

Alcalde, 2007). Individually, laccases catalyze the oxidation of a wide range of aromatic compounds: *ortho* and *para*-diphenols, methoxy-substituted phenols, aromatic amines, benzenethiols, hydroxyindols or syringaldazine. In addition, inorganic/organic metal compounds can also serve as substrates of laccase. Mn^{2+} is oxidized to Mn^{3+} and also, $Fe(EDTA)^{2-}$ is accepted by the enzyme (Alcalde, 2007). Moreover, the range of reducing substrates can be further expanded to non-phenolic compounds (that are otherwise difficult to oxidize) by including redox mediators from synthetic or natural sources in the so-called laccase mediator systems. Upon oxidation by laccases, redox mediators oxidize other compounds by non-enzymatic mechanisms, thereby allowing substrates with higher redox potential than laccases to be transformed (*e.g.* lignin model compounds or polycyclic aromatic hydrocarbons, PAHs). Acting as diffusible electron carriers, these mediators can oxidize large polymers such as lignin, cellulose or starch, circumventing the inherent problems of enzyme hindrance normally associated to these substrates (Cañas and Camarero, 2010).

Laccases can be found in plants, fungi, bacteria and a few insects. Plant and bacterial laccases belong to the group of low-redox potential laccases (with redox potential at the T1 site [E°_{T1}] around +400 mV), and in particular the latter are of especial interest since they generally display high thermal stability, a quality really appreciated for industrial settings. However, their practical application is still reduced due to the limited range of substrates that they are capable of accepting. On the other hand, bacterial laccases are useful models for protein engineers, who can take advantage of the ease of manipulation of the bacterial host to carry out rational design or directed evolution. Indeed, recent studies on the directed evolution of laccase CotA from *Bacillus subtilis* has been reported to improve substrate specificity, functional expression and more recently, to use protein surface display to screen mutant libraries (Gupta and Farinas, 2009, 2010; Gupta *et al.*, 2010).

Fungal laccases have been studied comprehensively because of their strong catalytic capacities and in particular, there have been many studies into directed evolution of fungal laccases in the last few years. This interest initially stemmed from the high redox potential of the enzyme that permits a broader array of substrates to be oxidised. Indeed, several laccases from white rot fungi (involved in lignin combustion) possess an E°_{T1} close to +800 mV (Kunamneni *et al.*, 2007; Rodgers *et al.*, 2010). Thus, fungal laccases, and especially high-redox potential laccases (HRPLs), may serve: i) to produce 2nd generation biofuels (*i.e.* bioethanol) from lignocellulosic material (*i.e.* laccase and/or laccase-mediator system can oxidize the lignin content of agricultural wastes), or in the manufacture of new products from starch, cellulose and lignin with high added value; ii) in the food industry to process drinks and in bakery products; iii) in the paper industry for pulp-kraft biobleaching, the manufacture of mechanical pulps at low energy cost and to treat effluents; iv) in the textile industry for the remediation of dyes in effluents and textile bleaching (*i.e.* jeans); v) in nanobiotechnology, since laccases belong

to the exclusive group of enzymes capable of accepting electrons directly from a cathodic compartment which enables them to be used in the engineering of biosensors (for phenols, oxygen, azides, morphine, codein, catecholamines or flavonoids) with clinical and environmental applications, or in biofuel cells; vi) in the bioremediation through the oxidation of polycyclic aromatic hydrocarbons (PAHs), dioxines, halogenate compounds, phenolic compounds, bencenic derivatives, nitroaromatic compounds and dyes; and vii) in the organic synthesis of complex polymers, drugs, antibiotics and cosmetics (Alcalde *et al.*, 2006a; Xu, 2005; Kunamneni *et al.*, 2008a,b).

There have been many attempts to use rational approaches to engineer fungal laccases over the last couple of decades. In pioneering research carried out by Dr. Xu, several residues in the neighborhood of the catalytic copper ions were subjected to site directed mutagenesis in order to determine what parameters define the catalytic activity and the redox potentials of these enzymes (Xu *et al.*, 1998; Xu *et al.*, 1999; Palmer *et al.*, 2003). One consequence of these comprehensive structure-function studies was the generation of a collection of mutants with structural perturbations at the T1 copper center. In addition, directed evolution of fungal laccases (especially HRPLs) has received a recent boost by overcoming the obstacles associated with their functional expression in hosts suitable for *in vitro* evolution experiments (Camarero *et al.*, 2010; García-Ruiz *et al.*, 2010; Maté *et al.*, 2010; Maté *et al.*, 2011a).

2.3.3. DIRECTED EVOLUTION OF FUNGAL LACCASES

For most of us, directed evolution represents an elegant shortcut to tailor enzymes with improved features. By mimicking the Darwinist algorithm of natural selection through iterative steps of random mutagenesis and/or DNA recombination, the temporal scale of evolution can be collapsed from millions of years into months rather than weeks of bench work (Bloom and Arnold, 2009; Romero and Arnold, 2009; Tracewell and Arnold, 2009). In general, it is important to bear in mind three essential aspects when performing laboratory evolution experiments:

i) It is necessary to have a reliable and sensitive screening assay to identify the small improvements obtained in each round of evolution, generally 2 to 10-fold improvements per evolutive cycle. In the last years, colorimetric high-throughput screening assays specifically designed for laccase evolution have emerged. All these assays are based on natural or surrogate substrates of different chemical nature and complexity (from phenols to recalcitrant compounds), and typically, ABTS, DMP, syringaldazine, iodide, anthracene or Poly R-478 have been used to screen mutant laccase libraries (Alcalde *et al.*, 2002; Alcalde *et al.*, 2003; Alcalde *et al.*, 2005; Zumárraga *et al.*, 2007a; Maté *et al.*, 2010). Depending on the approach, the screening assays can be combined in an attempt to enhance several features at once [*e.g.* activity and stability (García-Ruiz *et al.*, 2010) or to

avoid the laccase becoming dependent of one specific substrate during evolution (Maté *et al.*, 2010; Camarero *et al.*, 2010)].

ii) Diversity should be generated by random mutagenesis and *in vivo* or *in vitro* DNA recombination protocols (Alcalde, 2010). Other approaches such as circular permutation, combinatorial saturation mutagenesis and the combination of rational design with directed evolution are also frequently included in the evolutionary strategy, generally yielding good results (Arnold, 2006; Zumárraga *et al.*, 2008a; Maté *et al.*, 2010).

iii) It must be possible to functionally express the genetic products with the desired traits. Although *Escherichia coli* is the preferred host organism for directed evolution experiments, the broad differences between the eukaryotic expression system of fungal laccases and that of bacteria (codon usage, missing chaperones, post-translational modifications such as glycosylation or the formation of disulphide bridges, and copper uptake) are shortcomings that are not easily overcome. In fact, all attempts to functionally express fungal laccases in bacteria have resulted in misfolding and the formation of inclusion bodies. Alternatively, the secretory machinery of *Saccharomyces cerevisiae* permits post-translational modifications, and it is also an excellent host to carry out laboratory evolution experiments (Bulter and Alcalde, 2003; Bulter *et al.*, 2003b).

2.3.3.1. *Saccharomyces cerevisiae* for directed laccase evolution: a biomolecular tool box for the generation of diversity

There are four main reasons to use *S. cerevisiae* for the laboratory evolution of fungal laccases:

i) High transformation efficiencies: over 15,000 clones per transformation reaction can be generated.

ii) Episomal vectors are available that facilitates the recovery of interesting mutants without integration into the genomic DNA as generally happens in yeasts such as *Pichia pastoris*. However, engineering strategies for the evolution of hydroxynitrile lyases in *P. pastoris* have been designed recently, involving the integration of linear expression cassettes to construct and express mutant libraries (Liu *et al.*, 2008).

iii) The glycosylation and secretion of laccases avoids the tedious and cumbersome lysis steps required for bacteria. In addition, working with supernatants makes the validation of the screening assay easier since there is much less interference than with complex lysate mixtures.

iv) And last but not least, a high level of homologous DNA recombination can be achieved, which enables *in vivo* shuffled mutant libraries to be produced or the development of new tools to generate diversity (Alcalde *et al.*, 2006a; Zumárraga *et al.*, 2008b; Alcalde, 2010).

One of the first directed evolution experiments using *in vivo* DNA shuffling was carried out to engineer a low redox potential peroxidase from *Coprinus cinnereus* with oxidative stability (Cherry *et al.*, 1999). This pioneering work opened an array of possibilities that led to many research groups (among which we are included) beginning to develop new strategies of DNA recombination (Bulter *et al.*, 2003a; Okkels, 2004; Cusano *et al.*, 2009; Alcalde, 2010). Taking advantage of yeast physiology, our group has designed several *in vivo* DNA recombination methods (IVOE, IvAM) with the aim of generating suitable crossover events or varying the mutational bias in the framework of *in vitro* laccase evolution (**Figure 2.3.1**). Sequence splicing by IVOE (*I*n *V*ivo *O*verlap *E*xtension) is a robust and reliable method through which combinatorial saturation mutagenesis, deletion and/or insertion mutagenesis, site-directed recombination or site-directed mutagenesis can be accomplished straightforwardly (Alcalde *et al.*, 2006b; Alcalde, 2010). The method is based on the engineering of mutagenized primers that contain suitable overhangs, with homologous regions that anneal to each other to generate an autonomously replicating vector containing the mutant gene/s (**Figure 2.3.1A**). This strategy mimics the classical SOE (*S*equence *O*verlap *E*xtension) but it removes several steps, including the *in vitro* cloning. IVOE has been employed to construct mutant libraries for directed evolution of ascomycete and basidiomycete laccases, as well as to carry out semi-rational studies (*i.e.* combinatorial saturation mutagenesis coupled to high-throughput screenings (Zumárraga *et al.*, 2008b; Maté *et al.*, 2010). IvAM (*I*n *v*ivo *A*ssembly of *M*utant libraries) is another approach that has been successfully used to engineer fungal laccases for improved organic co-solvent tolerance (**Figure 2.3.1B**) (Zumárraga *et al.*, 2007a, 2008a). Generally, error-prone PCR methods are unsatisfactory because they are associated with a limited and predicted mutational spectrum derived from the intrinsic bias of each DNA polymerase. To overcome this problem, the mutation biases of different polymerases can be combined by alternating between them in successive rounds of evolution. IvAM has allowed us to explore the laccase sequence space through the *in vivo* DNA shuffling of several mutant libraries with different mutational spectra in a single round of evolution. It is also possible to bring together strategies for *in vitro* and *in vivo* DNA recombination to evolve enzymes in the laboratory. For example, CLERY (*C*ombinatorial *L*ibraries *E*nhanced by *R*ecombination in *Y*east) combines *in vitro* and *in vivo* DNA shuffling (Abécassis *et al.*, 2000). In a similar approach, we have combined mutagenic StEP (*St*aggered *E*xtension *P*rocess) with *in vivo* DNA shuffling to evolve ligninolytic peroxidases. There is also an interesting report on how to engineer chimeric fungal laccases from *Trametes* sp. C30 by *in vivo* DNA shuffling (Cusano *et al.*, 2009), where a low redox potential laccase gene was used in all the chimeric libraries to guarantee functional expression. This example constitutes a valuable point of departure for the potential application of the *S. cerevisiae* machinery for laccase chimeragenesis.

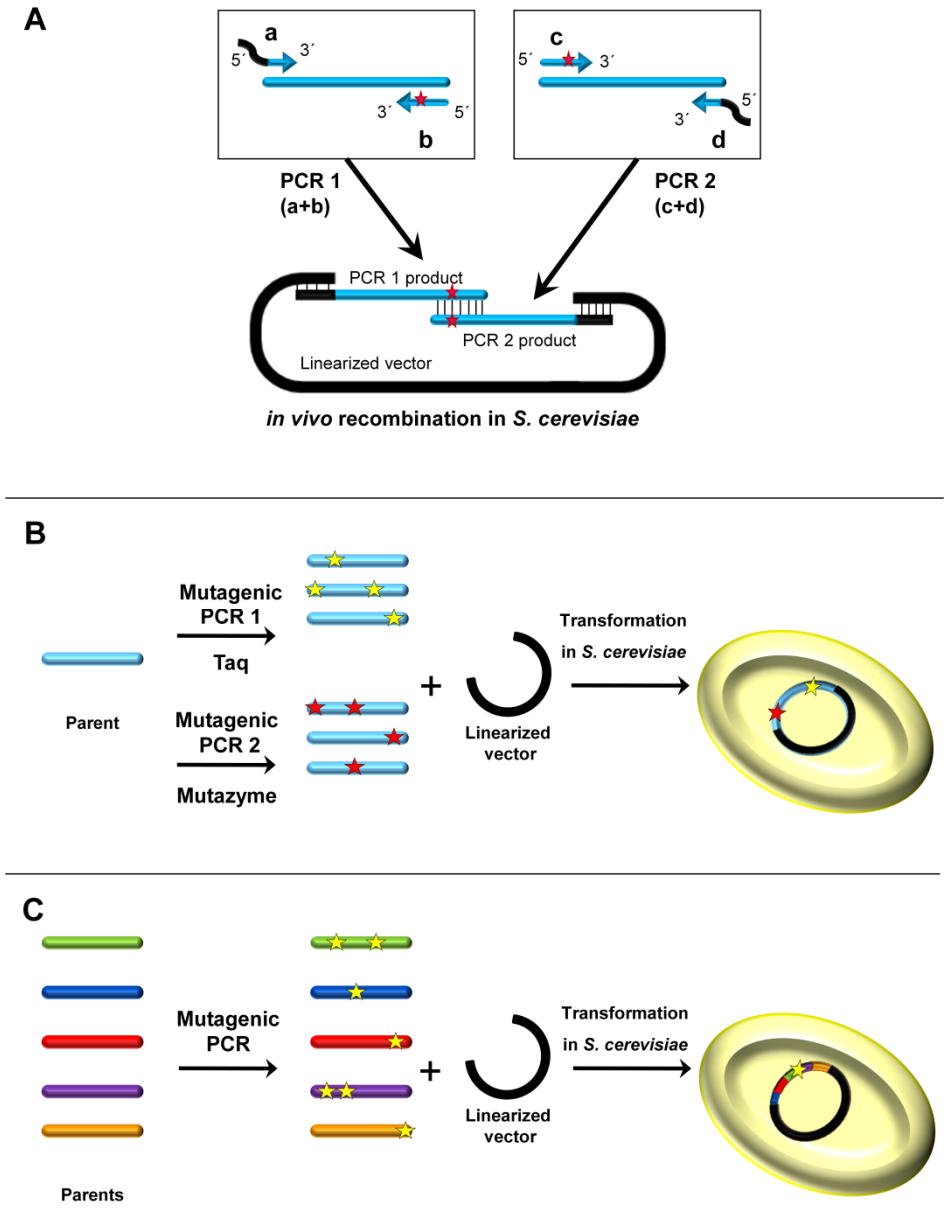

Figure 2.3.1. Different *in vivo* DNA recombination strategies based on the *S. cerevisiae* apparatus. (**A**) IVOE; (**B**) IvAM; (**C**) *in vivo* DNA shuffling combined with mutagenic PCR.

2.3.3.2. Directed evolution of ascomycete laccases

The first laccase gene subjected to directed evolution was the *Myceliophthora thermophila* laccase (MtL), a low-medium redox potential ascomycete laccase that is very thermostable (with T_{50} values ~75.6°C) (Bulter *et al.*, 2003a). In this work, 10 rounds of laboratory evolution were carried out to achieve the strongest functional expression of a laccase in *S. cerevisiae* yet reported

(up to 18 mg/L, **Figure 2.3.2.**). The basic tools for the generation of diversity included error prone PCR, StEP and *in vivo* DNA shuffling. The latter was modified in such a manner that error-prone PCR products were recombined *in vivo* to introduce new mutations in conjunction with recombination (**Figure 2.3.1C**). Furthermore, backcrossing recombination was employed to eliminate neutral mutations. In the final rounds of evolution, PCR and *in viv*o gap repair were used to recombine neighbouring mutations in a site-directed fashion, once again taking advantage of the eukaryotic apparatus (referred to as *in vivo* assembly recombination) which proved extremely useful to eliminate some deleterious mutations. The sequence targeted for directed evolution included the native prepro-leader, as well as the C-terminal tail of the gene that encode for parts of the protein that are cleaved during maturation. The ultimate evolutionary product obtained after screening over 20,000 clones, the T2 mutant, harboured 14 mutations (**Figure 2.3.3A**). The single most beneficial mutation was found in the C-terminal tail, introducing a cleavage site for the *KEX2* protease of the Golgi compartment of *S. cerevisiae*. This mutation probably adjusted the sequence to the different protease specificity of the heterologous host. In a later study, we employed the T2 evolved mutant to study the role of the C-terminal plug of ascomycete laccases. Using combinatorial saturation mutagenesis through IVOE, a direct relationship between the C-terminal plug and a conserved tripeptide in the vicinity of the reducing substrate binding site was determined (Zumárraga *et al.*, 2008b).

Many applications of fungal laccases (bioremediation, lignocellulose processing, organic synthesis, etc.) require high concentrations of organic co-solvents in which laccases may unfold and lose their activity (Kunamneni *et al.*, 2008a). In another recent study, we used the evolved MtL (T2 mutant) as our point of departure to confer organic co-solvent tolerance (Zumárraga *et al.*, 2008a). In this work, five rounds of laboratory evolution were carried out to explore 13,000 clones, using IVOE, IvAM and error-prone PCR, in combination with *in vivo* DNA shuffling for library creation. The laboratory evolution strategy was carefully planned according to the following rules:

i) Screening was performed (based on the oxidation of ABTS) in the presence of two co-solvents of different chemical nature and polarity in order to identify variants active in both co-solvents. The ultimate goal was to provide promiscuity in other water-solvent mixtures.

ii) To improve the activity and stability in organic co-solvents, only those mutant *hits* that retained their stability and that were more active were considered as candidates for further cycles of evolution.

iii) The extreme selective pressure, increasing the concentrations of organic co-solvents from 20% in the first cycles up to 60% in the last round, further drove the evolution.

iv) The spectro-electrochemistry of the variants was studied in depth to assess the influence of the evolution process on the transit of electrons through the laccase structure.

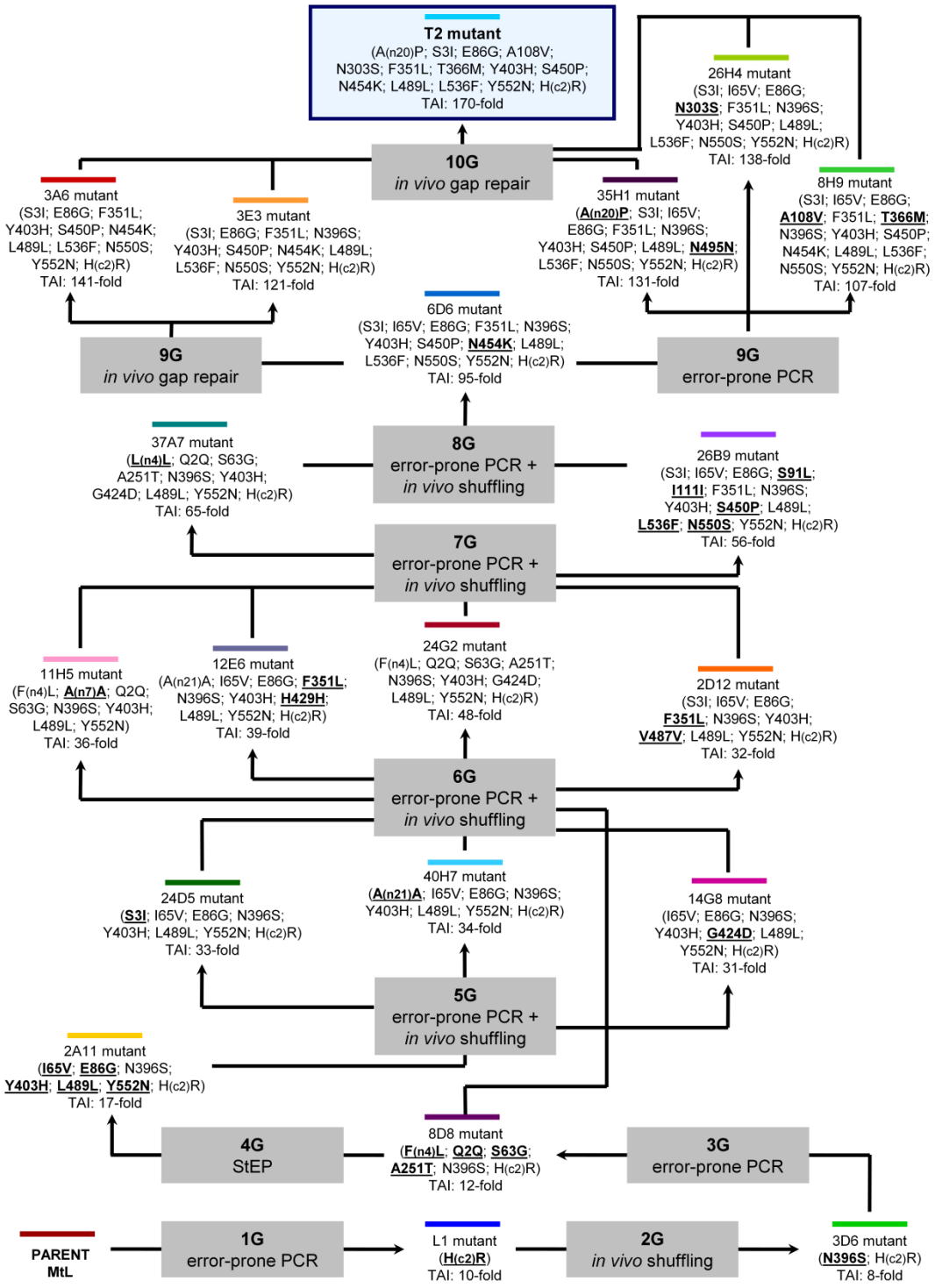

Figure 2.3.2. Artificial evolution pathway for MtL in yeast. TAI: total activity improvement over MtL parent type.

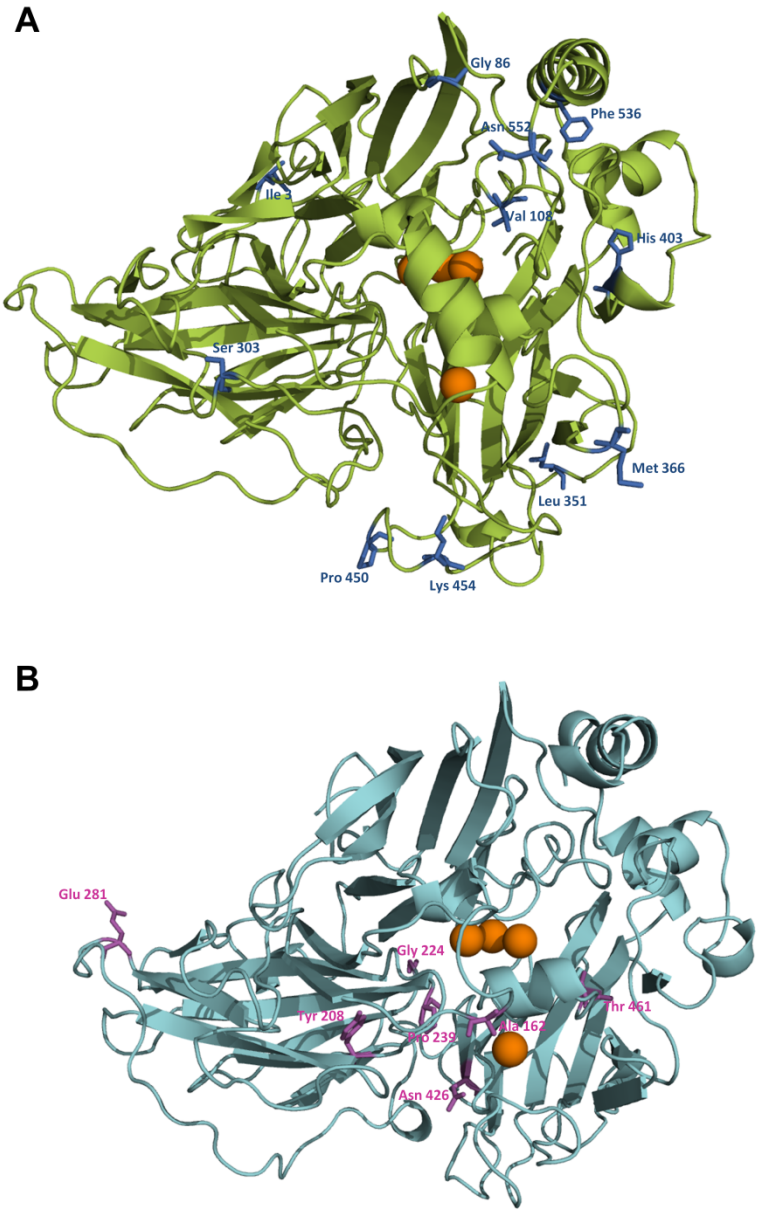

Figure 2.3.3. Amino acid substitutions accumulated in evolved laccases for functional expression in *S. cerevisiae*. (**A**) MtLT2-variant; (**B**) HRPL PM1 (OB-1 variant). Orange spheres represent copper atoms. Amino acid substitutions found in mature MtLT2 and OB-1 are highlighted with stick structures.

The final mutant (R2 variant) was fairly active and stable at concentrations as high as 50% of organic co-solvents, (retaining between 20-30% of its activity in aqueous solution). Moreover, this variant showed promiscuity for different organic co-solvents (DMSO, DMF, DMA, acetonitrile, acetone, ethanol and methanol). Significantly, the spectro-electrochemical features

of the enzyme were slightly modified (*i.e*. E°_{T1} and copper geometries), although these changes did not exert any important differences in either its kinetics or stability. R2 harboured four mutations in the mature protein (E182K, S280N, L429N and N552H), as well as two mutations at the C-terminal tail (G8D and E9K). The mutations at the C-terminal tail seemed to affect protein folding, whereas some mutations at the surface of the mature laccase established new interactions, either through salt bridges or hydrogen bonds. These novel interactions were reflected in the structural reinforcement of the regions amenable to denaturation under harsh conditions.

2.3.3.3. Directed evolution of HRPLs

The past successes with MtL evolution cannot easily be translated to their HRPL counterparts, in part because MtL is an ascomycete laccase that facilitates its functional expression in *S. cerevisiae*. Several directed evolution experiments have been attempted by error prone PCR using HRPLs from *Pleurotus ostreatus* (Festa *et al*., 2008; Miele *et al*., 2010a,b). The results confirmed a general improvement in the total activity but poor secretion limits their practical engineering for other purposes. We recently described for the first time how to engineer HRPLs that can be expressed strongly by *S. cerevisiae*, enhancing their activities and thermostabilities (Maté *et al*., 2010). Two different HRPLs were used to achieve this goal, the laccase from basidiomycete PM1 (Maté *et al*., 2011a) and the laccase from *Pycnoporus cinnabarinus* (PcL) (Camarero *et al*., 2010). Several fusion proteins were tested by replacing the native signal sequences with others used successfully during heterologous expression in yeast. The best result was obtained with the α-factor prepro-leader and accordingly, the α-PM1 and α-PcL fusion proteins could then be subjected to the corresponding artificial evolution pathways. Interestingly, the joint evolution of the α-factor prepro-leader plus the HRPL allowed us to adjust each to the different protease specificities of the heterologous host throughout its transit from the endoplasmic reticulum to the Golgi compartment. For α-PM1 laccase, eight rounds of evolution were carried out in combination with rational approaches (**Figure 2.3.4**.). After screening over 50,000 clones generated by random mutagenesis, *in vivo* DNA shuffling, IvAM and site directed mutagenesis, the total laccase activity (which is the product of its secretion and kinetics) was enhanced up to 34,000-fold, the largest improvement ever reported for this kind of system (Maté *et al*., 2010a). We attribute such a large improvement to the joint evolution of the prepro-leader and the laccase, which meant that a synergistic effect was produced during its exportation by yeast. The ultimate variant obtained through this evolutionary process, the OB-1 mutant, was readily secreted by *S. cerevisiae* (up to 8 mg/L) in a soluble, very active and very stable form, particularly with respect to temperature (with a T_{50} value of 73°C), pH and co-solvents (**Figure 2.3.3B**).

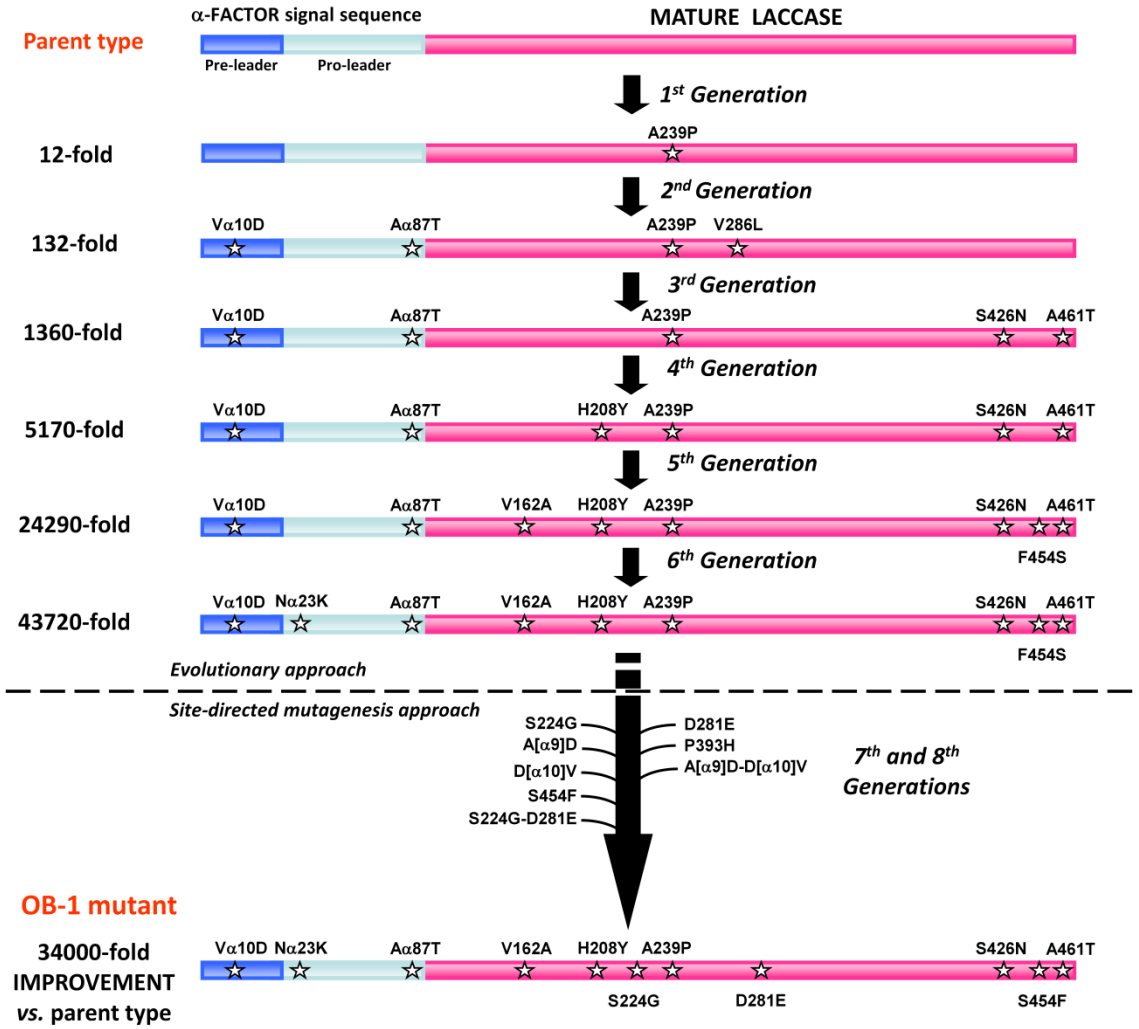

Figure 2.3.4. Combination of directed evolution and rational approaches for the engineering of HRPLs.

Among the strategies engineered to evolve HRPLs, the mutational exchange and the recovery of beneficial mutants should be highlighted. With mutational exchange, several mutations found in both evolutionary programmes (for the α-PM1 and the α-PcL) were switched from one system to another, taking advantage of their close sequence homology (above 75%). Interestingly, some mutations found in the hydrophobic core of the α-factor pre-leader were valuable in both systems, which opens the possibility of evolving the α-factor prepro-leader as a universal signal peptide for the heterologous expression of fungal laccases in yeast. With mutational recovery, some beneficial mutations ruled out by the yeast recombination apparatus could be recovered by site-directed mutagenesis of OB-1 having mapped them first in the family tree of the whole evolution experiment. Last but not least, we

paid special attention to protein stability since the overall philosophy of this work was to create a scaffold on which new functions could be developed and that was sufficiently stable to tolerate the introduction of a new set of beneficial mutations. Hence, the drops in stability produced during evolution by the accumulation of some beneficial but destabilizing mutations could be recovered by rational approaches, coupled with the screening of mutant libraries for thermostability (**Figure 2.3.5**.).

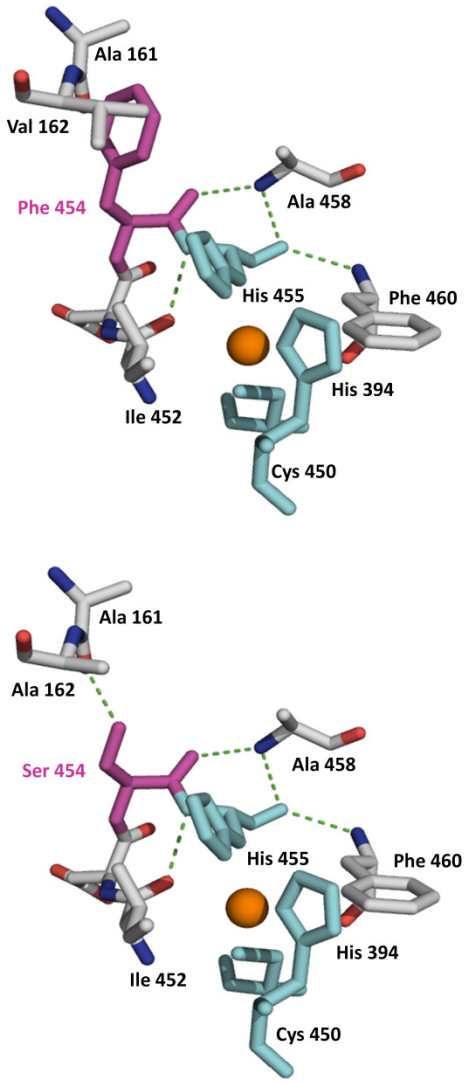

Figure 2.3.5. Rational approach for thermostability during the evolution of PM1 laccase. Mutation F454S discovered in the 5th round enhanced the activity but at the cost of reducing the thermal stability (a hydrogen bond formed with Ala161 may affect the distance coordination between His455 and the T1 Cu). The reverted variant S454F completely recovered its stability which allowed the introduction of a new set of beneficial mutations.

What have we learnt?

Over the years, *S. cerevisiae* has helped us to engineer strategies for the directed evolution of fungal laccases. The low redox potential laccase MtL was the first successful example (Bulter *et al.*, 2003b) and since then, we have designed specific approaches for the laboratory evolution of HRPLs that combine *in vivo* and *in vitro* tools with rational approaches (Sayut and Sun, 2010). The evolved fungal laccases mentioned in this review constitute unique platforms for further protein engineering through directed evolution, principally aimed at generating enzymes that can be used in attractive biotechnological applications. Indeed, we are now in a position to tailor HRPLs for different purposes, ranging from the engineering of 3D-nanobiodevices for analytical or biomedical use to the construction of cell factories in yeast (Rodgers *et al.*, 2010; Sayut and Sun, 2010). There are still some hurdles to overcome and some questions that should be answered: why is the functional expression of laccases in yeast so tremendously difficult?, would it be possible to evolve high-redox potential laccases in bacteria?, is it feasible to enhance the laccase redox potential beyond natural limits by directed evolution or by rational means without disturbing its stability?… and more significantly, would that improvement necessarily mean better activity? We hope that in the near future, new HRPLs engineered by directed evolution and rational approaches can affront the attractive challenges presented by traditional and modern biocatalysis.

CAPÍTULO 4

Switching from blue to yellow: altering the spectral properties of a high-redox potential laccase by directed evolution

Diana M. Mate, Eva Garcia-Ruiz, Susana Camarero, Vladimir V. Shubin, Magnus Falk, Sergey Shleev, Antonio O. Ballesteros and Miguel Alcalde

Published in *Biocatalysis and Biotransformations*, 2013, vol. 31, pp. 8-21.

2.4.1. SUMMARY

During directed evolution to functionally express the high redox potential laccase from the PM1 basidiomycete in *Saccharomyces cerevisiae*, the characteristic maximum absorption at the T1 copper site (Abs_{610}T1Cu) was quenched, switching the typical blue colour of the enzyme to yellow. To determine the molecular basis of this colour change, we characterized the original wild-type laccase and its evolved mutant. Peptide printing and MALDI-TOF analysis confirmed the absence of contaminating protein traces that could mask the Abs_{610}T1Cu, while conservation of the redox potential at the T1 site was demonstrated by spectroelectrochemical redox titrations. Both wild-type and evolved laccases were capable of oxidizing a broad range of substrates (ABTS, guaiacol, DMP, synapic acid) and they displayed similar catalytic efficiencies. The laccase mutant could only oxidize high redox potential dyes (Poly R-478, Reactive Black 5, Azure B) in the presence of exogenous mediators, indicating that the yellow enzyme behaves like a blue laccase. The main consequence of over-expressing the mutant laccase was the generation of a six-residue N-terminal acidic extension, which was associated with the failure of the *STE13* protease in the Golgi compartment giving rise to alternative processing. Removal of the N-terminal tail had a negative effect on laccase stability, secretion and its kinetics, although the truncated mutant remained yellow. The results of CD spectra analysis suggested that polyproline helixes were formed during the directed evolution altering spectral properties. Moreover, introducing the A461T and S426N mutations in the T1 environment during the first cycles of laboratory evolution appeared to mediate the alterations to Abs_{610}T1Cu by affecting its coordinating sphere. This laccase mutant is a valuable departure point for further protein engineering towards different fates.

2.4.2. INTRODUCTION

Fungal laccases (benzenediol:oxygen oxidoreductase, EC 1.10.3.2) are remarkable biocatalysts with broad substrate specificity and very few requirements (Riva, 2006; Rodgers *et al.*, 2010). These enzymes can oxidize a wide range of compounds using oxygen from the air and releasing water as the sole by-product. Fungal laccases oxidize ortho- and para-diphenols, methoxy-substituted phenols, aromatic amines, benzenethiols, hydroxyindols, syringaldazine and some inorganic/organic metal compounds, as well as other molecules (Alcalde, 2007). Furthermore, in the presence of redox mediators from natural or synthetic sources, laccases can expand their substrate specificity to oxidize higher redox potential compounds (including non-phenolic substrates such as lignin derivatives, synthetic organic dyes and PAHs) (Cañas and Camarero, 2010). Thus, fungal laccases may have many potential applications in the front line of green chemistry, in the bioremediation of pollutants, the production of second generation biofuels (bioethanol, biobutanol), the engineering of biosensors and biofuel cells, in the paper, textile and food industries and in the organic synthesis of antibiotics, drugs, cosmetics, polymers and other compounds (Xu, 2005; Alcalde *et al.*, 2006a; Kunamneni *et al.*, 2007; Kunamneni *et al.*, 2008a,b). Typically, laccases contain four copper atoms arranged in two highly conserved regions. The reducing substrate binds at the T1 Cu site, while the trinuclear Cu cluster (containing one T2 Cu and two T3 Cu) is involved in the binding of molecular oxygen, which is concomitantly reduced to two molecules of water. Upon purification, the paramagnetic T1 Cu (in its oxidized resting state, Cu^{2+}) confers the characteristic blue colour of laccase (with an extinction coefficient ranging from 4900 to 5700 $M^{-1}cm^{-1}$ at the Abs_{610}T1Cu) (Solomon *et al.*, 1996; Davies and Ducros, 2002). This particular feature accounts for the name of the blue-multicopper protein group, which is made up of laccases (fungal, bacterial, plant or insect), bacterial copper nitrite reductases, the plant ascorbate oxidases, the mammalian plasma proteins ceruloplasmins, and fungal and bacterial bilirubin oxidases (Baldrian, 2006; Alcalde, 2007). In addition to blue laccases, several other laccases with distinct spectral characteristics have been described, such as yellow-brown laccases obtained from white-rot fungi under solid-state fermentation conditions. These laccases do not contain Abs_{610}T1Cu, supposedly due to the presence of a putative natural mediator derived from lignin biodegradation located at the T1 Cu site (Leontievsky *et al.*, 1997a,b; Pozdnyakova *et al.*, 2004, 2006a). White laccases produced by different basidiomycete strains have also been described with a broad band at around 400 nm but no absorbance at 610 nm. These white laccases contain two atoms of zinc and one iron/manganese atom, instead of the characteristic trinuclear copper cluster (Palmieri *et al.*, 1997; Min *et al.*, 2001; Haibo *et al.*, 2009). Recently, a unique white laccase containing a single Cu atom and lacking any other metal content was also reported (Schückel *et al.*, 2011).

Formerly, we carried out the directed evolution of a high redox potential laccase from the basidiomycete PM1 to achieve functional heterologous expression in a soluble, stable and active form (Maté *et al.*, 2010). The final variant of this process (OB-1 mutant) was readily secreted by yeast, and it was stable at high temperatures (T_{50} = 73°C), in the presence of organic co-solvents and over a broad pH range (3.0 to 9.0). While the evolved laccase retained the general characteristics of the wild-type blue PM1 laccase (Coll *et al.*, 1993a), the mutant was yellow-brownish in colour. To further investigate this change in the spectral properties of the enzyme, we performed a comprehensive biochemical and spectroelectrochemical characterization of the evolved and wild-type laccases.

2.4.3. MATERIAL AND METHODS

2.4.3.1. Materials

The basidiomycete PM1, originally isolated from a waste-water from a paper factory, was obtained from the Spanish Type Culture Collection (CECT 2971). Laccase mutant OB-1 was engineered as described previously (Maté *et al.*, 2010). The laccase from *Trametes hirsuta* was kindly donated by Prof. A. Yaropolov (Institute of Biochemistry, Moscow, Russia) and the laccase from *Trametes versicolor* by Prof. Frances H. Arnold (California Institute of Technology [Caltech], Pasadena, CA, USA). The uracil-independent and ampicillin resistant shuttle vector pJRoC30 was also obtained from Caltech (CA, USA). The 2,2′-azino-bis(3-ethylbenzothiazoline-6-sulfonic acid) (ABTS), 2,6-dimethoxyphenol (DMP), guaiacol, sinapic acid, reactive black 5 (RB5), poly R-478, azure blue (Azure B), 1-hydroxybenzotriazole (HBT), acetosyringone, potassium ferrocyanide ($K_4[Fe(CN)_6]$) and potassium cyanomolybdate (IV) ($K_4[Mo(CN)_8]$) were all purchased from Sigma-Aldrich (Madrid, Spain). The *E. coli* XL2-Blue ultracompetent cells were obtained from Stratagene (La Jolla, CA, USA) and the protease-deficient *S. cerevisiae* strain BJ5465 from LGCPromochem (Barcelona, Spain). The Zymoprep Yeast Plasmid Miniprep kit, Zymoclean Gel DNA Recovery kit, and the DNA Clean and Concentrator-5 kit were all purchased from Zymo Research (Irvine, CA). The NucleoSpin Plasmid kit was obtained from Macherey-Nagel (Düren, Germany) and the restriction enzymes *Bam*HI and *Xho*I from New England Biolabs (Hertfordshire, UK). All chemicals were of reagent-grade purity.

2.4.3.2. Culture media

Minimal medium contained 100 mL 6.7% sterile yeast nitrogen base, 100 mL 19.2 g/L sterile yeast synthetic drop-out medium supplement lacking uracil, 100 mL sterile 20% raffinose, 700 mL *dd*H_2O and 1 mL 25 g/L chloramphenicol. Yeast Peptone (YP) medium contained 10 g yeast extract and 20 g peptone in 650 mL *dd*H_2O. Expression medium contained 720 mL YP, 67 ml 1 M

potassium phosphate buffer pH 6.0, 111 mL 20% galactose, 2 mM $CuSO_4$, 25 g/L ethanol and 1 ml 25g/L chloramphenicol, made up to 1000 mL with *dd*H_2O. YPD solution contained 10 g yeast extract, 20 g peptone, 100 mL 20% sterile glucose and 1 ml 25g/L chloramphenicol, made up to 1000 mL with *dd*H_2O. SC drop-out plates contained 100 mL 6.7% sterile yeast nitrogen base, 100 mL 19.2g/L sterile yeast synthetic drop-out medium supplement lacking uracil, 20 g bacto agar, 100 mL 20% sterile glucose and 1 mL 25g/L chloramphenicol, made up to 1000 mL with *dd*H_2O. GAE medium contained (per litre) 10 g glucose, 1 g asparagine, 0.5 g yeast extract, 0.5 g K_2HPO_4, 1 g $MgSO_4$ $7H_2O$ and 0.01 g $FeSO_4$ $7H_2O$.

2.4.3.3. Truncated variant (OB-1del mutant)

The extra N-terminal sequence was removed by deletion mutagenesis using *In Vivo* Overlap Extension (IVOE, **Figure 2.4.5.**, p. 141) (Alcalde *et al.*, 2006b; Alcalde, 2010). The primers used for PCR 1 were RMLN (5′-CCTCTATACTTTAACGTCAAGG-3′, which binds to bp 5′-420-441-3′ of pJRoC30-OB-1) and ALPHA2 (5′-ACCGTTGGAGATGGTGAGGTCTGCGACTGGCCCAATGCTTCTTTTCTCGAGAGATACCC CTTC-3′, which binds to bp 5′-701-781-3′ of pJRoC30-OB-1). The primers for PCR 2 were OB-1MAT (5′-AGCATTGGGCCAGTCGCAGAC-3′, which binds to bp 5-743-763-3′ of pJRoC30-OB-1) and RMLC (5′-GGGAGGGCGTGAATGTAAGC-3′, which binds to bp 5′-2288-2307-3′ of pJRoC30-OB-1). The pJRoC30 plasmid was linearized with *Xho*I and *Bam*HI, and subsequently, both the linearized plasmid and the PCR products were cleaned, concentrated and loaded onto a low melting point preparative agarose gel for purification using the Zymoclean Gel DNA Recovery kit (Zymo Research). The linearized plasmid (100 ng) was mixed with the products from PCR1 and PCR 2 (200 ng each) and transformed into competent *S. cerevisiae* cells. Individual clones were picked and cultured in 96-well plates (GreinerBio-One, Frichkenhausen, Germany) containing 50 μL of minimal medium per well and screened by the ABTS procedure as described previously (Maté *et al.*, 2010). Positive clones were re-screened (Maté *et al.*, 2010), and the *in vivo* repaired plasmid was recovered and the truncated fusion gene confirmed by DNA sequencing.

2.4.3.4. Production and purification of laccases

Production of the wild-type laccase in the PM1 basidiomycete (PM1L-wt)

The PM1 basidiomycete was cultured in GAE medium (2 x 50 mL in 250-mL flasks) for 5 days at 37°C and 240 rpm, and the pellets from the two flasks were homogenized in distilled water. A 4 mL suspension of the homogenate was used to inoculate 1-L flasks containing 300 mL of GAE medium supplemented with 300 μM $CuSO_4$. After 7 days of incubation (maximum laccase activity) the liquid cultures were filtered and the laccase was purified.

Production of the mutant laccase in S. cerevisiae

A single colony from the *S. cerevisiae* clone containing the mutant laccase gene (OB-1 and OB-1del) was picked from a synthetic complete (SC) drop-out plate, inoculated in 10 mL of minimal medium and incubated for 48 h at 30°C and 225 rpm (Micromagmix shaker, Ovan, Spain). An aliquot of cells was removed, inoculated into a final volume of 50 mL of minimal medium in a 500-mL flask (optical density, OD_{600} = 0.25), and incubated for two complete growth phases (6-8 h). Subsequently, 450 ml of the expression medium was inoculated with the 50 mL preculture in a 2.0-L baffled flask (OD_{600} = 0.1 and, after incubating for 92-96 h at 30°C and 225 rpm (maximal laccase activity; OD_{600} = 25-35), the cells were separated by centrifugation for 15 min at 6000 rpm and 4°C (Avantin J-E Centrifuge, Beckman Coulter, Fullerton, CA, USA) and the supernatant was double-filtered (through glass followed by a nitrocellulose membrane of 0.45 μm pore size).

Purification

Laccases OB-1 and OB-1del were purified by fast protein liquid chromatography (FPLC; LCC-500CI, Amersham Bioscience, Barcelona, Spain) and high performance liquid chromatography (HPLC, Waters 600E System with a PDA detector; Varian, USA). The crude extract was first subjected to fractional precipitation with 55% ammonium sulphate (first cut) and the pellet removed before subjecting the supernatant to precipitation with 75% ammonium sulphate (second cut). The final pellet was recovered in 20 mM Bis-Tris buffer pH 6.5 (BT buffer) and the sample filtered and loaded onto the FPLC, which was coupled to a strong anionic exchange column (HiTrap QFF, Amersham Bioscience) pre-equilibrated with BT buffer. The proteins were eluted with a linear gradient of 0 to 1 M NaCl in two phases at a flow rate of 1 mL/min: from 0 to 50% over 40 min and from 50 to 100% over 10 min. Fractions with laccase activity were pooled, concentrated, dialyzed against BT buffer and further purified by HPLC-PDA coupled with a 10 μm high resolution anion exchange Biosuite Q column (Waters, MA, USA) pre-equilibrated with BT buffer. The proteins were eluted using a linear gradient of 0 to 1 M NaCl at a flow rate of 1 mL/min in two phases: from 0-8% over 60 min and from 8-100% over 10 min. The fractions with laccase activity were pooled, dialyzed against 10 mM Britton and Robinson buffer pH 6.0, concentrated and stored at –20°C. Throughout the purification process the fractions were analyzed by SDS-polyacrylamide gel electrophoresis (SDS-PAGE) on 12% gels in which the proteins were stained with Coomassie Brilliant Blue G-250 (Protoblue Safe, National Diagnostics, GA, USA). All protein concentrations were determined using the Bio-Rad protein reagent (Bio-Rad Laboratories, Hercules, USA) and bovine serum albumin as a standard. For the PM1L-wt the protocol was similar to that used for the laccase mutants in *S. cerevisiae*, with some minor changes: the pellet from the fractional precipitation was recovered in BT buffer and the sample was filtered and loaded onto the FPLC coupled with the HiTrap

QFF column pre-equilibrated with BT buffer. The proteins were eluted with a linear gradient of 0 to 1 M NaCl in two phases at a flow rate of 1 mL/min: from 0-40% over 40 min and from 40-100% over 10 min. The fractions with laccase activity were pooled, dialyzed, concentrated and stored at –20°C.

2.4.3.5. Estimation of copper content

The copper content of the purified PM1L-wt and the OB-1 mutant was determined by Inductively Coupled Plasma-Optical Emission Spectrometry (ICP-OES), using a Perkin Elmer Optima model 3300 DV spectrometer (Walthman, MA, USA).

2.4.3.6. MALDI-TOF analysis

Matrix-Assisted Laser Desorption and Ionization-Time of Flight (MALDI-TOF) experiments were performed on an Autoflex III MALDI-TOF-TOF instrument (Bruker Daltonics, Bremen, Germany) with a smartbeam laser. The spectra were acquired at a laser power just above the ionization threshold, and the samples were analysed in the positive ion detection and delayed extraction linear mode. Typically, 1,000 laser shots were summed into a single mass spectrum. External calibration was performed, using BSA from Bruker, over a range of 30,000-70,000 Da. The 2,5-dihydroxy-acetophenone (2,5-DHAP) matrix solution was prepared by dissolving 7.6 mg (50 μmol) in 375 μL ethanol, to which 125 μL of 80 mM diammonium hydrogen citrate aqueous solution was added. For sample preparation, 2.0 μL of purified enzyme was diluted with 2.0 μL of 2% trifluoro acetic acid aqueous solution and 2.0 μL of matrix solution. A volume of 1.0 μL of this mixture was spotted onto the stainless steel target and allowed to dry at room temperature.

2.4.3.7. Protein identification by peptide mass fingerprinting

The purified OB-1 variant was digested with trypsin at the Proteomic and Genomic Services of the CIB (CSIC, Spain). Peptides were analyzed by MALDI-TOF and further sequenced. Peptides QAILVNDVFPSPLITGNKGDR; GPIVVYDPQDPHKSLYDVDDDSTVITLADWYHLA AK; SINTLNADLAVITVTK; YSFVLNADQDVDNYWIRALPNSGTRNFDGGVNSAILR and SAGSSTYNYANPVYR were compared with the data available from a primary sequence database (Mascot, http://www.matrixscience.com).

2.4.3.8. pI determination

The pI of purified laccases (8 μg of each) was determined by bi-dimensional electrophoresis (Proteomic and Genomic Services, CIB, CSIC, Spain).

2.4.3.9. N-terminal analysis

Purified laccases were resolved by SDS-PAGE and the proteins transferred to polyvinilydene difluoride (PVDF) membranes. The PVDF membranes were stained with Coomassie Brilliant Blue R-250, after which the enzyme bands were cut out and processed for N-terminal amino acid sequencing on a precise sequencer at the core facilities of the Helmholtz Centre for Infection Research (HZI; Braunschweig, Germany).

2.4.3.10. Kinetic parameters

As previously reported (Maté *et al.*, 2010), steady-state enzyme kinetics were determined using the following extinction coefficients: ABTS, ε_{418} = 36,000 M^{-1} cm^{-1}; DMP, ε_{469} = 27,500 M^{-1} cm^{-1} (relative to substrate concentration); guaiacol, ε_{465} = 12,100 M^{-1} cm^{-1}; sinapic acid, ε_{512} = 14,066 M^{-1} cm^{-1}. The activity of different laccase variants towards two substrates, potassium ferrocyanide, $K_4[Fe(CN)_6]$ and potassium octacyanomolybdate (IV), $K_4[Mo(CN)_8]$, was determined in homogenous solution by measuring oxygen consumption in a solution with a Clark electrode. This electrode measures oxygen on a catalytic platinum surface using the net reaction: $O_2 + 4\ e^- + 2\ H_2O \rightarrow 4\ OH^-$. The experiments were performed using the Oxygraph setup (Hansatech Instruments, King´s Lynn, UK). All Clark measurements were performed in 50 mM acetate buffer pH 4.0. For comparison, the activity of the *Trametes hirsuta* laccase (ThL), ($E°'_{T1}$ = +780 mV *vs.* NHE) was also determined, and laccase activities were determined using at substrate concentrations of 10 mM for $K_4[Fe(CN)_6]$ and 20 mM for $K_4[Mo(CN)_8]$, allowing each enzyme to reach its maximal catalytic rates.

2.4.3.11. Determination of thermostability

The thermostability of the different laccase samples was estimated by assessing their T_{50} values using 96/384 well gradient thermocyclers. Appropriate laccase dilutions were prepared, such that 20 µL aliquots produced a linear response in the kinetic mode. Subsequently, 50 µL samples were assessed at each point in the gradient scale and a temperature gradient profile ranging from 35 to 90°C was established as follows (in °C): 35.0, 36.7, 39.8, 44.2, 50.2, 54.9, 58.0, 60.0, 61.1, 63.0, 65.6, 69.2, 72.1, 73.9, 75.0, 76.2, 78.0, 80.7, 84.3, 87.1, 89.0 and 90.0. After a 10 min incubation, the samples were chilled on ice for 10 min and further incubated at room temperature for 5 min. Next, 20 µL of samples were subjected to the same ABTS-based colorimetric assay described above. Thermostability values were deduced from the ratio between the residual activities incubated at different temperature points and the initial activity at room temperature (García-Ruiz *et al.*, 2010).

2.4.3.12. Electrochemical characterization

Spectroelectrochemical analysis of PM1L-wt and the OB-1 mutant, as well as the ThL, was performed as described previously (Larsson *et al.*, 2001) using a micro-spectroelectrochemical cell with a gold capillary electrode. The potential of the gold capillary in the cell was controlled by a three-electrode BAS LC-3E potentiostat from Bioanalytical Systems (BAS, West Lafayette, IN, USA) using an Ag|AgCl|KCl reference electrode (BAS) and a platinum counter electrode. The absorbance spectra were monitored with a PC2000-UV-VIS miniature fibre optic spectrometer (Ocean Optics; Dunedin, FL, USA) with an effective range of 200-1100 nm. The redox potential of the T1 site of the enzymes was determined by mediated spectroelectrochemical redox titration (MRT). A complex mediator system containing two different mediators, $K_4[Fe(CN)_6]$ and $K_4[W(CN)_8]$, with formal redox potentials of +430 mV and +780 mV, respectively, against NHE, was used for the MRT in accordance with previously published methods (Christenson *et al.*, 2006).

2.4.3.13. Circular dichroism spectra

CD spectra were recorded with a Chirascan™ CD Spectrometer (Applied Photophysics, Leatherhead, UK). The measurements were performed under an atmosphere of N_2 with a 1 mm light path quartz cell (Hellma, Müllheim, Germany) using protein concentrations in the range from 0.05 up to 0.1 mg/mL. The protein concentration was determined in accordance with methodology presented in (Scopes, 1974). The parameters of the secondary structures were calculated using an in house program ("Protein-CD v. 1.5"; Moscow, Russia), as described previously (Shleev *et al.*, 2006). This software uses a ridge regression procedure in the method of linear regression and allows creation of the optimal selection from CD spectra in a database for mathematical treatment of a CD spectrum of interest. As known from X-ray studies of redox enzymes from different sources, laccases are β-structured proteins. Indeed, the CD database for our calculations contained only β-proteins. From 39 β-proteins only 25 examples were selected based on the criterion of root-mean-square similarities of their spectra with a CD spectrum of a wild-type laccase from *Coprinus cinereus*. For the learning sample containing 25 proteins, regression coefficients were obtained, which were used in the calculation of basic elements of protein secondary structures, *viz.* α-helix, 3_{10}-helix, β-sheet, β-turns, and random (unordered) structure. In order to determine calculating errors the learning sample was tested by alternated removal of each protein from the database.

2.4.3.14. DNA sequencing

The plasmid containing the OB-1del gene was sequenced with an ABI 3730 DNA Analyzer-Applied Biosystems Automatic Sequencer from Secugen (CIB, Madrid). The following primers,

designed using Fast-PCR software (University of Helsinki, Finland), were used: RMLN; PM1FS (5′-ACGACTTCCAGGTCCCTGACCAAGC-3′, which binds to bp 5′-1026-1050-3′ of pJRoC30-αPM1); PM1RS (5′-TCAATGTCCGCGTTCGCAGGGA -3′, which binds to bp 5′-1860-1881-3′ of pJRoC30-αPM1) and RMLC.

2.4.3.15. Protein modelling

The Protein Data Bank was searched for proteins with known structural homology to the PM1 laccase. The protein with the highest sequence similarity to PM1 was the laccase from *Trametes trogii*, the crystal structure of which was solved at a resolution of 1.58 Å and it exhibits 97% sequence identity to PM1 (PDB id: 2HRG) (Matera *et al.*, 2008). A model was generated using the Swiss-Model protein automated modelling server (http://swissmodel.expasy.org/), and analyzed using DeepView/Swiss-Pdb Viewer and PyMol Viewer.

2.4.4. RESULTS AND DISCUSSION

2.4.4.1. The yellow OB-1 mutant

The blue laccase from basidiomycete PM1 belongs to a group of high redox potential laccases discovered in the western Mediterranean region, which includes laccases from other white-rot fungi (*Trametes trogii*, *Trametes* sp. C30, *Coriolopsis gallica* and *Pycnoporus cinnabarinus*) (Colao *et al.*, 2006). These laccases share sequence identity of at least ~75% and they have been characterized as blue laccases, *i.e.*, with a copper content of 4 atoms per protein; displaying a shoulder at approximately 330 nm corresponding to the type III binuclear copper couple; and a peak at 610 nm associated with T1 Cu, also known as blue copper. We previously modified the PM1 laccase through eight rounds of directed evolution and screening, to achieve functional expression in *S. cerevisiae* (Maté *et al.*, 2010). In that study, a fusion gene comprising the α-factor prepro-leader and the mature PM1 laccase was constructed and improved by consecutive cycles of random mutagenesis, DNA recombination and semi-rational approaches, to generate the final OB-1 mutant that harboured a full set of coppers (estimated by *ICP-OES, see Experimental Procedures).* However, unlike the wild-type laccase produced by basidiomycete PM1 (PM1L-wt), the OB-1 mutant did not display the characteristic laccase absorption spectrum, but rather one similar to that of the yellow laccases (**Figure 2.4.1A**). The A_{280}/A_{610} ratio represents the combined absorbances of tryptophan and aromatic residues at 280 nm, divided by the absorbance of T1 Cu at 610 nm. Generally, blue laccases exhibit an A_{280}/A_{610} ratio of ~20, while that of the yellow laccases ranges from 90 to 150 (Leontievsky *et al.*, 1997a; Pozdnyakova *et al.*, 2006a). Thus the PM1L-wt is a blue-laccase, while the OB-1 mutant can be considered as yellow

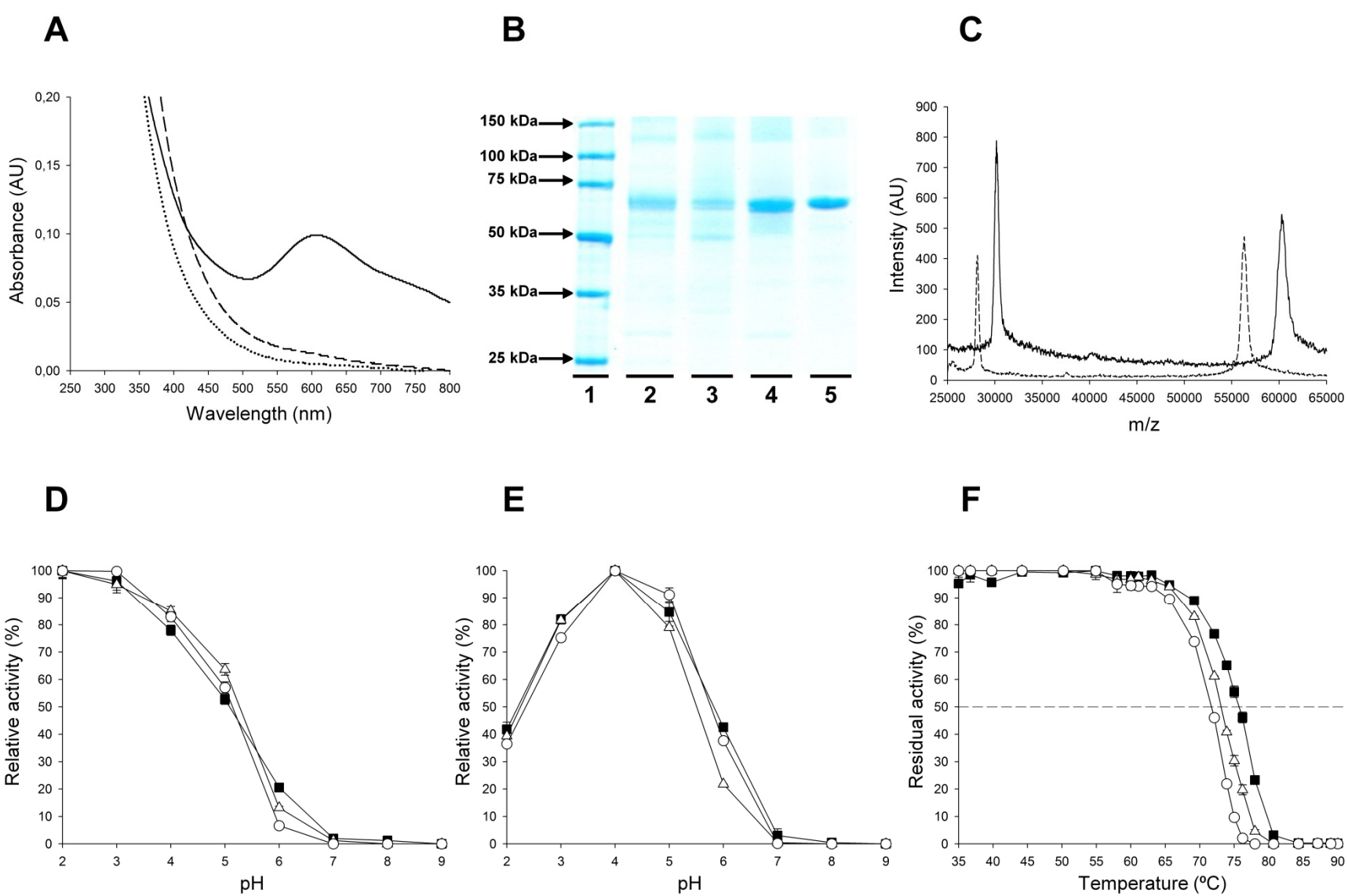
A
Absorbance (AU)
0,20
0,15
0,10
0,05
0,00
250 300 350 400 450 500 550 600 650 700 750 800
Wavelength (nm)
B
150 kDa
100 kDa
75 kDa
50 kDa
35 kDa
25 kDa
1 2 3 4 5
C
Intensity (AU)
900 800 700 600 500 400 300 200 100 0
25000 30000 35000 40000 45000 50000 55000 60000 65000
m/z
D
Relative activity (%)
100 90 80 70 60 50 40 30 20 10 0
2 3 4 5 6 7 8 9
pH
E
Relative activity (%)
100 90 80 70 60 50 40 30 20 10 0
2 3 4 5 6 7 8 9
pH
F
Residual activity (%)
100 90 80 70 60 50 40 30 20 10 0
35 40 45 50 55 60 65 70 75 80 85 90
Temperature (ºC)

Figure 2.4.1. Biochemical characterization. (**A**) UV-visible spectra of pure laccases recorded for 1.3 mg protein/mL. Solid line, PM1L-wt; dashed line, OB-1 mutant; dotted line, OB-1del mutant. (**B**) SDS-PAGE of the purified OB-1 mutant. Lanes: 1, protein ladder; 2, culture filtrate; 3, $(NH_4)_2SO_4$ fractional precipitation; 4, anion exchange (HiTrap QFF); 5, high resolution anion exchange (Biosuite Q). (**C**) MALDI-TOF mass spectra of purified laccases (PM1L-wt, dashed line; OB-1, solid line). The pH activity profiles of wild type and mutant laccases for ABTS (**D**) and DMP (**E**): black squares, PM1L-wt; white triangles, OB-1 mutant; white circles, OB-1del mutant. Activities were measured in 100 mM Britton and Robinson buffer at different pHs with 3 mM ABTS or DMP as the substrate. Laccase activity was normalized to the optimum activity value and each point (and the corresponding standard deviation) represents the average of three independent experiments. (**F**) Thermostability (T_{50}) of PM1L-wt (black squares), the OB-1 mutant (white triangles) and the OB-1del mutant (white circles). The T_{50} is defined as the temperature at which the enzyme retains 50% of its activity after a 10 min incubation. Each point (and the corresponding standard deviation) represents the average of three independent experiments.

laccase, based on its T1 Cu spectral features (**Table 2.4.1.**). OB-1 was purified to homogeneity (purification factor ~115; **Table 2.4.2**, **Figure 2.4.1B**) to rule out any possible contamination by other residual proteins that could mask absorbance at 610 nm. Subsequently, the purified mutant was analysed by MALDI-TOF mass spectrometry, which revealed a single peak for the mono- and di-protonated species, indicating a high level of purity in the preparation (**Figure 2.4.1C**). The purified OB-1 was then identified by peptide mass fingerprinting, resulting in a protein score of 480, matching that of the original PM1 laccase (accession number: CAA78144).

Table 2.4.1. Biochemical and spectrochemical features of PM1L-wt and the PM1 mutants.

Characteristic	PM1L-wt	OB-1	OB-1del
MW[a]	53,219	53,991	53,284
MW[b]	56,290	60,310	n.d.
Glycosylation (%)	6	12	12
Thermal stability, T_{50} (°C)	76.3	73.1	71.7
pI	5.4	5.1	5.3
Optimum pH (with ABTS)	3	3	3
Optimum pH (with DMP)	4	4	4
A_{280}/A_{610}	25.3	82.8	160.6
$E^{o'}$T1 Cu (mV)	759	n.m.	n.m.
CD spectra (minimum, nm)	215	207	216
N-terminal end	SIGP	**ETEAEF**SIGP	SIGP

[a]Estimated from the amino acid composition; [b]estimated by MALDI-TOF mass spectrometry; n.d.: not determined; n.m.: non-measurable. The extra N-terminal extension is highlighted in bold.

2.4.4.2. Biochemical characterization

Both laccases had similar isoelectric points and pH activity profiles for ABTS and DMP (see **Table 2.4.1.** for a summary of the main characteristics of PM1L-wt and the OB-1 mutant, and **Figures 2.4.1D**, **1E** and **1F**), although the degree of glycosylation differed, as might be expected for enzymes produced in different hosts (**Table 2.4.1.**). The kinetic parameters were assessed using different phenolic and non-phenolic compounds. It was not possible to characterize native PM1 laccase produced in *S. cerevisiae* due to its poor secretion (0.035 ABTS-U/L of supernatant). The k_{cat} of the OB-1 variant was close to that of PM1L-wt produced from the fungal strain (**Table 2.4.3.**). Bearing in mind that the total activity of PM1 laccase was enhanced round after round of evolution, our data indicate that the k_{cat} of the native laccase PM1 must be several folds lower when the enzyme is expressed in *S. cerevisiae* than in the original host. Our results agreed well with those for other laccases expressed in *S. cerevisiae*. For example, when the low redox potential laccase from *Myceliophthora thermophila* was functionally expressed in yeast, the k_{cat} of the enzyme decreased 10-fold in the *S. cerevisiae* expression system (Bulter *et al.*, 2003a).

Table 2.4.2. Purification of the OB-1 mutant.

Purification step	Volume (mL)	Volumetric activity (U/mL)	Protein (mg/mL)	Specific activity (U/mg)	Activity yield (%)	Purification factor
Culture filtrate	1,815	0.99	0.26	3.8	100	—
Fractional precipitation	29	62	5.04	12.3	100	3.2
HiTrap QFF	11	127	2.52	50.4	78	13.2
High resolution Biosuite Q	1.0	606	1.38	439	34	115

2.4.4.3. Laccase-mediator system

Redox mediators are small synthetic or natural molecules that can act as diffusible electron carriers. After oxidization by laccases, the mediator oxidizes the target substrate through non-enzymatic mechanisms (Baiocco *et al.*, 2003; Cañas and Camarero, 2010). Laccase-mediator

systems have been exhaustively investigated, as they permit the oxidation of high redox potential compounds that cannot be oxidized by laccases alone (including lignin derivatives, recalcitrant dyes and PAHs) (Morozova *et al.*, 2007b). Some fungal laccases produced in solid-phase cultures are yellow rather than the typical blue colour exhibited by the same laccases when produced in liquid cultures (Leontievsky *et al.*, 1997a, b; Pozdnyakova *et al.*, 2004, 2006a). In solid state fermentation of white-rot fungi using lignocellulosic materials (*e.g.,* wheat straw containing lignin), a natural lignin-derived compound can modify the T1 Cu, switching from the oxidized resting state (Cu^{2+}) to the reduced state (Cu^{1+}), and thus quenching the Abs_{610}T1Cu. Interestingly, once laccase binds to this natural and hitherto unknown molecule, the enzyme can oxidize higher redox potential compounds without the need for any exogenous mediator (Leontievsky *et al.*, 1997a,b; Rodakiewicz-Nowak *et al.*, 1999; Pozdnyakova *et al.*, 2004, 2006a). The presence of this putative "endogenous mediator" bound to the T1 Cu site in yellow laccases is one of the characteristic features of these enzymes. Although the OB-1 mutant was produced in conventional YP liquid media, the possible binding of a mediator that altered the Abs_{610}T1Cu cannot be ruled out. We analyzed the oxidation of several high redox potential dyes by the OB-1 mutant in the presence or absence of exogenous mediators (the artificial mediator HBT or the natural mediator acetosyringone, **Figure 2.4.2A**). RB5, Poly R-478 and Azure B were only oxidized efficiently in the presence of the mediator, with the best yields produced by the HBT-laccase system. Unlike all the yellow laccases described in literature, the OB-1 mutant oxidized none of the recalcitrant dyes in the absence of exogenous mediators. Similar results were obtained for the blue laccase from *Trametes versicolor* (TvL), confirming that the yellow OB-1 mutant behaves like a blue laccase in terms of its laccase-mediator requirements (**Figure 2.4.2B**).

2.4.4.4. Spectro-electrochemical characterization

To determine whether modification of the Abs_{610}T1Cu affects the laccase redox potential, midpoint potentials were measured for PM1L-wt and the OB-1 mutant to provide an estimate of the potential value of the T1 Cu site ($E°'_{T1}$). The $E°'_{T1}$ for PM1L-wt was +759 mV when compared to NHE from the mediated reductive redox titration, placing the PM1 laccase in the group of high redox potential laccases (**Figure 2.4.3A**). It was not possible to accurately estimate the $E°'_{T1}$ for the OB-1 mutant as the quenched signal at 610 nm prevented calculation of a reliable value. However, a constant increment was detected with increasing voltage (from +350 mV to +950 mV), indicating reduction of the T1 Cu (**Figure 2.4.3B**). The redox potential of the T1 site was also assessed in an activity assay based on the consumption of O_2 by the laccase. In all cases, activities with the $K_4[Fe(CN)_6]/K_4[Mo(CN)_8]$ pair fell within the same range (196 ± 12, 150 ± 3, 195 ± 8 s^{-1} for ThL, PM1L-wt and OB-1, respectively) indicating that the redox potential of the OB-1 mutant was, in all likelihood, unaltered after evolution (**Figure 2.4.3C**).

Table 2.4.3. Comparison of the kinetic parameters of PM1 mutants expressed in *S. cerevisiae* and wild type PM1 expressed in fungus.

Laccase	Mutations in mature protein	Substrate	K_m (mM)	k_{cat} (s^{-1})	k_{cat}/K_m ($mM^{-1}s^{-1}$)
PM1L-wt (fungus)	–	ABTS	0.0081 ± 0.0007	272 ± 7	33,580
		DMP	0.12 ± 0.01	153 ± 4	1,093
		Guaiacol	1.16 ± 0.03	65.9 ± 0.5	57
		Sinapic acid	0.048 ± 0.001	45 ± 3	923
OB-1 mutant	V162A, H208Y, S224G, A239P, D281E, S426N, A461T	ABTS*	0.0063 ± 0.0009	185 ± 6	29,365
		DMP*	0.14 ± 0.02	125 ± 4	893
		Guaiacol*	6.6 ± 0.5	44 ± 1	6.7
		Sinapic acid	0.073 ± 0.002	129 ± 9	1,778
OB-1del	V162A, H208Y, S224G, A239P, D281E, S426N, A461T (N-TERMINAL EXTENSION -ETEAEF- DELETED)	ABTS	0.006 ± 0.001	134 ± 6	23,124
		DMP	0.16 ± 0.01	49 ± 1	311
		Guaiacol	3.8 ± 0.3	21.2 ± 0.5	5.6
		Sinapic acid	0.074 ± 0.002	56 ± 6	757

*Data from Maté *et al.*, 2010.

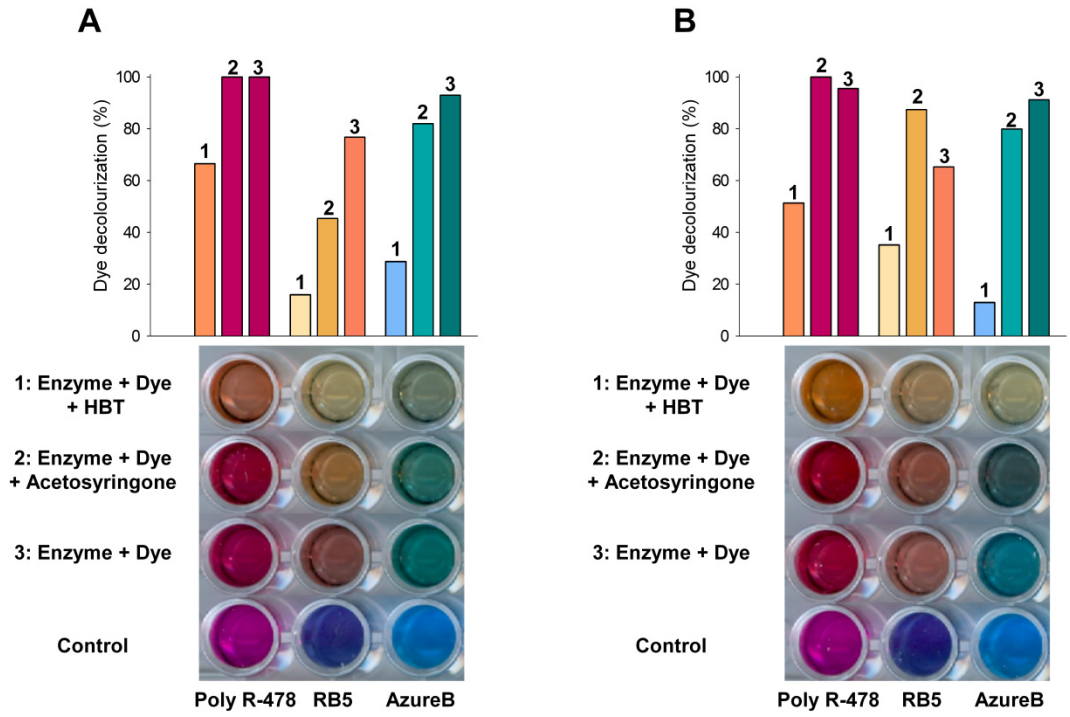

Figure 2.4.2. Dye decolourization by the laccase mediator system. The oxidation of high redox potential dyes was analyzed for the OB-1 mutant (**A**) and TvL (**B**) in the presence or absence of redox mediators. The percentage decolourization was measured after 21 hours at room temperature in a reaction mixture containing 0.01 U of laccase, with or without 1 mM of redox mediator (HBT or acetosiringone). The initial dye concentrations were 0.015, 0.0075 and 0.002% for Poly R-478, RB5 and Azure B, respectively (resulting in an initial absorbance at the corresponding wavelength of 1.2). Decolourization was monitored at 520, 598 and 647 nm for Poly R-478, RB5 and Azure B, respectively, and the data points represent the average of measurements performed in triplicate with a SD 10% of the mean.

The CD spectrum of the PM1L-wt (**Figure 2.4.3D**) was very similar to those of *Trametes hirsuta*, *Coprinus cinereus* and other fungal laccases (Schneider *et al.*, 1999; Shleev *et al.*, 2004). The calculated basic elements of the secondary structure of the wild-type enzyme correlated well with the content of α-helix, 3_{10}-helix, β-structure, β-turns, and unordered structures in *Coprinus cinereus* laccase obtained from X-ray analysis (**Table 2.4.4.**). CD spectra of mutants, however, differed significantly from the spectrum of the wild-type enzyme, *viz.* intensive negative band in the region of 200 nm occurred, which is a very distinguishing feature for proteins with irregular structures, such as collagens and polyproline helixes (Sreerama and Woody, 1994). In the frame of the calculation method used in our studies, this difference in CD spectra of mutants compared to the wild type laccase is described by the percentage increase of irregular (unordered) structure with concomitant small decrease in regular structures, *viz.* α-helix, β-structure, and β-turns. It is important to emphasize that a positive band in the region of 224 nm

do exist on CD spectra of mutants, also characteristic of polyproline helix structures. (Sreerama and Woody, 1994). Usually, polyproline helixes are short (only 3-6 amino acids) and they are classified as an unordered structure (Mansiaux *et al.*, 2011). Moreover, the specific ellipticity of polyproline helixes varies from 45,000 up to 100,000 degr·cm^2·dmol^{-1} (Sreerama and Woody, 1994). Since the specific ellipticity for mutants of laccase in the region of polyproline helix (*ca.* 200 nm) was calculated to be 9,000-12,000 degr·cm^2·dmol^{-1} (**Figure 2.4.3D**), it can be suggested that the observed spectral changes might be related to the transition of 15-30% amino acids into polyproline helix (polyproline II type helices) during the direct evolution of the wild-type laccase.

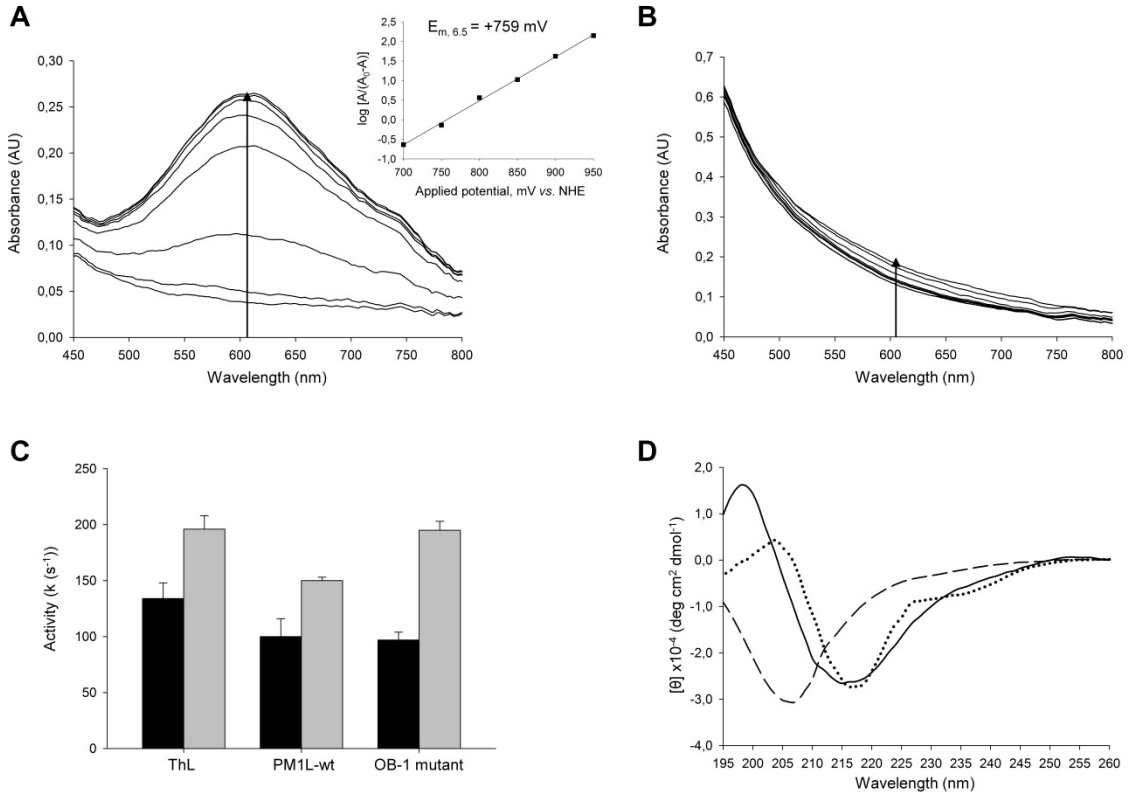

Figure 2.4.3. Spectro-electrochemical characterization. The E°′$_{T1}$ Cu for PM1L-wt (**A**) and the OB-1 mutant (**B**) was assessed by mediated redox reductive titration. Current densities of +400, +450, +500, +550, +600, +650, +700, +750 and +850 mV were applied to measure PM1L-wt. Current densities of +350, +400, +450, +500, +550, +600, +650, +700, +750, +800, +850, +900 and +950 were applied to measure the OB-1. The insert in A shows a typical Nernst plot of the dependence of the applied potential versus the absorbance at 600 nm and the averaged parameters calculated from the titrations. (**C**) O_2 consumption activity assays with $K_4[Fe(CN)_6]$ (black bars) and $K_4[Mo(CN)_8]$ (grey bars). For A, B and C, redox titration of the well-characterised *T. hirsuta* laccase (ThL) was also performed as a control. (**D**) CD spectra analysis. Solid line, PM1L-wt; dashed line, OB-1 mutant; dotted line, OB-1del mutant.

Table 2.4.4. CD analysis.

Laccase	α-helix	3_{10}- helix	β-sheet	β-turns	Unordered	∑
X-ray of laccase from *Coprinus cinereus* (PDB: 1HFU)	0.08	0.04	0.38	0.12	0.38	1.00
PM1L-wt	0.04	0.03	0.41	0.12	0.38	0.98
OB-1 mutant	0	0.05	0.37	0.10	0.47	0.99
OB-1 del mutant	0.02	0.05	0.36	0.10	0.48	1.01
RMS deviation	0.030	0.025	0.043	0.032	0.038	---

*RMS deviation for a set of 25 β-proteins used for calculations of secondary structures based on CD spectra.

2.4.4.5. OB-1 truncated variant

The OB-1 mutant was engineered by constructing of a fusion protein harbouring the α-factor prepro-leader from *S. cerevisiae* and the native mature laccase PM1. After screening over 50,000 clones in eight cycles of directed evolution, the OB-1 mutant contained the following mutations: V[α10]D, N[α23]K, G[α62]G, A[α87]T, E[α90]E, Q70Q, V162A, A167A, H208Y, S224G, A239P, D281E, S426N, L456L and A461T (synonymous mutations are underlined and brackets denote mutations in the α-factor prepro-leader). Mutations in the hydrophobic core of the evolved α-factor prepro-leader enhanced functional expression, whereas some mutations in the mature protein improved catalytic efficiency, folding and secretion by altering the interactions with the surrounding residues (Maté *et al.*, 2010).

The α-factor pro-leader is thought to be involved in vacuolar targeting and chaperone like-activity, and it is processed at the Golgi through the action of three proteases: *KEX2*, *STE13* and *KEX1* (Brake, 1990). *KEX2* is a membrane-bound endoproteinase that cleaves the carboxyl side of the Lys-Arg motif. Maturation is sustained by the action of *STE13*, a membrane-bound dipeptidyl aminopeptidase that removes Glu/Asp-Ala dipeptides from the N-terminus of the mature protein. Finally, the serine protease *KEX1* removes the Lys and Arg residues from the C-terminus, which is essential for the proper maturation of α-factor tandems but is not necessary for the heterologous expression of α-factor prepro-leader fusion proteins (Shuster, 1991).

Several studies have described incorrect processing in response to high levels of secreted proteins produced from fusion genes with the α-factor prepro-leader, ultimately resulting in extracellular proteins containing a spacer dipeptide sequence linked to the N-terminus (Romanos *et al.*, 1992). This effect is thought to reflect the low levels of *STE13* protease produced by yeast, insufficient to process the high levels of heterologous proteins expressed by these synthetic genes. When we sequenced the N-terminal end of the OB-1 mutant, an extra acidic N-terminal extension (ETEAEF) led the original mature protein, confirming that *STE13* fails to process the pro-leader (**Figure 2.4.4A**). ETEA is the spacer dipeptide for *STE13* (including mutation A[α87]T), whereas the EF dipeptide was introduced during the cloning strategy to fuse the α-factor prepro-leader to the mature OB-1. To determine the effect of this alternative processing on laccase characteristics (including the Abs_{610}T1Cu spectral properties, stability and kinetics), we deleted the portion of our evolved gene encoding the acidic tail. Accordingly, a truncated version of the OB-1 mutant (OB-1del) was engineered by deletion mutagenesis through IVOE (**Figure 2.4.5.**). The new variant was produced, purified and N-terminal sequenced, confirming the corrected processing and secretion in the absence of *STE13* cleavage (*i.e.*, through *KEX2* protease activity only, **Figure 2.4.4B**).

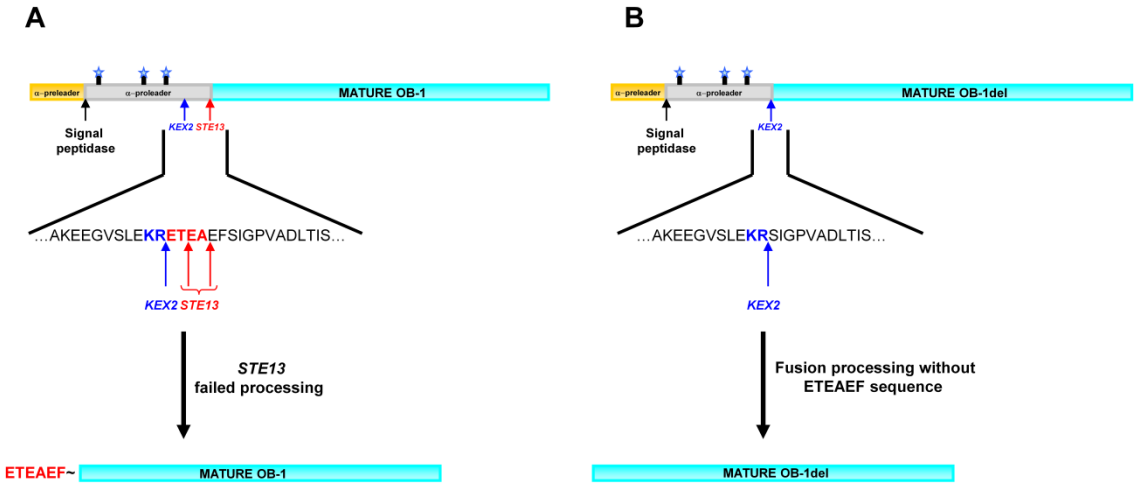

Figure 2.4.4. The extra N-terminal extension in the OB-1 mutant. (**A**) Alternative processing of the laccase OB-1 proposed in *S. cerevisiae*. (**B**) Fusion construct without the EAEA cleavage site and the role of *KEX2* in mature OB-1del secretion. The α-factor pre-leader is represented in yellow, the α-factor pro-leader in grey and the mature laccase in cyan blue. Blue stars indicate glycosylation sites in the pro-leader.

The OB-1del mutant had a similar yellow colour to OB-1 and moreover, the truncated version had an Abs280/Abs610 ratio of ~160 (**Figure 2.4.1A** and **Table 2.4.1.**). The pI shifted from 5.1 to 5.3 due to the loss of three acidic residues upon deletion. The removal of the acidic tail of the OB-1del mutant did not have associated significant changes in the CD spectra (**Figure**

2.4.3D and **Table 2.4.4.**). The OB-1del mutant had the same pH activity profile as OB-1 (**Figures 2.4.1D** and **1E**), although it was less stable (with a T_{50} 1.4°C less than that of OB-1, **Figure 2.4.1F**) and with worse kinetics (with k_{cat}/K_m 3 to 1.3-fold lower than that of OB-1; **Table 2.4.3.**). Finally, the truncated version was expressed more weakly in yeast (secretion dropped by ~40%). Removal of the charged spacer peptide made the fusion directly linked to the Lys-Arg processing site a poor substrate for the *KEX2* protease, indicating the importance of an acidic environment in the proximity of the *KEX2* cleavage site for secretion. This same effect was also observed for the α-factor leader-interferon-α1, which accumulated intracellularly and of which unprocessed and partially processed forms were secreted (Zsebo *et al.*, 1986), as well as in our laboratory during the directed evolution of a versatile peroxidase from *Pleurotus eryngii* (Garcia-Ruiz *et al.*, 2012).

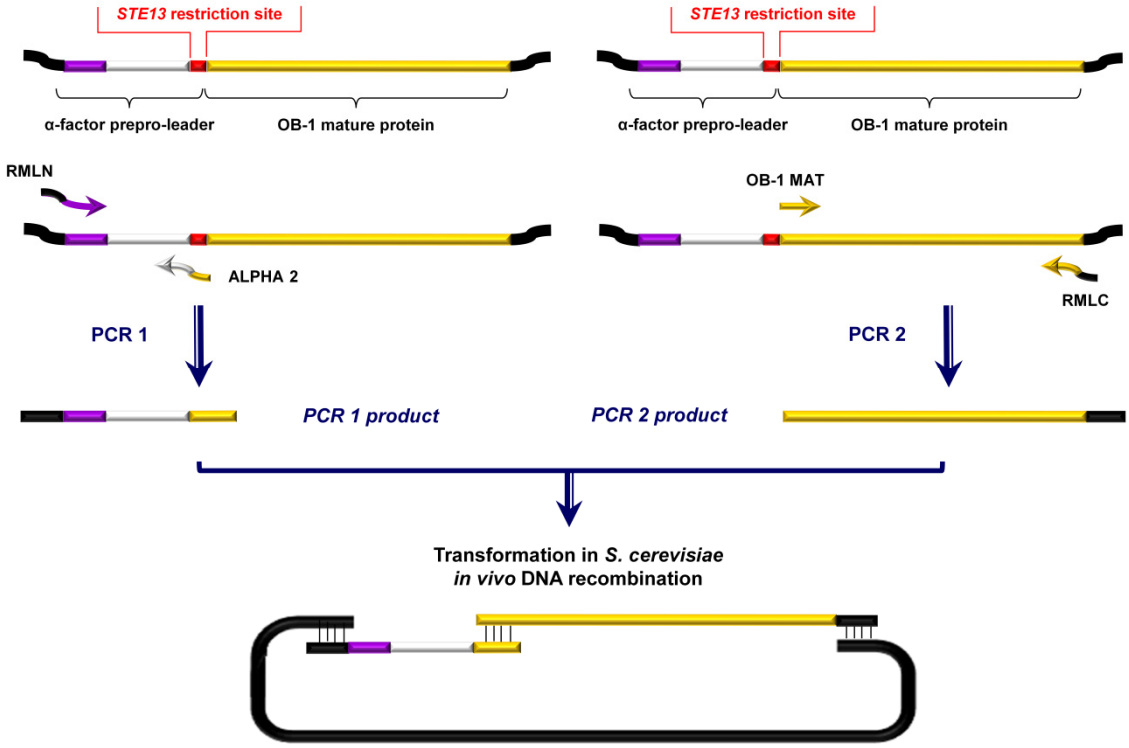

Figure 2.4.5. Generation of the truncated OB-1del mutant by *in vivo* overlap extension (IVOE) deletion mutagenesis. An autonomously replicating plasmid was generated by designing specific overhangs between fragments containing homologous regions, between which the truncated products were spliced into in the linearized vector. The products from PCR 1 and PCR 2 had overhangs separated by regions of 39, 40 and 66 bp homologous to the linearized vector for *in vivo* cloning. The α-factor pre-leader is represented in violet; the α-factor pro-leader in white; the *STE13* cleavage site in red; the OB-1 gene in yellow; and the shuttle vector in black.

2.4.4.6. Modification of the coordination sphere of the T1 Cu site

Despite the absence of Abs_{610}T1Cu, the yellow OB-1 mutant exhibited the primary biochemical features of a blue laccase. Given that the extra N-terminal extension was not responsible for the colour change, we could attribute the spectral changes to the polyproline helixes detected by CD. Moreover, some of the new amino acid changes induced by directed evolution in the mature OB-1 mutant may modify the T1 Cu environment. The mutant protein harbours seven beneficial mutations (V162A, H208Y, S224G, A239P, D281E, S426N and A461T), which were mapped in a 3D-structure model based on the crystal structure of the *Trametes trogii* laccase (97% identity). These beneficial mutations were at a distance of 8 to 40 Å of the T1 Cu site. The Cu T1 is trigonally coordinated to two His residues (His455 and His394, according to PM1 numbering) and Cys450. In PM1L-wt, the Abs_{610}T1Cu results from a covalent copper-cysteine bond (Davies and Ducros, 2002). Interestingly, mutations A461T and S426N are located near the T1 Cu site and may alter the coordination of the blue copper (**Figure 2.4.6.**).

According to our model, the A461T mutation (8.86 Å from T1 Cu) appears to establish a new H-bond with Phe460, which in turn is bound to the coordinating Cys450. It is likely that this change affects the overall geometry of the T1 Cu and hence, the Abs_{610}T1Cu, as the highly covalent Cu-S(Cys) bond is responsible for the pronounced blue colour of laccases. The S426N mutation (at 8.23 Å from T1 Cu) appears to break one H-bond with Gly428, while establishing a new H-bond with the adjacent Thr427. The T1 Cu ligand His394 is bound to Thr427 and thus, the newly established H-bond may alter the coordinating sphere of the T1 Cu. Reversal of these mutations may in turn reverse the effects on Abs_{610}T1Cu, albeit at the cost of expression. In fact, the A461T and S426N mutations were introduced in the early stages of evolution for functional secretion in yeast, in such a way that their consequent removal would jeopardize the secretion and stability of the entire protein, hindering the production of the mutant (Maté *et al.*, 2010).

2.4.5. CONCLUSIONS

The OB-1 mutant is a high redox potential laccase with specific spectral features derived from the presence of polyproline helixes together with modifications in T1 Cu coordinating sphere. The alterations in absorbance at the T1 Cu site observed in this mutant indicate that not all yellow laccases necessarily contain an endogenous mediator bound to the T1 Cu site, and more significantly, that not all yellow laccases are produced from solid state cultures, but they can also be obtained as genetically modified products. The yellow laccase OB-1 displays similar characteristics to the blue PM1L-wt laccase, in terms of kinetics, redox potential, laccase mediator requirements, pH profile and stability. This mutant contains an extra acidic N-terminal tail, which is involved in alternative processing and folding, and that facilitates laccase

secretion as an active, soluble and stable form. Thus, this mutant would appear to be a suitable vehicle for directed evolution experiments towards challenging destinies (from bioremediation to novel green processes) (Maté *et al.*, 2011b).

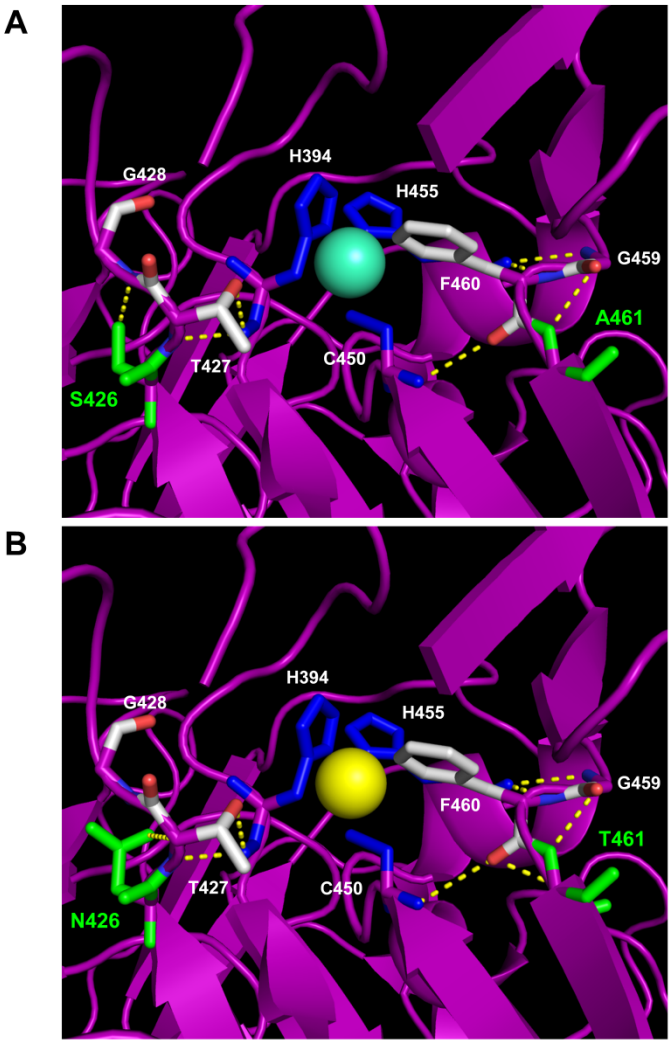

Figure 2.4.6. The coordination sphere of the T1 Cu site. Mutations A461T and S426N are highlighted in green in the PM1L-wt (**A**) and the OB-1 mutant (**B**). The T1 Cu for PM1L-wt and the OB1-mutant are represented in cyan blue and yellow, respectively. The residues involved in the coordination of the T1 Cu are represented in blue.

CAPÍTULO 5

Blood tolerant laccase by directed evolution

Diana M. Mate, David Gonzalez-Perez, Magnus Falk, Roman Kittl, Marcos Pita, Antonio L. De Lacey, Roland Ludwig, Sergey Shleev and Miguel Alcalde

Published in *Chemistry and Biology*, 2013, vol. 20, pp. 223-231.

2.5.1. SUMMARY

High-redox potential laccases are powerful biocatalysts with a wide range of applications in biotechnology. We have converted a thermostable laccase from a white-rot fungus into a blood tolerant laccase. Adapting the fitness of this laccase to the specific composition of human blood (above neutral pH, high chloride concentration) required several generations of directed evolution in a surrogate complex blood medium. Our evolved laccase was tested in both human plasma and blood, displaying catalytic activity whilst retaining a high redox potential at the T1 copper site. Mutations introduced in the second coordination sphere of the T1 site shifted the pH activity profile and drastically reduced the inhibitory effect of chloride. This proof of concept that laccases can be adapted to function in extreme conditions opens an array of opportunities for implantable nanobiodevices, chemical syntheses and detoxification.

2.5.2. INTRODUCTION

The extension of an enzymes' capacity to function in extreme environmental conditions is an issue that promises to deliver countless benefits. Due to their extraordinary versatility, the study of the ligninolytic enzymatic consortium of oxidoreductases secreted by white-rot fungi is of special biotechnological interest –mainly high-redox potential laccases (HRPLs), peroxidases and H_2O_2-supplying enzymes– (Martínez *et al.*, 2009). However, the absence of catalytic activity at neutral/basic pHs, along with the inhibition by modest concentrations of different substances (halides, metal ions, fatty acids, detergents), remain a serious obstacle to their further exploitation. HRPLs (EC 1.10.3.2) that are active under such inclement conditions would be very desirable to be used in applications that range from organic synthesis to bioremediation (Gianfreda *et al.*, 1999; Alcalde, 2007). In addition, HRPLs belong to the exclusive group of oxidoreductases that are capable of accepting electrons directly from the cathode of a biofuel cell or an amperometric biosensor. Indeed, the set of advantages that HRPLs have to offer (*i.e.*,

high current densities, direct electron transfer, low overpotential for O_2 reduction and high operational stability) situate them among the best suited candidates for enzyme-based bioelectronic devices (Shleev and Ruzgas, 2008). Possibly, one of the most attractive challenges in this field focuses on achieving implantable self-contained wireless 3D-nanobiodevices that work in different physiological fluids (blood, saliva, tears). Such nanobioelectronic devices are comprised of a biosensor array to detect different metabolites *in vivo* (glucose, insulin), a transmitter/transducer to externalize the information and a biofuel cell to power the entire system. The main shortcomings in the engineering of this type of technology stem from the difficulties in miniaturizing their individual elements (antenna, transducer), and in tailoring reliable and stable enzymes to catalyze the biocathode reaction in which the O_2 dissolved in the fluids is reduced to H_2O (Castillo *et al.*, 2004; Bullen *et al.*, 2006; Kim *et al.*, 2006). Unfortunately, HRPLs are inactive at blood pH (~7.4) and they are also strongly inhibited by chloride concentrations much lower than those found in blood (140-150 mM), which limits this specific application and the use in other areas where basic pHs or chloride ions are presented (*i.e.*, dye-stuff proccessing, waste-water treatment, pollutant remediation, pharmaceutical compound synthesis and food proccessing, to name a few (Gianfreda *et al.*, 1999; Riva, 2006; Alcalde, 2007; Rodgers *et al.*, 2010).

Here, we report the engineering by directed evolution of a HRPL that is functional in human blood. The ultimate mutant enzyme obtained through this evolutionary process was characterized comprehensively and its evolved features were tested on real human blood samples, revealing the mechanisms underlying this relevant improvement.

2.5.3. RESULTS AND DISCUSSION

2.5.3.1. Laboratory evolution approach

Our point of departure in this study was a HRPL (OB-1 mutant) previously tailored in our laboratory by *in vitro* evolution and semi-rational approaches to be active, soluble, highly thermostable and readily secreted by yeast (Maté *et al.*, 2010). To convert OB-1 to an active blood-tolerant laccase, we designed a screening assay based on human blood composition. As real plasma or blood are unsuitable for screening mutant libraries in the experimental context of directed evolution, we developed a surrogate complex medium ("blood buffer") mimicking the biochemical composition of human blood. This buffer contained a laccase colorimetric substrate but it lacked any cells and coagulating agents. Three consecutive rescreens were conducted to rule out the selection of false positives. Like all HRPLs, the OB-1 mutant exhibits neither activity nor significant internal electron transfer at pH 7.4 (Maté *et al.*, 2010). Accordingly, for the first generation the pH of the blood buffer was set at 6.5, resulting in a decrease in laccase activity of

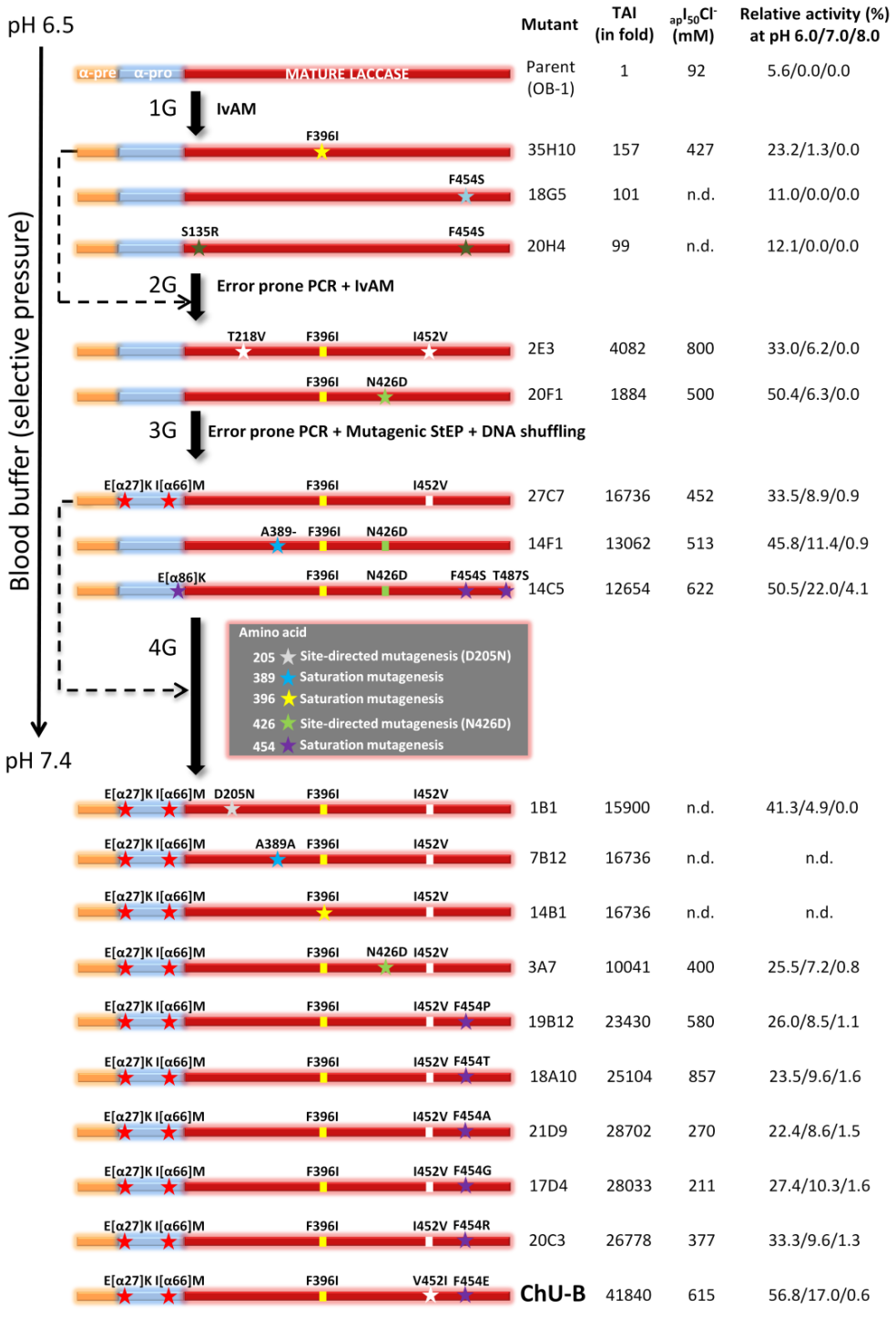

Figure 2.5.1. Directed laccase evolution. The parental type fusion gene (OB-1 mutant) (Maté *et al.*, 2010) is formed by the α-factor prepro-leader, replacing the original laccase signal sequence to improve secretion in *S. cerevisiae*, and the mature laccase. The α-factor pre-leader is represented in orange, the α-factor pro-

leader in blue and the mature laccase in red. New mutations are depicted as stars and accumulated mutations as squares; A389- is a deleted residue. TAI (total activity improvement in blood buffer): a value indicating the improvement in laccase activity detected in *S. cerevisiae* microcultures for each mutant compared with the parental OB-1. Measurements were performed in quintuplicate from supernatants of independent cultures grown in 96-well plates, using 3 mM ABTS as substrate. The $_{ap}I_{50}Cl^-$ (apparent I_{50} for NaCl) indicates the concentration of NaCl at which the enzyme retains 50% of its ABTS-activity, as determined in *S. cerevisiae* microcultures for each mutant after a 2 h incubation. Relative activity at different pH values was assessed with 3 mM ABTS as substrate. Dashed arrows indicate the mutant used as a parent in each generation. n.d., not determined. Silent mutations are not included. Over 10,000 clones were screened in four rounds of molecular evolution combining *in vivo* (IvAM, DNA shuffling, IVOE) and *in vitro* (error-prone PCR, mutagenic StEP) recombination/mutagenic methods. In the last cycle of evolution, the final variant (ChU-B) was obtained after analyzing several positions by site-directed mutagenesis and saturation mutagenesis. See also **Supplemental Results,** p. 161; **Tables 2.5.S1.** and **S5,** pp. 166 and 167, respectively; and **Figure 2.5.S3.**, p. 165.

over 90%. In successive generations selective pressure was progressively enhanced until physiological pH values were reached. We took advantage of the high frequency of homologous DNA recombination of the *Saccharomyces cerevisiae* machinery to create diversity (Alcalde, 2010; Gonzalez-Perez *et al*., 2012). Thus, in each evolution cycle different DNA recombination methods (both *in vivo* and *in vitro*) were combined to enhance the complexity of the mutant libraries in this pool. The last round of evolution was dedicated to the detailed rational evaluation of several positions that produced substantial improvements in the total activity by saturation mutagenesis, site directed mutagenesis and mutational recovery (**Figure 2.5.1.**; **Table 2.5.S1.,** p. 166; and **Supplemental Results,** p. 161). When the last variant of the evolutionary pathway was obtained (ChU-B mutant), it exhibited an increase in total activity in blood buffer over 40,000-fold versus the parental type.

2.5.3.2. Laccase mutant in blood

The behavior of the mutant laccase was tested in human plasma and blood. Oxygen consumption in physiological fluids enriched with ascorbic acid (a poor laccase substrate naturally present in blood) was monitored with a Clark electrode, revealing comparable responses for plasma and blood (185 and 127 min^{-1}, respectively, **Figure 2.5.2A**). The 1.5-fold increase in ChU-B activity in plasma suggested that blood cells interfere with the detection method. To confirm that the enzyme was active under physiological conditions regardless of the reducing substrate used, oxygen reduction against common laccase substrates −(2,2′-azino-bis(3-ethylbenzothiazoline-6-sulphonic acid) [ABTS] and $K_4[Fe(CN)_6]$− was measured in blood buffer, obtaining similar values for all compounds tested (**Figure 2.5.2A**).

Laccases contain four catalytic copper ions arranged at two different sites: the T1 site, at which the substrate is oxidized; and a trinuclear copper cluster (with one Cu T2 and two Cu T3), at which oxygen is reduced to water (Morozova *et al.*, 2007a). If the laccase is properly connected to an electrode via the T1 Cu, the electroactive surface of the device can replace the electron-donating natural substrates of the enzyme. Redox titration of the T1 Cu site was performed at physiological pH using a micro-spectroelectrochemical cell with a gold capillary electrode (**Figure 2.5.2B**). The ChU-B mutant exhibited a high redox potential (+720 mV *vs.* NHE) at pH 7.4, and it reversibly cycled between its fully oxidized and fully reduced state. To further verify that the mutant was electrochemically active under physiological conditions, ChU-B was adsorbed onto low-density graphite electrodes and the electrocatalytic response of O_2 reduction by direct electron transfer was recorded at pH 7.4 (**Figure 2.5.2C**). No responses were detected for any of the HRPLs tested at this pH.

2.5.3.3. Inhibition by halides and hydroxides

The novel properties of ChU-B were dissected in terms of its activity versus pH and halide inhibition. The pH activity profiles against phenolic (2,6-dimethoxyphenol, DMP) and nonphenolic (ABTS) compounds revealed a notable shift towards less acidic values, including a change in DMP optimum activity pH from 4.0 to 5.0-6.0 (**Figures 2.5.3A-3B**; and **2.5.S1A-S1B,** p. 163). At pH 7.0, ChU-B retained ~50% and ~20% of its activity for DMP and ABTS, respectively, whereas the parental type displayed negligible activity under these conditions. Similarly, ChU-B activity at pH 6.0 was over 90% and 50% for DMP and ABTS, respectively, while that of the parental type was ~20%. This drastic improvement in activity at near neutral pH led to a small but noticeable increase in ChU-B activity even at pH 8.0. To date, the engineering of chimeric laccases had only succeeded in slightly shifting the pH profile, at the expense of sacrificing redox potential (Cusano *et al.*, 2009). By contrast, ChU-B variant exhibits activity at neutral/alkaline pH values while keeping a high redox potential at the T1 Cu site.

It is well known that increases in pH inhibit laccase activity, due to a decrease in H^+ availability and the binding of OH^- ions to the T2 Cu, which in our laccase is tricoordinated with His64, His397 and one H_2O molecule (Xu, 1997, Matera *et al.*, 2008). HRPLs are also inhibited by halides (fluoride, chloride and bromide, but not iodide), with an inhibitory potency inversely proportional to the diameter of the anion ($F^->Cl^->Br^-$). This dependence is possibly due to an access limitation for the binding of the larger halide ions to the laccase catalytic sites (Xu, 1996; Xu, 1997). The I_{50} measured for the different halides (the concentration of halide at which the enzyme retains 50% of its initial activity) was independent of the substrate employed (**Table 2.5.S2.,** p. 167). The I_{50} of ChU-B for Cl^- improved from 176 to 1025 mM with ABTS as substrate (**Figure 2.5.3C**), to the best of our knowledge the highest I_{50Cl^-} reported for any basidiomycete

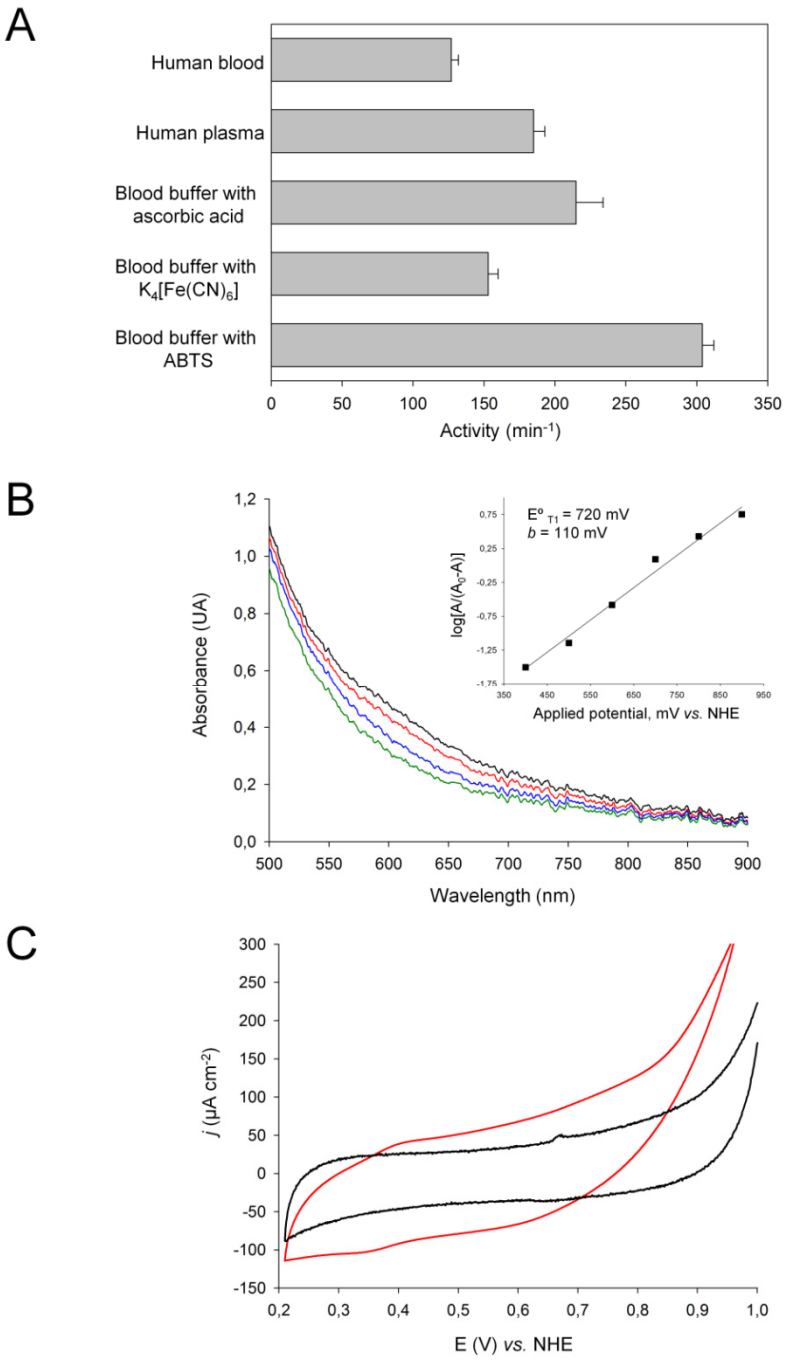

Figure 2.5.2. Activity in physiological fluids and spectro-electrochemical characterization. (**A**) Activity of the ChU-B mutant determined by measuring O_2 consumption. To monitor laccase activity in blood and plasma, the fluids were supplemented with 10 mM ascorbic acid and the pH adjusted to 7.4 prior to adding the enzyme. Each bar, including the standard deviation (SD), is from three independent experiments. (**B**) Redox titration of ChU-B at physiological pH values. Each redox titration was carried out

in both directions: from the fully oxidized to the fully reduced state of the enzyme (reductive titration) and vice versa (oxidative titration). The spectra of laccases were recorded at redox equilibrium and typical spectra of the oxidized, partly reduced and fully reduced enzymes are depicted. Equilibration of the T1 copper center at each potential applied was apparent from the stabilization of absorbance at 600 nm. As the redox mediators used are transparent above 500 nm, the spectral changes at 600 nm were attributed to the T1 Cu of the laccase. Spectra from the reductive titration, corresponding to oxidized laccase (black curve, applied potential +1000 mV *vs.* NHE), partly reduced enzymes (red and blue curves, +700 mV and +600 mV *vs*. NHE, respectively) and the fully reduced laccase (green curve, +300 mV *vs.* NHE) are shown. Inset: a typical Nernst plot of the dependence of the applied potential versus absorbance at 600 nm, and averaged parameters calculated from the reductive and oxidative titrations (midpoint value of +720 mV *vs.* NHE and a slope of 110 mV). (**C**) Cyclic voltammograms of O_2 reduction obtained using a polished, low-density graphite (LDG) electrode (black), and a LDG electrode with ChU-B laccase adsorbed to its surface (red). Measurements were carried out in a three-electrode electrochemical cell filled with 100 mM sodium phosphate buffer pH 7.4 and after bubbling O_2 at a pressure of 1 atm for 15 min, using a platinum wire as the counter electrode and a BAS Ag/AgCl reference electrode. Measurements were performed using Autolab PGSTAT30 controlled by GPES 4.9 software.

HRPL. It was not possible to measure Br^- inhibition for Chu-B, as the I_{50} of the parental type was already above 1300 mM, impeding measurement by surpassing the limit of substrate solubility at such high salt concentrations. As expected, there was strong inhibition in the presence of F^- (in the μM range), and although F^- inhibition was not a goal of the directed evolution study, the I_{50F^-} was slightly enhanced (from 70 to 109 μM, **Figure 2.5.3D**). Halide inhibition was also measured at physiological pH values and ChU-B was not sensitive to increasing concentrations of chloride (ranging from 100 to 800 mM) (**Figure 2.5.3E**). At pH 7.4, very little H_2O dissociation was observed, although the resulting 251 nM of OH^- may be enough to efficiently bind at the T2 Cu site and promote the inhibition of native HRPLs. The gradual increase in blood buffer pH throughout evolution reflects the $[OH^-]$ increase and $[H^+]$ decrease, and it permitted a selection of variants that were more tolerant to both hydroxyl and chloride ions in the same screening assay. Comparing ChU-B with other HRPLs revealed that, depending on the substrate, our variant was 12 to 20-fold less sensitive to F^- than the HRPLs from *Trametes trogii* and *Trametes villosa* (Xu, 1996; Garzillo *et al.*, 1998). Similarly, the I_{50Cl^-} of ChU-B was 26 to 164-fold higher than corresponding HRPLs. The ascomycete laccase from *Botrytis aclada* exhibited the highest I_{50Cl^-} described to date (1.4 M with DMP as substrate) (Kittl *et al.*, 2012b), yet its negligible activity at neutral pH and poor stability precludes its use in implantable biocathodes or other environmental processes. Comparing ChU-B with laccases from bacterial sources revealed a 1.5-fold better chloride tolerance than that of the halide-resistant polyphenol oxidase from *Marinomonas mediterranea* (Jimenez-Juarez *et al.*, 2005). This halide tolerance of the Chu-B mutant is remarkable given that, as a rule, fungal laccases are much more sensitive to halide inhibition than low-redox potential laccases from bacteria (Niladevi *et al.*, 2008; Singh *et al.*, 2011).

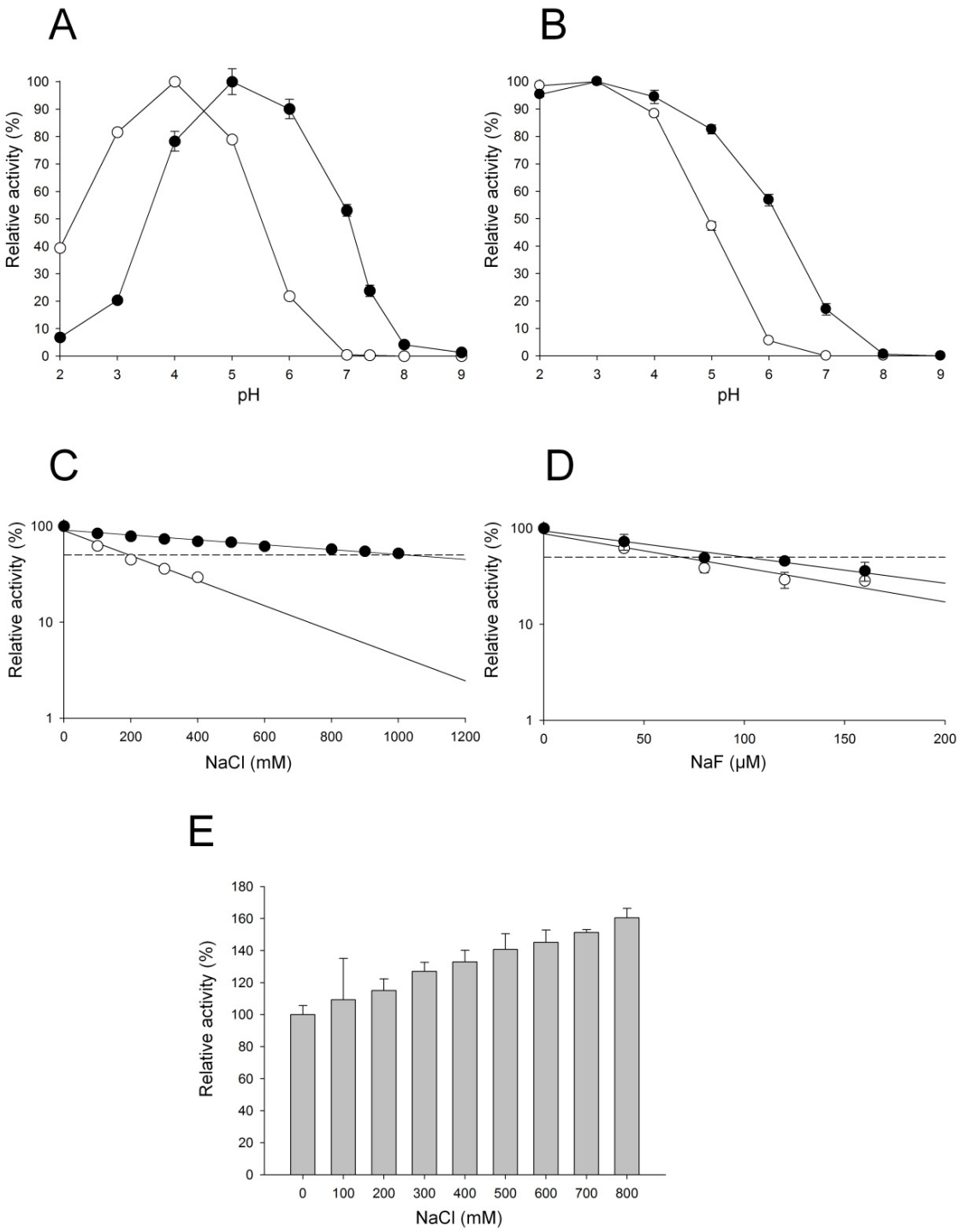

Figure 2.5.3. Biochemical characterization. (**A** and **B**) pH activities profiles were measured in 100 mM Britton and Robinson buffer at different pH values with 3 mM DMP (**A**) or ABTS (**B**) as substrates. White circles, parental type; black circles, ChU-B mutant. Laccase activity was normalized to the optimum

activity value. (**C-E**) Inhibition by halides. (**C**) Cl^- inhibition measured with 2.4 mM ABTS in 100 mM sodium acetate buffer pH 4.0. (**D**) F^- inhibition measured with 2.4 mM ABTS in 100 mM sodium acetate buffer pH 4.0. (**E**) Cl^- inhibition of ChU-B measured with 2.4 mM ABTS in 100 mM sodium phosphate buffer pH 7.4. Each value represents the mean and SD derived from three independent experiments. See also **Figure 2.5.S1.**, p. 163; and **Tables 2.5.S2.** and **S3**, p. 167 both.

We assessed maximum turnover rates of ChU-B in blood buffer. The synergic effect that improved activity at physiological pH in association with a strong chloride tolerance resulted in initial rates of 427 and 143 mol substrate/min/mol enzyme for DMP and ABTS, respectively. In equivalent conditions, the parental type showed almost no activity. Significantly, the turnover rates of the ChU-B mutant was 3- to 4-fold lower than that of the parental type under optimal conditions (*i.e.*, acidic pH and in the absence of inhibitors; **Table 2.5.S3.**, p. 167). Intrigued by these results, we analyzed mutations in the laccase structure.

2.5.3.4. Structural analysis of mutations

The laccase catalytic scaffold is formed by the T1 Cu site close to the surface, although the copper is not solvent-exposed. The T1 Cu is trigonally coordinated by His455, His394 and Cys450, the latter forming part of the highly-conserved His451-Cys450-His449 tripeptide, which connects to the trinuclear cluster located 12 Å away. The electrons from T1 Cu are transferred through two intramolecular electron transfer pathways governed by the aforementioned tripeptide to the T2/T3 trinuclear Cu cluster, where O_2 binds and is reduced to two molecules of H_2O. This second active site is buried deep in the laccase structure, with a T2 Cu tricoordinated by two His residues, one molecule of water and two tetracoordinated T3 coppers. The entrance of O_2 and the exit of H_2O to the T2/T3 site occur via two solvent channels. Bearing in mind that halide/OH^- inhibition allegedly occurs at the T2/T3 cluster, interrupting the internal electron transfer (Naqui and Varfolomeev, 1980; Naki and Varfolomeev, 1981), we expected to find mutations located in the surroundings of the trinuclear copper cluster, or in either of the two channels for oxygen and water transit (Xu *et al.*, 1998; Matera *et al.*, 2008). However, the two mutations introduced in the mature ChU-B (F396I and F454E) were located at the second coordination sphere of the T1 Cu site (**Figure 2.5.4.**). Indeed, most of the mutations discovered during the course of evolution were placed in the same region (at an average distance of 7.5 Å from the T1 Cu site), indicating an important influence of this region on halide/OH^- inhibition (**Figure 2.5.S2.**, p. 164; **Table 2.5.S4.**, p. 167).

F396I was discovered in the first generation, and it provoked the greatest improvement in activity of the entire evolutionary process (157-fold increase in activity over the parental type). Additional saturation mutagenesis at this position did not confer any further improvement (**Figure 2.5.1.**, p. 147). The highly conserved Phe396 plays a key role in the redox potential of the T1 site, and hence in HRPL catalysis (Matera *et al.*, 2008). Phe396 acts as a bridge connecting the

T1 Cu and T2/T3 Cu cluster via Pro395 (contiguous to the coordinating His394 of the T1 Cu) and His397, which coordinates the T2 Cu (**Figure 2.5.4.**). The F454E mutation was generated by subjecting position 454 to saturation mutagenesis and subsequent screening, as some mutants discovered in the first and third generations already contained a mutation at this position (**Figures 2.5.1.**, p. 147; and **2.5.S3.**, p. 165). We selected six different mutants with F454P/T/A/G/R/E substitutions, which boosted activity in blood buffer up to 2.5-fold (**Supplemental Results**, p. 162). The F454E mutation is contiguous to the coordinating His455 of the T1 Cu. Analysis of our model revealed that upon mutation, an H-bond with the imidazole group of His455 appears to be established (**Figure 2.5.4.**). It is generally accepted that electron transfer from the substrate to the T1 Cu is the rate-limiting step of laccase catalysis (Gianfreda *et al.*, 1999; Alcalde, 2007). Modification of the second coordination sphere of the T1 Cu reduces activity at acidic pH values and simultaneously compensates for T2 Cu inhibition so that ChU-B maintains activity in the presence of halides and OH^-. These results are consistent with previous studies of an ascomycete low-redox potential laccase subjected to comprehensive site-directed mutagenesis at the T1 region (Xu *et al.*, 1998). Recently, the parental type of the current research -the HRPL OB-1 mutant evolved for secretion and stability in yeast (Maté *et al.*, 2010)- was analyzed by a computational algorithm to understand the physical forces that rule the stability of the variant (Christensen and Kepp, 2012). Indeed, the combination of *in silico* computational methods (based on Montecarlo simulations and molecular dynamics) may provide a new twist in the study of this blood tolerant laccase. In particular, the use of quantum mechanics/molecular mechanics (QM/MM) methods −for mapping internal electron transfer pathways (Guallar and Wallrapp, 2008)− as well as the protein energy landscape exploration (PELE) −for assessing the traffic of halides and hydroxides through the laccase structure (Borrelli *et al.*, 2005)− could be valuable approaches to discern the hidden physicochemical principles behind the laccase improvements.

2.5.4. SIGNIFICANCE

HRPLs are considered by many as the green biocatalysts of the 21st century: they easily oxidize hundreds of compounds using oxygen from air and release water as the only byproduct (Maté *et al.*, 2011b). Moreover, they can be immobilized onto electrodes and they mediate direct electron transfer, permitting their integration into nanobioelectronic devices. Our blood tolerant laccase displays all these properties, thereby enabling its incorporation into physiological fluids. We are currently designing a full wireless 3D-nanobiodevice prototype for use in human blood, containing an *ad hoc* transmitter and a biosensor powered by a biofuel cell, to which ChU-B is attached (manuscript in preparation). This technology should permit less invasive and more reliable real-time *in situ* monitoring. Indeed, nanobiodevices can minimize the often critical time to detect a potentially life threatening physiological imbalance and shorten the intervention

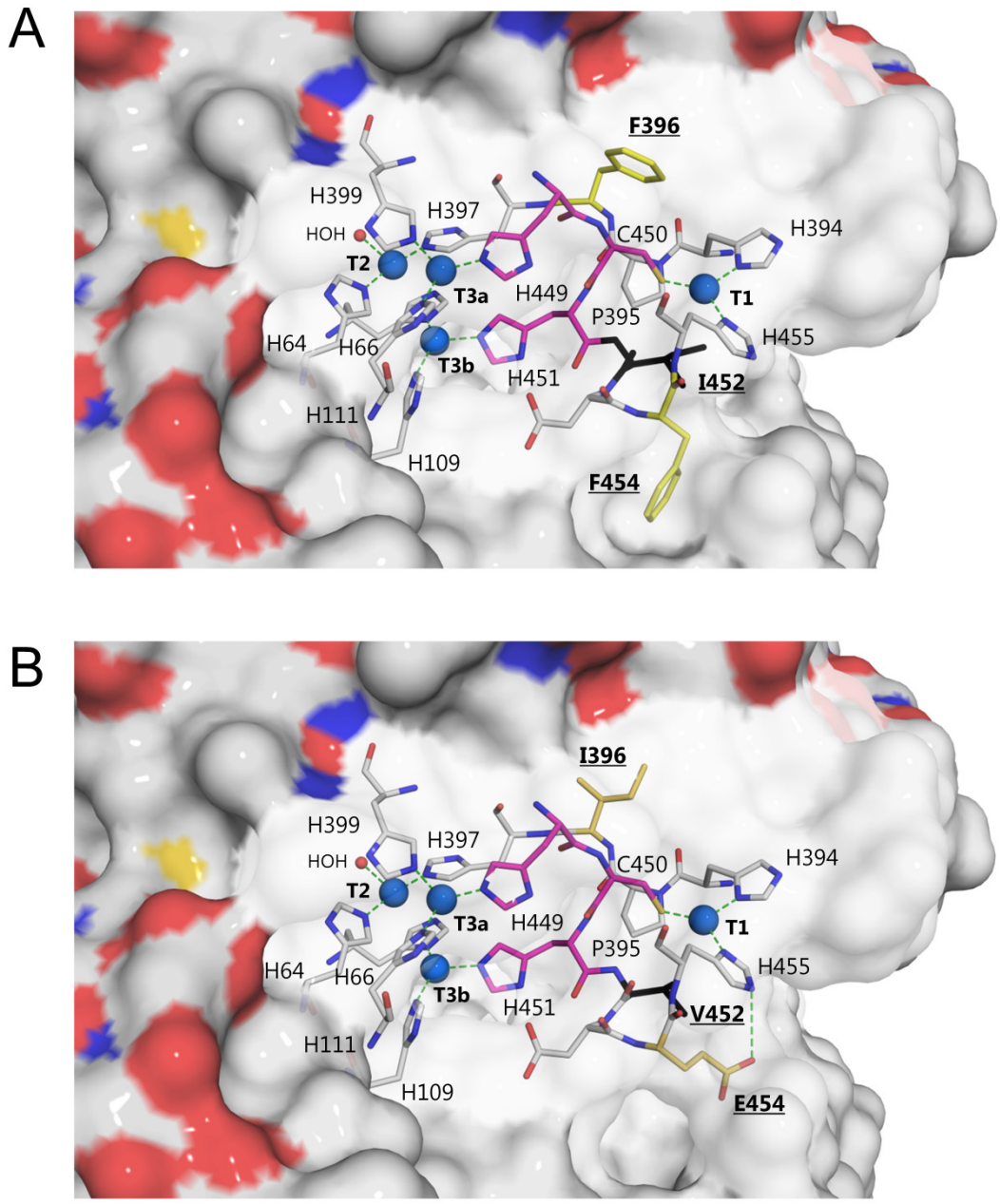

Figure 2.5.4. Mutations in evolved laccase. (**A** and **B**) Details of the mutations in the ChU-B variant (**B**) compared with the corresponding residues in the parental type (**A**). The F396I and F454E mutations are shown in yellow, and the I452V mutation (reverted in ChU-B) in black. Blue spheres represent copper atoms. The residues of the internal transfer pathway from T1 Cu to T2/T3 cluster are colored magenta. Residues involved in the first coordination sphere of the catalytic coppers and their interactions (as green dashes) are also represented. The electrostatic surface of the protein structure is shown in the background. The 3D-structure model is based on the crystal structure of the *Trametes trogii* laccase (97% identity, PDB: 2HRG) (Matera *et al.*, 2008). See also **Figure 2.5.S2.**, p. 164, and **Table 2.5.S4.**, p. 167).

time for medical teams. With an extraordinary resistance to halides and significant activity at neutral/alkaline pH values, the benefits of our evolved HRPL may also be extended to applications such as the development of medical bioassays, bioremediation (*e.g.*, oxidation of pesticides, PAHs, contained-waste waters, dye processing), pulp-kraft biobleaching, organic syntheses, and cofactor/coenzyme regeneration, among other processes in which high pH and/or strong salt contents represent major hurdles (Alcalde *et al.*, 2006a; Couto and Herrera, 2006; Riva, 2006; Kunamneni *et al.*, 2008a; Witayakran and Ragauskas, 2009).

2.5.5. EXPERIMENTAL PROCEDURES

All chemical reagents were of the highest purity commercially available. The oligonucleotides used along the evolutionary process (**Table 2.5.S5**, p. 168) were purchased from Isogen Life Science (De Meern, The Netherlands). Culture media were prepared as described previously (Maté *et al.*, 2010).

2.5.5.1. Laboratory evolution

For each generation, PCR fragments were cleaned, concentrated and loaded onto a low melting point preparative agarose gel (Bio-Rad, Hercules, CA), and then purified using the Zymoclean gel DNA recovery kit (Zymo Research, Orange, CA). PCR products were cloned under the control of GAL1 promoter of the pJRoC30 expression shuttle vector (kindly donated by Prof. F.H. Arnold from Caltech, CA), replacing the parent gene in pJRoC30. To remove the parent gene, the pJRoC30 plasmid was linearized with *Bam*HI and *Xho*I (New England Biolabs, Hertfordshire, UK), and the linear plasmid was concentrated and purified as described above for the PCR fragments.

First generation: IvAM

Using the OB-1 mutant as the parental type (Maté *et al.*, 2010), a library of over 3,000 clones was constructed by *in vivo* assembly of mutant libraries with different mutational spectra (IvAM) (Zumárraga *et al.*, 2008a). Independent mutagenic PCR reactions with *Taq*/$MnCl_2$ (Sigma-Aldrich, Madrid, Spain) and Mutazyme II DNA polymerase (Genemorph II Random mutagenesis kit, Stratagene, CA) were carried out on a gradient thermocycler (Mycycler, Bio-Rad) using the following parameters: 95°C for 2 min (1 cycle); 94°C for 0.75 min, 53°C for 0.75 min, 74°C for 3 min (28 cycles); 74°C for 10 min (1 cycle). In a final volume of 50 μL, the *Taq*/$MnCl_2$ PCR amplification contained 90 nM RMLN, 90 nM RMLC, 0.1 ng/μL template, 0.3 mM dNTPs (0.075 mM each), 3% DMSO, 1.5 mM $MgCl_2$, 0.01 mM $MnCl_2$ and 0.05 U/μL *Taq* polymerase. Mutazyme II amplification was carried out with 372 nM RMLN, 372 nM RMLC, 40 ng/μL template, 0.8 mM dNTPs (0.2 mM each), 3% DMSO and 0.05 U/μL Mutazyme II per 50

μL of reaction product. Under these conditions the mutational rates of *Taq*/$MnCl_2$ and Mutazyme II libraries were 0-3 and 4.5-9 mutations per 1,000 bp, respectively. To promote *in vivo* ligation, overhangs of 40 and 66 bp homologous to the linear vector were designed. The two libraries were mixed in equimolar amounts and transformed into competent *S. cerevisiae* cells of the protease-deficient strain BJ5465 (LGC Promochem, Barcelona, Spain) using the yeast transformation kit (Sigma-Aldrich, Madrid, Spain) together with the linearized vector (ratio vector/library 1:4). Transformed cells were plated in synthetic complete drop-out plates and incubated for 3 days at 30°C. Then, colonies were picked and subjected to the screening assay and to three successive re-screenings, as describes below.

Second generation: error-prone PCR + IvAM

Using the 35H10 mutant from the first generation as the parental type, three mutant libraries (~700 clones each) were constructed and independently screened. The first library was prepared with *Taq*/$MnCl_2$, the second with Mutazyme II and the third with IvAM, as described for the first generation.

Third generation: mutagenic StEP and in vivo DNA shuffling

Two independent libraries were created and explored using the two best mutants from the second round, 2E3 and 20F1, as the parental types. For the first library, the parental types were independently prepared with *Taq*/$MnCl_2$ and the mutagenic products *in vivo* shuffled in *S. cerevisiae*. The second library was prepared by *in vitro* recombination through staggered extension process (StEP) (Zhao *et al.*, 1998). The StEP-PCR reaction (50 μL final volume) contained 0.5 μM RMLN, 0.5 μM RMLC, 0.1 ng/μL of each DNA template, 0.8 mM dNTPs (0.2 mM each), 3% DMSO, 1 mM $MgCl_2$, 0.01 mM $MnCl_2$ and 0.02 U/μL iProof high fidelity DNA polymerase (Bio-Rad). The PCR conditions were as follows: 95°C for 2 min (1 cycle); 94°C for 0.5 min, 55°C for 0.33 min (90 cycles). An electrophoretic band of ~2 kb was purified and further subjected to mutagenic PCR with Mutazyme II. This mutagenic product was *in vivo* shuffled as described above.

Fourth generation: site-directed and saturation mutagenesis studies

Two individual mutants and three saturation mutagenesis libraries were constructed by in vivo overlap extension (IVOE) (Alcalde, 2010) using the 27C7 mutant as the parental template. The PCR reactions were carried out using the iProof high fidelity DNA polymerase.

D205N mutant. The primers for PCR 1 were RMLN and D205N-REV and for PCR 2 were D205N-FOR and RMLC.

N426D mutant. The primers for PCR 1 were RMLN and N426D-REV and for PCR 2 were N426D-FOR and RMLC.

Saturation mutagenesis at position 389. The primers for PCR 1 were RMLN and SAT389-REV and for PCR 2 were SAT389-FOR and RMLC.

Saturation mutagenesis at position 396. The primers for PCR 1 were RMLN and SAT396-REV and for PCR 2 were SAT396-FOR and RMLC.

Saturation mutagenesis at position 454. The primers for PCR 1 were RMLN and SAT454-REV and for PCR 2 were SAT454-FOR and RMLC.

2.5.5.2. Screening assay and high-throughput protocol

Laccase mutant libraries were screened in a medium (blood buffer) containing the colorimetric laccase substrate ABTS and that simulates the composition of human blood, although it lacks coagulating agents and cells. Blood buffer composition: 150 mM NaCl, 18 mM $NaHCO_3$, 1 mg/mL D-(+)-glucose, 4.3 mM urea, 0.87 mM $MgSO_4$, 0.4 mM D-(+)-fructose, 0.1 mM L-cysteine and 4.29 mM ABTS in 100 mM sodium phosphate buffer. The blood buffer pH was set at 6.5 for the first generation and was gradually increased throughout evolution to reach physiological pH (7.4) in generation 4. The general HTP-screening protocol was as reported previously (Maté *et al.*, 2010) with some modifications. Individual clones were picked and cultured in 96-well plates (Greiner Bio-One, Frickenhausen, Germany) containing 50 μL of minimal medium per well. In each plate, column number 6 was inoculated with the parental type and one well (H1-control) was left uninoculated. Plates were sealed to prevent evaporation and incubated at 30°C and 80% relative humidity on a shaker at 225 rpm (Minitron-INFORS, Biogen, Spain). After 48 h, 160 μL of expression medium was added to each well and the plates were incubated for 24 h. The plates (master plates) were then centrifuged (Eppendorf 5810R centrifuge, Germany) for 5 min at 3000 x *g* at 4°C and 60 μL of the supernatant was transferred from the master plate onto a replica plate with the help of a robot (Liquid Handler Quadra 96-320, Tomtec, Hamden, CT). The replica plate was filled with 140 μL of blood buffer, and after briefly stirring the plates and allowing substrate oxidation in blood buffer, absorption was measured at 418 nm ($\varepsilon_{ABTS^{\bullet+}}$=36,000 M^{-1} cm^{-1}) in a plate reader (SpectraMax Plus384, Molecular Devices, Sunnyvale, CA). The plates were incubated at room temperature until a green color developed and the absorption was measured again. Relative activities were calculated as the difference between absorption before and after incubation, and normalized against the parental type used as reference in the corresponding plate (the reference parental types were as follows: 1G, OB-1; 2G, 35H10; 3G, 2E3; 4G, 27C7). To rule out false positives, two consecutive re-screenings were carried out according to our previously described protocol (Maté *et al.*, 2010), but using the blood buffer assay described above. A third re-screening was introduced to obtain

a breakdown of the improvements detected in terms of pH activity profile, Cl^- tolerance and thermostability.

2.5.5.3. Laccase production and purification

Laccase variants were produced in *S. cerevisiae* (with secretion levels of 8 mg/L) and purified to homogeneity as described previously (Maté *et al.*, 2010). For spectroelectrochemical studies, mutants were overproduced in *Pichia pastoris* after cloning them into the pPICZαA vector under the control of the methanol-inducible AOX1 promoter (*Pichia* expression kit, Life Technologies, Carlsbad, CA). Secretions levels of 43 mg/L were achieved in a 42 L autoclavable stainless steel bioreactor (Applikon Biotechnology, Schiedam, The Netherlands).

2.5.5.4. Measurement of laccase activity in human plasma and blood

Human blood was collected in BD Vacutainer blood collection tubes (Plymoth, UK). Blood samples were centrifuged for 10 min at 3,000 rpm to obtain human plasma, discarding the pellet after having carefully extracted the supernatant. Both plasma and blood were supplemented with 10 mM ascorbic acid as substrate and the pH adjusted to 7.4. The activity of the ChU-B mutant in both physiological fluids was determined by measuring oxygen consumption in solution with a Clark electrode. These experiments were performed using the Oxygraph system (Hansatech Instruments, King´s Lynn, UK), taking into account the stoichiometry of the reaction: one molecule of O_2 is reduced by oxidizing four substrate molecules. The activity of the ChU-B mutant was further measured in blood buffer using the same protocol described above and the following substrates: $K_4[Fe(CN)_6]$ (5 mM final concentration); ABTS (5 mM final concentration); and ascorbic acid (10 mM final concentration). Human plasma and blood manipulation was officially authorized by the Faculty of Health and Society of the Malmö University (Sweden).

2.5.5.5. Biochemical characterization

Determination of maximum turnover rates in blood buffer

The initial turnover rates were determined in blood buffer (pH 7.4) for ABTS and DMP. A typical reaction started upon the addition of the enzyme (4.7 and 22.7 nM for ABTS and DMP, respectively) to the assay mixture (1.3 mM ABTS or 2.8 mM DMP in blood buffer). All measurements were performed in triplicate.

pH-activity profiles

The pH profiles were determined over a range of pH 2.0-9.0 as described previously (Camarero *et al.*, 2012).

Halide inhibition (I_{50} determination)

The inhibitory effect of fluoride, chloride and bromide was measured using two laccase substrates (ABTS and DMP) at their corresponding optimal pH activity values (in 100 mM sodium acetate buffer pH 4.0 for ABTS and 100 mM sodium tartrate buffer pH 5.0 for DMP), as well as at physiological pH (in 100 mM sodium phosphate buffer pH 7.4). Inhibition was determined by the I_{50} value (the halide concentration at which the 50% of the initial laccase activity is retained), as the complexity of the plots complicated the extraction of the inhibition constant (K_i). The assay mixture contained 2.4 mM ABTS or DMP, halide (concentrations ranging from 0 to 1100 mM) and purified laccase (0.2 and 1.7 nM for ABTS and DMP, respectively). Each data point represents the mean value determined in at least three independent experiments.

Thermostability (T_{50} determination)

The thermostability of the different laccase samples was estimated by determining their T_{50} values as reported in a previous work (García-Ruiz *et al.*, 2010).

2.5.5.6. Spectro-electrochemical studies

Determination of laccase redox potential

The redox titration of yellow laccase mutants was carried out as described previously for the OB-1 parental type (Mate *et al.*, 2013a), with some modifications. Briefly, a micro-spectroelectrochemical cell containing a gold capillary electrode was used, with the potential controlled by a three-electrode BAS LC-3E potentiostat (Bioanalytical Systems, West Lafayette, IN) where a Ag|AgCl|KCl electrode was used as reference electrode (BAS) and a platinum wire as counter electrode. The absorbance spectra were monitored on a HR4000 high resolution spectrometer with an effective range of 200-1100 nm using a DH-2000 light source, both from Ocean Optics (Dunedin, FL). The redox potential of the T1 site of the enzyme was determined by mediated redox titration (MRT) using the spectroelectrochemical set-up described above. A complex mediator system was used for the MRT containing three different redox mediators: $K_4[Fe(CN)_6]$ and $K_4[Mo(CN)_8]$ with formal redox potentials of +430 mV and +780 mV *vs.* NHE, respectively, and $K_4[W(CN)_8]$ with a formal redox potential of +520 mV *vs.* NHE, synthesized as

described previously (Leipoldt *et al.*, 1974). All experiments were performed in 50 mM sodium phosphate buffer pH 7.4.

Electrochemical measurements

Electrochemical experiments were performed with an Autolab PGSTAT30 analyzer controlled by GPES 4.9 software (Eco Chemie, The Netherlands). Experiments were run in a 3-electrode glass cell using a BAS Ag|AgCl|KCl reference electrode (+210 mV *vs.* NHE) and a platinum wire counter electrode. The low-density graphite (LDG) electrodes were abraded with sandpaper and sonicated. A 5 μL drop of laccase (13 mg/mL) was deposited on a clean LDG electrode and after it had been absorbed for 20 min, the electrode was set into the electrochemical cell, which was bubbled with O_2 (g) at 1 atm pressure for 15 min. For electrocatalytic measurements, current densities are expressed relative to the geometric area of the electrodes and potentials are described relative to that of the NHE. Cyclic voltammograms were recorded from +1100 mV to +210 mV *vs.* NHE using a 10-mV/s scan rate.

2.5.5.7. Protein modelling

Protein models of the parental and evolved laccases were generated and analyzed as described previously (Maté *et al.*, 2010).

2.5.6. SUPPLEMENTAL RESULTS

In the generation 4, the following positions were subjected to site-directed mutagenesis and saturation mutagenesis (see also **Figure 2.5.1.**, p. 147; and **Table 2.5.S1.**, p. 166).

D205N

This mutation reportedly provokes a shift in the optimum pH value of the *Trametes versicolor* laccase (a 1.4 unit increase with DMP as the substrate) (Madzak *et al.*, 2006). The same substitution was tested in this study, giving rise to the 1B1 mutant, which resulted in a comparable improvement (2.0 unit increase over the parental type with DMP as the substrate). 1B1 was finally excluded due to its low TAI value and activity with non-phenolic compounds at physiological pH values.

N426D

This beneficial mutation was first discovered in the 20F1 mutant (2G) but it was eventually lost because of the low likelihood of a crossover event with the nearby I452V. N426D was introduced in 27C7 to create the 3A7 variant, resulting in a 0.6-fold decrease in activity.

Saturation mutagenesis at positions 389, 396 and 454

The Ala389 residue was deleted in the third round of evolution, enhancing the TAI ~3-fold compared to the best performing parent in the previous generation (2E3 mutant). After saturation mutagenesis and screening, only A389A mutants were discovered, indicating that unless the whole residue is removed, no other amino acid is better suited at this position.

Phe396 was subjected to saturation mutagenesis because the F396I mutation conferred the greatest improvement in the entire evolution experiment (a 157-fold improvement in the 35H10 mutant, 1G). Besides, this mutation changed by itself the pH profile for DMP as substrate (from 4.0 to 5.0) without jeopardizing the thermal stability (**Figure 2.5.S1.**, following page). After saturation mutagenesis and screening, all variants found contained the same substitution, confirming Ile396 as the residue best suited to this position in the context of our activity assay.

The F454S mutation was discovered at different stages of the directed evolution (18G5 and 20H4 mutants, 1G; 14C5 mutant, 3G) suggesting an important role in overcoming halide/OH^- inhibition. In our previous work, this substitution was already discovered and reported as destabilizing mutation (Maté *et al.*, 2010). Indeed, a decrease in the T_{50} (with drops of 5°C and 10°C for 18G5 and 20H4, respectively) was detected along with a dramatic lost during its long-term storage (loosing 30% of their activity after two weeks at 4°C). For this reason these variants were not initially chosen as parental types for new rounds of evolution. Interestingly, F454S shifted the pH profile for DMP (from 4.0 to 5.0) as happened with F396I. We explored the position by saturation mutagenesis in an attempt to find a compromise between activity at physiological conditions and stability. After saturating the position, noticeable improvements were detected for several variants with substitutions including non-polar to polar amino acids (F454P/T/A/G/ R/E). From this array of variants, the ChU-B mutant was chosen based on its TAI values, pH profiles, ${}_{ap}I_{50}^{Cl^-}$ and stability (ChU-B kept 100% of stability during long-term storage for months with a T_{50} close to 64°C). ChU-B harbored three mutations (E[α27]K, I[α66]M and the silent mutation D[α49]D) in the α-factor prepro-leader (related to laccase secretion)), and five mutations in the mature protein (two beneficial mutations, F396I and F454E; two silent mutations, E380E and T413T; and a reverted mutation, V452I).

2.5.7. SUPPLEMENTAL FIGURES AND TABLES

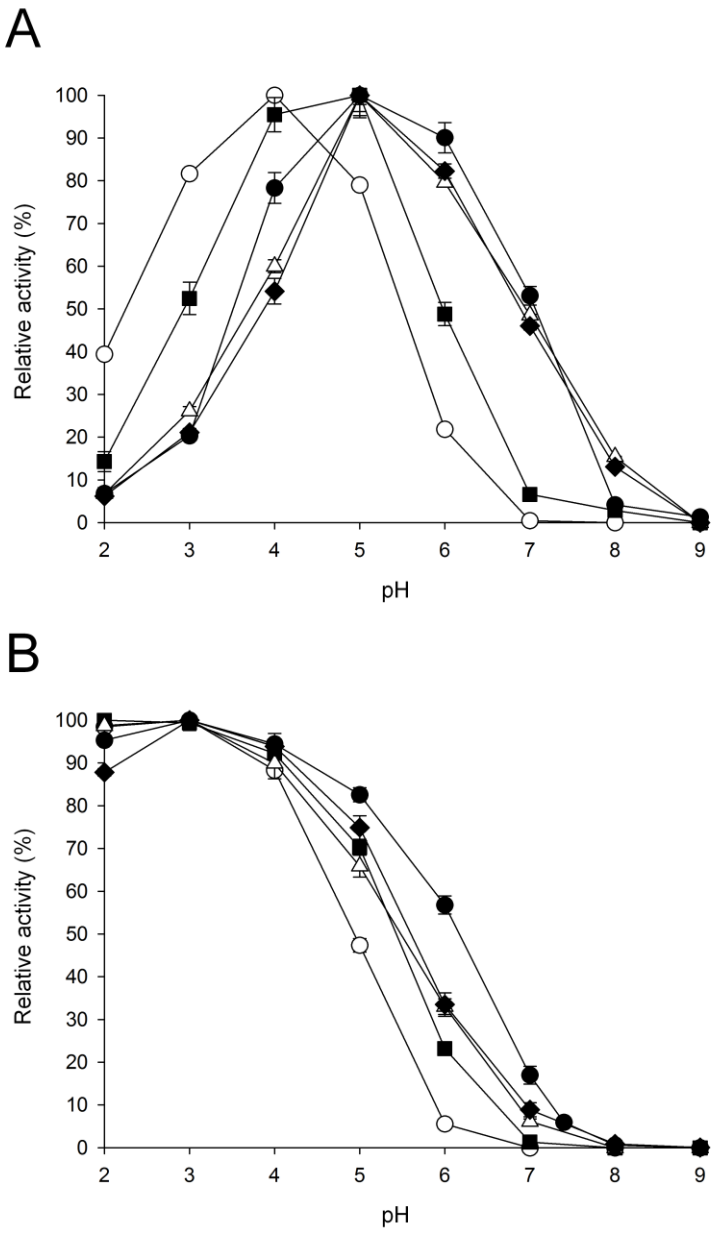

Figure 2.5.S1. pH activity profiles of the parental laccase and the best mutants of each round of evolution. Activities were measured in 100 mM Britton and Robinson buffer at different pH values with 3 mM DMP (**A**) or ABTS (**B**) as substrates. White circles, parental type; black squares, 35H10 mutant (1G); white triangles, 2E3 mutant (2G); black diamonds, 27C7 mutant (3G); black circles, ChU-B mutant (4G). Laccase activity was normalized to the optimum activity, each value representing the mean and standard deviation derived from three independent experiments.

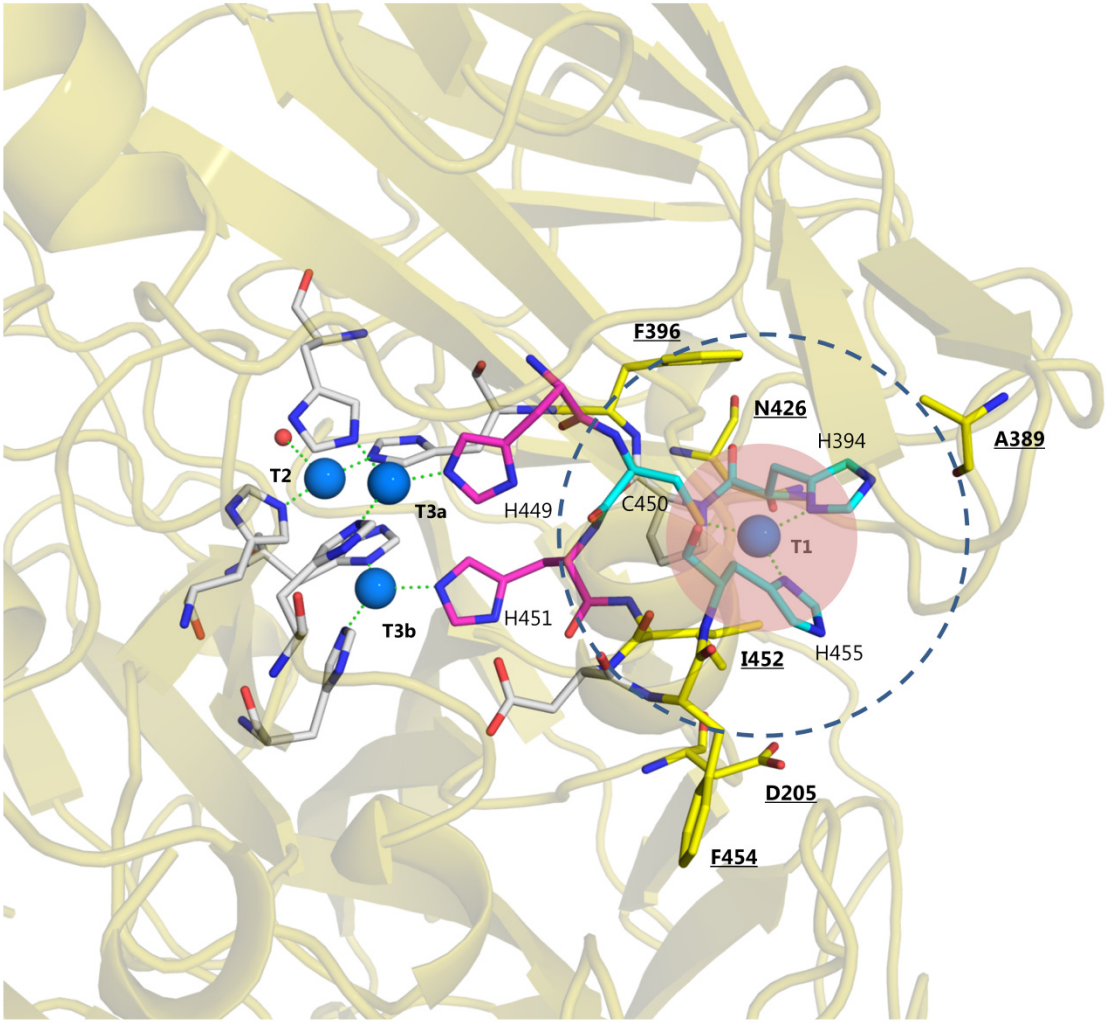

Figure 2.5.S2. Overview of the mutations in the laccase structure. All the residues mutated in this study are highlighted in yellow. The first coordination sphere of the T1 Cu (His394, His455 and Cys450) is indicated with a red circle. Dashed concentric circle indicates the second coordination sphere. The His residues of the internal electron transfer pathway from the T1 Cu to T2/T3 cluster are depicted in magenta. Blue spheres represent copper atoms. The 3D-structure model is based on the crystal structure of the *T. trogii* laccase (97% identity) (Matera *et al.*, 2008).

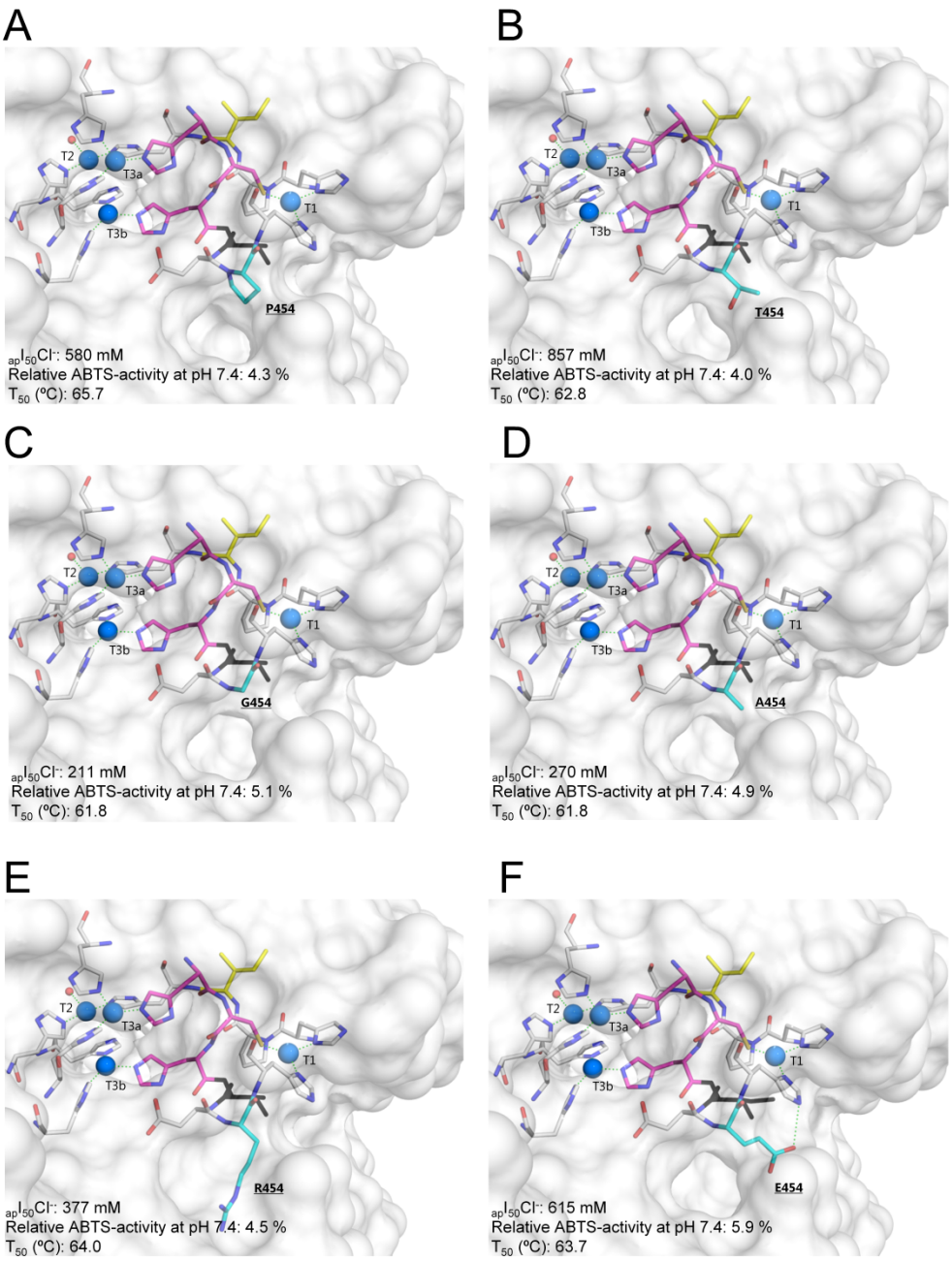

Figure 2.5.S3. Saturation mutagenesis at residue 454 (shown in cyan and underlined): (**A**) 19B12 variant; (**B**) 18A10 variant; (**C**) 17D4 variant; (**D**) 21D9 variant; (**E**) 20C3 variant; (**F**) ChU-B variant. Blue spheres represent copper atoms. The residues of the internal transfer pathway from the T1 Cu to T2/T3 cluster are depicted in magenta. The residues involved in the first coordination sphere of the catalytic coppers and their interactions (green dashes) are also represented. The electrostatic surface of the protein structure is shown in the background. The 3D-structure model is based on the crystal structure of the *T. trogii* laccase (97% identity) (Matera *et al.*, 2008).

Table 2.5.S1. Mutations introduced during the directed evolution process. +, new mutation; o, accumulated mutation; ●, mutation introduced by site-directed mutagenesis; ■, mutation introduced by saturation mutagenesis; □, reverted mutation (V452I, **G**TC/**A**TC). Silent mutations are underlined; subscript indicates codon usage in *S. cerevisiae*. TAI, total activity improvement in blood buffer.

Generation		1G			2G		3G			4G									
Mutation		35H10	18G5	20H4	2E3	20F1	27C7	14F1	14C5	1B1	7B12	14B1	3A7	19B12	18A10	21D9	17D4	20C3	ChU-B
Amino acid	Codon																		
E(α27)K	**G**AA/**A**AA						+			o	o	o	o	o	o	o	o	o	o
D(α49)D	GAT$_{38}$/GA**C**$_{20}$	+			o	o	o	o	o	o	o	o	o	o	o	o	o	o	o
I(α66)M	AT**A**/AT**G**						+			o	o	o	o	o	o	o	o	o	o
E(α86)K	**G**AG/**A**AG								+										
S135R	AG**C**/AG**G**			+															
D205N	**G**AC/**A**AC									●									
T218V	A**C**C/A**T**C				+														
D363D	GA**C**$_{20}$/GA**T**$_{38}$		+																
E380E	GA**G**$_{19}$/GA**A**$_{46}$						+			o	o	o	o	o	o	o	o	o	o
A389-	GCC/---							+											
A389A	GCC$_{13}$/GC**G**$_{6}$										■								
F396I	**T**TC/**A**TC	+			o	o	o	o	o	o	o	■	o	o	o	o	o	o	o
F403F	TTC$_{18}$/TT**T**$_{26}$		+																
T413T	AC**G**$_{8}$/AC**A**$_{18}$						+			o	o	o	o	o	o	o	o	o	o
N426D	**A**AC/**G**AC					+		o	o				●						
I452V	**A**TC/**G**TC				+		o			o	o	o	o	o	o	o	o	o	□
F454S	T**T**C/T**C**C		+	+					+										
F454P	**TTC**/**CCC**													■					
F454T	**TTC**/**ACG**														■				
F454A	**TTC**/**GCG**															■			
F454G	**TTC**/**GGC**																■		
F454R	**TTC**/**CGG**																	■	
F454E	**TTC**/**GAG**																		■
A458A	GC**T**$_{21}$/GC**C**$_{13}$								+										
F460F	TT**C**$_{18}$/TT**T**$_{26}$								+										
T487S	A**C**C/A**G**C								+										
TAI (in fold)		157	101	99	4082	1884	16736	13062	12654	15900	16736	16736	10041	23430	25104	28702	28033	26778	41840
Apparent I_{50} NaCl (mM)		427	n.d.	n.d.	800	500	452	513	622	n.d.	n.d.	n.d.	400	580	857	270	211	377	615
Relative activity (%) at pH 7.0		1.3	0.0	0.0	6.2	6.3	8.9	11.4	22.0	4.9	n.d.	n.d.	7.2	8.5	9.6	8.6	10.3	9.6	17.0
T_{50} (°C)		69.5	68.1	65.1	68.0	69.0	68.5	66.8	60.0	n.d.	n.d.	n.d.	68.9	65.7	62.8	61.8	61.8	64.0	63.7

Table 2.5.S2. Parental and ChU-B mutant I_{50} values (in mM) for different halides.

Inhibitor	Substrate	pH[a]	OB-1 mutant	ChU-B mutant
NaF	ABTS	4.0	0.070	0.109
	DMP	5.0	0.167	0.183
NaCl	ABTS	4.0	176	1025
	DMP	5.0	208	818
NaBr	DMP	4.0	1306	n.m.[b]

[a]Experiments were carried out at the optimum pH value for each substrate. [b]n.m., non measurable.

Table 2.5.S3. Maximum turnover rates (mol substrate/min/mol enzyme) for the parental laccase and ChU-B mutant under optimum conditions and in blood buffer.

Substrate	pH	Parent type	ChU-B mutant
ABTS	3.0	44215 ± 1061	14895 ± 654
	7.4 (blood buffer)	n.m.	143 ± 9
DMP	Optimum[a]	20820 ± 710	4767 ± 216
	7.4 (blood buffer)	n.m.	427 ± 32

[a]Optimum pH activity value (4.0 and 5.0 for parent and ChU-B, respectively). n.m., non measurable.

Table 2.5.S4. Mutations introduced into the mature laccase during the directed evolution process.

Mutation	Distance to T1 Cu (Å)	Distance to T2 Cu (Å)	Distance to T3a-T3b Cu (Å)	Domain	Secondary structure motif
I452V	4.8	12.4	9.6	III	Loop (H451-I452)
F454E[a]	7.6	15.8	12.2	III	α-helix (D453-A458)
F396I[a]	7.6	9.9	9.0	III	β-sheet (P395-L398)
A389-	7.7	21.4	18.4	III	Loop (L383-H394)
N426D	9.3	14.5	13.7	III	β-sheet (V424-N426)
D205N	7.8	15.2	11.8	II	Loop (L202-N207)

[a]Mutations present in the final ChU-B variant.

Table 2.5.S5. Primers employed in this project. The codons subjected to mutagenesis are highlighted in bold, where N is A/T/G/C and S is G/C.

Oligo	Sequence	Annealing site (bp) in pJRoC30
RMLN forward	5′-CCTCTATACTTTAACGTCAAGG-3′	5′-420-441-3′
RMLC reverse	5′-GGGAGGGCGTGAATGTAAGC-3′	5′-2288-2307-3′
D205N forward	5′-CTGGTGTCGCTGTCATGC**AAC**CCGAATTACACGTTCAGC-3′	5′-1337-1375-3′
D205N reverse	5′-GCTGAACGTGTAATTCGG**GTT**GCATGACAGCGACACCAG-3′	5′-1337-1375-3′
N426D forward	5′-GTCTACCGCGACGTCGTC**GAC**ACGGGCTCGCCCGGGGAC-3′	5′-2000-2038-3′
N426D reverse	5′-GTCCCCGGGCGAGCCCGT**GTC**GACGACGTCGCGGTAGAC-3′	5′-2000-2038-3′
SAT389 forward	5′-CTCCCCGCCACCTCCGCC**NNS**CCCGGCTTCCCGCAC-3′	5′-1889-1924-3′
SAT389 reverse	5′-GTGCGGGAAGCCGGG**SNN**GGCGGAGGTGGCGGGGAG-3′	5′-1889-1924-3′
SAT396 forward	5′-CCCGGCTTCCCGCACCCC**NNS**CACTTGCACGGGCACACC-3′	5′-1910-1948-3′
SAT396 reverse	5′-GGTGTGCCCGTGCAAGTG**SNN**GGGGTGCGGGAAGCCGGG-3′	5′-1910-1948-3′
SAT454 forward	5′-CTCCACTGCCACGTCGAC**NNS**CACCTTGAGGCTGGGTTC-3′	5′-2084-2122-3′
SAT454 reverse	5′-GAACCCAGCCTCAAGGTG**SNN**GTCGACGTGGCAGTGGAG-3′	5′-2084-2122-3′

CAPÍTULO 6

Functional expression of a blood tolerant laccase in *Pichia pastoris*

Diana M. Mate, David Gonzalez-Perez, Roman Kittl,
Roland Ludwig and Miguel Alcalde

Published in *BMC Biotechnology*, 2013, vol. 13, issue 38.

2.6.1. SUMMARY

Background: Basidiomycete high-redox potential laccases (HRPLs) working in human physiological fluids (pH 7.4, 150mM NaCl) arise great interest in the engineering of 3D-nanobiodevices for biomedical uses. In two previous reports, we described the directed evolution of a HRPL from basidiomycete PM1 strain CECT 2971: i) to be expressed in an active, soluble and stable form in *Saccharomyces cerevisiae*, and ii) to be active in human blood. In spite of the fact that *S. cerevisiae* is suited for the directed evolution of HRPLs, the secretion levels obtained in this host are not high enough for further research and exploitation. Thus, the search for an alternative host to over-express the evolved laccases is mandatory.

Results: A blood-active laccase (ChU-B mutant) fused to the native/evolved α-factor prepro-leader was cloned under the control of two different promoters (P_{AOX1} and P_{GAP}) and expressed in *Pichia pastoris*. The most active construct, which contained the P_{AOX1} and the evolved prepro-leader, was fermented in a 42-L fed-batch bioreactor yielding production levels of 43 mg/L. The recombinant laccase was purified to homogeneity and thoroughly characterized. As happened in *S. cerevisiae*, the laccase produced by *P. pastoris* presented an extra N-terminal extension (ETEAEF) generated by an alternative processing of the α-factor pro-leader at the Golgi compartment. The laccase mutant secreted by *P. pastoris* showed the same improved properties acquired after several cycles of directed evolution in *S. cerevisiae* for blood tolerance: a characteristic pH-activity profile shifted to the neutral-basic range and a greatly increased resistance against inhibition by halides. Slight biochemical differences between both expression systems were found in glycosylation, thermostability and turnover numbers.

Conclusions: The tandem-yeast system based on *S. cerevisiae* to perform directed evolution and *P. pastoris* to over-express the evolved laccases constitutes a promising approach for the *in vitro* evolution and production of these enzymes towards different biocatalytic and bioelectrochemical applications.

2.6.2. BACKGROUND

Laccases (benzenediol:oxygen oxidoreductase, E.C. 1.10.3.2.) are extracellular, multicopper oxidases widely distributed in fungi, higher plants, bacteria, lichens and insects (Baldrian, 2006; Laufer *et al.*, 2009; Singh *et al.*, 2011). They contain a T1 copper atom at which the reducing substrate is oxidized and a trinuclear copper cluster at which oxygen is reduced to water (Davies and Ducros, 2002). Laccases are able to oxidize a broad range of phenolic and non-phenolic compounds expanding further its broad substrate specificity through the inclusion of redox mediators from natural or artificial sources (Cañas and Camarero, 2010). The physiological roles of laccases are diverse and depend on their origin. In plants, these enzymes seem to be involved in wound response, fruiting body formation, cell-wall reconstitution and synthesis of lignin (Alcalde, 2007). Role attributes for bacterial laccases cover copper homeostasis, morphogenesis and pigmentation of spores to confer resistance to stress factors (Singh *et al.*, 2011). In fungi, laccases carry out a variety of physiological roles including morphogenesis, fungal plant-pathogen/host interaction and lignin mineralization (Baldrian, 2006). Among fungal laccases, those produced by the basidiomycete white-rot fungi are of great biotechnological interest due to their higher redox potential at the T1 site (Christenson *et al.*, 2004). Thus, high-redox potential laccases (HRPLs) find applications in the production of second generation biofuels, pulp-kraft biobleaching, bioremediation, organic syntheses and the development of biosensors and miniature biofuel cells for medical uses (Heller, 2004; Xu, 2005; Rodgers *et al.*, 2010).

Over 20 fungal laccases have been heterologously expressed in the yeasts *Pichia pastoris* and *Saccharomyces cerevisiae* for different purposes (Piscitelli *et al.*, 2010; Maté *et al.*, 2011). In general terms, both organisms are suitable for the expression of eukaryotic genes. These hosts are easy to manipulate due to the availability of a large set of molecular biology tools; besides, they have the ability to perform post-translational modifications (disulfide bridge formation, C- and N-terminal processing, glycosylation) readily secreting active enzymes to the culture broth (Romanos *et al.*, 1992). Particularly, *S. cerevisiae* arise a great interest in synthetic biology and protein engineering by directed evolution (Cobb *et al.*, 2012; Gonzalez-Perez *et al.*, 2012). With a sophisticated eukaryotic device supported by a high frequency of homologous DNA recombination, the construction of complex metabolic pathways by *in vivo* splicing expression cassettes and/or the directed evolution of cumbersome systems (*e.g.*, ligninolytic enzyme consortiums) are simply performed (Shao *et al.*, 2009; Gonzalez-Perez *et al.*, 2012). Indeed, the battery of reliable *in vivo* recombination methods based on *S. cerevisiae* physiology make this budding yeast a powerful cell factory for plenty of potential applications (Gonzalez-Perez *et al.*, 2012). Despite these advantages, the practical use of *S. cerevisiae* in different industrial settings is limited by its rather low secretion levels (Piscitelli *et al.*, 2010). Although the methylotrophic

yeast *P. pastoris* is not the favorite host for directed evolution experiments (the lack of episomal vectors together with low transformation efficiencies constrain the building of mutant libraries) (Pourmir and Johannes, 2012), it does show some attractive features which may complement *S. cerevisiae* in the synthetic evolutionary scenario: specifically, the ability to grow at very high cell densities under the control of strong promoters and secrete high amounts of protein (Daly and Hearn, 2005). Even though the expression levels reported for recombinant fungal laccases in these yeasts are diverse (**Table 2.6.1.**), overall they are much higher in *P. pastoris*, ranging from 4.9 to 517 mg/L (Otterbein *et al.*, 2000; Soden *et al.*, 2002; Colao *et al.*, 2006; Cui *et al.*, 2007; Li *et al.*, 2007; Kittl *et al.*, 2012a,b), than in *S. cerevisiae*, where they vary from 2 to 18 mg/L (Bulter *et al.*, 2003a; Klonowska *et al.*, 2005; Andberg *et al.*, 2009; Maté *et al.*, 2010; Camarero *et al.*, 2012).

Table 2.6.1. List of fungal laccases heterologously expressed in *P. pastoris* and *S. cerevisiae*.

Heterologous host	Laccase source	Expression yields (mg/L)	Promoter	Reference
P. pastoris	*Botrytis aclada*[a]	517	GAP[c]	Kittl *et al.*, 2012a
P. pastoris	*Botrytis aclada*[a]	495	AOX1[d]	Kittl *et al.*, 2012b
P. pastoris	*Pleurotus sajor-caju*[b]	4.9	AOX1[d]	Soden *et al.*, 2002
P. pastoris	*Pycnoporus cinnabarinus*[b]	8	AOX1[d]	Otterbein *et al.*, 2000
P. pastoris	*Trametes* sp. 420[b]	136	AOX1[d]	Cui *et al.*, 2007
P. pastoris	*Trametes* sp. AH28-2[b]	31.6	AOX1[d]	Li *et al.*, 2007
P. pastoris	*Trametes trogii*[b]	17	AOX1[d]	Colao *et al.*, 2006
S. cerevisiae	*Melanocarpus albomyces*[a]	7	GAL1[d]	Andberg *et al.*, 2009
S. cerevisiae	*Myceliophthora thermophila*[a,*]	18	ADH1[c]	Bulter *et al.*, 2003a
S. cerevisiae	PM1[b,*]	8	GAL1[d]	Maté *et al.*, 2010
S. cerevisiae	*Pycnoporus cinnabarinus*[b,*]	2	GAL1[d]	Camarero *et al.*, 2012
S. cerevisiae	*Trametes* sp. C30[b]	2	GAL10[d]	Klonowska *et al.*, 2005

[a]Ascomycete; [b]basiodiomycete; [c]constitutive promoter; [d]inducible promoter. [*]Laccase functional expression achieved by directed evolution.

In a previous work we tackled the directed evolution of the HRPL from the white-rot fungus PM1 strain CECT 2971 to be secreted in *S. cerevisiae* (with levels of ~8 mg/L) (Maté *et al.*, 2010). This evolved PM1 laccase was recently tailored to be active in human blood (at pH 7.4 and high NaCl concentration -150 mM-) (Mate *et al.*, 2013b). HRPLs are strongly inhibited by modest concentrations of OH^- and Cl^-, which tightly bind to the catalytic copper centers interrupting the catalysis. To surpass such inhibition, several rounds of laboratory evolution in combination

with semi-rational approaches were carried out using a screening assay based on the biochemical composition of human blood. Here, we describe the cloning and over-expression of this blood tolerant laccase in *P. pastoris*. The recombinant enzyme was tested with different promoters and fermentation conditions. The fermentation of the best construct was scaled up in a 42 L-bioreactor to 20 L fermentation volume, purified, and biochemically characterized. Laccase properties were compared to those obtained for the same mutant enzyme expressed by *S. cerevisiae*.

2.6.3. RESULTS AND DISCUSSION

2.6.3.1. Heterologous functional expression of blood tolerant laccases in *P. pastoris*

The departure point of the present study is a thermostable laccase from basidiomycete PM1, which was first subjected to eight generations of *in vitro* evolution for functional expression in *S. cerevisiae* (Maté *et al.*, 2010) and thereafter to four further cycles of evolution to become active in human blood (Mate *et al.*, 2013b). The final variant of this process (ChU-B mutant) is formed by the α-factor prepro-leader plus the mature laccase. The ChU-B whole fusion gene harbours 22 mutations (eight silent) (**Figure 2.6.1.**). Beneficial mutations enhancing functional expression or activity are both located in the signal sequence (five mutations) and in the mature protein (seven mutations). Besides, the mature protein presents two mutations, F396I and F454E, placed at the second coordination sphere of the T1 Cu, which are responsible for the activity shown in human blood (**Figure 2.6.1.**).

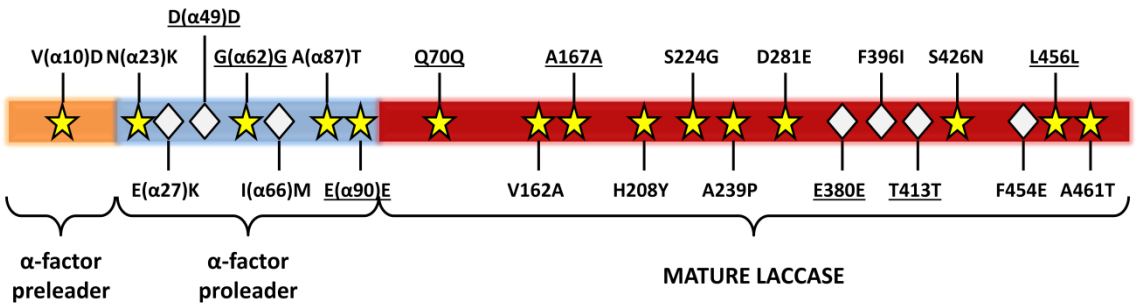

Figure 2.6.1. Mutations in the ChU-B mutant fusion gene. The α-factor pre-leader is depicted in orange, the α-factor pro-leader in blue, and the mature laccase in red. The fifteen mutations accumulated in the directed evolution for functional expression in yeast are represented as yellow stars, while the seven mutations resulted from the evolutionary process for activity in blood are shown as grey diamonds. Silent mutations are underlined.

To test ChU-B expression levels in *P. pastoris*, four different constructs were built, including native and evolved α-factor prepro-leaders in combination with two expression vectors: pPICZαA under the control of the methanol inducible alcohol oxidase promoter (P_{AOX1}) and pGAPZαA under the control of the constitutive glyceraldehyde 3-phosphate dehydrogenase promoter (P_{GAP}) (**Figure 2.6.2.**). Transformed clones were pre-screened for laccase expression on agar plates supplemented with ABTS, resulting in all four cases in a green halo around the colonies due to substrate oxidation by laccase. The apparent most active clones were further subjected to microtiter fermentations (in 96 deep-well plates). Of this set of experiments, P_{AOX1} clones showed the highest ABTS-activity and they were subjected to small scale fed-batch fermentation (500 mL bioreactor, **Figures 2.6.3A** and **B**). Laccase activity was *ca.* 1.7-fold higher for the construct containing the evolved prepro-leader (*i.e.*, 580 ABTS-U/L *vs.* 990 ABTS-U/L for the laccase with the original and the mutated α-factor signal sequence, respectively). Accordingly, production of the construct with the evolved prepro-leader was scaled up in a 20-L fermentation (**Figure 2.6.3C**). The maximum volumetric activity was reached after 151 h (3220 ABTS-U/L). Cultivation was not stopped at this time since wet biomass was still increasing and we could expect higher amounts of enzyme to be secreted. Unfortunately, laccase activity diminished to 2830 ABTS-U/L at harvesting time (165 h), an effect that may be ascribed to proteolytic degradation by released intracellular proteases (Cregg *et al.*, 2000). Under these conditions, the final laccase production was 43 mg/L. This was 5.4-fold higher than that obtained in shake-flask cultures of *S. cerevisiae* (8 mg/L); the latter cannot yield the high cell density levels of *P. pastoris* (Cregg *et al.*, 2000), which precludes its use in bioreactor (Maté *et al.*, 2010). Compared to other basidiomycete laccases secreted by *P. pastoris*, the ChU-B secretion was 9-, 5- and 2.5-fold higher than those of laccases from *Pleurotus sajor-caju*, *Pycnoporus cinnabarinus* and *Trametes trogii*, respectively, and very similar to that of the *Trametes* sp. AH28-2 laccase (**Table 2.6.1.**). The production yields achieved with the laccase from *Trametes* sp. 420 and the ascomycete *Botrytis aclada* laccase were much higher (**Table 2.6.1.**).

2.6.3.2. Biochemical characterization

Glycosylation and thermostability

The ChU-B laccase produced in *P. pastoris* was purified by three chromatographic steps resulting in a homogeneous sample, which was compared with the purified counterpart from *S. cerevisiae* (Mate *et al.*, 2013b). The molecular mass deduced from SDS-PAGE was ~60 kDa for the enzyme secreted by *P. pastoris* and *S. cerevisiae* (**Figure 2.6.4A**). The MALDI-TOF (Matrix-Assisted Laser Desorption and Ionization-Time Of Flight) mass spectrometry analysis allowed a more accurate estimation of molecular masses (62,541 Da and 60,310 Da for the laccase from *P. pastoris* and *S. cerevisiae*, respectively). From the molecular mass determined using the amino acid composition (53,939 Da), glycosylation patterns of 16% and 12% for the laccase from *P.*

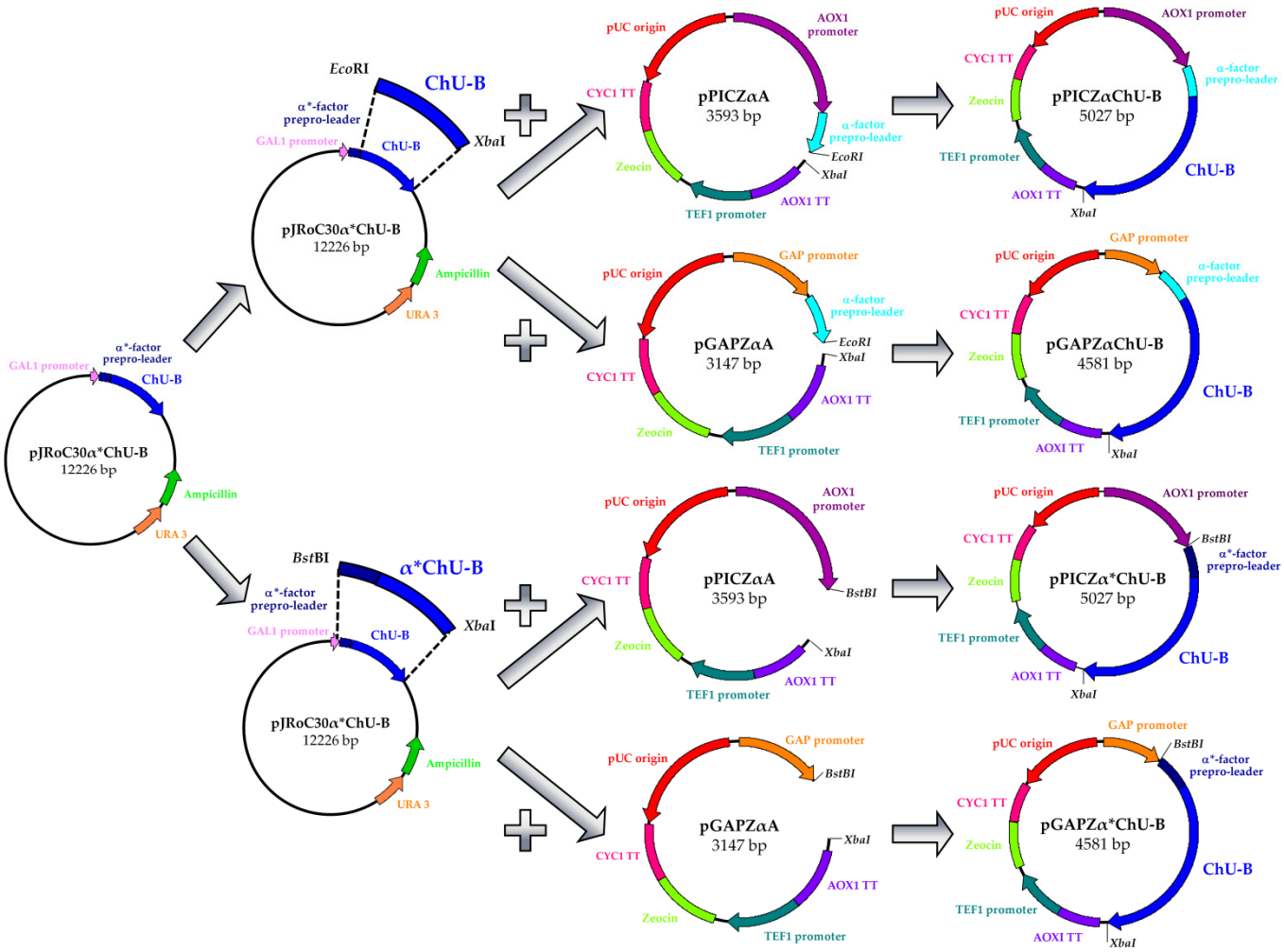

Figure 2.6.2. Cloning strategy for the construction of pPICZαChU-B, pGAPZαChU-B, pPICZα*ChU-B and pGAPZα*ChU-B plasmids. The pJRoC30α*ChU-B was used as template to amplify ChU-B with/without the evolved α-factor prepro-leader (α*) from *S. cerevisiae*. See **Methods section**, p. 183, for details.

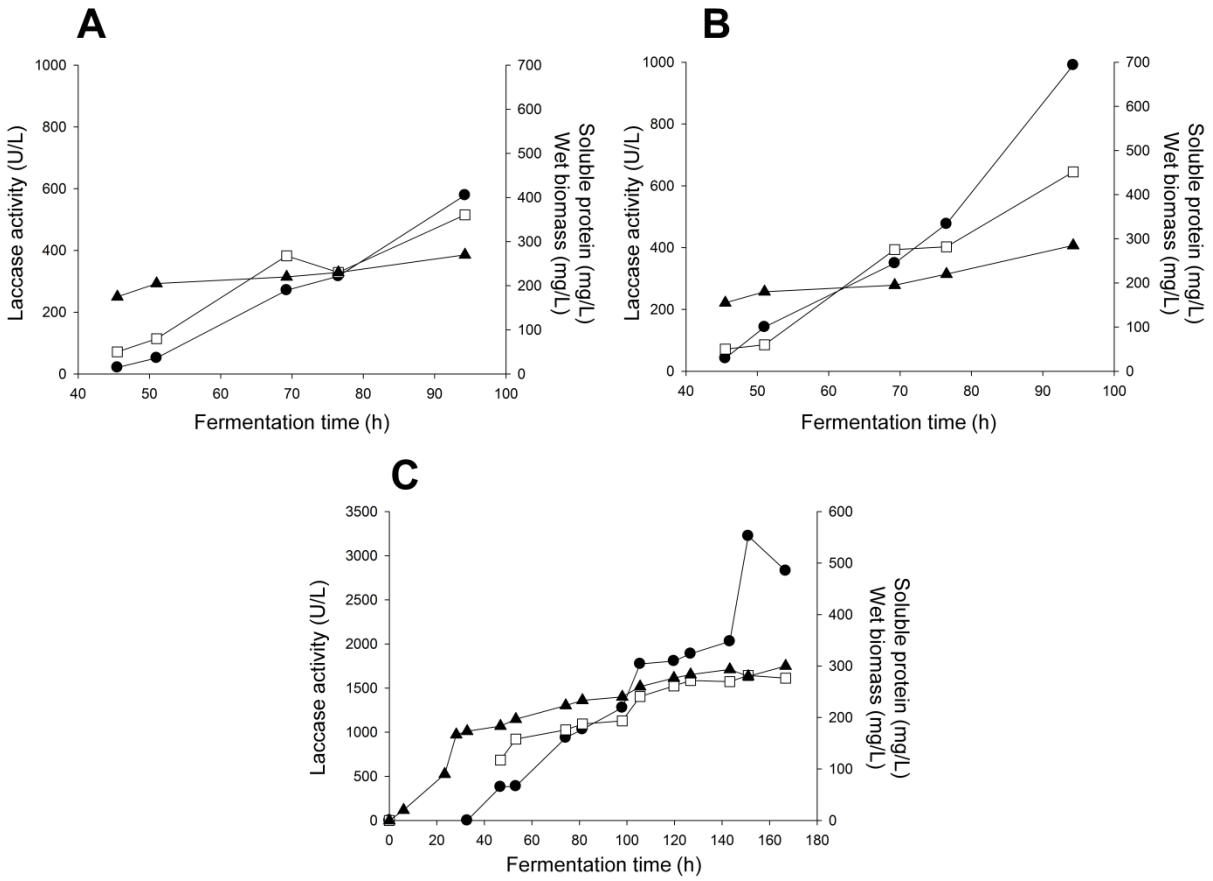

Figure 2.6.3. Laccase expression in *P. pastoris*. (**A** and **B**) Fermentation in a 500-mL bioreactor of *P. pastoris* transformants expressing the ChU-B mutant joined to the original (**A**) and the evolved (**B**) α-factor prepro-leader under the control of the P_{AOX1}. After 22 h of batch phase, glycerol feed was maintained for 5 hours and thereafter the methanol induction started. Methanol was pumped to the culture so that a DO level ~4% was maintained throughout the fermentation. (**C**) 20-L fermentation in a 42-L bioreactor of a *P. pastoris* clone transformed with pPICZα*ChU-B. Fermentation comprised four steps: batch phase for 22 h, glycerol phase for 5 h, transition phase for 5 h to adapt the culture to grow on methanol, induction phase for 136 h. Black circles, laccase activity at the induction phase; black triangles, wet biomass; white squares, extracellular protein concentration.

pastoris and *S. cerevisiae* were calculated (**Table 2.6.2.**). Unlike *S. cerevisiae*, whose tendency to add in high extent mannose moieties at the Golgi compartment led to hyperglycosylated heterologous proteins, *P. pastoris* is known to introduce outer sugar chains to a lesser extent (being more appropriate than *S. cerevisiae* to produce, for example, proteins for crystallization studies) (Romanos *et al.*, 1992). These results address a longer residence time at the Golgi of ChU-B mutant in *P. pastoris* than in *S. cerevisiae*. Comparing our data with other HRPLs expressed in *P. pastoris,* the degree of glycosylation is similar to that of the highly related *T. trogii* laccase (97% of sequence identity with ChU-B; Matera *et al.*, 2008) but much lower than that of the hyperglycosylated *P. cinnabarinus* laccase (with ~75% of sequence identity with ChU-B laccase), which probably has to face several bottlenecks during exocytosis (with glycosylation degrees of 36% and ~50% in *P. pastoris* and *S. cerevisiae*, respectively (Otterbein *et al.*, 2000; Camarero *et al.*, 2012).

Kinetic thermostability was determined by measuring the T_{50} (the temperature at which the enzyme retains 50% of its activity after ten minutes of incubation). In spite of the fact that hyperglycosylation is generally reported to confer higher thermostability (Wang *et al.*, 1996), the T_{50} of the laccase variant produced in *P. pastoris* was ~6°C behind its counterpart from *S. cerevisiae* (**Table 2.6.2**). Only the careful examination of thermodynamic stability could give us new clues about whether the laccase overglycosylation in *P. pastoris* is affecting the protein folding and stability.

Table 2.6.2. Biochemical characteristics of ChU-B mutant produced in *P. pastoris* and *S. cerevisiae*.

Feature	ChU-B from *P. pastoris*	ChU-B from *S. cerevisiae*
Expression levels (mg/L)	43	8
MW[1]	53,939	53,939
MW[2]	62,541	60,310
Glycosylation (%)	16	12
N-terminal end	**ETEAEF**SIGP	**ETEAEF**SIGP
Optimum pH (with ABTS)	4.0	4.0
Optimum pH (with DMP)	5.0	5.0
T_{50} (°C)	57.9	63.7

[1]Calculated from the amino acid composition (http://web.expasy.org/compute_pi/); [2]determined by MALDI-TOF mass spectrometry. The extra N-terminal extension is highlighted in bold.

N-terminal end

We recently reported an extra N-terminal extension of six amino acids in our evolved laccase, as consequence of an alternative processing at the Golgi compartment. It was concluded that this extra tail was beneficial for secretion without jeopardizing the biochemical laccase properties (Mate *et al.*, 2013a). In order to know whether similar processing takes place in *P. pastoris*, ChU-B was subjected to end-terminal sequencing. Indeed, the same N-terminal extension ETEAEF was detected in the mature protein revealing the lack of sufficient amount of *STE13* protease in *P. pastoris* for a correct cleavage of the α-factor pro-leader. Our results are in good agreement with several studies in which *STE13* was not capable of processing the high levels of α-factor prepro-leader fusion genes, resulting in an extra N-terminal tail linked to the mature protein (Romanos *et al.*, 1992; Garcia-Ruiz *et al.*, 2012; Mate *et al.*, 2013a).

Evolved properties of ChU-B laccase

a) pH activity profiles

HRPLs are fully inactive at neutral or basic pHs due to a reversible OH^- inhibition process. One of the most remarkable improvements of ChU-B mutant after directed evolution was the shift in the pH activity profile towards the neutral-alkaline side (pH of human blood is around 7.4). ChU-B produced by *S. cerevisiae* retained ~20% and ~10% of its initial activity at physiological pH with DMP and ABTS as substrates, respectively, whereas the activity of parent type (OB-1 mutant) at this pH was negligible (Mate *et al.*, 2013b). Almost identical pH activity shapes (with the same optimal pH values at 5.0 for DMP and 4.0 for ABTS) were detected with independency of the producing yeast indicating that this important acquired feature was also shown by the mutant expressed in *P. pastoris* (**Figures 2.6.4B** and **C**). Even though the pH profile was shifted (including a change in the optimum pH for DMP from 4.0 to 5.0), as occurs for the rest of fungal laccases a bell shaped profile was observed for the phenolic substrate DMP, which is the result of two opposite effects: i) activation in the acidic range due to higher redox potential difference between the phenol and the T1 Cu (the redox potential of phenols decreases when pH increases while the redox potential of the laccase hardly varies), and ii) inactivation at alkaline pH due to the accumulation of OH^-, which bind to the T2 site interrupting the internal electron transfer from the T1 to the T2/T3 centers (Xu, 1997). Concerning the non-phenolic substrate ABTS, the pH activity profile showed the expected monotonic shape as the oxidation of this compound does not include proton exchange and the only effect involved is the inhibition by OH^-.

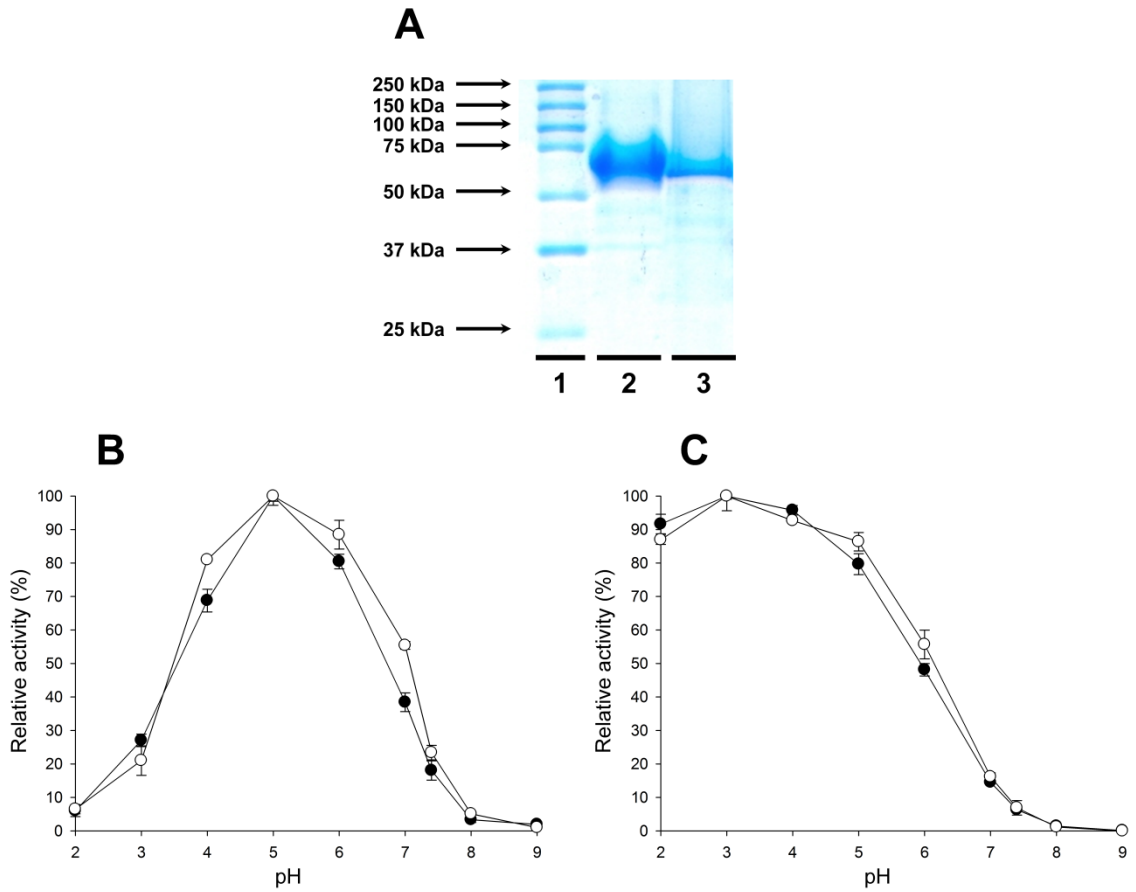

Figure 2.6.4. Biochemical characterization of ChU-B mutant. (**A**) SDS-PAGE: Lane 1, protein standards; lane 2, ChU-B from *P. pastoris*; lane 3, ChU-B from *S. cerevisiae*. Samples were resolved on a 12% SDS-polyacrylamide gel and stained with Coomassie Brilliant Blue. (**B** and **C**) pH activity profiles. Black circles, ChU-B from *P. pastoris*; white circles, ChU-B from *S. cerevisiae*. Activities were measured in 100 mM Britton and Robinson buffer in the pH range from 3.0 to 9.0 with 3 mM DMP (**B**) or 3 mM ABTS (**C**) as the reducing substrates. Relative activity (in %) was calculated with respect to the activity at the optimum pH and each point, including the standard deviation, is the average of three independent experiments.

b) Inhibition by halides

HRPLs are strongly inhibited by the presence of modest concentrations of halides (Cl^-, Br^-, F^- but not I^-) (Gianfreda *et al.*, 1999). Therefore, the use of HRPLs in miniature biofuel cells operative in mammal physiological fluids (with ~150 mM NaCl) is limited, on the one hand by the negligible activity at neutral-alkaline pH, and on the other, by the low laccase tolerance against Cl^-. The ChU-B mutant greatly surpassed the halide inhibition by directed evolution and this important property was checked in the variant expressed by *P. pastoris*. The I_{50} values (the

concentration of halide at which the enzyme keeps 50% of its initial activity) were determined at acidic and physiological pH using ABTS and DMP as substrates. Whilst the $I_{50}Cl^-$ of parent type (the OB-1 mutant) was 176 mM and 208 mM for ABTS and DMP at acidic pH, respectively, these values were risen up in the ChU-B variant from *S. cerevisiae* to 1025 mM and 818 mM for these substrates. Additionally, a slight increase in the $I_{50}F^-$ value for both substrates at acidic pH was also observed (parent type: 70 μM and 167 μM for ABTS and DMP, respectively; ChU-B mutant from *S. cerevisiae*: 109 μM and 183 μM for ABTS and DMP, respectively) (Mate *et al.*, 2013b). These improved $I_{50}F^-$ and $I_{50}Cl^-$ were maintained in the mutant expressed in *P. pastoris* being similar in both yeasts (*i.e.* $I_{50}Cl^-$ ~1000 mM and $I_{50}F^-$ above 100 μM both for ABTS and DMP at acidic pH; **Table 2.6.3.** and **Figures 2.6.5A** and **B**). Since the smaller the ionic diameter of the halide the easier the access to the T2/T3 trinuclear copper cluster (Xu, 1996b), an inhibition potency $F^->Cl^-$ was observed with independence of the substrate tested (**Table 2.6.3.**; **Figures 2.6.5A** and **B**). When halide inhibition was measured at physiological pH, the enzyme expressed in both yeasts showed $I_{50}F^-$ which rose from the μM range at acid pH to the mM range at blood pH, **Figure 2.6.5A**. Moreover, laccase activity was not affected by increasing concentrations of Cl^- (**Figure 2.6.5C**). This data is consistent with the described effect by which the halide inhibition of laccase activity is weaker at alkaline pH values. Under such conditions, the presence of a deprotonated water molecule coordinating the T2 Cu results in a competition with the halide for binding to the T2 site (Naki and Varfolomeev, 1982; Xu, 1997; Xu *et al.*, 1998).

Table 2.6.3. I_{50} values (in mM) of sodium halides for ChU-B mutant produced in *P. pastoris* and *S. cerevisiae*.

Inhibitor	Substrate	pH	ChU-B from *P. pastoris* I_{50} (mM)	ChU-B from *S. cerevisiae* I_{50} (mM)
NaF	ABTS	4.0	0.134	0.109
	ABTS	7.4 (blood buffer)	40	42
	DMP	5.0	0.174	0.183
NaCl	ABTS	4.0	1106	1025
	ABTS	7.4	n.m.	n.m.
	DMP	5.0	931	818

n.m.: non-measurable. Inhibition studies were performed at the optimum pH activity value for each substrate tested (4.0 and 5.0 for ABTS and DMP, respectively) and at physiological pH (7.4) with ABTS as reducing substrate.

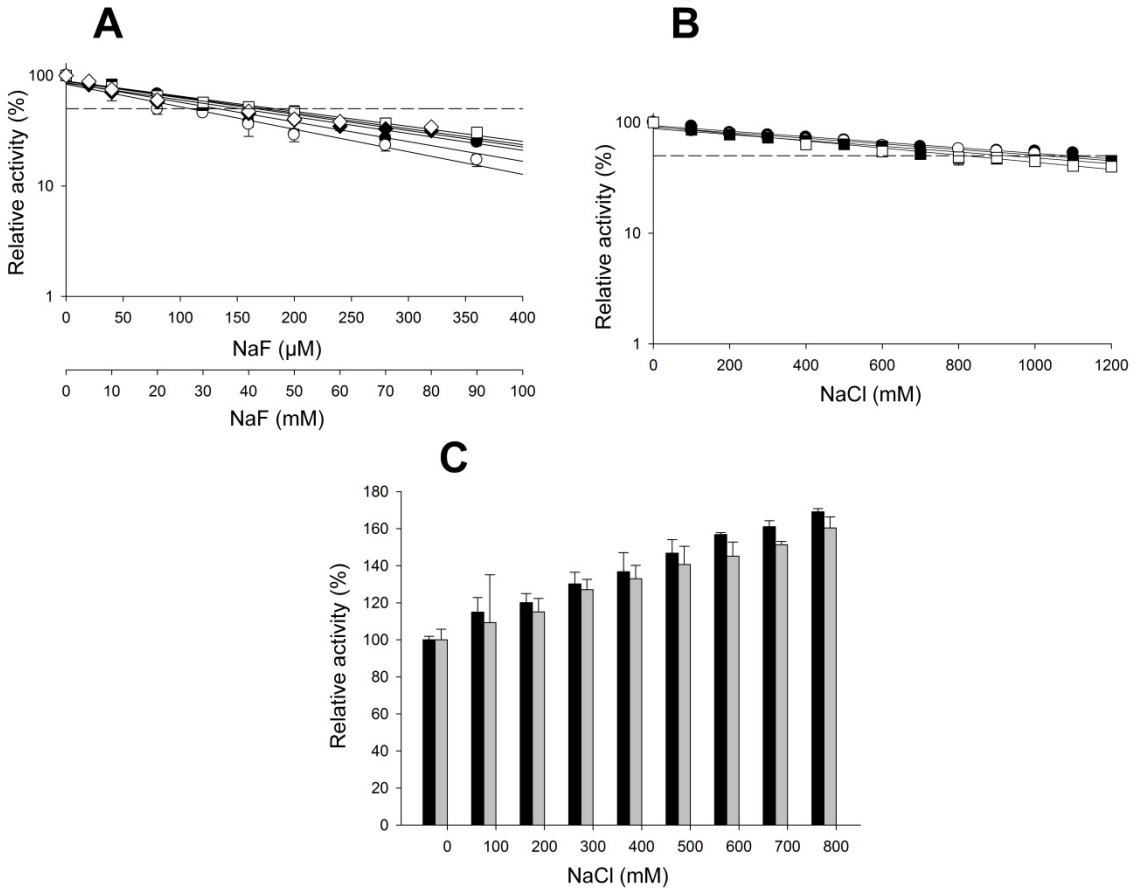

Figure 2.6.5. Inhibition of ChU-B by halides. (**A**) NaF inhibition with: i) ABTS at pH 4.0 (X-axis in μM; black circles, ChU-B from *P. pastoris*; white circles, ChU-B from *S. cerevisiae*); ii) DMP at pH 5.0 (X-axis in mM; black squares, ChU-B from *P. pastoris*; white squares, ChU-B from *S. cerevisiae*; and iii) ABTS at pH 7.4 (X-axis in mM; black diamonds, ChU-B from *P. pastoris*; white diamonds, ChU-B from *S. cerevisiae*). (**B**) NaCl inhibition with: i) ABTS at pH 4.0 (black circles, ChU-B from *P. pastoris*; white circles, ChU-B from *S. cerevisiae*); and ii) DMP at pH 5.0 (black squares, ChU-B from *P. pastoris*; white squares, ChU-B from *S. cerevisiae*). (**C**) NaCl inhibition at physiological pH (7.4) with ABTS as substrate (black bars, ChU-B from *P. pastoris*; grey bars, ChU-B from *S. cerevisiae*).

Kinetics

Kinetics parameters were measured for phenolic and non-phenolic substrates at optimum and physiological pH (**Table 2.6.4.**). The K_m for ABTS and DMP was similar for the laccase produced either by *S. cerevisiae* or *P. pastoris*. By contrast, the k_{cat} values for the two substrates were around 2.7 and 4.8-fold higher for the laccase from *S. cerevisiae* than those of the laccase from *P. pastoris*. Possibly, the detected glycosylation differences between both laccases are in part responsible for this effect. Further crystallization studies along with computational analysis

would be important to clarify the differences in k_{cat} values and thermostabilities (Christensen and Kepp, 2012). When comparing kinetics with the original parent type expressed in *S. cerevisiae* (Maté *et al.*, 2010), the K_m at acidic pH was increased around 4- and 14-fold whereas the k_{cat} was ~3.5- and 7-fold lower than those of the parental type, for ABTS and DMP respectively. Mutations F396I and F454E, both located at the second coordination sphere of the T1 Cu, enabled the enzyme to be active under physiological conditions albeit at the cost of catalytic efficiency (**Figure 2.6.6.**). The activity of ChU-B from *P. pastoris* in physiological fluids was determined by measuring the oxygen consumption in human plasma and blood. Comparable responses for both human fluids were obtained (31 ± 7 and 27 ± 1 min^{-1} for blood and plasma, respectively). Since for the application of this enzyme in 3D-nanodevices working in physiological conditions, the laccase is directly connected to the cathode of a biofuel cell, the reducing substrates are replaced by a direct electronic current from the anode, which is the rate limiting step in the catalytic mechanism. In fact, ChU-B is functional in blood because of the slowed down kinetics. As we have recently reported, the modification of the second coordination sphere of the T1 Cu comes at the cost of reducing the activity at acidic values, which simultaneously compensates for T2 Cu inhibition activating ChU-B in the presence of halides and OH^- (Mate *et al.*, 2013b).

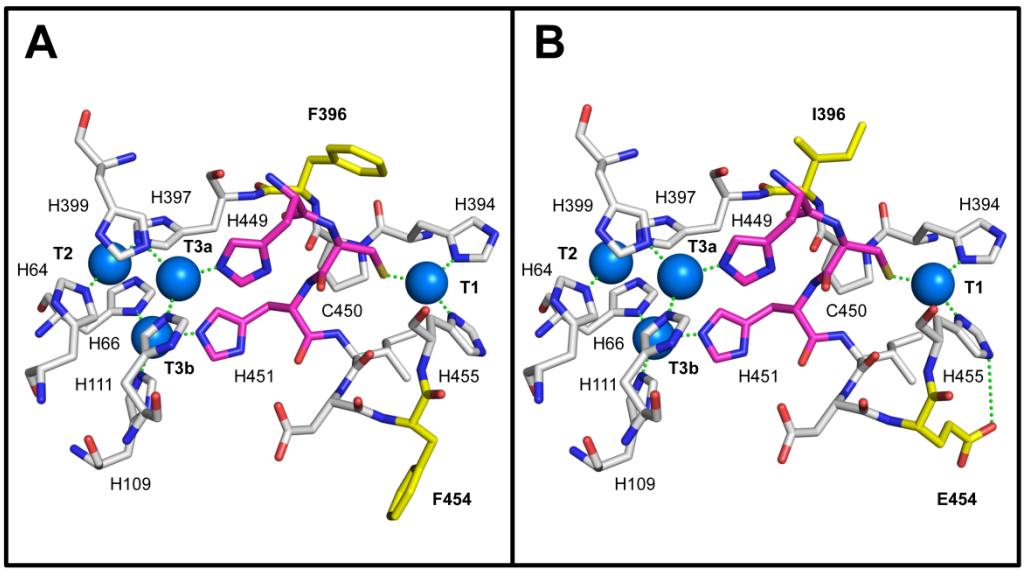

Figure 2.6.6. Location of the two mutations responsible for blood tolerance in the ChU-B mutant (B) compared with the corresponding residues in the parental type OB-1 (A). The F396I and F454E mutations are shown in yellow sticks and copper ions are depicted as blue spheres. The three residues in charge of the internal electron transfer from T1 Cu to T2/T3 cluster are displayed as magenta sticks. Residues involved in the first coordination sphere of the catalytic coppers and their interactions (green dashes) are also represented. The 3D-structure model is based on the crystal structure of the *Trametes trogii* laccase (97% identity, PDB: 2HRG; Matera *et al.*, 2008).

Table 2.6.4. Steady-state kinetic parameters of ChU-B mutant expressed in *P. pastoris* and *S. cerevisiae*.

Substrate	pH	ChU-B from *P. pastoris*			ChU-B from *S. cerevisiae*			(Parental type, OB-1mutant[a])		
		K_m (mM)	k_{cat} (s^{-1})	k_{cat}/K_m ($mM^{-1}s^{-1}$)	K_m (mM)	k_{cat} (s^{-1})	k_{cat}/K_m ($mM^{-1}s^{-1}$)	K_m (mM)	k_{cat} (s^{-1})	k_{cat}/K_m ($mM^{-1}s^{-1}$)
ABTS	3.0	0.024 ± 0.002	22.3 ± 0.5	929	0.023 ± 0.001	57.0 ± 0.9	2478	0.0063 ± 0.0009	200 ± 7	31746
	7.4	0.26 ± 0.01	1.13 ± 0.02	4.35	0.32 ± 0.02	3.09 ± 0.07	9.66	n.d.	n.d.	n.d.
DMP	5.0	1.91 ± 0.05	5.65 ± 0.05	2.96	2.0 ± 0.2	19.5 ± 0.5	9.75	0.14 ± 0.02	134 ± 5	957
	7.4	0.23 ± 0.03	0.41 ± 0.02	1.78	0.22 ± 0.03	1.95 ± 0.05	8.86	n.d.	n.d.	n.d.

[a]Data from Maté *et al.*, 2010. n.d.: not determined.

2.6.4. CONCLUSIONS

The blood tolerant laccase engineered by laboratory evolution in *S. cerevisiae* is easily secreted in *P. pastoris* with higher production yields whilst maintaining its evolved properties in terms of halide tolerance and pH activity profiles. These results support the use of *S. cerevisiae* as the preferred host to evolve ligninolytic enzymes and *P. pastoris* to over-express them for different purposes. Indeed, the application of this tandem-yeast evolution/expression system can be extended from laccases to other ligninolytic oxidoreductases (lignin-, manganese- and versatile-peroxidases, aromatic peroxygenases, aryl alcohol oxidases), whose engineering for challenging biocatalytic applications are currently pursued by many research groups.

2.6.5. METHODS

2.6.5.1. Strains and chemicals

The *P. pastoris* expression vectors pPICZαA and pGAPZαA, the *Escherichia coli* strain DH5α, the *P. pastoris* strain X-33 and the antibiotic Zeocin were purchased from Invitrogen (Carlsbad, CA, USA). Restriction endonucleases, the Rapid DNA Ligation Kit, containing T4 DNA ligase, and the shrimp alkaline phosphatase were obtained from Fermentas (Burlington, Canada). Nucleic acid amplifications were done employing Phusion High-Fidelity DNA Polymerase from New England Biolabs (Beverly, USA), dNTP mixture from Thermo Fisher Scientific (Waltham, MA, USA) and oligonucleotide primers from VBC Biotech (Vienna, Austria). The Illustra GFX PCR DNA and gel band purification kit was obtained from GE Healthcare (Buckinghamshire, UK). All chemicals and media components were of the highest purity available.

2.6.5.2. Laccase functional expression in *P. pastoris*

Laccase constructs for P. pastoris

A 1.5-kDa DNA fragment containing the coding region of the ChU-B mutant laccase gene was cloned with the original and the mutated α-factor prepro-leader from *S. cerevisiae* into the expression vectors pPICZαA and pGAPZαA. The vector pJRoC30α*ChU-B, resulting from a previous directed evolution experiment (Mate *et al.*, 2013b), was used to amplify the laccase gene without the evolved α-factor signal peptide with the primers 5PM1EcoR1 (5′-AA**GAATTC**AGCATTGGGCCAGTCGCAG-3′) and 3PM1Xba1 (5′-AGG**TCTAGA**TTACTGGTCGTCAGGCGAG-3′), which included targets for *Eco*RI and *Xba*I restriction enzymes, respectively (in bold). The laccase gene fused to the evolved α-factor signal

sequence was amplified using the primers 5ALPHABst1 (5′-AT**TTCGAA**ACGATGAGATTTCCTTCAATTTTTACTGC-3′), which included the *Bst*BI target (in bold), and 3PM1Xba1. PCR reactions were performed using a GeneAmp PCR System 2700 thermocycler (Applied Biosystems, Foster City, CA, USA) in a final volume of 25 μL containing 0.6 μM of each primer, 2 ng template, 800 μM dNTPs (200 μM each), 3% dimethyl sulfoxide (DMSO), 1.5 mM $MgCl_2$ and 0.5 U of Phusion polymerase. The PCR conditions were 98°C for 30 sec (1 cycle); 98°C for 10 sec, 62°C for 20 sec, 72°C for 45 sec (30 cycles); and 72°C for 7 min (1 cycle). The PCR products were purified using the Illustra GFX PCR DNA and gel band purification kit and then digested with the restriction enzymes *Bst*BI and *Xba*I -in the case of the fusion gene- or *Eco*RI and *Xba*I -in the case of the gene encoding the mature protein- at 37°C for 3 h. The pPICZαA and pGAPZαA vectors were equally treated and then their 5′ and 3′ ends were dephosphorylated using shrimp alkaline phosphatase at 37°C for 1 h. The PCR product and the linearized vector were ligated with T4 DNA ligase at room temperature for 30 min. After transformation of the constructs into chemically competent *E. coli* DH5α cells, the plasmids were proliferated, linearized with the restriction enzyme *Sac*I at 37°C for 1 h and transformed into electro-competent *P. pastoris* X-33 cells. Electro-competent *Pichia* cells were prepared and transformed following the condensed protocol of Lin-Cereghino *et al.* (Lin-Cereghino *et al.*, 2005). Transformants were grown on YPD plates (10 g/L yeast extract, 20 g/L peptone, 4 g/L glucose and 15 g/L agar) containing 25 mg/L zeocin and screened on indicator agar plates with BMM agar (100 mM potassium phosphate buffer pH 6.0, 3.5 g/L yeast nitrogen base without amino acids nor ammonium sulfate, 10 g/L ammonium sulfate, 400 μg/L biotin, 0.5% methanol, 20 g/L agar) containing 0.2 mM ABTS and 0.1 mM $CuSO_4$.

Small scale fed-batch fermentation

P. pastoris clone harbouring the ChU-B mutant with the original (α) and/or the mutated (α*) -factor signal peptide under control of the AOX1 promoter was cultivated in a 500-mL Multifors bioreactor (Infors HT, Bottmingen, CH) with a starting volume of 300 mL basal salts medium (26.7 mL/L 85% phosphoric acid, 0.93 g/L $CaSO_4 \cdot 2H_2O$, 14.9 g/L $MgSO_4 \cdot 7H_2O$, 18.2 g/L K_2SO_4, 4.13 g/L KOH; 40 g/L glycerol). After sterilization, the medium was supplemented with 4.35 mL/L PTM_1 trace salts (as described by Invitrogen), 100 μL Antifoam 204 (Sigma, St. Louis, MO, USA) and 0.1 mM $CuSO_4$. The pH of the medium was adjusted to pH 5.0 with 28% ammonium hydroxide and maintained at this value throughout the whole fermentation process. The fermentations were started by adding 25 mL of preculture grown on YPD medium in 250-mL baffled shake flasks at 125 rpm and 30°C overnight. The cultivations were performed according to the *Pichia* Fermentation Process Guidelines of Invitrogen with some modifications. The batch was run at 30°C, 500 rpm and an air flow of 0.2 L/min. After depletion of the glycerol in the batch medium, the fed-batch phase was started with a feed of 50% (w/v) glycerol containing 12 mL/L PTM1 trace salts for 5 h to increase the cell biomass under limiting conditions. For

induction, the temperature was reduced to 25°C and the feed was switched to 100% methanol with 12 mL/L PTM_1 trace salts at an initial feed rate of 0.6 mL/h until the culture was fully adapted to methanol. Subsequently the feed rate was adjusted to keep the oxygen saturation constant at 4% at a constant air supply of 2 L/min and a stirrer speed of 800 rpm. Samples were taken regularly and clarified by centrifugation. The wet biomass was measured by weighing centrifuged tubes containing culture samples after removing the supernatant. The soluble protein concentration was quantified using the Bio-Rad Protein Assay (Bio-Rad, CA, USA), with bovine serum albumin as standard. The volumetric activity was assayed spectrophotometrically using ABTS (ε_{418}=36,000 M^{-1} cm^{-1}) as substrate. The reaction was followed for 5 min at room temperature in a Lambda 35 UV/Vis spectrophotometer (Perkin Elmer). The ABTS-based assay contained 3 mM ABTS final concentration in 100 mM sodium acetate buffer pH 4.0.

Large scale fed-batch fermentation

The α*-ChU-B mutant under control of the AOX1 promoter (pPICZα*ChU-B construct) was large-scale produced in *P. pastoris* using a 42-L autoclavable stainless steel bioreactor (Applikon Biotechnology, *Schiedam*, The Netherlands) filled with 10 L of basal salts medium. After sterilization, 4.35 mL/L PTM_1 trace salts and 2 mL Antifoam 204 were added to the medium. Furthermore, the pH was set to pH 5.0 with 28% ammonium hydroxide, keeping it at this value throughout the entire process. The fermentation was started by adding 1 L of *P. pastoris* preculture grown on YPD medium in several 1-L baffled shake flasks at 200 rpm and 30ºC overnight. According to the *Pichia* Fermentation Process Guidelines aforementioned, the batch was run at 30°C and 600 rpm, keeping the dissolved oxygen (DO) concentration above 4%. Once all the glycerol was consumed from the batch growth phase, the glycerol fed phase was started with a feed of 50% (w/v) glycerol containing 12mL/L PTM_1 trace salts for 5 h to increase the biomass. Afterwards, 0.5% (v/v) methanol with 12 mL/L PTM_1 trace salts and 0.1 mM $CuSO_4$ were injected aseptically into the fermenter. From this time on, the temperature was set to 25°C and the stirrer speed to 750 rpm. After 5 h of transition phase, the feed was switched to 100% methanol containing 12 mL/L PTM_1 trace salts and it was regulated to keep the DO concentration between 1 and 3%. Samples were taken regularly and wet biomass, protein concentration and laccase activity were determined as mentioned above.

Purification of the laccase produced in P. pastoris

The culture broth of ChU-B mutant containing the *P. pastoris* cells was clarified by centrifugation at 6000 rpm for 20 min at 4°C (Sorvall Evolution RC Superspeed Centrifuge, Thermo Fisher Scientific) and solid ammonium sulphate was slowly added to the supernatant to 30% saturation at 4°C. The suspension was centrifuged at 6000 rpm for 30 min at 4°C to discard the precipitated protein (without laccase activity). Then, the supernatant-containing

laccase activity was applied to a 750-mL PHE sepharose 6 FF column (chromatographic equipment and materials from GE Healthcare) equilibrated with 50 mM sodium acetate buffer pH 5.0 containing 30% saturation ammonium sulphate. Proteins were eluted within a linear gradient from 30 to 0% ammonium sulphate at a flow rate of 20 L/min for 2 h. Fractions with laccase activity were pooled, dialyzed and concentrated in 20 mM Bis-Tris HCl buffer pH 6.5 (buffer A) using a hollow fiber cross-flow module (Microza UF module SLP-1053, 10 kDa cut-off, Pall Corporation, Port Washington, NY, USA). The sample was loaded onto a 19-mL Mono Q column, previously equilibrated with buffer A. Proteins were eluted with a linear gradient from 0 to 0.4 M of NaCl at a flow rate of 2 mL/min for 1 h. Active fractions were pooled and applied to a 70 mL PHE source column. Laccase was eluted with a linear gradient from 15 to 0% ammonium sulphate at a flow rate of 1 mL/min for 6 h. The fractions with laccase activity were pooled, dialyzed against buffer A, concentrated and stored at 4°C.

2.6.5.3. Production and purification of the laccase expressed in *S. cerevisiae*

The ChU-B mutant was expressed in the protease deficient *Saccharomyces cerevisiae* strain BJ5465 (LGC Promochem, Barcelona, Spain) and purified to homogeneity following the protocol reported in a former work (Maté *et al.*, 2010).

2.6.5.4. Biochemical characterization

Kinetic thermostability (T_{50} determination)

The thermostability of the different laccase samples was estimated by assessing their T_{50} values using 96/384 well gradient thermocyclers. Appropriate laccase dilutions were prepared, such that 20 μL aliquots produced a linear response in the kinetic mode. Subsequently, 50 μL samples were assessed at each point in the gradient scale and a temperature gradient profile ranging from 35 to 90°C was established as follows (in °C): 35.0, 36.7, 39.8, 44.2, 50.2, 54.9, 58.0, 60.0, 61.1, 63.0, 65.6, 69.2, 72.1, 73.9, 75.0, 76.2, 78.0, 80.7, 84.3, 87.1, 89.0 and 90.0. After 10 min of incubation, the samples were chilled on ice for 10 min and further incubated at room temperature for 5 min. Next, 20 μL of samples were subjected to the same ABTS-based colorimetric assay described above. Thermostability values were deduced from the ratio between the residual activities incubated at different temperature points and the initial activity at room temperature.

pH activity profiles

Appropriate laccase dilutions were prepared in such a way that 10 µl aliquots produced a linear response in the kinetic mode. Plates containing 10 µl of laccase samples and 180 µl of 100 mM Britton and Robinson buffer were prepared at pH values of 2.0, 3.0, 4.0, 5.0, 6.0, 7.0, 8.0 and 9.0. The assay commenced when 10 µl of 60 mM ABTS or DMP was added to each well to give a final substrate concentration of 3 mM. The activities were measured in triplicate in kinetic mode and the relative activity (in %) is based on the maximum activity for each variant in the assay.

Halide inhibition (I_{50} determination)

The inhibitory effect of fluoride and chloride was measured using two laccase substrates (ABTS and DMP) at their corresponding optimal pH activity values (in 100 mM sodium acetate buffer (pH 4.0) for ABTS and 100 mM sodium tartrate buffer (pH 5.0) for DMP, as well as at physiological pH (in 100 mM sodium phosphate buffer, pH 7.4). Inhibition was determined by the I_{50} value (the halide concentration at which only 50% of the initial laccase activity is retained), as the complexity of the plots complicated the extraction of the inhibition constant (K_i). The assay mixture contained 2.4 mM ABTS or DMP, halide (concentrations ranging from 0 to 1100 mM) and purified laccase (0.2 and 1.7 nM for ABTS and DMP, respectively). Each data point represents the mean value determined in at least three independent experiments.

Kinetics parameters

As previously reported (Maté *et al.*, 2010), steady-state enzyme kinetics were determined using the following extinction coefficients: ABTS, ε_{418} = 36,000 M^{-1} cm^{-1}; DMP, ε_{469} = 27,500 M^{-1} cm^{-1} (relative to substrate concentration). To calculate the values of K_m and $k_{cat,}$ the average v_{max} was represented versus substrate concentration and fitted to a single rectangular hyperbola function in SigmaPlot 10.0, where parameter *a* equals k_{cat} and parameter *b* equals K_m.

Determination of laccase activity in human plasma and blood

Human blood was collected in BD Vacutainer® blood collection tubes (Plymoth, UK). Blood samples were centrifuged for 10 min at 3000 rpm to obtain human plasma, discarding the pellet after having extracted the supernatant. Both plasma and blood were supplemented with 10 mM ascorbic acid as laccase substrate and the pH adjusted to 7.4. The activity of the ChU-B mutant in both physiological fluids was determined by measuring oxygen consumption in solution with a Clark electrode. These experiments were performed using the Oxygraph system (Hansatech Instruments, King´s Lynn, UK).

MALDI-TOF analysis

Matrix Assisted Laser Desorption and Ionization-Time Of Flight (MALDI-TOF) experiments were performed on an Autoflex III MALDI-TOF-TOF instrument (Bruker Daltonics, Bremen, Germany) with a smartbeam laser. The spectra were acquired at a laser power just above the ionization threshold, and the samples were analysed in the positive ion detection and delayed extraction linear mode. Typically, 1000 laser shots were summed into a single mass spectrum. External calibration was performed, using BSA from Bruker, over a range of 30000-70000 Da. The 2,5-dihydroxy-acetophenone (2,5-DHAP) matrix solution was prepared by dissolving 7.6 mg (50 μmol) in 375 μL ethanol, to which 125 μL of 80 mM diammonium hydrogen citrate aqueous solution was added. For sample preparation, 2.0 μL of purified enzyme was diluted with 2.0 μL of 2% trifluoro acetic acid aqueous solution and 2.0 μL of matrix solution. A volume of 1.0 μL of this mixture was spotted onto the stainless steel target and allowed to dry at room temperature.

N-terminal analysis

Purified laccases were resolved by SDS-PAGE and the proteins transferred to polyvinylidene difluoride (PVDF) membranes. The PVDF membranes were stained with Coomassie Brilliant Blue R-250, after which the enzyme bands were cut out and processed for N-terminal amino acid sequencing on a precise sequencer at the Core facilities of the Helmholtz Centre for Infection Research (HZI; Braunschweig, Germany).

2.6.5.5. Protein modelling

The 3D-structure models of the PM1 mutant laccases are based on the crystal structure of the *Trametes trogii* laccase (PDB: 2HRG, 97% sequence identity with the PM1 laccase; Matera *et al.*, 2008). The protein models were generated and analyzed as formerly reported (Maté *et al.*, 2010).

3. RESUMEN GENERAL

3.1. INTRODUCCIÓN

Este apartado recoge y discute de manera sucinta los diferentes trabajos presentados para optar al grado de Doctor (**Capítulos 1 al 6**) al tiempo que se desarrollan conceptos relevantes que no se comentaron en los artículos mencionados y que completan adecuadamente el conjunto de esta memoria. Finalmente se incluyen las principales conclusiones.

Esta Tesis Doctoral ha abordado el diseño de una lacasa de alto potencial redox para que sea activa en presencia de sangre humana, lo cual es de gran interés para la preparación de nanobiodispositivos tridimensionales implantables con fines biomédicos. En primer lugar, se llevó a cabo su evolución dirigida con la finalidad de obtener un sistema de expresión funcional robusto y estable en *S. cerevisiae*. El mejor mutante de este proceso (OB-1) fue exhaustivamente caracterizado y empleado como punto de partida para obtener una lacasa funcional en sangre mediante nuevos ciclos de evolución dirigida. Por último, se analizaron las diferentes propiedades del mutante tolerante a sangre (ChU-B), el cual se clonó en *P. pastoris* para su posterior fermentación en biorreactor de 42 L.

3.2. EVOLUCIÓN DIRIGIDA DE LA LACASA PM1 PARA EXPRESIÓN FUNCIONAL EN *S. cerevisiae*

3.2.1. Punto de partida

El **Capítulo 1** describe el proceso de evolución *in vitro* de la lacasa PM1 para conseguir su expresión funcional en *S. cerevisiae*. Esta enzima es producida por el basidiomiceto del mismo nombre y se caracteriza por tener un elevado potencial redox y ser altamente estable frente a la temperatura y en un amplio rango de pH. El cDNA de la lacasa PM1 incluyendo su péptido señal nativo fue clonado en un vector episómico bifuncional pero, desafortunadamente, esta construcción no permitió su expresión funcional. Por ello, el péptido señal nativo fue reemplazado por tres secuencias señales diferentes que favorecían la expresión funcional de sus correspondientes proteínas en la levadura: la lacasa evolucionada (mutante T2) de *M. thermophila*, la glucosa oxidasa de *A. niger* y la feromona de apareamiento factor α. De las tres construcciones, tan sólo la formada por el prepro-líder del factor α fusionada al gen de la lacasa PM1 madura (construcción α-PM1) dio lugar a niveles de expresión mínimos pero detectables, y en consecuencia, dicha construcción fue seleccionada como punto de partida para abordar el proceso de mejora de la expresión funcional.

3.2.2. Diseño evolutivo

Se sometió el gen de fusión completo α-PM1 a ocho ciclos de evolución dirigida. La evolución conjunta de la secuencia prepro-líder del factor α y la lacasa facilitó su producción funcional y exocitosis por *S. cerevisiae*. En las primeras seis generaciones, la creación de diversidad génica se llevó a cabo mediante la mutagénesis aleatoria de los diferentes genes parentales (introduciendo entre 1 y 3 cambios aminoacídicos por gen) junto con su recombinación *in vivo*. La introducción de mutaciones aleatorias y su recombinación simultánea resultó ser una aproximación extremadamente útil que promovió la acumulación de mutaciones beneficiosas procedentes de diferentes parentales de manera rápida y precisa. Este planteamiento experimental basado en una estrategia de *adaptative walk* en conjunción con procesos de recombinación *in vivo* variados (DNA *shuffling*, IvAM, IVOE), ha sido empleado de manera eficaz para la evolución de otras enzimas eucariotas en nuestro laboratorio como las lacasas de *Myceliophthora thermophila* (MtL) (Bulter *et al*., 2003a; Zumárraga *et al*., 2007) y de *Pycnoporus cinnabarinus* (Camarero *et al*., 2012), la peroxidasa versátil (VP) de *Pleurotus eryngii* (Garcia-Ruiz *et al*., 2012), la peroxigenasa inespecífica (UPO) de *Agrocybe aegerita* (material no publicado) y la β-fructofuranosidasa de *Schwanniomyces occidentalis* (de Abreu *et al*., 2013). En los dos últimos ciclos de evolución dirigida, se incorporaron dos estrategias racionales basadas en principios diferentes: i) la recuperación de mutaciones beneficiosas que se perdieron durante los eventos de recombinación en la levadura (por encontrarse estas mutaciones a una distancia nucleotídica que limitaba las posibilidades de entrecruzamiento), y ii) el intercambio mutacional con mutaciones descubiertas en experimentos evolutivos paralelos llevados a cabo en nuestro laboratorio con la lacasa de *P. cinnabarinus* (PcL, con una identidad de secuencia del 77% respecto a la lacasa PM1) (**Figura 3.1.**). En este sentido, es importante mencionar que el mutante final de la evolución de la lacasa PM1 hacia expresión funcional (variante OB-1) junto con el mejor mutante de la evolución dirigida de la PcL (variante 3PO) fueron empleados recientemente para la generación de lacasas quiméricas (Pardo *et al*., 2012). A través de protocolos de recombinación *in vitro* e *in vivo*, la lacasa OB-1 se recombinó con la lacasa 3PO en un mismo ciclo de evolución, dando lugar a un conjunto de lacasas quiméricas de elevado potencial redox. Se llegaron a localizar hasta seis eventos de recombinación por gen mientras que muchas de las propiedades enzimáticas fueron modificadas (perfiles de pH, afinidad por sustratos). De especial interés fue el aumento de la termoestabilidad cinética en algunas variantes, como consecuencia de la acumulación de mutaciones neutras a través de procesos de deriva genética.

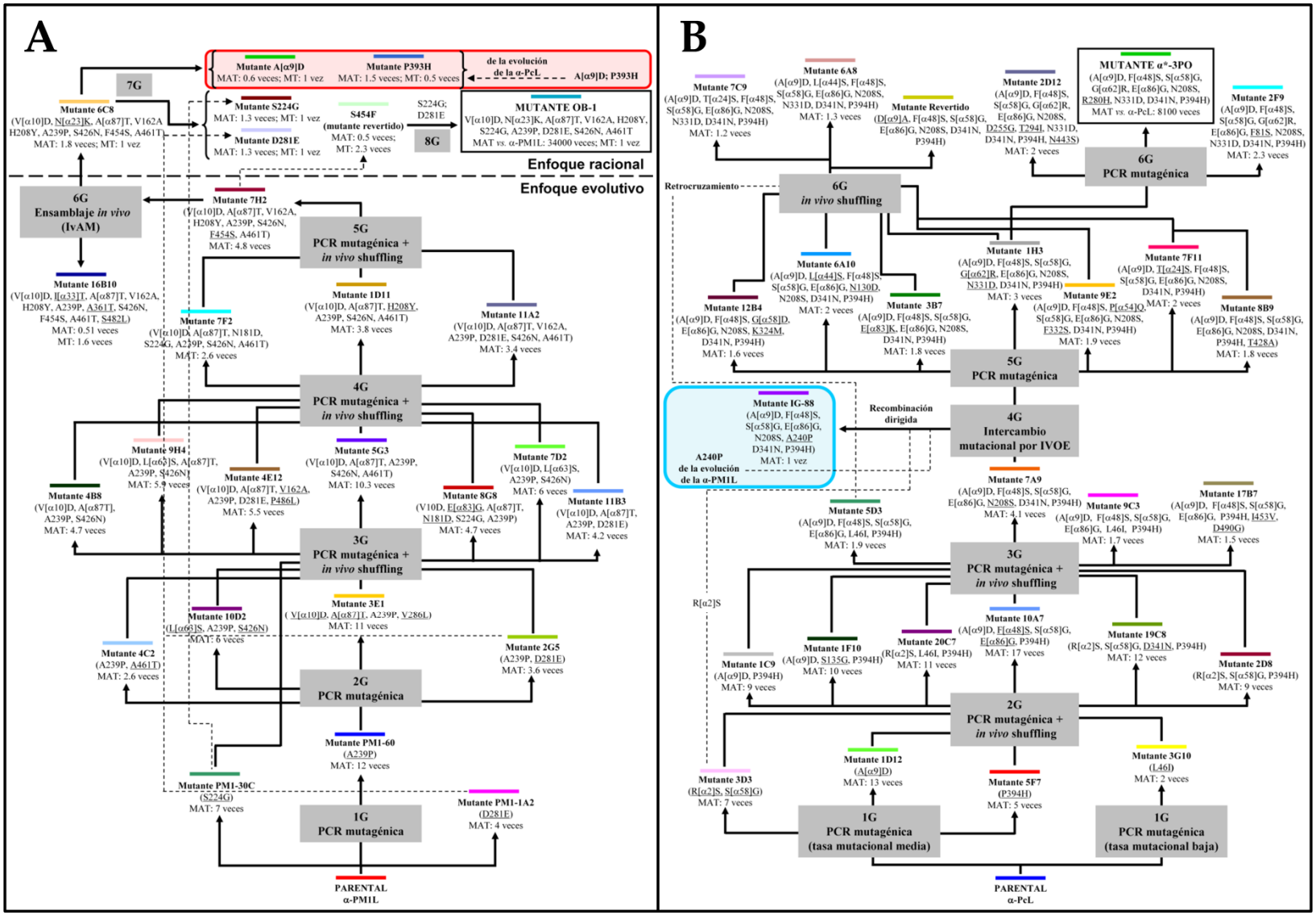
A
Mutante A[α9]D
MAT: 0.6 veces; MT: 1 vez
Mutante P393H
MAT: 1.5 veces; MT: 0.5 veces
de la evolución de la α-PcL
A[α9]D; P393H
7G
Mutante 6C8
(V[α10]D, N[α23]K, A[α87]T, V162A H208Y, A239P, S426N, F454S, A461T)
MAT: 1.8 veces; MT: 1 vez
Mutante S224G
MAT: 1.3 veces; MT: 1 vez
Mutante D281E
MAT: 1.3 veces; MT: 1 vez
S454F
(mutante revertido)
MAT: 0.5 veces; MT: 2.3 veces
S224G; D281E
8G
MUTANTE OB-1
V[α10]D, N[α23]K, A[α87]T, V162A, H208Y, S224G, A239P, D281E, S426N, A461T
MAT vs. α-PM1L: 34000 veces; MT: 1 vez
Enfoque racional
Enfoque evolutivo
6G
Ensamblaje in vivo
(IvAM)
Mutante 7H2
(V[α10]D, A[α87]T, V162A, H208Y, A239P, S426N, F454S, A461T)
MAT: 4.8 veces
5G
PCR mutagénica +
in vivo shuffling
Mutante 16B10
(V[α10]D, I[α33]T, A[α87]T, V162A, H208Y, A239P, A361T, S426N, F454S, A461T, S482L)
MAT: 0.51 veces
MT: 1.6 veces
Mutante 7F2
(V[α10]D, A[α87]T, N181D, S224G, A239P, S426N, A461T)
MAT: 2.6 veces
Mutante 1D11
(V[α10]D, A[α87]T, H208Y, A239P, S426N, A461T)
MAT: 3.8 veces
Mutante 11A2
(V[α10]D, A[α87]T, V162A, A239P, D281E, S426N, A461T)
MAT: 3.4 veces
4G
PCR mutagénica +
in vivo shuffling
Mutante 9H4
(V[α10]D, L[α63]S, A[α87]T, A239P, S426N)
MAT: 5.5 veces
Mutante 4E12
(V[α10]D, A[α87]T, V162A, A239P, D281E, P486L)
MAT: 5.5 veces
Mutante 5G3
(V[α10]D, A[α87]T, A239P, S426N, A461T)
MAT: 10.3 veces
Mutante 7D2
(V[α10]D, L[α63]S, A239P, S426N)
MAT: 6 veces
Mutante 4B8
(V[α10]D, A[α87T], A239P, S426N)
MAT: 4.7 veces
Mutante 8G8
(V10D, E[α83]G, A[α87]T, N181D, S224G, A239P)
MAT: 4.7 veces
Mutante 11B3
(V[α10]D, A[α87]T, A239P, D281E)
MAT: 4.2 veces
3G
PCR mutagénica +
in vivo shuffling
Mutante 10D2
(L[α66]S, A239P, S426N)
MAT: 6 veces
Mutante 3E1
(V[α10]D, A[α87]T, A239P, V286L)
MAT: 11 veces
Mutante 4C2
(A239P, A461T)
MAT: 2.6 veces
Mutante 2G5
(A239P, D281E)
MAT: 3.6 veces
2G
PCR mutagénica
Mutante PM1-60
(A239P)
MAT: 12 veces
Mutante PM1-30C
(S224G)
MAT: 7 veces
Mutante PM1-1A2
(D281E)
MAT: 4 veces
1G
PCR mutagénica
PARENTAL
α-PM1L
B
Mutante 7C9
(A[α9]D, T[α24]S, F[α48]S, S[α58]G, E[α86]G, N208S, N331D, D341N, P394H)
MAT: 1.2 veces
Mutante 6A8
(A[α9]D, L[α44]S, F[α48]S, S[α58]G, E[α86]G, N208S, N331D, D341N, P394H)
MAT: 1.3 veces
Mutante Revertido
(D[α9]A, F[α48]S, S[α58]G, E[α86]G, N208S, D341N, P394H)
Mutante 2D12
(A[α9]D, F[α48]S, S[α58]G, G[α62]R, E[α86]G, N208S, D255G, T294I, N331D, D341N, P394H, N443S)
MAT: 2 veces
MUTANTE α*-3PO
(A[α9]D, F[α48]S, S[α58]G, G[α62]R, E[α86]G, N208S, R280H, N331D, D341N, P394H)
MAT vs. α-PcL: 8100 veces
Mutante 2F9
(A[α9]D, F[α48]S, S[α58]G, G[α62]R, E[α86]G, F81S, N208S, N331D, D341N, P394H)
MAT: 2.3 veces
6G
PCR mutagénica
Retrocruzamiento
6G
in vivo shuffling
Mutante 6A10
(A[α9]D, L[α44]S, F[α48]S, S[α58]G, E[α86]G, N130D, N208S, D341N, P394H)
MAT: 2 veces
Mutante 1H3
(A[α9]D, F[α48]S, S[α58]G, G[α62]R, E[α86]G, N208S, N331D, D341N, P394H)
MAT: 3 veces
Mutante 7F11
(A[α9]D, T[α24]S, F[α48]S, S[α58]G, E[α86]G, N208S, D341N, P394H)
MAT: 2 veces
Mutante 12B4
(A[α9]D, F[α48]S, G[α58]D, E[α86]G, N208S, K324M, D341N, P394H)
MAT: 1.6 veces
Mutante 3B7
(A[α9]D, F[α48]S, S[α58]G, E[α83]K, E[α86]G, N208S, D341N, P394H)
MAT: 1.8 veces
Mutante 9E2
(A[α9]D, F[α48]S, P[α54]Q, S[α58]G, E[α86]G, N208S, F332S, D341N, P394H)
MAT: 1.9 veces
Mutante 8B9
(A[α9]D, F[α48]S, S[α58]G, E[α86]G, N208S, D341N, P394H, T428A)
MAT: 1.8 veces
5G
PCR mutagénica
Mutante IG-88
(A[α9]D, F[α48]S, S[α58]G, E[α86]G, N208S, A240P D341N, P394H)
MAT: 1 vez
A240P
de la evolución
de la α-PM1L
Recombinación dirigida
4G
Intercambio
mutacional por IVOE
Mutante 7A9
(A[α9]D, F[α48]S, S[α58]G, E[α86]G, N208S, D341N, P394H)
MAT: 4.1 veces
Mutante 9C3
(A[α9]D, F[α48]S, S[α58]G, E[α86]G, L46I, P394H)
MAT: 1.7 veces
Mutante 17B7
(A[α9]D, F[α48]S, S[α58]G, E[α86]G, P394H, I453V, D490G)
MAT: 1.5 veces
Mutante 5D3
(A[α9]D, F[α48]S, S[α58]G, E[α86]G, L46I, P394H)
MAT: 1.9 veces
3G
PCR mutagénica +
in vivo shuffling
R[α2]S
Mutante 1C9
(A[α9]D, P394H)
MAT: 9 veces
Mutante 1F10
(A[α9]D, S135G, P394H)
MAT: 10 veces
Mutante 20C7
(R[α2]S, L46I, P394H)
MAT: 11 veces
Mutante 10A7
(A[α9]D, F[α48]S, S[α58]G, E[α86]G, P394H)
MAT: 17 veces
Mutante 19C8
(R[α2]S, S[α58]G, D341N, P394H)
MAT: 12 veces
Mutante 2D8
(R[α2]S, S[α58]G, P394H)
MAT: 9 veces
2G
PCR mutagénica +
in vivo shuffling
Mutante 3D3
(R[α2]S, S[α58]G)
MAT: 7 veces
Mutante 1D12
(A[α9]D)
MAT: 13 veces
Mutante 5F7
(P394H)
MAT: 5 veces
Mutante 3G10
(L46I)
MAT: 2 veces
1G
PCR mutagénica
(tasa mutacional media)
1G
PCR mutagénica
(tasa mutacional baja)
PARENTAL
α-PcL

Figura 3.1. Rutas evolutivas artificiales de las lacasas α-PM1 (A) y α-PcL (B) hacia expresión funcional en *S. cerevisiae*. El intercambio mutacional entre ambas enzimas está indicado por los recuadros sombreados en rojo (mutaciones descubiertas durante la evolución de la α-PcL e introducidas en la α-PM1, **A**) y en azul (mutaciones descubiertas durante la evolución de la α-PM1 e incorporadas en la α-PcL, **B**). MAT: mejora en la actividad total (combinación de la expresión funcional y la actividad específica frente a ABTS) en número de veces con respecto al parental (o al mejor de los parentales) del ciclo anterior. MT: mejora en la termoestabilidad frente al parental (o al mejor de los parentales) del ciclo anterior. Las nuevas mutaciones se muestran subrayadas. Figura adaptada de Maté *et al.*, 2010 y Camarero *et al.*, 2012.

3.2.3. Buscando un compromiso entre actividad y estabilidad

En el transcurso de los ciclos de evolución dirigida de la lacasa PM1, se identificaron posiciones que resultaron críticas para el balance entre la actividad y la estabilidad de la enzima, algo muy frecuente en diseño evolutivo. El caso más llamativo fue el mutante 7H2 de la quinta generación, que aumentó 4.8 veces su actividad total frente al mejor mutante del ciclo anterior (1D11), pero a expensas de su estabilidad (**Figura 3.1.**). De hecho, la termoestabilidad cinética se redujo considerablemente (con valores de T_{50} 5°C más bajos que los de 1D11, lo cual afectó incluso a su conservación a tiempos largos con pérdidas de actividad de en torno al 30% tras dos semanas a 4°C). El mutante 7H2 fue el resultado de la recombinación de los mutantes de la cuarta generación 1D11 y 11A2 más la incorporación de la mutación F454S que, como se explicó en el **Capítulo 1** (**Figura 2.1.3.**, pág. 59), es la principal responsable del desequilibrio encontrado entre la actividad y estabilidad cinética de la enzima. También es importante destacar que la mutación F454S resultó en el desplazamiento en una unidad del pH óptimo de la lacasa para el sustrato fenólico DMP (de 4.0 a 5.0; **Figura 3.2.**), algo que fue redundante cuando se evolucionó la enzima hacia su actividad en sangre (ver **Subapartado 3.3.**, pág. 206).

Con el objetivo de recuperar parte de la estabilidad perdida, en el sexto ciclo de evolución se incorporó un ensayo HTS de termoestabilidad cinética (**Capítulo 2**). Con este *screening* dual de actividad y termoestabilidad se identificó el mutante 6C8, 1.8 veces más activo que 7H2 y con una T_{50} prácticamente idéntica, y el mutante 16B10 (mutante de estabilidad), la mitad de activo que 7H2 pero con una T_{50} mejorada en 3°C. En los ciclos finales, se optó por revertir la mutación F454S ya que los niveles de secreción (actividad total) alcanzados en los últimos estadios de la evolución fueron los suficientemente elevados como para que la reversión de esta mutación no afectase sobremanera a la actividad catalítica al tiempo que se recuperaba la termoestabilidad pérdida. Tras la reversión de la mutación F454S se recuperaron los 5°C de termoestabilidad y el perfil de pH original (**Figura 3.2.**), al tiempo que la actividad total del mutante fue aumentada gracias a la acumulación e inclusión de mutaciones de generaciones anteriores (**Figuras 2.1.1.** y **2.1.3C**, pág. 55 y 59, respectivamente).

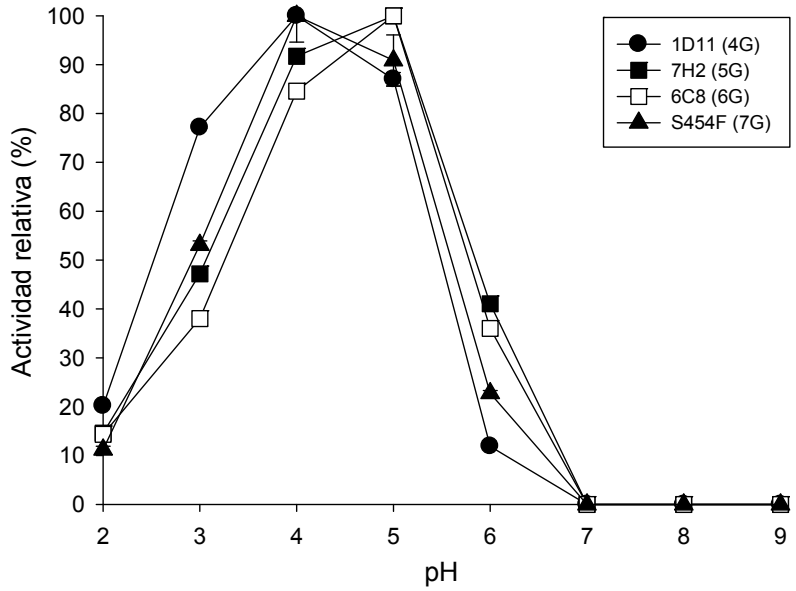

Figura 3.2. Perfil de actividad frente al pH utilizando DMP como sustrato reductor. Se puede apreciar cómo 7H2 (5G; con la mutación F454S) desplaza su perfil de pH con respecto a 1D11 (parental de la 4G). El mutante de estabilidad 6C8 (que conserva la mutación F454S) mantiene un perfil de pH similar a 7H2. Tras la reversión de la mutación en el mutante S454F (7G), se recuperó el perfil de pH original.

Nuestros resultados ponen de manifiesto el sutil equilibrio que existe entre la actividad y la estabilidad para posiciones determinadas en la estructura proteica, algo que ya ha sido documentado con anterioridad en diferentes estudios. Un ejemplo que ilustra este fenómeno se encuentra en la historia de la evolución *in vitro* del citocromo P450 BM-3 de *Bacillus megaterium* ($P450_{BM-3}$) para convertirlo en una alcano monooxigenasa (Romero y Arnold, 2009). Esta enzima cataliza de manera natural la hidroxilación de ácidos grasos de cadena larga (C12 a C18) en posiciones subterminales ω-1, ω-2 y ω-3. Durante sucesivos ciclos de evolución dirigida se forzó a la enzima para que aceptara alcanos como sustratos y los convirtiera en los correspondientes alcoholes (el objetivo último fue que se comportarse como una propano monooxigenasa) (Glieder *et al.*, 2002; Peters *et al.*, 2003; Fasan *et al.*, 2007). Como se muestra en la **Figura 3.3.**, la acumulación de mutaciones que aumentaron la eficiencia de la enzima en la hidroxilación de alcanos (**Figuras 3.3A** y **3.3C**) conllevó la disminución gradual de la termoestabilidad, con pérdidas de más de 10°C en la T_{50} (**Figura 3.3D**). Este efecto fue perjudicial para la evolución dirigida puesto que la enzima no fue capaz de tolerar la introducción de nuevas mutaciones beneficiosas (pero desestabilizantes). Por ello en la octava generación se hizo imprescindible la incorporación de mutaciones que estabilizaran la estructura proteica. Sin embargo, y al igual que ocurre en nuestro caso, la inclusión de mutaciones estabilizantes supuso una pérdida notable de actividad catalítica lo que pone de manifiesto la dificultad en la evolución conjunta de ambas propiedades.

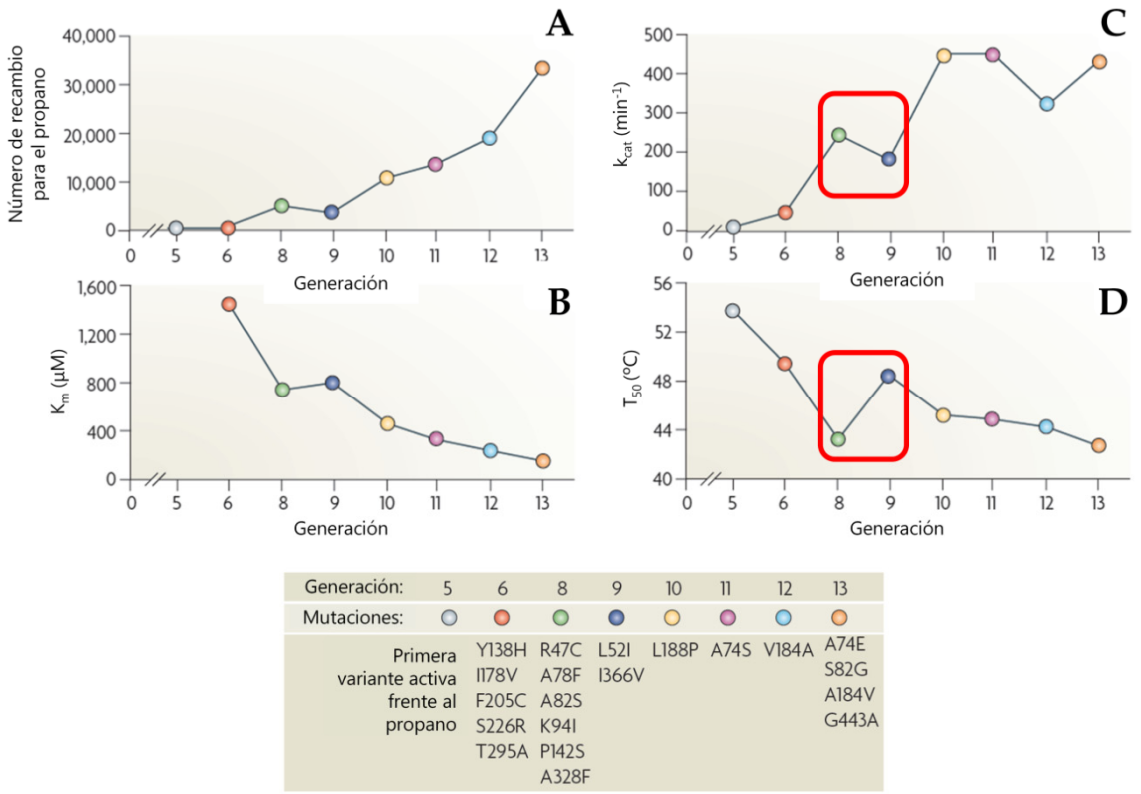

Figura 3.3. Evolución dirigida del citocromo P450$_{BM-3}$ para hidroxilación de alcanos. Se muestra el desequilibrio entre actividad y estabilidad a partir del quinto ciclo de evolución (en el cual se obtuvo el primer mutante activo frente al propano): (**A**) Número de recambio (moles de propanol producidos por mol de P450$_{BM-3}$). (**B**) y (**C**) Valores de K_m y de k_{cat} de la reacción de hidroxilación del propano. (**D**) Termoestabilidad (valores de T_{50}). La selección de mutantes se llevó a cabo en función de la actividad frente al propano en todas las generaciones salvo en la novena, en la cual el *screening* se realizó en base a la T_{50}. Los recuadros rojos muestran el efecto negativo que tuvo la introducción de mutaciones estabilizantes sobre la actividad del P450$_{BM-3}$. Figura adaptada de Romero y Arnold, 2009.

Finalmente, es importante señalar que el proceso de evolución dirigida descrito para la lacasa PM1 ha sido escogido recientemente como modelo para validar un método computacional que permite cuantificar la estabilidad relativa proteica (en base al ΔΔG de plegamiento) (Christensen y Kepp, 2012). Este algoritmo está basado en el software FoldX que permite el *screening in silico* de librerías de mutantes. La versión de FoldX utilizada en este trabajo tiene en cuenta las relaciones estructura-función, lo que permite aumentar la precisión en la predicción de estabilidades proteicas. El FoldX se aplicó a nueve mutantes de la lacasa PM1 (1D11 (4G), 11A2 (4G), 6C8 (6G), 16B10 (6G), S454F-revertido (7G), P393H (7G), D281E (4G), S224G (7G) y OB-1 (8G)) y, a pesar de que este software no tiene en cuenta la contribución de los carbohidratos en la estabilidad absoluta de la estructura proteica, las estabilidades

relativas experimentales procedentes de nuestro estudio de evolución dirigida y las calculadas con este algoritmo de dinámica molecular mostraron, en todos los casos, una correlación muy elevada. El modelo desarrollado permite predecir las fuerzas físicas que gobiernan la alta estabilidad de las lacasas fúngicas, principalmente las interacciones hidrofóbicas y las fuerzas de van der Waals existentes en el estado plegado.

3.2.4. Caracterización de la lacasa mutante de secreción OB-1

3.2.4.1. Caracterización bioquímica y cinética

El mutante OB-1, con una mejora en la actividad total de 34000 veces respecto a la lacasa α-PM1, fue escogido como la variante final de la evolución hacia expresión funcional.

OB-1 fue purificado a homogeneidad y ampliamente caracterizado (**Capítulos 1** y **4**). Sus niveles de secreción en *S. cerevisiae* fueron de 8 mg/L, su actividad específica de 400 U/mg y su masa molecular de 60310 kDa, de la cual en torno al 10% corresponde a carbohidratos. Este grado de glicosilación es muy inferior a los de las lacasas de *P. cinnabarinus* y *M. thermophila* expresadas en *S. cerevisiae* (ambas con alrededor un 50% de glicosilación; Bulter *et al.*, 2003a; Camarero *et al.*, 2012), lo que sugiere un menor tiempo de residencia del mutante OB-1 en el aparato de Golgi (en el que tiene lugar la adición de cadenas de entre 50 y 150 unidades de manosa). La secuenciación del extremo N-terminal de OB-1 confirmó la presencia de una extensión de seis aminoácidos adicionales (ETEAEF) correspondientes a la secuencia de corte de la peptidasa *STE13* (ETEA, incluyendo la mutación A[α87]T aparecida en el segundo ciclo de evolución) y la secuencia de reconocimiento de la enzima de restricción *Eco*RI (EF, introducida durante la construcción del plásmido pJRoC30-αPM1). Idéntico efecto se observó en el procesamiento de otras proteínas fusionadas al prepro-líder del factor α, como fueron la VP de *P. eryngii* (Garcia-Ruiz *et al.*, 2012) o las proteínas humanas β-endorfina, interferón α1 y el factor de crecimiento epidérmico (hEGF) (Brake *et al.*, 1990). La presencia de dicha extensión N-terminal se ha atribuido a unos niveles insuficientes de *STE13* en el aparato de Golgi como para procesar las grandes cantidades de proteína recombinante expresada.

Con el fin de valorar la contribución de la extensión N-terminal en las mejoras observadas en el mutante OB-1 secretado por *S. cerevisiae*, los seis aminoácidos extra se eliminaron mediante mutagénesis de deleción por IVOE (**Figura 2.4.5.**, pág. 141) dando lugar al mutante OB-1del. Tanto las propiedades espectroscópicas (UV-visible y dicroísmo circular) como los perfiles de actividad frente al pH de OB-1del fueron muy similares a los de OB-1. Sin embargo, la variante truncada mostró, respecto a OB-1: i) un pI 0.2 unidades más básico como consecuencia de la deleción de tres Glu; ii) una estabilidad frente a la temperatura ligeramente inferior; iii) peores parámetros cinéticos respecto a todos a los sustratos utilizados (ABTS, DMP, guayacol y ácido

sinápico); y iv) una disminución del 40% en los niveles de expresión. Este último resultado puede explicarse considerando que la eliminación de las repeticiones (Glu-Ala) pudo afectar a la actividad de *KEX2* ya que, de acuerdo con lo descrito en la bibliografía, la eficiencia de dicha aminopeptidasa está favorecida por la presencia de residuos ácidos en los alrededores de su sitio de corte (Lys-Arg).

Los bajos niveles de expresión de la lacasa α-PM1 impidieron su producción en cantidades suficientes para ser purificada y así poder ser comparada con OB-1. En consecuencia, se produjeron y purificaron los mejores mutantes del segundo, tercer y cuarto ciclo (variantes 3E1, 5G3 y 1D11, respectivamente) para de esta manera poder estudiar el efecto de la acumulación de mutaciones en las constantes cinéticas. En este punto es importante señalar que hubiera sido interesante emplear el prepro-líder del factor α evolucionado para fusionarlo a la lacasa PM1 parental y así poder desglosar, de una manera más adecuada, las mejoras obtenidas en la actividad total, además de poder establecer una comparación fidedigna en términos catalíticos con la PM1 parental secretada por la levadura. Esta aproximación sí que se llevó a cabo en la evolución dirigida paralela de la PcL (Camarero *et al.*, 2012), siendo una estrategia que hemos estandarizado en nuestro laboratorio para otros sistemas (como en la evolución dirigida de la UPO, material no publicado).

Se apreció una notable mejora en las eficiencias catalíticas (k_{cat}/K_m) a lo largo de la evolución para diferentes sustratos (ABTS, DMP y guayacol). Curiosamente, los mutantes de las primeras generaciones presentaron valores de k_{cat}/K_m muy inferiores a los descritos para lacasas de características similares (lacasa de *T. trogii* y lacasa de *Trametes* C30, **Tabla 2.1.1.**, pág. 62), lo cual indica que la actividad de la lacasa PM1 parental producida en *S. cerevisiae* fue mucho menor que la producida homólogamente por el hongo PM1 (PM1 nativa), tal y como se describe en el **Capítulo 4** (**Tabla 2.4.3.**, pág. 136). Desconocemos las razones por las que la lacasa PM1 parental expresada en levadura muestra peores eficiencias, algo que no sucede con la PcL parental en el mismo hospedador (Camarero et al. 2012). No obstante, en experimentos previos llevados a cabo con la MtL en *S. cerevisiae* la lacasa expresada mostró notables disminuciones en sus eficiencias catalíticas, siendo mejoradas en ciclos sucesivos de evolución dirigida (Bulter *et al.*, 2003a), tal y como sucede en el caso de la evolución de la lacasa PM1: el mutante OB-1, tras ocho ciclos de evolución, muestra unas cinéticas similares a la PM1 nativa.

La estabilidad de OB-1 fue analizada en términos de temperatura, pH y tolerancia a disolventes orgánicos:

- Termoestabilidad cinética. La T_{50} de OB-1 fue superior a la de otras lacasas de alto potencial redox como son las lacasas de *P. cinnabarinus*, *Trametes hirsuta* y *Pleurotus ostreatus*, muy similar a la de las lacasas de *Coriolopsis gallica* y *Trametes versicolor*, y ligeramente inferior a la de la lacasa PM1 nativa (**Tabla 3.1.**).

- Estabilidad frente al pH. OB-1 es altamente estable en el rango de pH de 3.0 a 9.0, reteniendo por encima del 85% de actividad tras 6 h de incubación.
- Estabilidad frente a disolventes orgánicos. OB-1 conserva entre el 30% y el 95% de su actividad después de 4 h de incubación en presencia de un 50% (v/v) de disolventes orgánicos de diferente naturaleza química y polaridad.

En consecuencia, las mutaciones incorporadas a lo largo del proceso evolutivo resultaron en una lacasa altamente estable en términos de temperatura, pH y tolerancia a disolventes orgánicos, lo cual concuerda con estudios anteriores en los que enzimas con elevada termoestabilidad fueron más resistentes a otros factores desnaturalizantes como son el pH o los disolventes orgánicos (Van den Burg *et al.*, 1998; Wang *et al.*, 2000).

Tabla 3.1. T_{50} de la lacasa PM1, del mutante OB-1 y de otras lacasas de alto potencial redox.

Lacasa	T_{50} (°C)
PM1 nativa	76.3
Coriolopsis gallica	73.6
OB-1	73.1
Trametes versicolor	72.5
P. cinnabarinus	68.9
Trametes hirsuta	65.6
Pleurotus ostreatus	60.0

3.2.4.2. Caracterización espectro-electroquímica

Como se ha descrito en el **Capítulo 4**, el mutante OB-1 no presentó, tras su purificación, el característico color azul del resto de lacasas –entre ellas, la PM1 nativa– sino que su espectro UV-visible fue similar a los reportados para las lacasas amarillas. Así, mientras que el cociente Abs_{280}/Abs_{610} de la PM1 nativa fue de 25.3 (valor típico de lacasas azules), en el caso de OB-1 fue de 82.8, que está dentro del intervalo de cocientes Abs_{280}/Abs_{610} característicos de las lacasas amarillas. Se descartó que la falta de absorbancia a 610 nm fuera debida a la presencia de otras proteínas procedentes del medio de cultivo, ya que tanto el gel de poliacrilamida en condiciones denaturalizantes, el espectro de MALDI-TOF y los estudios de huella peptídica confirmaron que la enzima tenía un elevado grado de pureza (**Figuras 2.4.1B** y **C**, pág. 133). También se excluyó que el cambio de color se debiera a alteraciones en el contenido en cobre de la proteína recombinante: los resultados obtenidos mediante ICP-OES confirmaron que OB-1 presentaba cuatro átomos de cobre por molécula de enzima. No obstante, y a diferencia de lo que ocurre con el resto de lacasas amarillas, OB-1 no fue capaz de oxidar colorantes de alto potencial redox

en ausencia de mediadores redox, un resultado idéntico al obtenido para la lacasa azul de *T. versicolor* (**Figura 2.4.2.**, pág. 137).

La falta de absorbancia a 610 nm de OB-1 impidió la determinación del potencial redox de su sitio T1 ($E°_{T1}$) mediante valoración redox convencional. Sin embargo, sus valores de actividad medidos en base al consumo de O_2 necesario para la oxidación de $K_4[Fe(CN)_6]$ y $K_4[Mo(CN)_8]$ fueron muy similares a los obtenidos para la PM1 nativa y la lacasa de *T. hirsuta*. Estos resultados, junto con la capacidad de OB-1 de oxidar de manera mediada diferentes colorantes de alto potencial redox, sugieren que el $E°_{T1}$ de la enzima no se vio afectado por la evolución y que OB-1 tiene un $E°_{T1}$ próximo al de la PM1 nativa (+759 mV *vs.* ENH; **Figura 2.4.3A**, pág. 138).

A fin de conocer si el proceso evolutivo dio lugar a un cambio en la estructura secundaria de la proteína, se registraron los espectros de dicroísmo circular tanto de la PM1 nativa como de OB-1 (**Figura 2.4.3D**, pág. 138 y **Tabla 2.4.4.**, pág. 139). La PM1 nativa mostró un espectro de dicroísmo circular (con unos porcentajes de los diferentes tipos de estructura secundaria) muy similar al de la lacasa de *Coprinus cinereus* (Schneider *et al.*, 1999). Por el contrario, OB-1 presentó un aumento en el contenido de estructuras desordenadas así como una banda negativa a 200 nm. Dicha banda es característica de las hélices de poliprolina e indica un cambio significativo en la estructura secundaria de la enzima. Por este motivo, suponemos que el cambio de color de azul (PM1 nativa) a amarillo (mutante OB-1) pudo ser debido a la combinación del aumento en el contenido de hélices de poliprolina y a la modificación de la esfera de coordinación del sitio T1 como consecuencia de la aparición de las mutaciones S426N y A461T, tal y como se explica en el **Capítulo 4**.

3.2.4.3. Caracterización mutacional

La secuencia de OB-1 contiene quince mutaciones (cinco silenciosas) distribuidas a lo largo del gen de fusión de la siguiente manera: una mutación en el prelíder del factor α (V[α10]D), cuatro mutaciones en el prolíder del factor α (N[α23]K, G[α62]G, A[α87]T y E[α90]E) y diez mutaciones en la proteína madura (Q70Q, V162A, A167A, H208Y, S224G, A239P, D281E, S426N, L456L y A461T) (**Tabla 2.1.S1.**, pág. 86). Tres de las cinco mutaciones silenciosas (subrayadas) favorecieron el uso de codones en *S. cerevisiae*. Por su parte, se cree que la mutación en el prelíder del factor α pudo mejorar la interacción con la partícula de reconocimiento de señal implicada en dirigir la proteína al retículo endoplasmático, mientras que las mutaciones en el prolíder pudieron favorecer el transporte de la proteína desde el retículo endoplasmático hasta el aparato de Golgi y su posterior secreción al medio extracelular. En cuanto a las mutaciones en la proteína madura, tres de ellas (V162A, S426N y A461T) están localizadas en el entorno del Cu T1. De acuerdo con el modelo tridimensional generado a partir de la estructura cristalográfica de la lacasa de *Trametes trogii* (PDB: 2HRG; 97% de identidad de secuencia con la PM1), estas

tres mutaciones dan lugar a la formación o ruptura de enlaces de hidrógeno que parecen conducir a ligeras modificaciones en la geometría de coordinación del Cu T1, lo cual, a su vez, explicaría la mejora en las propiedades cinéticas de la enzima así como el mencionado cambio en su propiedades espectroscópicas. Las cuatro mutaciones restantes presentes en la proteína madura (H208Y, S224G, A239P y D281E) se encuentran alejadas de los centros de cobre y en zonas de la proteína para las cuales, hasta la publicación del **Capítulo 1**, no se había descrito que estuvieran involucradas en la funcionalidad de las lacasas.

3.3. EVOLUCIÓN DIRIGIDA DE LA LACASA PM1 PARA SER ACTIVA EN SANGRE

Como se comentó en el **Apartado 1** (**Introducción general)** y en el **Capítulo 5**, las lacasas de alto potencial redox tienen la capacidad de aceptar electrones directamente desde la superficie de un electrodo, presentando además un bajo sobrepotencial de oxígeno y una elevada estabilidad operacional. Estas propiedades las convierten en candidatas excelentes para ser empleadas como biocatalizadores en biosensores y biopilas de combustible. No obstante, entre las características intrínsecas de este tipo de lacasas se encuentran la ausencia de actividad a pH superiores a 7.0 y el efecto inhibitorio de moderadas concentraciones de haluros. Estas condiciones son típicas de fluidos fisiológicos (*p. ej.,* la sangre humana tiene un pH aproximado de 7.4 y contiene en torno a 140-150 mM de NaCl), lo que dificulta su aplicación en biodispositivos operativos en condiciones fisiológicas. Además, también impide su implementación en diversos procesos industriales que tienen lugar a pH neutro o básico y en presencia de elevadas concentraciones de haluros.

3.3.1. Estrategia evolutiva

El mutante de secreción en levadura OB-1 fue escogido como enzima parental para un proceso de evolución dirigida con el objetivo de conseguir una lacasa activa en sangre humana (**Capítulo 5**). Para ello se diseñó un método de HTS para la selección de mutantes de lacasa en función de su actividad en un medio que simulaba las condiciones sanguíneas pero en ausencia de glóbulos rojos y agentes coagulantes. Dicho medio (al que se denominó *buffer de sangre*) contenía los principales metabolitos presentes en condiciones normales en la sangre (entre ellos, 150 mM de NaCl) así como el sustrato colorimétrico ABTS para la cuantificación de la actividad lacasa. El empleo del *buffer de sangre* fue necesario ante la imposibilidad de llevar a cabo el HTS con sangre real, puesto que los diferentes tipos de células sanguíneas así como los factores de coagulación hubiesen generado interferencias en las medidas. Dado que OB-1 no es activo a pH neutro, el primer ciclo de evolución se llevó a cabo en *buffer de sangre* a pH 6.5, aumentándose

progresivamente la presión selectiva en los ciclos sucesivos hasta alcanzar el pH fisiológico (pH 7.4). Es importante destacar que se incorporaron tres *re-screenings* consecutivos para descartar la presencia de falsos positivos. En particular, en el último *re-screening* se desglosaron las propiedades de cada mutante seleccionado en función de sus perfiles de pH, resistencias aparentes al cloruro y termoestabilidades.

En las tres primeras generaciones, la creación de diversidad genética se llevó a cabo mediante el empleo de diferentes DNA polimerasas propensas a error. Las genoteca mutagénicas resultantes fueron posteriormente recombinadas mediante distintas estrategias (*in vivo* DNA *shuffling*, IvAM y StEP), de manera equivalente a como se procedió en la evolución dirigida hacia secreción. Este procedimiento permitió el descubrimiento de tres nuevas mutaciones en el prepro-líder del factor α (E[α27]K, I[α66]M y E[α86]K), relacionadas exclusivamente con una mejora en la secreción de lacasa, y de seis nuevas mutaciones (S135R, T218V, N426D, I452V, F454S y T487S) más una deleción (A389-) en la proteína madura, que dieron lugar a mutantes con actividades notablemente mejoradas en *buffer de sangre*.

La cuarta y última generación se dedicó al estudio mediante mutagénesis dirigida y mutagénesis saturada de cuatro posiciones aminoacídicas que aumentaron de forma significativa la actividad lacasa en las condiciones del ensayo de *screening*, así como de una posición cuya importancia en el comportamiento de la enzima frente al pH fue descrita en estudios racionales con otra lacasa de alto potencial redox.

3.3.1.1. Mutagénesis dirigida D205N

En un trabajo anterior (Madzak *et al.*, 2006), el análisis de la estructura cristalográfica de la lacasa de *T. versicolor* reveló que el Asp en la posición 206 estaba directamente involucrado en la unión de la amina aromática 2,5-xilidina. Por alineamiento con las secuencias de lacasas de varias especies de hongos y plantas, los autores de dicho estudio decidieron sustituir el Asp206 por: i) Ala; ii) Glu, presente en dicha posición en varias lacasas de ascomicetos; y iii) Asn, típica en la posición 206 de las lacasas de plantas. Su objetivo era el determinar el efecto que tiene la modificación de esta posición en la actividad de la enzima en función del pH. En el caso de la oxidación del sustrato no fenólico ABTS, ninguno de los tres cambios dio lugar a modificaciones significativas en el perfil de actividad frente al pH. Sin embargo, cuando se empleó el sustrato fenólico DMP, el efecto de las mutaciones sobre el perfil de pH fue mucho más marcado. El cambio de Asp por residuos no cargados dio lugar al desplazamiento del pH óptimo de actividad hacia un pH más básico: la mutación D206A lo desplazó de 3.4 a ~4.0 ($\Delta pH_{óptimo}$ = ~0.6) mientras que el cambio D206N lo aumentó hasta 4.8 ($\Delta pH_{óptimo}$ = 1.4).

Dado que la lacasa PM1 comparte un alto grado de identidad de secuencia con la de *T. versicolor* (80%), se decidió llevar a cabo la mutagénesis dirigida en la posición 205 (equivalente

a la 206 en la de *T. versicolor*) a fin de averiguar si el cambio D205N ejercía el mismo efecto sobre los perfiles de pH. En efecto, el mutante 1B1 (con la mutación D205N) mostró un perfil de pH para ABTS muy similar al de 27C7 (su parental de la cuarta generación) manteniendo el pH óptimo en 3.0 (**Figura 3.4A**), mientras que con DMP desplazó su pH óptimo de actividad hasta 6.0, una y dos unidades por encima que los de 27C7 y OB-1, respectivamente (**Figura 3.4B**). A pesar de esta notable mejora, el mutante 1B1 fue finalmente descartado porque su actividad en *buffer de sangre* fue muy inferior a la de 27C7, lo cual parece indicar que la mutación D205N, si bien desplaza el perfil de pH para sustratos fenólicos, no tiene incidencia en el perfil de pH para ABTS y tampoco parece ser relevante en la tolerancia a haluros.

3.3.1.2. Mutagénesis dirigida N426D

Esta mutación apareció en la segunda generación (mutante 20F1) y su efecto beneficioso quedó demostrado al aumentar la actividad en *buffer de sangre* 12 veces respecto a la del mutante 35H10 de la primera generación (**Figura 2.5.1.**, pág. 147). Desafortunadamente, esta mutación se perdió en los eventos de recombinación del tercer ciclo dada su proximidad a la I452V. Por este motivo, se decidió incorporar el cambio N426D en 27C7, dando lugar a una lacasa (mutante 3A7) 0.6 veces menos activa que el correspondiente parental y, en consecuencia, esta mutación fue también descartada.

3.3.1.3. Mutagénesis saturada en la posición 389

El mutante 14F1 (3G) presentó una mejora en la actividad en buffer de sangre de 7 veces respecto a la del mutante 20F1 (2G), siendo su secuencia idéntica a la de 20F1 (2G) salvo por la deleción de la Ala situada en la posición 389. La supresión de este residuo fue debida probablemente a un fallo durante los procesos de anillamiento y extensión truncada a los que se sometió el gen de la lacasa durante el proceso de StEP para promover la recombinación de diferentes parentales.

La importancia de este resultado radica en dos aspectos. En primer lugar, el fallo suprimió tres nucleótidos consecutivos que formaban parte del mismo codón, de tal forma que su deleción no influyó en la pauta de lectura del ribosoma durante la traducción. En segundo lugar, la lacasa mutante codificada por el gen 'incompleto' presentó una elevada actividad en *buffer de sangre* respecto a los parentales de su ciclo, lo cual valida el protocolo de HTS diseñado. Aunque existen técnicas que permiten la construcción de librerías de mutantes con deleciones en aminoácidos puntuales (*p. ej.*, el método RAISE, *RAndom Insertional-deletional Strand Exchange mutagenesis*; Fujii *et al.*, 2006), en la bibliografía no se han encontrado estudios sobre evolución dirigida en los que se describa la selección de mutantes mejorados con posiciones delecionadas.

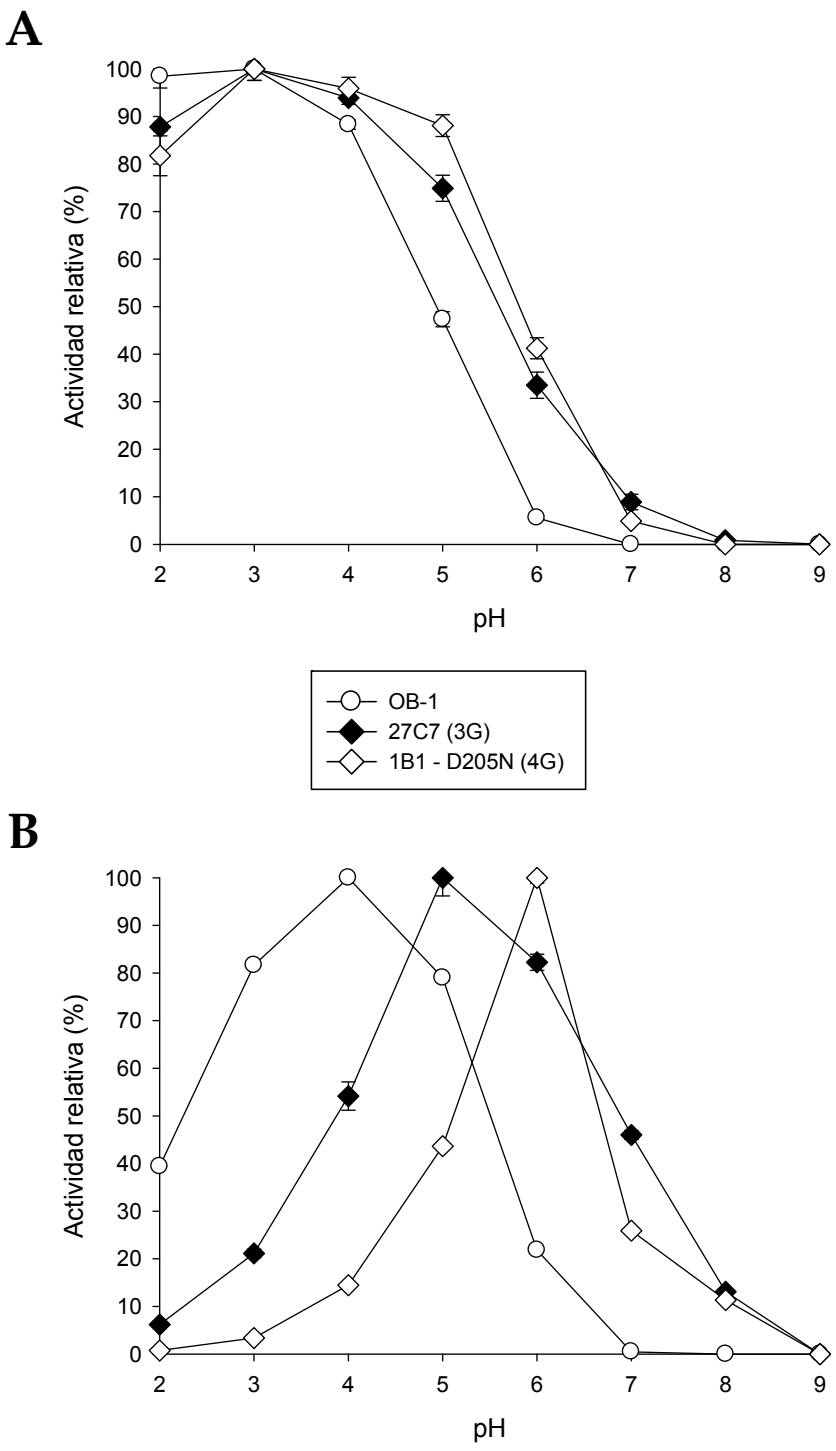

Figura 3.4. Perfiles de actividad frente al pH de los mutantes OB-1 (parental), 27C7 (3G) y 1B1- D205N (4G) empleando ABTS (A) y DMP (B) como sustratos.

Esta posición fue explorada por mutagénesis saturada obteniéndose únicamente mutantes con la Ala inicial, lo que significa que tan sólo la eliminación del aminoácido, y no su sustitución por cualquiera de los otros 19, produce mejoras en la actividad de la enzima en las condiciones del ensayo de *screening*. Cuando se analizó la posición 389 en el modelo de la lacasa, se apreció cómo la Ala389, situada a 7.7 Å del Cu T1, parecía establecer un puente de hidrógeno con la His394 que coordina dicho cobre (**Figura 3.5.**). Finalmente, se decidió no incluir la deleción en la variante final del proceso evolutivo porque, a pesar de su resistencia a las condiciones fisiológicas, la ausencia de este residuo supuso una disminución en la termoestabilidad de la lacasa de 1.7°C (**Tabla 2.5.S1**, pág. 166), y además, la supresión del enlace con la His394 podría comprometer el potencial redox del sitio T1 de la enzima.

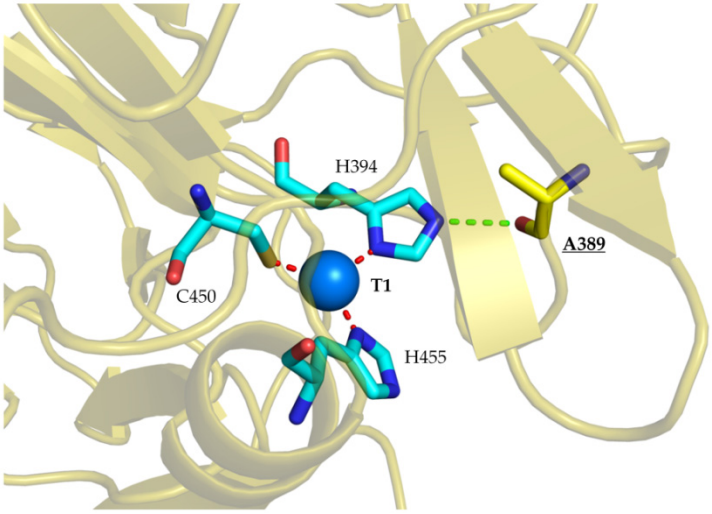

Figura 3.5. Análisis estructural de la Ala389. La esfera azul representa el Cu T1. Los ligandos del Cu T1 se muestran en azul y la Ala389 en amarillo. La interacción entre la His394 y la Ala389 está indicada por la línea discontinua verde y las interacciones Cu T1-ligandos por las líneas discontinuas rojas.

3.3.1.4. Mutagénesis saturada en la posición 396

El cambio de Phe a Ile en la posición 396 apareció en el mutante 35H10 de la primera generación, produciendo el aumento de actividad más alto de todo el proceso evolutivo (157 veces respecto al parental OB-1). Además, esta mutación resultó en un desplazamiento significativo del perfil de pH. El pH óptimo de actividad para el DMP aumentó en una unidad –pasó de 3.0 en OB-1 a 4.0 en 35H10–, de manera similar a lo que ocurrió con la mutación F454S (mutantes 7H2 (5G) y 6C8 (6G) del proyecto evolutivo hacia expresión funcional; **Figura 3.2.**).

Cuando la posición 396 fue estudiada por mutagénesis saturada, la exploración de la librería mutagénica dio lugar a un mutante (14B1) con la mutación F396I, lo cual pone de manifiesto

que el cambio descubierto por mutagénesis aleatoria en la primera generación fue el más adecuado para la propiedad en estudio y, por tanto, no susceptible de optimización adicional.

3.3.1.5. Mutagénesis saturada en la posición 454

Como se mencionó en el **Subapartado 3.2.** (pág. 194), la mutación F454S, aparecida en el quinto ciclo de evolución hacia expresión funcional en levadura, supuso un notable aumento de la actividad de la enzima a expensas de su termoestabilidad cinética y un desplazamiento considerable del pH frente a sustratos fenólicos. Esta posición fue redescubierta en el proceso de evolución dirigida hacia actividad en sangre, algo por otro lado presumible si se tienen en cuenta las condiciones del ensayo de *screening*. En concreto, los mutantes 18G5 y 20H4, ambos de la primera generación, y 14C5 de la tercera se obtuvieron a partir de genotecas construidas por diferentes metodologías (18G5 y 20H4 a partir de IvAM, y 14C5 procedente de una librería de StEP mutagenizada recombinada, a su vez, mediante *in vivo* DNA *shuffling*), dando lugar en todos los casos al aumento en la actividad a expensas de la disminución en la estabilidad térmica (**Tabla 3. 2.**).

Tabla 3.2. Número de veces de mejora en la actividad total (MAT) y T_{50} de la lacasa parental (mutante OB-1) y de las variantes que contienen la mutación F454S. *El MAT está referido al parental (o al mejor de los parentales) empleado en el correspondiente ciclo de evolución.

Lacasa	MAT*	T_{50} (°C)
OB-1 (parental)	-	73.1
18G5 (1G)	101	68.5
20H4 (1G)	99	65.1
14C5 (3G)	3.1	60.0

Estos resultados confirmaron de nuevo que el cambio de una Phe por una Ser en la posición 454 da lugar a un incremento de la actividad total de la lacasa a pH básico (es decir, disminuye el efecto inhibitorio de los iones hidroxilo), a la vez que desestabiliza la estructura proteica, de manera similar a lo que se observó para el mutante 7H2 del quinto ciclo hacia expresión funcional. Debido a su reducida termoestabilidad y a la pérdida de actividad durante su almacenamiento, los mutantes 18G5 (1G), 20H4 (1G) y 14C5 (3G) fueron descartados como parentales para los ciclos posteriores, si bien la posición 454 fue finalmente explorada mediante mutagénesis saturada con el objetivo de descubrir cambios diferentes a Phe→Ser que permitieran aumentar la actividad en condiciones fisiológicas afectando en menor medida a la estabilidad. Tras la exploración de la librería de mutagénesis saturada, se seleccionaron seis

mutantes en los que la Phe454 fue sustituida por Pro, Thr, Ala, Gly, Arg y Glu, resultando en mejoras en la actividad total en *buffer de sangre* entre 1.4 y 2.5 veces y T_{50} similares o hasta 6.7°C inferiores con respecto al parental 27C7 (**Tabla 3.3.**). Cabe señalar que la mutación F454S no fue redescubierta, lo cual indica que la mutagénesis saturada acoplada al ensayo HTS para seleccionar mutantes activos en sangre resultó eficaz en la optimización de esta posición. También es importante indicar que las seis mutaciones reveladas supusieron el cambio de 2 ó 3 de los nucleótidos componentes del codón original (TTC) (**Tabla 3.3.**), lo cual revela su inaccesibilidad mediante estrategias de mutagénesis aleatoria convencionales.

Tabla 3.3. T_{50} del mutante parental 27C7 (3G) y de las diferentes variantes obtenidas a partir de éste mediante mutagénesis saturada en la posición 454.

Lacasa	Aminoácido en la posición 454	Codón	T_{50} (°C)
27C7 (3G)	Phe	TTC	68.5
19B12 (4G)	Pro	CCC	65.7
18A10 (4G)	Thr	ACG	62.8
21D9 (4G)	Ala	GCG	61.8
17D4 (4G)	Gly	GGC	61.8
20C3 (4G)	Arg	CGG	64.0
ChU-B (4G)	Glu	GAG	63.7

El mutante con el cambio F454E (mutante ChU-B) fue escogido como variante final debido a que fue la lacasa con la actividad total en condiciones fisiológicas más elevada de todo el proceso evolutivo (41840 veces respecto a OB-1), toleró altas concentraciones de iones cloruro ($_{ap}I_{50}Cl^-$ de 650 mM frente a 92 mM de OB-1) y mostró actividad catalítica incluso a pH 8.0. Es importante mencionar que la introducción de F454E vino acompañada de la reversión no planeada de la mutación beneficiosa V452I (posiblemente debido a un fallo durante las reacciones de amplificación del DNA). Desconocemos si la combinación de dichas mutaciones daría lugar a un mutante todavía con mejores características, o por el contrario, dicha variante no fue descubierta durante el *screening* debido a incompatibilidades estructurales entre ambas posiciones. Únicamente la introducción mediante mutagénesis dirigida de la V452I en ChU-B aclararía este aspecto de la investigación. En cualquier caso, el hecho de que sólo dos mutaciones fueran las responsables finales de conferir a ChU-B tolerancia a la sangre indica que la re-especialización de esta lacasa para adaptarla a un ambiente tan inhóspito sólo necesitó del

0.4 % de su secuencia aminoacídica. Finalmente es también notorio el hecho de que ChU-B redujo su termoestabilidad drásticamente (con una caída en los valores de T_{50} de ~10°C frente al parental OB-1), aunque mantuvo una buena estabilidad durante su almacenamiento, sin merma detectable en su actividad tras varias semanas de conservación. La reducción en su termoestabilidad es predecible si se analizan de manera individual sus mutaciones (F454E disminuyó la T_{50} en 4.8°C mientras que F396I en 3.6°C; **Tabla 2.5.S1**, pág. 166). En un futuro próximo, podría mejorarse la termoestabilidad de ChU-B mediante la introducción de un conjunto de mutaciones estabilizantes (incluyendo por ejemplo, las mutaciones estabilizantes A361T y S482L descritas en los **Capítulos 1** y **2**) o realizando un nuevo ciclo de evolución hacia termoestabilidad.

3.3.2. Caracterización de la lacasa mutante activa en sangre ChU-B

La secuencia de aminoácidos del mutante ChU-B presentó cuatro mutaciones no silenciosas respecto a la secuencia del mutante de secreción OB-1. Por un lado, dos mutaciones en el prolíder del factor α (E[α7]K e I[α66]M), relacionadas con la expresión de lacasa por parte de la levadura, y por otro, dos mutaciones beneficiosas en la proteína madura (F396I y F454E), responsables de la actividad en condiciones fisiológicas. ChU-B fue producido en *S. cerevisiae*, purificado a homogeneidad y caracterizado desde un punto de vista bioquímico y electroquímico, a fin de estudiar el efecto que ejercieron en las propiedades de la enzima las dos mutaciones aparecidas en la proteína madura.

Cabe señalar que, una vez purificado, ChU-B recuperó el típico color azul propio de las lacasas. El cambio de color amarillo a azul podría ser debido al posible efecto ejercido por las mutaciones F396I y F454E en las esferas de coordinación del Cu T1. Para confirmar que los cambios de color de azul (PM1 nativa) a amarillo (OB-1) y su reversión final a azul (ChU-B) son consecuencia de alteraciones en la geometría del Cu T1, el estudio detallado mediante EPR sería de gran interés. Tampoco es descartable el diseño de nuevos pasos de purificación con el fin de estudiar la posible presencia de contaminantes de origen no proteico que puedan distorsionar la señal a 610 nm del Cu T1.

3.3.2.1. Ensayos de actividad en sangre y plasma humanos

Tras llevar a cabo la evolución dirigida en un medio sustituto de la sangre, fue necesario demostrar que la enzima era catalíticamente activa en sangre y plasma humanos reales. Para ello, se diseñó un experimento en el que se cuantificó el consumo de oxígeno por parte de la lacasa mutante sumergida en muestras de sangre y plasma. En estas medidas de actividad se enriqueció la sangre y el plasma con ácido ascórbico. Este compuesto se encuentra de manera natural en la sangre (el enantiómero L es la vitamina C) y es un pobre sustrato de las lacasas. La

frecuencia de recambio de ChU-B en sangre y plasma fue de 185 ± 8 y 127 ± 5 min^{-1}, respectivamente, confirmando la capacidad de esta lacasa para actuar en condiciones fisiológicas reales (**Figura 2.5.2A**, pág. 150). Idénticos experimentos se realizaron en *buffer de sangre* a pH 7.4 con ácido ascórbico, ABTS y $K_4[Fe(CN)_6]$. Los valores de actividad fueron similares para los tres compuestos, demostrando que ChU-B es capaz de llevar a cabo la oxidación en condiciones fisiológicas con independencia de la naturaleza química del sustrato (**Figura 2.5.2A**).

Ya que ChU-B fue diseñado con el propósito de que aceptara electrones desde un compartimento catódico sumergido en sangre, se inmovilizó el mutante en un electrodo de grafito de baja densidad y se registró de manera exitosa la corriente catódica generada por la reducción del oxígeno a pH fisiológico (**Figura 2.5.2C**, pág. 150). Además, se determinó que el potencial redox del sitio T1 de la enzima es de 740 mV *vs.* ENH a pH fisiológico (**Figura 2.5.2B**, pág. 150), 19 mV inferior al $E°_{T1}$ obtenido para el sitio T1 de la PM1 nativa a pH ácido (**Figura 2.4.3A**, pág. 138). Esta disminución en el potencial redox es atribuible al pH al que se realizó la medida e indica que ChU-B muestra un $E°_{T1}$ similar al de la PM1 nativa y, por tanto, pertenece al grupo de las lacasas de alto potencial.

3.3.2.2. Tolerancia a los iones haluro e hidroxilo

Las propiedades evolucionadas del mutante ChU-B fueron minuciosamente desglosadas mediante el análisis de sus perfiles de pH y resistencia a la inhibición por haluros.

Los perfiles de actividad frente al pH mostraron un desplazamiento significativo hacia pH alcalino tanto para ABTS como DMP (**Figuras 2.5.3A** y **B**, pág. 152). Por ejemplo, a pH neutro, ChU-B retuvo en torno al 20 y al 50% de su actividad para ABTS y DMP, respectivamente, mientras que la actividad de OB-1 en estas condiciones y para ambos sustratos fue nula. El aumento de la actividad a pHs alcalinos fue tan importante que ChU-B incluso mostró actividad a pH 8.0. Estos resultados confirman la disminución del efecto inhibitorio que tienen los iones hidroxilo sobre la enzima y convierten a ChU-B en la primera lacasa de alto potencial redox que muestra actividad a pHs neutros/alcalinos.

En lo que respecta a la inhibición por haluros, se determinaron las I_{50} para fluoruro y cloruro a pH ácido usando ABTS y DMP como sustratos (**Figuras 2.5.3C-D** y **Tabla 2.5.S2.**, pág. 152 y 167, respectivamente). En todos los casos, e independientemente del sustrato empleado, la I_{50} de ChU-B fue superior a la del parental OB-1. Por ejemplo, a pH ácido y con ABTS como sustrato, ChU-B fue 6 veces más tolerante a los cloruros ($I_{50}Cl^-$ = 1025 mM) que OB-1 ($I_{50}Cl^-$ = 176 mM), así como 15 y 26 veces más que las lacasas de alto potencial redox de *Trametes trogii* y *Trametes villosa* (con $I_{50}Cl^-$ de 70 y 40 mM, respectivamente; Garzillo *et al.*, 1998; Xu, 1996b). El fluoruro ejerció un mayor efecto inhibitorio que el cloruro, con valores de $I_{50}F^-$ en el orden micromolar.

Este resultado coincidió con lo esperado puesto que la fuerza inhibitoria de los haluros es inversamente proporcional al tamaño del anión: al ser más pequeños que los cloruros, los fluoruros acceden más fácilmente al *cluster* trinuclear, uniéndose al Cu T2 e interrumpiendo la transferencia intramolecular de electrones procedentes del sitio T1. No obstante, y a pesar de su elevado poder inhibitorio y de que la tolerancia a fluoruro no era objetivo de la evolución, ChU-B mejoró ligeramente las $I_{50}F^-$ para ABTS y DMP con respecto a las del parental OB-1.

Además, la inhibición de la actividad lacasa por los cloruros fue menor a pH alcalino debido a que los iones hidroxilo compiten con los haluros por la unión al sitio T2 (**Figuras 2.5.3E**, pág. 152). Así, ChU-B mantuvo el 100% de su actividad en presencia de concentraciones de cloruro en el intervalo de 100 a 800 mM, un comportamiento muy cercano al descrito en otros estudios como el de la polifenol oxidasa resistente a haluros producida por la bacteria *Marinomonas mediterranea* (Jimenez-Juarez *et al.*, 2005).

3.3.2.3. Análisis estructural de las mutaciones de ChU-B

Las mutaciones F396I y F454E confirieron a la lacasa resistencia a la inhibición por altas concentraciones de iones hidroxilo y cloruro, lo que a su vez resultó en una actividad catalítica detectable en sangre y plasma humanos. De acuerdo con una serie de estudios llevados a cabo por el Prof. F. Xu con lacasas de alto y medio potencial redox, la inhibición por parte de haluros e hidroxilos tiene fundamentalmente lugar en el *cluster* T2/T3, donde el inhibidor se une al Cu T2, interrumpiendo la transferencia de electrones procedentes del sitio T1 (Xu, 1996b; Xu, 1997; Xu *et al.*, 1998; Xu, 2001). Por este motivo, *a priori* cabría esperar que las mutaciones que confieren tolerancia a estos inhibidores hubiesen aparecido en las proximidades del *cluster* trinuclear. Sin embargo, las dos mutaciones se encontraron en el entorno del Cu T1 (ambas a 7.6 Å de distancia). En este punto es importante mencionar que mientras que la actividad de ChU-B a pH fisiológico se generó a partir de valores prácticamente nulos del parental OB-1, la actividad a pH óptimo fue drásticamente disminuida, siendo entre 3 y 4 veces (dependiendo del sustrato empleado) más baja que la del parental (**Tabla 2.5.S3.**, pág. 167). La modificación de la segunda esfera de coordinación del Cu T1, donde se sitúan las mutaciones F396I y F454E, si bien ralentiza la catálisis a pH ácidos, es fundamental para que la enzima sea funcional a valores de pH fisiológico, resultados que coinciden con los ensayos realizados mediante mutagénesis dirigida en la región del Cu T1 para la MtL (Xu *et al.*, 1998). Recientemente, hemos llevado a cabo la conversión mediante evolución dirigida de la MtL en una lacasa alcalofílica, descubriendo en este estudio mutaciones en el entorno del *cluster* trinuclear T2/T3 (Torres-Salas *et al.*, 2013). Asimismo, existen diversos trabajos donde se describen mecanismos diferentes para la inhibición por fluoruros y cloruros de la lacasa de *T. versicolor*, y que postulan que el fluoruro actúa como inhibidor no competitivo y el cloruro como inhibidor competitivo, bloqueando ambos la transferencia electrónica intramolecular (Naqui y Varfolomeev, 1980; Naki y

Varfolomeev, 1981). Más recientemente, se ha comprobado que la orientación adecuada de la lacasa de *T. hirsuta* en la superficie de un electrodo vía el sitio T1 (Vaz-Dominguez *et al.*, 2008) o la incorporación de la enzima en un polímero redox optimizado (Beyl *et al.*, 2011) permite reducir de manera significativa, e incluso anular totalmente, la inhibición por cloruros sin apenas alterar la inhibición por fluoruros.

Cabe señalar que en la actualidad se están llevando a cabo estudios computacionales en colaboración con el Prof. Víctor Guallar (Centro Nacional de Supercomputación, BSC-CNS) mediante simulaciones de Montecarlo usando el algoritmo PELE (*Protein Energy Landscape Exploration*) con el fin de determinar las posibles interacciones de los haluros en la estructura de la lacasa nativa y sus mutantes. Los primeros resultados indican que los haluros presentan mayor tendencia por unirse al *cluster* trinuclear T2/T3 que al Cu T1 (con relaciones 20/100 frente 1/100 para cada sitio, respectivamente; Prof. Guallar, comunicación personal).

En conclusión, la inhibición por haluros e hidroxilos de lacasas es un proceso extremadamente complejo y con al menos dos mecanismos diferentes relacionados con su unión al Cu T1 o al *cluster* T2/T3 de estas enzimas.

3.3.3. Sobreexpresión de ChU-B en *Pichia pastoris*

El desarrollo de la presente Tesis estuvo enmarcado dentro del proyecto *3D-nanobiodevice* (Ref. NMP4-SL-2009-229255) del Séptimo Programa Marco. El principal objetivo del proyecto fue la construcción de nanobiodispositivos tridimensionales implantables y capaces de monitorizar las concentraciones de glucosa y oxígeno presentes en biomatrices de diferente composición (*p. ej.*, sangre, plasma, saliva o lágrimas). Dentro del proyecto, nuestra labor fue el diseño mediante evolución *in vitro* de lacasas de alto potencia redox activas en sangre, así como su posterior producción en cantidades superiores a 50 mg a fin de poder ser suministradas al resto de grupos de investigación participantes e inmovilizarlas en los diferentes materiales susceptibles de formar el compartimento catódico de la biopila y/o del biosensor.

La expresión de ChU-B en *S. cerevisiae* tuvo lugar a niveles de ~8 mg/L, valores elevados teniendo en cuenta que los niveles de secreción en esta levadura conseguidos para lacasas de alto potencial redox no evolucionadas son prácticamente nulos (ver el **Apartado 1** -**Introducción general**- y el **Capítulo 2**). A pesar de ello, el rendimiento en la producción de enzima era claramente insuficiente de cara a conseguir la cantidad de lacasa pura necesaria para el proyecto.

Dado que la levadura metanotrófica *Pichia pastoris* se ha empleado para la expresión en elevadas cantidades de una gran variedad de proteínas heterólogas y, más concretamente, de

diferentes lacasas fúngicas (con niveles de producción entre 4.9 y 517 mg/L), esta levadura fue elegida para llevar a cabo la sobreproducción del mutante ChU-B (**Capítulo 6**).

El gen de la proteína madura de ChU-B unido tanto al prepro-líder del factor α nativo como evolucionado fue clonado, de manera independiente, bajo el control del promotor de la alcohol oxidasa 1 (P_{AOX1}, inducible por metanol) y del promotor de la gliceraldehído-3-fosfato deshidrogenasa (P_{GAP}, constitutivo), ambos de *P. pastoris* (**Figura 2.6.2.**, pág. 174). Los cuatro plásmidos resultantes se transformaron en *P. pastoris* y los correspondientes clones se sometieron a un pre-*screening* en placas de agar con ABTS, apreciándose como las construcciones con el prepro-líder nativo y evolucionado bajo el control del P_{AOX1} daban lugar a los clones más activos. A continuación, se realizaron fermentaciones *fed-batch* en biorreactores de 500 mL de las dos construcciones con el P_{AOX1} (**Figuras 2.6.3A** y **B**, pág. 175). Se comprobó así que las mutaciones en el prepro-líder del factor α favorecían de manera significativa la secreción de lacasa en esta levadura (niveles de expresión 1.7 veces más altos con el prepro-líder evolucionado que con el nativo). Seguidamente, y de acuerdo con los resultados anteriores, se decidió llevar a cabo una fermentación *fed-batch* en un biorreactor de 42 L de la construcción de ChU-B unido al prepro-líder evolucionado (**Figuras 2.6.3C**, pág. 175). La máxima actividad volumétrica conseguida fue de 3220 U-ABTS/L, similar a la obtenida en *S. cerevisiae* (2200 U-ABTS/L). Sin embargo, los niveles de producción de lacasa en biorreactor se incrementaron notablemente, alcanzándose valores de 43 mg/L como consecuencia directa de la elevada cantidad de biomasa generada por *P. pastoris* durante la fermentación.

3.3.3.1. Caracterización bioquímica de ChU-B expresado en *P. pastoris*

Los perfiles de actividad frente al pH para ABTS y DMP y la tolerancia frente a haluros de ChU-B producido en *P. pastoris* fueron muy similares a los obtenidos para la enzima expresada en *S. cerevisiae* (**Figuras 2.6.4B-C** y **2.6.5**, pág. 178 y 180, respectivamente, y **Tabla 2.6.3.**, pág. 179). Además, y al igual que lo observado para OB-1, el mutante ChU-B expresado en ambas levaduras mostró el tetrapéptido ETEAEF unido al extremo N-terminal de la enzima como consecuencia del procesamiento parcial del prolíder del factor α (**Tabla 2.6.2.**, pág. 176). Por otro lado, se comprobó que la enzima expresada en *P. pastoris* era menos termoestable y eficiente en la oxidación de ABTS y DMP a pH ácido (**Tabla 2.6.4.**, pág. 182) pero se mostró catalíticamente activa en sangre y plasma humanos.

El mutante ChU-B producido en *P. pastoris* fue distribuido entre los diferentes grupos del proyecto *3D-nanobiodevice* y fue empleado en el diseño final de un prototipo del dispositivo tridimensional capaz de reportar señal inalámbrica durante la monitorización de glucosa en condiciones fisiológicas (publicación en preparación).

3.4. CONCLUSIONES

1. Se ha conseguido la expresión en *S. cerevisiae* de la lacasa nativa del basidiomiceto PM1 en forma soluble, estable y funcional. Para ello se sustituyó la secuencia señal nativa por la del prepro-líder del factor α de *S. cerevisiae* (α-PM1).

2. La estrategia de evolución dirigida para mejorar la secreción de esta lacasa en *S. cerevisiae* consistió en: i) someter el gen de fusión α-PM1 a ciclos sucesivos de mutagénesis aleatoria, recombinación y *screening*; ii) incorporar estudios semi-racionales de intercambio mutacional y recuperación de mutaciones beneficiosas perdidas durante los eventos de entrecruzamiento; y iii) salvaguardar la termoestabilidad cinética mediante la incorporación de mutaciones estabilizantes a través del empleo de un protocolo de HTS de termoestabilidad.

3. Tras explorar más de 50000 clones en ocho ciclos de evolución dirigida, se obtuvo el mutante OB-1, que presentó quince mutaciones, originando un aumento en la actividad total de 34000 veces respecto a la enzima parental α-PM1 con niveles de secreción de 8 mg/L. A las cinco mutaciones en la secuencia señal del factor α (dos silenciosas) se les atribuyó la mejora en la secreción de la proteína. Las diez mutaciones restantes se localizaron en la secuencia de la proteína madura (tres silenciosas). Las siete mutaciones no silenciosas en la proteína madura (V162A, H208Y, S224G, A239P, D281E, S426N y A461T) fueron responsables de la mejora de las propiedades catalíticas de la enzima frente a sustratos fenólicos y no fenólicos, pudiendo también tener influencia sobre el plegamiento proteico y exocitosis.

4. El mutante OB-1 presentó una extensión de seis aminoácidos adicionales en el extremo N-terminal como consecuencia de una alteración durante el procesamiento del prolíder del factor α por parte de la peptidasa *STE13* en el aparato de Golgi. Se construyó el correspondiente mutante truncado (OB-1del) y se comprobó que la extensión N-terminal no influye de manera significativa en las propiedades bioquímicas de la lacasa pero sí que reduce considerablemente su secreción por la levadura.

5. El mutante OB-1 presentó unas propiedades espectroscópicas similares a las de las lacasas amarillas. Este hecho fue atribuido a la presencia de hélices de poliprolina y a modificaciones en la esfera de coordinación del sitio de Cu T1 como consecuencia de las mutaciones incorporadas durante el proceso de evolución.

6. El mutante OB-1 fue seleccionado como enzima parental para el diseño de una lacasa activa en sangre humana mediante evolución dirigida. Para ello se elaboró un protocolo

HTS basado en la medida de actividad lacasa en un medio complejo que simulaba la composición bioquímica de la sangre.

7. Este segundo experimento evolutivo comprendió tres ciclos consecutivos de mutagénesis aleatoria combinada con recombinación *in vivo* e *in vitro*, y un ciclo de mutagénesis dirigida y saturada. La última generación se llevó a cabo con el fin de: i) introducir dos mutaciones beneficiosas perdidas en el curso de la evolución, así como una mutación responsable del desplazamiento hacia pH alcalino en la lacasa de *T. versicolor*; y ii) explorar mediante mutagénesis saturada tres posiciones aminoacídicas importantes en la tolerancia de la enzima hacia iones cloruro e hidroxilo.

8. Tras más de 10000 clones explorados en cuatro generaciones de evolución dirigida se obtuvo el mutante final ChU-B, con la capacidad de ser catalíticamente activo en sangre y plasma humanos. El desglose de sus propiedades mostró una gran tolerancia al cloruro (con valores de I_{50} en torno a 1 M) y un perfil de pH notablemente desplazado hacia la zona alcalina (lo que le permite funcionar a pH fisiológico).

9. El mutante ChU-B presentó siete mutaciones con respecto a la lacasa parental (mutante de secreción OB-1). De estas siete mutaciones, tres se localizaron en la secuencia señal del factor α (una silenciosa) y las cuatro restantes en la proteína madura (dos silenciosas). Las dos mutaciones beneficiosas de la proteína madura (F396I y F454E) fueron responsables de la adaptación de la enzima al medio sanguíneo.

10. El mutante ChU-B fue clonado en *P. pastoris* y fermentado en biorreactor de 42 L, alcanzando niveles de producción de 43 mg/L y mostrando un comportamiento catalítico en fluidos fisiológicos similar al de la variante producida en *S. cerevisiae*.

11. La lacasa de alto potencial redox tolerante a sangre diseñada en esta Tesis Doctoral constituye un punto de partida prometedor para su inmovilización en biopilas de combustible y biosensores integrados dentro de nanodispositivos con aplicaciones biomédicas. Además, la actividad de esta lacasa a pH neutro/alcalino y su baja sensibilidad a la presencia de iones cloruro posibilitan su estudio en otros ámbitos como son la síntesis orgánica, el procesado de decolorantes industriales o su aplicación en la industria del blanqueo del papel.

4. BIBLIOGRAFÍA

Abécassis, V., Pompon, D. y Truan, G. (**2000**) High efficiency family shuffling based on multi-step PCR and *in vivo* DNA recombination in yeast: statistical and functional analysis of a combinatorial library between human cytochrome P450 1A1 and 1A2. *Nucleic Acids Res.* 28: e88.

Abyanova, A.R., Chulkin, A.M., Vavilova, E.A., Fedorova, T.V., Loginov, D.S., Koroleva, O.V. y Benevolensky, S.V. (**2010**) A heterologous production of the *Trametes hirsuta* laccase in the fungus *Penicillium canescens*. *Appl. Biochem. Microb.* 46: 313-317.

Aharoni, A., Griffiths, A.D. y Tawfik, D.S. (**2005**) High-throughput screens and selections of enzyme-encoding genes. *Curr. Opin. Chem. Biol.* 9: 210-216.

Alcalde, M. (**2003**) Evolución molecular dirigida. *Investigación y Ciencia* 326: 69-77.

Alcalde, M. (**2007**) Laccases: biological functions, molecular structure and industrial applications. En *Industrial Enzymes. Structure, Function and Applications*. Eds. J. Polaina y A. P. MacCabe. Springer (Dordrecht, Países Bajos). pág. 461-476.

Alcalde, M. (**2010**) Mutagenesis protocols in *Saccharomyces cerevisiae* by *in vivo* overlap extension. En *In vitro Mutagenesis Protocols. Methods in Molecular Biology*. Ed. J. Braman. Humana Press (Totowa, Nueva Jersey). Vol. 634. pág. 3-14.

Alcalde M. (**2012**) Fundamentos de evolución molecular dirigida de enzimas. En *Monografías de la Real Academia Nacional de Farmacia, Monografía XXXV: Biocatálisis Aplicada a la Obtención de Fármacos y Productos de Alto Valor Añadido.* Eds. J. M. Sánchez Montero, F. Ortega Ortiz de Apodaca y A. Doadrio Villarejo. Real Academia Nacional de Farmacia (Madrid). pág. 289-316.

Alcalde, M. y Bulter, T. (**2003**) Colorimetric assays for screening laccases. En *Directed Enzyme Evolution: Screening and Selection Methods*. *Methods in Molecular Biology*. Eds. F.H. Arnold y G. Georgiou. Humana Press (Totowa, Nueva Jersey). pág. 193-201.

Alcalde, M., Bulter, T. y Arnold, F.H. (**2002**) Colorimetric assays for biodegradation of polycyclic aromatic hydrocarbons by fungal laccases. *J. Biomol. Screen.* 7: 547-553.

Alcalde, M., Bulter, T., Zumarraga, M., Garcia-Arellano, H., Mencia, M., Plou, F.J. y Ballesteros, A. (**2005**) Screening mutant libraries of fungal laccases in the presence of organic solvents. *J. Biomol. Screen.* 10: 624-631.

Alcalde, M., Ferrer, M., Plou, F.J. y Ballesteros, A. (**2006a**) Environmental biocatalysis: from remediation with enzymes to novel green processes. *Trends Biotechnol.* 24: 281-287.

Alcalde, M., Zumárraga, M., Polaina, J., Ballesteros, A. y Plou, F.J. (**2006b**) Combinatorial saturation mutagenesis by *in vivo* overlap extension for the engineering of fungal laccases. *Comb. Chem. High T. Scr.* 9: 719-727.

Alves, A.M.C.R., Record, E., Lomascolo, A., Scholtmeijer, K., Asther, M., Wessels, J.G.H. y Wosten, H.A.B. (**2004**) Highly efficient production of laccase by the basidiomycete *Pycnoporus cinnabarinus*. *Appl. Environ. Microbiol.* 70**:** 6379-6384.

Andberg, M., Hakulinen, N., Auer, S., Saloheimo, M., Koivula, A., Rouvinen, J. y Kruus, K. (**2009**) Essential role of the C-terminus in *Melanocarpus albomyces* laccase for enzyme production, catalytic properties and structure. *FEBS J.* 276: 6285-6300.

Arnold, F.H. (**1990**) Engineering enzymes for nonaqueous solvents. *Trends Biotechnol.* 8: 244-249.

Arnold, F.H. (**1996**) Directed evolution: Creating biocatalysts for the future. *Chem. Eng. Sci.* 51: 5091-5102.

Arnold, F.H. (**2006**) Fancy footwork in the sequence space shuffle. *Nat. Biotechnol.* 24: 328-330.

Arnold, F.H. (**2009**) How proteins adapt: lessons from directed evolution. *Cold Spring Harb. Symp. Quant. Biol.* 74: 41-46.

Arnold, F.H. y Volkov, A.A. (**1999**) Directed evolution of biocatalysts. *Curr. Opin. Chem. Biol.* 3: 54-59.

Arnold, F.H. y Georgiou, G. (**2003**) Directed enzyme evolution: screening and selection methods. En *Methods in Molecular Biology*. Humana Press (Totowa, Nueva Jersey).

Arnold, F.H., Giver, L., Gershenson, A., Zhao, H.M. y Miyazaki, K. (**1999**) Directed evolution of mesophilic enzymes into their thermophilic counterparts. *Ann. N. Y. Acad. Sci.* 870: 400-403.

Bailey, M.R., Woodard, S.L., Callaway, E., Beifuss, K., Magallanes-Lundback, M., Lane, J.R., Horn, M.E., Mallubhotla, H., Delaney, D.D., Ward, M., Van Gastel, F., Howard, J.A. y Hood, E.E. (**2004**) Improved recovery of active recombinant laccase from maize seed. *Appl. Microbiol. Biot.* 63: 390-397.

Baiocco, P., Barreca, A.M., Fabbrini, M., Galli, C. y Gentili, P. (**2003**) Promoting laccase activity towards non-phenolic substrates: a mechanistic investigation with some laccase-mediator systems. *Org. Biomol. Chem.* 1:191-197.

Baker, C.J.O. y White, T.C. (**2001**) Expression of laccase I and IV genes from *Trametes versicolor* in *Trichoderma reesei*. En *Oxidative Delignification Chemistry. ACS Symposium Series*. Ed. D. S. Argyropoulos. American Chemical Society (Washington). pág. 413-426.

Baldrian, P. (**2006**) Fungal laccases-occurrence and properties. *FEMS Microbiol. Rev.* 30: 215-242.

Bao, W., O'Malley, D.M., Whetten, R. y Sederoff, R.R. (**1993**) A laccase associated with lignification in Loblolly pine xylem. *Science* 260: 672-674.

Beloqui, A., Pita, M., Polaina, J., Martinez-Arias, A., Golyshina, O.V., Zumarraga, M., Yakimov, M.M., Garcia-Arellano, H., Alcalde, M., Fernandez, V.M. *et al.* (**2006**) Novel polyphenol oxidase mined from a metagenome expression library of bovine rumen - Biochemical properties, structural analysis, and phylogenetic relationships. *J Biol. Chem.* 281: 22933-22942.

Bento, I., Silva, C.S., Chen, Z., Martins, L.O., Lindley, P.F. y Soares, C.M. (**2010**) Mechanisms underlying dioxygen reduction in laccases. Structural and modelling studies focusing on proton transfer. *BMC Struct. Biol.* 10: 28.

Berka, R.M., Schneider, P., Golightly, E.J., Brown, S.H., Madden, M., Brown, K.M., Halkier, T., Mondorf, K. y Xu, F. (**1997**) Characterization of the gene encoding an extracellular laccase of *Myceliophthora thermophila* and analysis of the recombinant enzyme expressed in *Aspergillus oryzae*. *Appl. Environ. Microbiol.* 63: 3151-3157.

Bershtein, S. y Tawfik, D.S. (**2008**) Advances in laboratory evolution of enzymes. *Curr. Opin. Chem. Biol.* 12: 151-158.

Bertrand, T., Jolivalt, C., Briozzo, P., Caminade, E., Joly, N., Madzak, C. y Mougin, C. (**2002**) Crystal structure of a four-copper laccase complexed with an arylamine: Insights into substrate recognition and correlation with kinetics. *Biochemistry* 41: 7325-7333.

Beyl, Y., Guschin, D.A., Shleev, S. y Schuhmann, W. (**2011**) A chloride resistant high potential oxygen reducing biocathode based on a fungal laccase incorporated into an optimized Os-complex modified redox hydrogel. *Electrochem. Commun.* 13**:** 474-476.

Bleve, G., Lezzi, C., Mita, G., Rampino, P., Perrotta, C., Villanova, L. y Grieco, F. (**2008**) Molecular cloning and heterologous expression of a laccase gene from *Pleurotus eryngii* in free and immobilized *Saccharomyces cerevisiae* cells. *Appl. Microbiol. Biot.* 79: 731-741.

Bloom, J.D. y Arnold, F.H. (**2009**) In the light of directed evolution: Pathways of adaptive protein evolution. *P. Natl. Acad. Sci. USA* 106: 9995-10000.

Bloom, J.D., Wilke, C.O., Arnold, F.H. y Adami, C. (**2004**) Stability and the evolvability of function in a model protein. *Biophys. J.* 86: 2758-2764.

Bloom, J.D., Meyer, M.M., Meinhold, P., Otey, C.R., MacMillan, D. y Arnold, F.H. (**2005**) Evolving strategies for enzyme engineering. *Curr. Opin. Struc. Biol.* 15: 447-452.

Bloom, J.D., Labthavikul, S.T., Otey, C.R. y Arnold, F.H. (**2006**) Protein stability promotes evolvability. *P. Natl. Acad. Sci. USA* 103: 5869-5874.

Bloom, J.D., Romero, P.A., Lu, Z. y Arnold, F.H. (**2007**) Neutral genetic drift can alter promiscuous protein functions, potentially aiding functional evolution. *Biol. Direct* 2:17.

Bohlin, C., Jonsson, L.J., Roth, R. y vanZyl, W. H. (**2006**) Heterologous expression of *Trametes versicolor* laccase in *Pichia pastoris* and *Aspergillus niger*. *Appl. Biochem. Biotech.* 129: 195-214.

Bommarius, A.S., Broering, J.M., Chaparro-Riggers, J.F. y Polizzi, K. M. (**2006**) High-throughput screening for enhanced protein stability. *Curr. Opin. Biotech.* 17: 606-610.

Borrelli, K.W., Vitalis, A., Alcantara, R. y Guallar, V. (**2005**) PELE: Protein energy landscape exploration. A novel Monte Carlo based technique. *J. Chem. Theory Comput.* 1: 1034-1311.

Boyd, D. y Beckwith, J. (**1990**) The role of charged amino-acids in the localization of secreted and membrane-proteins. *Cell* 62: 1031-1033.

Bragd, P.L., van Bekkum, H. y Besemer, A.C. (**2004**) TEMPO-mediated oxidation of polysaccharides: survey of methods and applications. *Topics in Catalysis* 27: 49-66.

Braiuca, P., Ebert, C., Basso, A., Linda, P. y Gardossi, L. (**2006**) Computational methods to rationalize experimental strategies in biocatalysis. *Trends Biotechnol.* 24: 419-425.

Brake, A.J. (**1990**) α-factor leader-directed secretion of heterologous proteins from yeast. *Methods Enzymol.* 185: 408-421.

Brakmann, S. (**2001**) Discovery of superior enzymes by directed molecular evolution. *ChemBioChem* 2: 865-871.

Bullen, R.A., Arnot, T.C., Lakeman, J.B. y Walsh, F.C. (**2006**) Biofuel cells and their development. *Biosens. Bioelectron.* 21: 2015-2045.

Bulter, T. y Alcalde, M. (**2003**) Preparing libraries in *Saccharomyces cerevisiae*. En *Directed Evolution Library Creation*. *Methods in Molecular Biology*. Eds. F.H. Arnold y G. Georgiou. Humana Press (Totowa, Nueva Jersey). pág. 17-22.

Bulter, T., Alcalde, M., Sieber, V., Meinhold, P., Schlachtbauer, C. y Arnold, F.H. (**2003a**) Functional expression of a fungal laccase in *Saccharomyces cerevisiae* by directed evolution. *Appl. Environ. Microbiol.* 69: 987-995.

Bulter, T., Sieber, V. y Alcalde, M. (**2003b**) Screening mutant libraries in *Saccharomyces cerevisiae*. En *Directed Enzyme Evolution: Screening and Selection Methods*. *Methods in Molecular Biology*. Eds. F.H. Arnold y G. Georgiou. Humana Press (Totowa, Nueva Jersey). pág. 99-107.

Calabrese Barton, S., Gallaway, J. y Atanassov, P. (**2004**) Enzymatic biofuel cells for implantable and microscale devices. *Chem. Rev.* 104: 4867-4886.

Call, H.P. y Mucke, I. (**1997**) History, overview and applications of mediated lignolytic systems, especially laccase-mediator-systems (Lignozym®-process). *J. Biotechnol.* 53: 163-202.

Camarero, S., Cañas, A., Martínez, M.J., Martínez, A.T., Ballesteros, A., Plou, F.J., Record, E., Asther, M. y Alcalde, M. (**2010**). Laccases having high redox potential obtained through directed evolution. Patente internacional WO 2010/058057.

Camarero, S., Pardo, I., Cañas, A.I., Molina, P., Record, E., Martinez, A.T., Martinez, M.J. y Alcalde, M. (**2012**) Engineering platforms for directed evolution of laccase from *Pycnoporus cinnabarinus*. *Appl. Environ. Microbiol.* 78: 1370-1384.

Cañas, A.I. y Camarero, S. (**2010**) Laccases and their natural mediators: Biotechnological tools for sustainable eco-friendly processes. *Biotechnol. Adv.* 28: 694-705.

Castillo, J., Gaspar, S., Leth, S., Niculescu, M., Mortari, A., Bontidean, I., Soukharev, V., Dorneanu, S.A., Ryabov, A.D. y Csoregi, E. (**2004**) Biosensors for life quality - Design, development and applications. *Sensor. Actuat. B-Chem.* 102: 179-194.

Cereghino, J.L. y Cregg, J.M. (**2000**) Heterologous protein expression in the methylotrophic yeast *Pichia pastoris*. *FEMS Microbiol. Rev.* 24: 45-66.

Chen, T., Barton, S.C., Binyamin, G., Gao, Z.Q., Zhang, Y.C., Kim, H.H. y Heller, A. (**2001**) A miniature biofuel cell. *J. Am. Chem. Soc.* 123: 8630-8631.

Chernykh, A., Myasoedova, N., Kolomytseva, M., Ferraroni, M., Briganti, F., Scozzafava, A. y Golovleva, L. (**2008**) Laccase isoforms with unusual properties from the basidiomycete *Steccherinum ochraceum* strain 1833. *J. Appl. Microbiol.* 105: 2065-2075.

Cherry, J.R. y Fidantsef, A.L. (**2003**) Directed evolution of industrial enzymes: an update. *Curr. Opin. Biotech.* 14: 438-443.

Cherry, J.R., Lamsa, M.H., Schneider, P., Vind, J., Svendsen, A., Jones, A. y Pedersen, A.H. (**1999**) Directed evolution of a fungal peroxidase. *Nat. Biotechnol.* 17: 379-384.

Chica, R.A., Doucet, N. y Pelletier, J.N. (**2005**) Semi-rational approaches to engineering enzyme activity: combining the benefits of directed evolution and rational design. *Curr. Op. Biotech.* 16: 378-384.

Christensen, N.J. y Kepp, K.P. (**2012**) Accurate stabilities of laccase mutants predicted with a modified FoldX protocol. *J. Chem. Inf. Model.* 52: 3028-3042.

Christenson, A., Dimcheva, N., Ferapontova, E.E., Gorton, L., Ruzgas, T., Stoica, L., Shleev, S., Yaropolov, A.L., Haltrich, D., Thorneley, R.N.F. y Aust, S.D. (**2004**) Direct electron transfer between ligninolytic redox enzymes and electrodes. *Electroanal.* 16: 1074-1092

Christenson, A., Shleev, S., Mano, N., Heller, A. y Gorton, L. (**2006**) Redox potentials of the blue copper sites of bilirubin oxidases. *Biochim. Biophys. Acta* 1757:1634-1641.

Cirino, P.C., Mayer, K.M. y Umeno, D. (**2003**) Generating mutant libraries using error-prone PCR. En *Directed Evolution Library Creation*. *Methods in Molecular Biology*. Eds. F.H. Arnold y G. Georgiou. Humana Press (Totowa, Nueva Jersey). pág. 3-9.

Claus, H. (**2004**) Laccases: structure, reactions, distribution. *Micron* 35: 93-96.

Cliffe, S., Fawer, M.S., Maier, G., Takata, K. y Ritter, G. (**1994**) Enzyme assays for the phenolic content of natural juices. *J. Agr. Food Chem.* 42: 1824-1828.

Cline, J., Braman, J.C. y Hogrefe, H.H. (**1996**) PCR fidelity of Pfu DNA polymerase and other thermostable DNA polymerases. *Nucleic Acids Res.* 24**:** 3546-3551.

Cline, J. y Hogrefe, H. (**2000**) Randomize gene sequences with new PCR mutagenesis kit. *Stratagene Strategies* 13:157-161.

Cobb, R.E., Si, T. y Zhao, H. (**2012**) Directed evolution: an evolving and enabling synthetic biology tool. *Curr. Opin. Chem. Biol.* 16: 285-291.

Coco, W.M., Levinson, W.E., Crist, M.J., Hektor, H.J., Darzins, A., Pienkos, P.T., Squires, C.H. y Monticello, D.J. (**2001**) DNA shuffling method for generating highly recombined genes and evolved enzymes. *Nat. Biotechnol.* 19: 354-359.

Colao, M.C., Garzillo, A.M., Buonocore, V., Schiesser, A. y Ruzzi, M. (**2003**) Primary structure and transcription analysis of a laccase-encoding gene from the basidiomycete *Trametes trogii*. *Appl. Microb. Biot.* 63: 153-158.

Colao, M.C., Lupino, S., Garzillo, A.M., Buonocore, V. y Ruzzi, M. (**2006**) Heterologous expression of lcc 1 gene from *Trametes trogii* in *Pichia pastoris* and characterization of the recombinant enzyme. *Microb. Cell Fact.* 5: 31-42.

Coll, P.M., Fernández-Abalos, J.M., Villanueva, J.R., Santamaría, R. y Pérez, P. (**1993a**) Purification and characterization of a phenoloxidase (laccase) from the lignin-degrading basidiomycete PM1 (CECT 2971). *Appl. Environ. Microbiol.* 59: 2607-2613.

Coll, P.M., Tabernero, C., Santamaría, R. y Pérez, P. (**1993b**) Characterization and structural analysis of the laccase I gene from the newly isolated ligninolytic basidiomycete PM1 (CECT 2971). *Appl. Environ. Microbiol.* 59: 4129-4135.

Collins, P.J. y Dobson, A.D.W. (**1997**) Regulation of laccase gene transcription in *Trametes versicolor*. *Appl. Environ. Microbiol.* 63: 3444-3450.

Coman, V., Vaz-Dominguez, C., Ludwig, R., Herreither, W., Haltrich, D., De Lacey, A.L., Ruzgas, T., Gorton, L. y Shleev, S. (**2008**) A membrane-, mediator-, cofactor-less glucose/oxygen biofuel cell. *Phys. Chem. Chem. Phys.* 10: 6093-6096.

Coman, V., Ludwig, R., Herreither, W., Haltrich, D., Gorton, L., Ruzgas, T. y Shleev, S. (**2010**) A direct electron transfer-based glucose/oxygen biofuel cell operating in human serum. *Fuel Cells* 10: 9-16.

Couto, S.R. y Herrera, J.L.T. (**2006**) Industrial and biotechnological applications of laccases: A review. *Biotechnol. Adv.* 24: 500-513.

Crameri, A., Whitehorn, E.A., Tate, E. y Stemmer, W.P.C. (**1996**) Improved green fluorescent protein by molecular evolution using DNA shuffling. *Nat. Biotechnol.* 14: 315-319.

Cregg, J.M., Cereghino, J. L., Shi, J. Y. y Higgins, D.R. (**2000**) Recombinant protein expression in *Pichia pastoris*. *Mol. Biotechnol.* 2000, 16: 23-52.

Cui, T.J., Wang, X.T., Zhou, H.M., Hong, Y.Z., Xiao, Y.Z., Cui, T.J., Wang, X.T. y Pu, C.L. (**2007**) High output of a *Trametes* laccase in *Pichia pastoris* and characterization of recombinant enzymes. *Chinese J. Biotechnol.* 23: 1055-1059.

Cusano, A.M., Mekmouche, Y., Meglecz, E. y Tron, T. (**2009**) Plasticity of laccase generated by homeologous recombination in yeast. *FEBS J.* 276: 5471-5480.

Dalby, P.A. (**2011**) Strategy and success for the directed evolution of enzymes. *Curr. Opin. Struc. Biol.* 21: 473-480.

Daly, R. y Hearn, M.T.W. (**2005**) Expression of heterologous proteins in *Pichia pastoris*: A useful experimental tool in protein engineering and production. *J. Mol. Recognit.* 18: 119-138.

Daugherty, P.S., Chen, G., Iverson, B.L. y Georgiou, G. (**2000**) Quantitative analysis of the effect of the mutation frequency on the affinity maturation of single chain Fv antibodies. *P. Natl. Acad. Sci. USA* 97: 2029-2034.

Davies, G.J. y Ducros, V. (**2002**) Laccase. En *Handbook of Metalloproteins*. Ed. A. Messerschmidt, R. Huber, K. Wieghardt y T. Poulos. Wiley (Hoboken, Nueva Jersey). pág. 1359-1368.

de Abreu, M. A. Álvaro-Benito, M., Sanz-Aparicio, J., Plou, F. J., Fernández-Lobato, M., Alcalde, M. (**2013**) Synthesis of 6-kestose using a highly efficient β-fructofuranosidase engineered by directed evolution. *Adv. Synth. Catal.* DOI: 10.1002/adsc.201200769.

de Wilde, C., Uzan, E., Zhou, Z.Y., Kruus, K., Andberg, M., Buchert, J., Record, E., Asther, M. y Lomascolo, A. (**2008**) Transgenic rice as a novel production system for *Melanocarpus* and *Pycnoporus* laccases. *Transgenic Res.* 17: 515-527.

Di Fusco, M., Tortolini, C., Deriu, D. y Mazzei, F. (**2010**) Laccase-based biosensor for the determination of polyphenol index in wine. *Talanta* 81**:** 235-240.

Dix, D.B. y Thompson, R.C. (**1989**) Codon choice and gene-expression - Synonymous codons differ in translational accuracy. *P. Natl. Acad. Sci. USA* 86: 6888-6892.

Ducros, V., Brzozowski, A.M., Wilson, K.S., Brown, S.H., Ostergaard, P., Schneider, P., Yaver, D. S., Pedersen, A.H. y Davies, G.J. (**1998**) Crystal structure of the type-2 Cu depleted laccase from *Coprinus cinereus* at 2.2 angstrom resolution. *Nat. Struct. Biol.* 5: 310-316.

Durao, P., Bento, I., Fernandes, A.T., Melo, E.P., Lindley, P.F. y Martins, L.O. (**2006**) Perturbations of the T1 copper site in the CotA laccase from *Bacillus subtilis*: structural, biochemical, enzymatic and stability studies. *J. Biol. Inorg. Chem.* 11: 514-526.

Edens, W.A., Goins, T.Q., Dooley, D. y Henson, J.M. (**1999**) Purification and characterization of a secreted laccase of *Gaeumannomyces graminis* var. *tritici*. *Appl. Environ. Microbiol.* 65: 3071-3074.

Emond, S., Mondon, P., Pizzut-Serin, S., Douchy, L., Crozet, F., Bouayadi, K., Kharrat, H., Potocki-Veronese, G., Monsan, P. y Remaud-Simeon, M. (**2008**) A novel random mutagenesis approach using human mutagenic DNA polymerases to generate enzyme variant libraries. *Protein Eng. Des. Sel.* 21: 267-274.

Enguita, F.J., Martins, L.O., Henriques, A.O. y Carrondo, M.A. (**2003**) Crystal structure of a bacterial endospore coat component - A laccase with enhanced thermostability properties. *J. Biol. Chem.* 278: 19416-19425.

Esvelt, K.M., Carlson, J.C. y Liu, D.R. (**2011**) A system for the continuous directed evolution of biomolecules. *Nature* 472: 499-503.

Falk, M., Andoralov, V., Blum, Z., Sotres, J., Suyatin, D.B., Ruzgas, T., Arnebrant, T. y Shleev, S. (**2012**) Biofuel cell as a power source for electronic contact lenses. *Biosens. Bioelectron.* 37: 38-45.

Farver, O., Skov, L.K., Pascher, T., Karlsson, B.G., Nordling, M., Lundberg, L.G., Vanngard, T. y Pecht, I. (**1993**) Intramolecular electron-transfer in single-site-mutated azurins. *Biochemistry* 32: 7317-7322.

Fasan, R., Chen, M.M., Crook, N.C. y Arnold, F.H. (**2007**) Engineered alkane-hydroxylating cytochrome $P450_{BM3}$ exhibiting nativelike catalytic properties. *Angew. Chem. Int. Ed.* 46: 8414-8418.

Feng, X.J., Sanchis, J., Reetz, M.T. y Rabitz, H. (**2012**) Enhancing the efficiency of directed evolution in focused enzyme libraries by the adaptive substituent reordering algorithm. *Chem. Eur. J.* 18: 5646-5654.

Fengel, D. y Wegener, G. (**1984**) *Wood: Chemistry, ultrastructure, reactions*. De Gruyter (Boston, Massachusetts).

Festa, G., Autore, F., Fraternali, F., Giardina, P. y Sannia, G. (**2008**) Development of new laccases by directed evolution: Functional and computational analyses. *Proteins* 72: 25-34.

Floudas, D., Binder, M., Riley, R., Barry, K., Blanchette, R.A., Henrissat, B., Martinez, A.T., Otillar, R., Spatafora, J.W., Yadav, J.S. *et al.* (**2012**) The paleozoic origin of enzymatic lignin decomposition reconstructed from 31 fungal genomes. *Science* 336: 1715-1719.

Frederick, K.R., Tung, J., Emerick, R.S., Masiarz, F.R., Chamberlain, S.H., Vasavada, A., Rosenberg, S., Chakraborty, S., Schopfer, L.M. y Schopfer, L.M. (**1990**). Glucose oxidase from *Aspergillus niger*. Cloning, gene sequence, secretion from *Saccharomyces cerevisiae* and kinetic analysis of a yeast-derived enzyme. *J. Biol. Chem.* 265: 3793-3802.

Fujii, R., Kitaoka, M. y Hayashi, K. (**2006**) RAISE: a simple and novel method of generating random insertion and deletion mutations. *Nucleic Acids Res.* 34: e30.

Gao, F., Yan, Y.M., Su, L., Wang, L. y Mao, L.Q. (**2007**) An enzymatic glucose/O_2 biofuel cell: Preparation, characterization and performance in serum. *Electrochem. Commun.* 9: 989-996.

García, E., Martínez, M.J., Dueñas, J., Martínez, A.T. y Alcalde M. (**2010**) High redox potential peroxidases designed by directed evolution. Patente internacional WO 2010/130862.

García-Ruiz, E., Maté, D., Ballesteros, A., Martinez, A.T., and Alcalde, M. (**2010**). Evolving thermostability in mutant libraries of ligninolytic oxidoreductases expressed in yeast. *Microb. Cell. Fact.* 9: 17. **Capítulo 2 de la Tesis**.

Garcia-Ruiz, E., Gonzalez-Perez, D., Ruiz-Dueñas, F.J., Martinez, A.T. y Alcalde, M. (**2012**) Directed evolution of a temperature-, peroxide- and alkaline pH-tolerant versatile peroxidase. *Biochem. J.* 441: 487-498.

Gardiol, A.E., Hernandez, R.J., Reinhammar, B. y Harte, B.R. (**1996**) Development of a gas-phase oxygen biosensor using a blue copper-containing oxidase. *Enzyme Microb. Technol.* 18: 347-352.

Garzillo, A.M.V., Colao, M.C., Caruso, C., Caporale, C., Celletti, D. y Buonocore, V. (**1998**) Laccase from the white-rot fungus *Trametes trogii*. *Appl. Microbiol. Biot.* 49: 545-551.

Garzillo, A.M., Colao, M.C., Buonocore, V., Oliva, R., Falcigno, L., Saviano, M., Santoro, A.M., Zappala, R., Bonomo, R.P., Bianco, C., Giardina, P., Palmieri, G. y Sannia, G. (**2001**) Structural and kinetic characterization of native laccases from *Pleurotus ostreatus*, *Rigidoporus lignosus*, and *Trametes trogii*. *J. Protein Chem.* 20: 191-201.

GeneMorph® II Random Mutagenesis Kit: Instruction Manual. Stratagene. http://www.bioc.rice.edu/bios576/proteng/200550.pdf

Georgescu, R., Bandara, G. y Sun, L. (**2003**) Saturation mutagenesis. En *Directed Evolution Library Creation. Methods in Molecular Biology*. Eds. F.H. Arnold y G. Georgiou. Humana Press (Totowa, Nueva Jersey). pág. 75-83.

Ghindilis, A.L., Gavrilova, V.P. y Yaropolov, A.I. (**1992**) Laccase-based biosensor for determination of polyphenols - determination of catechols in tea. *Biosens. Bioelectron.* 7: 127-131.

Gianfreda, L., Xu, F. y Bollag, J.M. (**1999**) Laccases: a useful group of oxidoreductive enzymes. *Bioremediat. J.* 3: 1-25.

Giardina, P., Faraco, V., Pezzella, C., Piscitelli, A., Vanhulle, S. y Sannia, G. (**2010**) Laccases: a never-ending story. *Cel. Mol. Life Sci.* 67: 369-385.

Gibbs, M.D., Nevalainen, K.M.H. y Bergquist, P.L. (**2001**) Degenerate oligonucleotide gene shuffling (DOGS): a method for enhancing the frequency of recombination with family shuffling. *Gene* 271: 13-20.

Gibson, D.G. (**2009**) Synthesis of DNA fragments in yeast by one-step assembly of overlapping oligonucleotides. *Nucleic Acids Res.* 37: 6984-6990.

Giver, L., Gershenson, A., Freskgard, P.O. y Arnold, F.H. (**1998**) Directed evolution of a thermostable esterase. *P. Natl. Acad. Sci. USA* 95: 12809-12813.

Glieder, A., Farinas, E.T. y Arnold, F.H. (**2002**) Laboratory evolution of a soluble, self-sufficient, highly active alkane hydroxylase. *Nat. Biotechnol.* 20: 1135-1139.

Gonzalez-Perez, D., Garcia-Ruiz, E. y Alcalde, M. (**2012**) *Saccharomyces cerevisiae* in directed evolution: An efficient tool to improve enzymes. *Bioengineered* 3: 172-177.

Greimel, K.J., Perz, V., Herrero Acero, E. y Guebitz, G.M. (**2012**) Replacing toxic heavy metals for the drying of alkyd resins using laccase/mediator systems. *OxiZymes*. Comunicación oral. Marsella, 16-19 Septiembre.

Guallar, V. y Wallrapp, F. (**2008**) Mapping protein electron transfer pathways with QM/MM methods. *J. R. Soc. Interface* 5: S233-S239.

Guo, M., Lu, F.P., Du, L.X., Pu, J. y Bai, D.Q. (**2006**) Optimization of the expression of a laccase gene from *Trametes versicolor* in *Pichia methanolica*. *Appl. Microbiol. Biot.* 71: 848-852.

Gupta, N. y Farinas, E.T. (**2009**) Narrowing laccase substrate specificity using active site saturation mutagenesis. *Comb. Chem. High T. Scr.* 12: 269-274.

Gupta, N. y Farinas, E.T. (**2010**) Directed evolution of CotA laccase for increased substrate specificity using *Bacillus subtilis* spores. *Protein Eng. Des. Sel.* 23: 679-682.

Gupta, N., Lee, F.S. y Farinas, E.T. (**2010**) Laboratory evolution of laccase for substrate specificity. *J. Mol. Catal. B-Enzym.* 62: 230-234.

Haibo, Z., Yinglong, Z., Feng, H., Peiji, G. y Jiachuan, C. (**2009**) Purification and characterization of a thermostable laccase with unique oxidative characteristics from *Trametes hirsuta*. *Biotechnol. Lett.* 31: 837-843.

Hakulinen, N., Kiiskinen, L.L., Kruus, K., Saloheimo, M., Paananen, A., Koivula, A. y Rouvinen, J. (**2002**) Crystal structure of a laccase from *Melanocarpus albomyces* with an intact trinuclear copper site. *Nat. Struct. Biol.* 9: 601-605.

Hao, J.J. y Berry, A. (**2004**) A thermostable variant of fructose bisphosphate aldolase constructed by directed evolution also shows increased stability in organic solvents. *Protein Eng. Des. Sel.* 17: 689-697.

Heller, A. (**2004**) Miniature biofuel cells. *Phys. Chem. Chem. Phys.* 6: 209-216.

Hidalgo, A., Schliessmann, A., Molina, R., Hermoso, J. y Bornscheuer, U.T. (**2008**) A one-pot, simple methodology for cassette randomisation and recombination for focused directed evolution. *Protein Eng. Des. Sel.* 21: 567-576.

Hildén, K., Hakala, T.K. y Lundell, T. (**2009**) Thermotolerant and thermostable laccases. *Biotechnol. Lett.* 31: 1117-1128.

Hoegger, P.J., Kilaru, S., James, T.Y., Thacker, J.R. y Kues, U. (**2006**) Phylogenetic comparison and classification of laccase and related multicopper oxidase protein sequences. *FEBS J.* 273: 2308-2326.

Höfer, C. y Schlosser, D. (**1999**) Novel enzymatic oxidation of Mn^{2+} to Mn^{3+} catalyzed by a fungal laccase. *FEBS Lett.* 451: 186-190.

Hofrichter, M., Ullrich, R., Pecyna, M.J., Liers, C. y Lundell, T. (**2010**) New and classic families of secreted fungal heme peroxidases. *Appl. Microbiol. Biot.* 87: 871-897.

Hong, F., Meinander, N.Q. y Jonsson, L.J. (**2002**) Fermentation strategies for improved heterologous expression of laccase in *Pichia pastoris*. *Biotechnol. Bioeng.* 79: 438-449.

Hoshida, H., Nakao, M., Kanazawa, H., Kubo, K., Hakukawa, T., Morimasa, K., Akada, R. y Nishizawa, Y. (**2001**) Isolation of five laccase gene sequences from the white-rot fungus *Trametes sanguinea* by PCR, and cloning, characterization and expression of the laccase cDNA in yeasts. *J. Biosci. Bioeng.* 92: 372-380.

Hoshida, H., Fujita, T., Murata, K., Kubo, K. y Akada, R. (**2005**) Copper-dependent production of a *Pycnoporus coccineus* extracellular laccase in *Aspergillus oryzae* and *Saccharomyces cerevisiae*. *Biosci. Biotech. Bioch.* 69: 1090-1097.

Iaropolov, A.I., Sukhomlin, T.K., Kariakin, A.A., Varfolomeev, S.D. y Berezin, I.V. (**1981**) The possibility of electron tunnel transfer in the enzymatic catalysis of electrode processes. *Dokl. Akad. Nauk SSSR* 260: 1192-1196.

Iffland, A., Tafelmeyer, P., Saudan, C. y Johnsson, K. (**2000**) Directed molecular evolution of cytochrome c peroxidase. *Biochemistry* 39: 10790-10798.

IUPAC. Compendium of Chemical Terminology (**1997**) Eds. A. D. McNaught y A. Wilkinson (Oxford). ISBN 0-86542-684-8.

Jäckel, C. y Hilvert, D. (**2010**) Biocatalysts by evolution. *Curr. Opin. Biotech.* 21: 753-759.

Jimenez-Juarez, N., Roman-Miranda, R., Baeza, A., Sánchez-Amat, A., Vazquez-Duhalt, R. y Valderrama, B. (**2005**) Alkali and halide-resistant catalysis by the multipotent oxidase from *Marinomonas mediterranea*. *J. Biotechnol.* 117: 73-82.

Johannes, T.W. y Zhao, H.M. (**2006**) Directed evolution of enzymes and biosynthetic pathways. *Curr. Opin. Microbiol.* 9: 261-267.

Johannes, T.W., Woodyer, R.D. y Zhao, H.M. (**2005**) Directed evolution of a thermostable phosphite dehydrogenase for NAD(P)H regeneration. *Appl. Environ. Microbiol.* 71: 5728-5734.

Jolivalt, C., Madzak, C., Brault, A., Caminade, E., Malosse, C. y Mougin, C. (**2005**) Expression of laccase IIIb from the white-rot fungus *Trametes versicolor* in the yeast *Yarrowia lipolytica* for environmental applications. *Appl. Microbiol. Biot.* 66: 450-456.

Jung, H.C., Xu, F. y Li, K.C. (**2002**) Purification and characterization of laccase from wood-degrading fungus *Trichophyton rubrum* LKY-7. *Enzyme Microb. Technol.* 30: 161-168.

Júnior, A.R.S. y Rebelo, M.J.F. (**2008**) Biosensors for the polyphenolic content of wine determination. *Port. Electrochim. Acta* 26**:** 117-124.

Kallio, J.P., Gasparetti, C., Andberg, M., Boer, H., Koivula, A., Kruus, K., Rouvinen, J. y Hakulinen, N. (**2011**) Crystal structure of an ascomycete fungal laccase from *Thielavia arenaria* - common structural features of asco-laccases. *FEBS J.* 278: 2283-2295.

Kaneko, S., Cheng, M., Murai, H., Takenaka, S., Murakami, S. y Aoki, K. (**2009**) Purification and characterization of an extracellular laccase from *Phlebia radiata* strain BP-11-2 that decolorizes fungal melanin. *Biosci. Biotech. Bioch.* 73: 939-942.

Katz, E. y Willner, I. (**2003**) A biofuel cell with electrochemically switchable and tunable power output. *J. Am. Chem. Soc.* 125: 6803-6813.

Katz, E., Buckmann, A.F. y Willner, I. (**2001**) Self-powered enzyme-based biosensors. *J. Am. Chem. Soc.* 123: 10752-10753.

Kawarasaki, Y., Griswold, K.E., Stevenson, J.D., Selzer, T., Benkovic, S.J., Iverson, B.L. y Georgiou, G. (**2003**) Enhanced crossover SCRATCHY: construction and high-throughput screening of a combinatorial library containing multiple non-homologous crossovers. *Nucleic Acids Res.* 31: e126.

Keightley, P.D. y Eyre-Walker, A. (**2000**) Deleterious mutations and the evolution of sex. *Science* 290: 331-333.

Kiiskinen, L.L., Kruus, K., Bailey, M., Ylosmaki, E., Siika-aho, M. y Saloheimo, M. (**2004**) Expression of *Melanocarpus albomyces* laccase in *Trichoderma reesei* and characterization of the purified enzyme. *Microbiology* 150: 3065-3074.

Kim, J., Jia, H.F. y Wang, P. (**2006**) Challenges in biocatalysis for enzyme-based biofuel cells. *Biotechnol. Adv.* 24: 296-308.

Kim, J.M., Park, S.M. y Kim, D.H. (**2010**) Heterologous expression of a tannic acid-inducible laccase3 of *Cryphonectria parasitica* in *Saccharomyces cerevisiae*. *BMC Biotechnol.* 10: 18.

Kittl, R., Gonaus, C., Pillei, C., Haltrich, D. y Ludwig, R. (**2012a**) Constitutive expression of *Botrytis aclada* laccase in *Pichia pastoris*. *Bioengineered* 3: 172-177.

Kittl, R., Mueangtoom, K., Gonaus, C., Khazaneh, S.T., Sygmund, C., Haltrich, D. y Ludwig, R. (**2012b**) A chloride tolerant laccase from the plant pathogen ascomycete *Botrytis aclada* expressed at high levels in *Pichia pastoris*. *J. Biotechnol.* 157: 304-314.

Klonowska, A., Gaudin, C., Fournel, A., Asso, M., Le Petit, J., Giorgi, M. y Tron, T. (**2002**) Characterization of a low redox potential laccase from the basidiomycete C30. *Eur. J. Biochem.* 269: 6119-6125.

Klonowska, A., Gaudin, C., Asso, M., Fournel, A., Reglier, M. y Tron, T. (**2005**) LAC3, a new low redox potential laccase from *Trametes* sp. strain C30 obtained as a recombinant protein in yeast. *Enzyme Microb. Technol.* 36: 34-41.

Kojima, Y., Tsukuda, Y., Kawai, Y., Tsukamoto, A., Sugiura, J., Sakaino, M. y Kita, Y. (**1990**) Cloning, sequence-analysis, and expression of ligninolytic phenoloxidase genes of the white-rot basidiomycete *Coriolus hirsutus*. *J. Biol. Chem.* 265: 15224-15230.

Kolkman, J.A. y Stemmer, W.P.C. (**2001**) Directed evolution of proteins by exon shuffling. *Nat. Biotechnol.* 19: 423-428.

Kuchner, O. y Arnold, F.H. (**1997**) Directed evolution of enzyme catalysts. *Trends Biotechnol.* 15: 523-530.

Kunamneni, A., Ballesteros, A., Plou, F.J. y Alcalde M. (**2007**) Fungal laccase - a versatile enzyme for biotechnological applications. En *Communicating Current Research and Educational Topics and Trends in Applied Microbiology* Ed. A. Méndez-Vilas. Formatex (Badajoz). pág. 233-245.

Kunamneni, A., Camarero, S., García-Burgos, C., Plou, F.J., Ballesteros, A. y Alcalde, M. (**2008a**) Engineering and applications of fungal laccases for organic synthesis. *Microb. Cell Fact.* 7: 32.

Kunamneni, A., Plou, F.J., Ballesteros, A. y Alcalde, M. (**2008b**) Laccases and their applications: a patent review. *Recent Pat. Biotechnol.* 2: 10-24.

Lang, M., Kanost, M.R. y Gorman, M.J. (**2012**) Multicopper oxidase-3 is a laccase associated with the peritrophic matrix of *Anopheles gambiae*. *PLOS ONE 7*: e33985.

Larsson, T., Lindgren, A. y Ruzgas, T. (**2001**) Spectroelectrochemical study of cellobiose dehydrogenase and diaphorase in a thiol-modified gold capillary in the absence of mediators. *Bioelectrochemistry* 53:243-249.

Laufer, Z., Beckett, R.P., Minibayeva, F.V., Luthje, S. y Bottger, M. (**2009**) Diversity of laccases from lichens in suborder *Peltigerineae*. *Bryologist* 112: 418-426.

Lee, I.Y., Jung, K.H., Lee, C.H. y Park, Y.H. (**1999**) Enhanced production of laccase in *Trametes vesicolor* by the addition of ethanol. *Biotechnol. Lett.* 21: 965-968.

Leech, D. y Daigle, F. (**1998**) Optimisation of a reagentless laccase electrode for the detection of the inhibitor azide. *Analyst* 123: 1971-1974.

Leemhuis, H., Kelly, R.M. y Dijkhuizen, L. (**2009**) Directed evolution of enzymes: Library screening strategies. *IUBMB Life* 61: 222-228.

Leontievsky, A.A., Vares, T., Lankinen, P., Shergill, J.K., Pozdnyakova, N.N., Myasoedova, N.M., Kalkkinen, N., Golovleva, L.A., Cammack, R., Thurston, C.F. y Hatakka, A. (**1997a**) Blue and yellow laccases of ligninolytic fungi. *FEMS Microbiol. Lett.* 156: 9-14.

Leontievsky, A., Myasoedova, N., Pozdnyakova, N. y Golovleva, L. (**1997b**) 'Yellow' laccase of *Panus tigrinus* oxidizes non-phenolic substrates without electron-transfer mediators. *FEBS Lett.* 413: 446-448.

Leung, D.W., Chen, E. y Goeddel, D.V. (**1989**) A method for random mutagenesis of a defined DNA segment using a modified polymerase chain reaction. *Technique* 1: 11-15.

Leung, S. y Lai, J. (**2011**) Advanced dehydrogenase biofuel cell modified with highly branched polymers and nano gold sol-gel. *ICABE 2011 - International Conference on Agricultural and Biosystems Engineering.* Hong Kong, 20-21 Febrero.

Leipoldt, J.G., Bok, L.D.C. y Cilliers, P.J. (**1974**) Preparation of potassium octacyanotungstate (IV) dihydrate. *Z. Anorg. Allg. Chem.* 407: 350-352.

Li, K.C., Xu, F. y Eriksson, K.E.L. (**1999**) Comparison of fungal laccases and redox mediators in oxidation of a nonphenolic lignin model compound. *Appl. Environ. Microbiol.* 65: 2654-2660.

Li, H., Webb, S.P., Ivanic, J. y Jensen, J.H. (**2004**) Determinants of the relative reduction potentials of type-1 copper sites in proteins. *J. Am. Chem. Soc.* 126: 8010-8019.

Li, J., Hong, Y., Xiao, Y., Xu, Y. y Fang, W. (**2007**) High production of laccase B from *Trametes* sp. in *Pichia pastoris*. *World J. Microb. Biot.* 23: 741-745.

Lin-Cereghino, J., Wong, W.W., Xiong, S., Giang, W., Luong, L.T., Vu, J., Johnson, S.D. y Lin-Cereghino, G.P. (**2005**) Condensed protocol for competent cell preparation and transformation of the methylotrophic yeast *Pichia pastoris*. *Biotechniques* 38: 44.

Lin-Goerke, J.L., Robbins, D.J. y Burczak, J.D. (**1997**) PCR-based random mutagenesis using manganese and reduced dNTP concentration. *Biotechniques* 23: 409-412.

Liu, Y. y Dong, S. (**2008**) Electrochemical characteristics of mediated laccase-catalysis and electrochemical detection of environmental pollutants. *Electroanal.* 20: 827-832.

Liu, W., Chao, Y., Liu, S., Bao, H. y Qian, S. (**2003**) Molecular cloning and characterization of a laccase gene from the basidiomycete *Fome lignosus* and expression in *Pichia pastoris*. *Appl. Microb. Biot.* 63: 174-181.

Liu, Z., Pscheidt, B., Avi, M., Gaisberger, R., Hartner, F.S., Schuster, C., Skranc, W., Gruber, K., Glieder, A. (**2008**) Laboratory evolved biocatalysts for stereoselective syntheses of substituted benzaldehyde cyanohydrins. *ChemBioChem* 9: 58-61.

Lopez-Camacho, C., Salgado, J., Lequerica, J.L., Madarro, A., Ballestar, E., Franco, L. y Polaina, J. (**1996**) Amino acid substitutions enhancing thermostability of *Bacillus polymyxa* beta-glucosidase A. *Biochem. J.* 314: 833-838.

Lyashenko, A.V., Bento, I., Zaitsev, V.N., Zhukhlistova, N.E., Zhukova, Y.N., Gabdoulkhakov, A.G., Morgunova, F.Y., Voelter, W., Kachalova, G.S., Stepanova, E.V. *et al.* (**2006**) X-ray structural studies of the fungal laccase from *Cerrena maxima*. *J. Biol. Inorg. Chem.* 11: 963-973.

Lutz, S. (**2010**) Beyond directed evolution - Semi-rational protein engineering and design. *Curr. Op. Biotech.* 21: 734-743.

Lutz, S., Ostermeier, M. y Benkovic, S.J. (**2001a**) Rapid generation of incremental truncation libraries for protein engineering using alpha-phosphothioate nucleotides. *Nucleic Acids Res.* 29: e16.

Lutz, S., Ostermeier, M., Moore, G.L., Maranas, C.D. y Benkovic, S.J. (**2001b**) Creating multiple-crossover DNA libraries independent of sequence identity. *P. Natl. Acad. Sci. USA* 98: 11248-11253.

Madzak, C., Otterbein, L., Chamkha, M., Moukha, S., Asther, M., Gaillardin, C. y Beckerich, J.M. (**2005**) Heterologous production of a laccase from the basidiomycete *Pycnoporus cinnabarinus* in the dimorphic yeast *Yarrowia lipolytica*. *FEMS Yeast Res.* 5: 635-646.

Madzak, C., Mimmi, M.C., Caminade, E., Brault, A., Baumberger, S., Briozzo, P., Mougin, C. y Jolivalt, C. (**2006**) Shifting the optimal pH of activity for a laccase from the fungus *Trametes versicolor* by structure-based mutagenesis. *Protein Eng. Des. Sel.* 19: 77-84.

Majors, B.S., Chiang, G.G. y Betenbaugh, M.J. (**2009**) Protein and genome evolution in mammalian cells for biotechnology applications. *Mol. Biotechnol.* 42: 216-223.

Manivasakam, P., Weber, S.C., Mcelver, J. y Schiestl, R.H. (**1995**) Micro-homology mediated PCR targeting in *Saccharomyces cerevisiae*. *Nucleic Acids Res.* 23: 2799-2800.

Mano, N., Mao, F. y Heller, A. (**2003**) Characteristics of a miniature compartment-less glucose-O_2 biofuel cell and its operation in a living plant. *J. Am. Chem. Soc.* 125: 6588-6594.

Mansiaux, Y., Joseph, A.P., Gelly, J.C. y de Breven, A.G. (**2011**) Assignment of polyproline II conformation and analysis of sequence-structure relationship. *PLOS ONE* 6: e18401.

Martínez, A.T., Speranza, M., Ruiz-Dueñas, F.J., Ferreira, P., Camarero, S., Guillén, F., Martínez, M.J., Gutiérrez, A. y del Río, J.C. (**2005**) Biodegradation of lignocellulosics: microbial, chemical, and enzymatic aspects of the fungal attack of lignin. *Int. Microbiol.* 8: 195-204.

Martínez, A.T., Ruiz-Dueñas, F.J., Martínez, M.J., del Río, J.C. y Gutiérrez, A. (**2009**) Enzymatic delignification of plant cell wall: from nature to mill. *Curr. Opin. Biotech.* 20: 348-357.

Maté, D., García-Burgos, C., García-Ruiz, E., Ballesteros, A.O., Camarero, S. y Alcalde, M. (**2010**). Laboratory evolution of high-redox potential laccases. *Chem. Biol.* 17: 1030-1041. **Capítulo 2 de la Tesis**.

Maté, D., Valdivieso, M., Fernández, L. y Alcalde, M. (**2011a**) Laccase with high redox potential. Patente internacional WO 2011/144784.

Maté, D., García-Ruiz, E., Camarero, S. y Alcalde, M. (**2011b**). Directed evolution of fungal laccases. *Curr. Genomics* 12: 113-122. **Capítulo 3 de la Tesis**.

Mate, D.M., Garcia-Ruiz, E., Camarero, S., Shubin, V.V., Falk, M., Shleev, S., Ballesteros, A.O., y Alcalde, M. (**2013a**) Switching from blue to yellow: Altering the spectral properties of a high redox potential laccase by directed evolution. *Biocatal. Biotransfor.* 31: 8-21. **Capítulo 4 de la Tesis**.

Mate, D.M., Gonzalez-Perez, D., Falk, M., Kittl, R., Pita, M., De Lacey, A.L., Ludwig, R., Shleev, S. y Alcalde, M. (**2013b**) Blood tolerant laccases by directed evolution. *Chem. Biol.* 20: 223-231. **Capítulo 5 de la Tesis**.

Matera, I., Gullotto, A., Tilli, S., Ferraroni, M., Scozzafava, A. y Briganti, F. (**2008**) Crystal structure of the blue multicopper oxidase from the white-rot fungus *Trametes trogii* complexed with *p*-toluate. *Inorg. Chim. Acta* 361: 4129-4137.

Mayer, A.M. y Staples, R.C. (**2002**) Laccase: new functions for an old enzyme. *Phytochemistry* 60: 551-565.

Mekmouche, Y., Zhou, S., Cusano, A.M., Record, E., Lomascolo, A., Robert, V., Simaan, A.J., Rousselot-Pailley, P. y Tron, T. (**2012**) Optimisation of a fungal laccase production in the host *Aspergillus niger*. *OxiZymes*. Póster. Marsella, 16-19 Septiembre.

Melo, E.P., Fernandes, A.T., Durao, P. y Martins, L.O. (**2007**) Insight into stability of CotA laccase from the spore coat of *Bacillus subtilis*. *Biochem. Soc. Trans.* 35: 1579-1582.

Messerschmidt, A., Ladenstein, R., Huber, R., Bolognesi, M., Avigliano, L., Petruzzelli, R., Rossi, A. y Finazziagro, A. (**1992**) Refined crystal-structure of ascorbate oxidase at 1.9 Å resolution. *J. Mol. Biol.* 224: 179-205.

Messerschmidt, A. (**1997**) *Multi-copper oxidases*. World Scientific (Singapur).

Miele, A., Giardina, P., Notomista, E., Piscitelli, A., Sannia, G. y Faraco, V. (**2010a**) A semi-rational approach to engineering laccase enzymes. *Mol. Biotechnol.* 46: 149-156.

Miele, A., Giardina, P., Sannia, G. y Faraco, V. (**2010b**) Random mutants of a *Pleurotus ostreatus* laccase as new biocatalysts for industrial effluents bioremediation. *J. Appl. Microbiol.* 108: 998-1006.

Miessner, M., Crescenzi, O., Napolitano, A., Prota, G., Andersen, S.O. y Peter, M.G. (**1991**) Biphenyltetrols and dibenzofuranones from oxidative coupling of resorcinols with 4-alkylpyrocatechols - New clues to the mechanism of insect cuticle sclerotization. *Helv. Chim. Acta* 74: 1205-1212.

Milligan, C. y Ghindilis, A. (**2002**) Laccase based sandwich scheme immunosensor employing mediatorless electrocatalysis. *Electroanal.* 14: 415-419.

Min, K.L., Kim, Y.H., Kim, Y.W., Jung, H.S. y Hah, Y.C. (**2001**) Characterization of a novel laccase produced by the wood-rotting fungus *Phellinus ribis*. *Arch. Biochem. Biophys.* 392: 279-286.

Miyazaki, K., Takenouchi, M., Kondo, H., Noro, N., Suzuki, M. y Tsuda, S. (**2006**) Thermal stabilization of *Bacillus subtilis* family-11 xylanase by directed evolution. *J. Biol. Chem.* 281: 10236-10242.

Mondon, P., Grand, D., Souyris, N., Emond, S., Bouayadi, K. y Kharrat, H. (**2010**) Mutagen: a random mutagenesis method providing a complementary diversity generated by human error-prone DNA polymerases. En *In vitro Mutagenesis Protocols. Methods in Molecular Biology*. Ed. J. Braman. Humana Press (Totowa, Nueva Jersey). pág. 373-386.

Moore, J. C. y Arnold, F.H. (**1996**) Directed evolution of a *para*-nitrobenzyl esterase for aqueous-organic solvents. *Nat. Biotechnol.* 14: 458-467.

Morawski, B., Lin, Z.L., Cirino, P.C., Joo, H., Bandara, G. y Arnold, F.H. (**2000**) Functional expression of horseradish peroxidase in *Saccharomyces cerevisiae* and *Pichia pastoris*. *Protein Eng.* 13: 377-384.

Morawski, B., Quan, S. y Arnold, F.H. (**2001**) Functional expression and stabilization of horseradish peroxidase by directed evolution in *Saccharomyces cerevisiae*. *Biotechnol. Bioeng.* 76: 99-107.

Morozova, O.V., Shumakovich, G.P., Gorbacheva, M.A., Shleev, S.V. y Yaropolov, A.I. (**2007a**) "Blue" laccases. *Biochemistry-Moscow* 72: 1136-1150.

Morozova, O.V, Shumakovich, G.P., Shleev, S.V. y Yaropolov, Y.I. (**2007b**) Laccase-mediator systems and their applications: A review. *Appl. Biochem. Microb.* 43: 523-535.

Moţ, A.C., Parvu, M., Damian, G., Irimie, F.D., Darula, Z., Medzihradszky, K.F., Brem, B. y Silaghi-Dumitrescu, R. (**2012**) A "yellow" laccase with "blue" spectroscopic features, from *Sclerotinia sclerotiorum*. *Process Biochem.* 47: 968-975.

Naki, A. y Varfolomeev, S.D. (**1981**) Mechanism of the inhibition of laccase activity from *Polyporus versicolor* by halide ions. *Biochemistry-Moscow* 46: 1694-1702.

Naqui, A. y Varfolomeev, S.D. (**1980**) Inhibition mechanism of *Polyporus* laccase by fluoride ion. *FEBS Lett.* 113: 157-160.

Niladevi, K.N., Jacob, N. y Prema, P. (**2008**) Evidence for a halotolerant-alkaline laccase in *Streptomyces psammoticus*: Purification and characterization. *Process Biochem.* 43: 654-660.

Nothwehr, S.F. y Gordon, J.I. (**1990**) Targeting of proteins into the eukaryotic secretory pathway - Signal peptide structure-function-relationships. *BioEssays* 12: 479-484.

Ogino, H. y Ishikawa, H. (**2001**) Enzymes which are stable in the presence of organic solvents. *J. Biosci. Bioeng.* 91: 109-116.

Oh, K.H., Nam, S.H. y Kim, H.S. (**2002**) Improvement of oxidative and thermostability of N-carbamyl-D-amino acid amidohydrolase by directed evolution. *Protein Eng.* 15: 689-695.

Okkels, J.S. (**2004**) *In vivo* gene shuffling in yeast: a fast and easy method for directed evolution of enzymes. En *Enzyme Functionality: Design, Engineering and Screening*. Ed. A. Svendsen. CRC Press (Nueva York). pág. 413-424.

Oktem, H.A., Senyurt, O., Eyidogan, F.I., Bayrac, C. y Yilmaz, R. (**2012**) Development of a laccase based paper biosensor for the detection of phenolic compounds. *J. Food Agric. Environ.* 10: 1030-1034.

Okuda-Shimazaki, J., Kakehi, N., Yamazaki, T., Tomiyama, M. y Sode, K. (**2008**) Biofuel cell system employing thermostable glucose dehydrogenase. *Biotechnol. Lett.* 30: 1753-1758.

Oldenburg, K.R., Vo, K.T., Michaelis, S. y Paddon, C. (**1997**) Recombination-mediated PCR-directed plasmid construction *in vivo* in yeast. *Nucleic Acids Res.* 25: 451-452.

Osma, J.F., Toca-Herrera, J.L. y Rodriguez-Couto, S. (**2010**) Uses of laccases in the food industry. *Enzyme Res.* 2010: 918761.

Ostermeier, M., Shim, J.H. y Benkovic, S.J. (**1999**) A combinatorial approach to hybrid enzymes independent of DNA homology. *Nat. Biotechnol.* 17: 1205-1209.

Otterbein, L., Record, E., Longhi, S., Asther, M. y Moukha, S. (**2000**) Molecular cloning of the cDNA encoding laccase from *Pycnoporus cinnabarinus* I-937 and expression in *Pichia pastoris*. *Eur. J. Biochem.* 267: 1619-1625.

Palmer, A.E., Szilagyi, R.K., Cherry, J.R., Jones, A., Xu, F. y Solomon, E.I. (**2003**) Spectroscopic characterization of the Leu513His variant of fungal laccase: Effect of increased axial ligand interaction on the geometric and electronic structure of the type 1 Cu site. *Inorg. Chem.* 42: 4006-4017.

Palmieri, G., Giardina, P., Bianco, C., Scaloni, A., Capasso, A. y Sannia, G. (**1997**) A novel white laccase from *Pleurotus ostreatus*. *J. Biol. Chem.* 272: 31301-31307.

Palmore, G.T. y Whitesides, G.M. (**1994**) Microbial and enzymatic biofuel cells. En *Enzymatic Conversion of Biomass for Fuels Production*. Eds. M.E. Himmel, J.O. Baker y R.P. Overend. ACS Symposium Series. pág. 271-290.

Pardo, I., Vicente, A.I., Mate, D.M., Alcalde, M. y Camarero, S. (**2012**) Development of chimeric laccases by directed evolution. *Biotechnol. Bioeng.* 109: 2978-2986.

Patel, P.H., Kawate, H., Adman, E., Ashbach, M., Loeb, L.K. (**2001**) A single highly mutable catalytic site amino acid is critical for DNA polymerase fidelity. *J. Biol. Chem.* 276: 5044-5051

Perez-Jimenez, R., Ingles-Prieto, A., Zhao, Z.M., Sanchez-Romero, I., Alegre-Cebollada, J., Kosuri, P., Garcia-Manyes, S., Kappock, T., Tanokura, M., Holmgren, A., Sanchez-Ruiz, J.M., Gaucher, E.A. y Fernandez, J.M. (**2011**) Single-molecule paleoenzymology probes the chemistry of resurrected enzymes. *Nat. Struct. Mol. Biol.* 18: 592-596.

Peters, M.W., Meinhold, P., Glieder, A. y Arnold, F.H. (**2003**) Regio- and enantioselective alkane hydroxylation with engineered cytochromes P450 BM-3. *J. Am. Chem. Soc.* 125**:** 13442-13450.

Piontek, K., Antorini, M. y Choinowski, T. (**2002**) Crystal structure of a laccase from the fungus *Trametes versicolor* at 1.90-angstrom resolution containing a full complement of coppers. *J. Biol. Chem.* 277: 37663-37669.

Piscitelli, A., Giardina, P., Mazzoni, C. y Sannia, G. (**2005**) Recombinant expression of *Pleurotus ostreatus* laccases in *Kluyveromyces lactis* and *Saccharomyces cerevisiae*. *Appl. Microbiol. Biot.* 69: 428-439.

Piscitelli, A., Pezzella, C., Giardina, P., Faraco, V. y Giovanni, S. (**2010**) Heterologous laccase production and its role in industrial applications. *Bioengineered.* 1: 252-262.

Pizzariello, A., Stredansky, M. y Miertus, S. (**2002**) A glucose/hydrogen peroxide biofuel cell that uses oxidase and peroxidase as catalysts by composite bulk-modified bioelectrodes based on a solid binding matrix. *Bioelectrochemistry* 56: 99-105.

Pourmir, A. y Johannes, T.W. (**2012**) Directed evolution: selection of the host microorganism. *Comput. Struct. Biotechnol. J.* 2: e201209012.

Pozdnyakova, N.N., Rodakiewicz-Nowak, J. y Turkovskaya, O.V. (**2004**) Catalytic properties of yellow laccase from *Pleurotus ostreatus* D1. *J. Mol. Catal. B-Enzym.* 30: 19-24.

Pozdnyakova, N.N., Turkovskaya, O.V., Yudina, E.N. y Rodakiewicz-Nowak, Y. (**2006a**) Yellow laccase from the fungus *Pleurotus ostreatus* D1: purification and characterization. *Appl. Biochem. Microb.* 42: 56-61.

Pozdnyakova, N.N., Rodakiewicz-Nowak, J., Turkovskaya, O.V. y Haber, J. (**2006b**) Oxidative degradation of polyaromatic hydrocarbons and their derivatives catalyzed directly by the yellow laccase from *Pleurotus ostreatus* D1. *J. Mol. Catal. B-Enzym.* 41: 8-15.

Rakestraw, J.A., Sazinsky, S.L., Piatesi, A., Antipov, E. y Wittrup, K.D. (**2009**) Directed evolution of a secretory leader for the improved expression of heterologous proteins and full-length antibodies in *Saccharomyces cerevisiae*. *Biotechnol. Bioeng.* 103: 1192-1201.

Reading, N.S. y Aust, S.D. (**2000**) Engineering a disulfide bond in recombinant manganese peroxidase results in increased thermostability. *Biotechnol. Progr.* 16: 326-333.

Record, E., Punt, P.J., Chamkha, M., Labat, M., van den Hondel, C.A.M.J.J. y Asther, M. (**2002**) Expression of the *Pycnoporus cinnabarinus* laccase gene in *Aspergillus niger* and characterization of the recombinant enzyme. *Eur. J. Biochem.* 269: 602-609.

Reetz, M.T. (**2011**) Laboratory evolution of stereoselective enzymes: A prolific source of catalysts for asymmetric reactions. *Angew. Chem. Int. Ed.* 50: 138-174.

Reetz, M.T., Carballeira, D. y Vogel, A. (**2006**) Iterative saturation mutagenesis on the basis of B factors as a strategy for increasing protein thermostability. *Angew. Chem. Int. Ed.* 45: 7745-7751.

Reetz, M.T., Kahakeaw, D. y Lohmer, R. (**2008**) Addressing the numbers problem in directed evolution. *ChemBioChem* 9: 1797-1804.

Reinhammar, B.R.M. (**1972**) Oxidation-reduction potentials of the electron acceptors in laccases and stellacyanin. *BBA-Bioenergetics* 275: 245-259.

Riva, S. (2006) Laccases: blue enzymes for green chemistry. *Trends Biotechnol.* 24: 219-226.

Robert, V., Mekmouche, Y., Pailley, P.R. y Tron, T. (**2011**) Engineering laccases: in search for novel catalysts. *Curr. Genomics* 12: 123-129.

Rodakiewicz-Nowak, J., Haber. J., Pozdnyakova, N., Leontievsky, A. y Golovleva, L.A. (**1999**) Effect of ethanol on enzymatic activity of fungal laccases. *Bioscience Rep.* 19:589-600.

Rodgers, C.J., Blanford, C.F., Giddens, S.R., Skamnioti, P., Armstrong, F.A. y Gurr, S.J. (**2010**) Designer laccases: a vogue for high-potential fungal enzymes? *Trends Biotechnol.* 28: 63-72.

Rodriguez-Mozaz, S., de Alda, M.J.L. y Barcelo, D. (**2006**) Biosensors as useful tools for environmental analysis and monitoring. *Anal. Bioanal. Chem.* 386: 1025-1041.

Romanos, M.A., Scorer, C.A. y Clare, J.J. (**1992**) Foreign gene expression in yeast - A review. *Yeast* 8: 423-488.

Romero, P.A. y Arnold, F.H. (**2009**) Exploring protein fitness landscapes by directed evolution. *Nat. Rev. Mol. Cell Bio.* 10: 866-876.

Roodveldt, C., Aharoni, A. y Tawfik, D.S. (**2005**) Directed evolution of proteins for heterologous expression and stability. *Curr. Opin. Struc. Biol.* 15: 50-56.

Ruiz-Dueñas, F.J., Martínez, M.J. y Martínez, A.T. (**1999**) Heterologous expression of *Pleurotus eryngii* peroxidase confirms its ability to oxidize Mn^{2+} and different aromatic substrates. *Appl. Environ. Microbiol.* 65**:** 4705-4707.

Ruiz-Dueñas, F.J., Morales, M., Pérez-Boada, M., Choinowski, T., Martinez, M.J., Piontek, K. y Martínez, A.T. (**2007**) Manganese oxidation site in *Pleurotus eryngii* versatile peroxidase: A site-directed mutagenesis, kinetic, and crystallographic study. *Biochemistry* 46: 66-77.

Ruiz-Dueñas, F.J., Morales, M., García, E., Miki, Y., Martinez, M.J. y Martínez, A.T. (**2009**) Substrate oxidation sites in versatile peroxidase and other basidiomycete peroxidases. *J. Exp. Bot.* 60: 441-452.

Rydén, L.G. y Hunt, L.T. (**1993**) Evolution of protein complexity: the blue copper-containing oxidases and related proteins. *J. Mol. Evol.* 36: 41-66.

Sahdev, S., Khattar, S.K. y Saini, K.S. (**2008**) Production of active eukaryotic proteins through bacterial expression systems: a review of the existing biotechnology strategies. *Mol. Cel. Biochem.* 307: 249-264.

Salazar, O. y Sun, L. (**2003**) Evaluating a screen and analysis of mutant libraries. En *Directed Enzyme Evolution: Screening and Selection Methods*. *Methods in Molecular Biology*. Eds. F.H. Arnold y G. Georgiou. Humana Press (Totowa, Nueva Jersey). pág. 85-97.

Salazar, O., Cirino, P.C. y Arnold, F.H. (**2003**) Thermostabilization of a cytochrome P450 peroxygenase. *ChemBioChem* 4: 891-893.

Saloheimo, M. y Niku-Paavola, M.L. (**1991**) Heterologous production of a ligninolytic enzyme - expression of the *Phlebia radiata* laccase gene in *Trichoderma reesei*. *Nat. Biotechnol.* 9: 987-990.

Salony, Garg, N., Baranwal, R., Chhabra, M., Mishra, S., Chaudhuri, T.K. y Bisaria, V. S. (**2008**) Laccase of *Cyathus bulleri*: structural, catalytic characterization and expression in *Escherichia coli*. *Biochim. Biophys. Acta* 1784: 259-268.

Sayut, D.J. y Sun, L. (**2010**) Creating designer laccases. *Chem. Biol.* 17: 918-920.

Schneider, P., Caspersen, M.B., Mondorf, K., Halkier, T., Skov, L.K., Ostergaard, P.R., Brown, K. M., Brown, S.H. y Xu, F. (**1999**) Characterization of a *Coprinus cinereus* laccase. *Enzyme Microb. Technol.* 25: 502-508.

Schneider, K.P., Gewessler, U., Flock, T., Heinzle, A., Schenk, V., Kaufmann, F., Sigl, E. y Guebitz, G.M. (**2012**) Signal enhancement in polysaccharide based sensors for infections by incorporation of chemically modified laccase. *New Biotechnol.* 29: 502-509.

Schückel, J., Matura, A. y van Pée, K. H. (**2011**) One-copper laccase-related enzyme from *Marasmius* sp.: Purification, characterization and bleaching of textile dyes. *Enzyme Microb. Technol.* 48: 278-284.

Scopes, R.K. (**1974**) Measurements of protein by spectrophotometry at 205 nm. *Anal. Biochem.* 59:277-282.

Shafikhani, S., Siegel, R.A., Ferrari, E. y Schellenberger, V. (**1997**) Generation of large libraries of random mutants in *Bacillus subtilis* by PCR-based plasmid multimerization. *Biotechniques* 23: 304-310.

Shaner, N.C., Lin, M.Z., McKeown, M.R., Steinbach, P.A., Hazelwood, K.L., Davidson, M.W. y Tsien, R.Y. (**2008**) Improving the photostability of bright monomeric orange and red fluorescent proteins. *Nat. Methods* 5: 545-551.

Shao, Z.Y., Zhao, H. y Zhao, H.M. (**2009**) DNA assembler, an *in vivo* genetic method for rapid construction of biochemical pathways. *Nucleic Acids Res.* 37: e16.

Shleev, S.V., Morozova, O., Nikitina, O., Gorshina, E.S., Rusinova, T., Serezhenkov, V.A., Burbaev, D.S., Gazaryan, I.G. y Yaropolov, A.I. (**2004**) Comparison of physico-chemical characteristics of four laccases from different basidiomycetes. *Biochimie* 86: 693-703.

Shleev, S., Tkac, J., Christenson, A., Ruzgas, T., Yaropolov, A.I., Whittaker, J.W. y Gorton, L. (**2005a**) Direct electron transfer between copper-containing proteins and electrodes. *Biosens. Bioelectron.* 20: 2517-2554.

Shleev, S., Jarosz-Wilkolazka, A., Khalunina, A., Morozova, O., Yaropolov, A., Ruzgas, T. y Gorton, L. (**2005b**) Direct electron transfer reactions of laccases from different origins on carbon electrodes. *Bioelectrochemistry* 67: 115-124.

Shleev, S., Nikitina, O., Christenson, A., Reimann, C.T., Yaropolov, A.I., Ruzgas, T. y Gorton, L. (**2007**) Characterization of two new multiforms of *Trametes pubescens* laccase. *Bioorg. Chem.* 35: 35-49.

Shleev, S. y Ruzgas, T. (**2008**) Transistor-like behavior of a fungal laccase. *Angew. Chem. Int. Ed.* 47: 7270-7274.

Shivange, A.V., Marienhagen, J., Mundhada, H., Schenk, A. y Schwaneberg, U. (**2009**) Advances in generating functional diversity for directed protein evolution. *Curr. Opin. Chem. Biol.* 13: 19-25.

Shuster, J.R. (**1991**) Gene expression in yeast: protein secretion. *Curr. Opin. Biotech.* 2: 685-690.

Sieber, V., Martinez, C.A. y Arnold, F.H. (**2001**) Libraries of hybrid proteins from distantly related sequences. *Nat. Biotechnol.* 19: 456-460.

Singh, G., Bhalla, A., Kaur, P., Capalash, N. y Sharma, P. (**2011**) Laccase from prokaryotes: A new source for an old enzyme. *Rev. Environ. Sci. Biotechnol.* 10: 309-326.

Soden, D.M., O'Callaghan, J. y Dobson, A.D.W. (**2002**) Molecular cloning of a laccase isozyme gene from *Pleurotus sajor-caju* and expression in the heterologous *Pichia pastoris* host. *Microbiology* 148: 4003-4014.

Solomon, E.I., Sundaram, U.M. y Machonkin, T.E. (**1996**) Multicopper oxidases and oxygenases. *Chem. Rev.* 96**:** 2563-2605.

Sonoki, T., Kajita, S., Ikeda, S., Uesugi, M., Tatsumi, K., Katayama, Y. y Iimura, Y. (**2005**) Transgenic tobacco expressing fungal laccase promotes the detoxification of environmental pollutants. *Appl. Microbiol. Biot.* 67: 138-142.

Soukharev, V., Mano, N. y Heller, A. (**2004**) A four-electron O_2-electroreduction biocatalyst superior to platinum and a biofuel cell operating at 0.88 V. *J. Am. Chem. Soc.* 126: 8368-8369.

Sreerama, N. y Woody, R.W. (**1994**) Poly(Pro)II helixes in globular proteins - Identification and circular dichroic analysis. *Biochemistry* 33:10022-10025.

Stemmer, W.P.C. (**1994**) Rapid evolution of a protein *in vitro* by DNA shuffling. *Nature* 370: 389-391.

Stoica, L., Dimcheva, N., Ackermann, Y., Karnicka, K., Guschin, D.A., Kulesza, P.J., Rogalski, J., Haltrich, D., Ludwig, R., Gorton, L. y Schuhmann, W. (**2009**) Membrane-less biofuel cell based on

cellobiose dehydrogenase (anode)/laccase (cathode) wired via specific os-redox polymers. *Fuel Cells* 9: 53-62.

Suen, W. C., Zhang, N. Y., Xiao, L., Madison, V. y Zaks, A. (**2004**) Improved activity and thermostability of *Candida antarctica* lipase B by DNA family shuffling. *Protein Eng. Des. Sel.* 17: 133-140.

Sun, L., Petrounia, I.P., Yagasaki, M., Bandara, G. y Arnold, F.H. (**2001**) Expression and stabilization of galactose oxidase in *Escherichia coli* by directed evolution. *Protein Eng.* 14: 699-704.

Terron, M.C., Gonzalez, T., Carbajo, J.M., Yague, S., Arana-Cuenca, A., Tellez, A., Dobson, A.D. W. y Gonzalez, A.E. (**2004**) Structural close-related aromatic compounds have different effects on laccase activity and on lcc gene expression in the ligninolytic fungus *Trametes* sp. I-62. *Fungal Genet. Biol.* 41**:** 954-962.

Theerachat, M., Emond, S., Cambon, E., Bordes, F., Marty, A., Nicaud, J., Chulalaksananukul, W., Guieysse, D., Remaud-Simeon, M. y Morel, S. (**2012**) Engineering and production of laccase from *Trametes versicolor* in the yeast *Yarrowia lipolytica*. *Bioresource Technol.* 125**:** 267-274.

Thurston, C.F. (**1994**) The structure and function of fungal laccases. *Microbiology* 140: 19-26.

Tobias, A.V. y Joern, J.M. (**2003**) Solid-phase screening using digital image analysis. En *Directed Enzyme Evolution: Screening and Selection Methods*. *Methods in Molecular Biology*. Eds. F.H. Arnold y G. Georgiou. Humana Press (Totowa, Nueva Jersey). pág. 109-115.

Torres-Salas, P., Mate, D.M., Ghazi, I., Plou, F.J., Ballesteros, A.O. y Alcalde, M. (**2013**) Widening the pH activity profile of a fungal laccase by directed evolution. *ChemBioChem*. DOI: 10.1002/cbic.201300102.

Tracewell, C.A. y Arnold, F.H. (**2009**) Directed enzyme evolution: climbing fitness peaks one amino acid at a time. *Curr. Opin. Chem. Biol.* 13: 3-9.

Trudeau, F., Daigle, F. y Leech, D. (**1997**) Reagentless mediated laccase electrode for the detection of enzyme modulators. *Anal. Chem.* 69: 882-886.

Tuller, T., Waldman, Y.Y., Kupiec, M. y Ruppin, E. (**2010**) Translation efficiency is determined by both codon bias and folding energy. *P. Natl. Acad. Sci. USA* 107: 3645-3650.

Van den Burg, B., Vriend, G., Veltman, O.R. y Eijsink, V.G.H. (**1998**) Engineering an enzyme to resist boiling. *P. Natl. Acad. Sci. USA* 95**:** 2056-2060.

Vaz-Dominguez, C., Campuzano, S., Rudiger, O., Pita, M., Gorbacheva, M., Shleev, S., Fernandez, V.M. y De Lacey, A.L. (**2008**) Laccase electrode for direct electrocatalytic reduction of O_2 to H_2O with high-operational stability and resistance to chloride inhibition. *Biosens. Bioelectron.* 24**:** 531-537.

Wahleithner, J.A., Xu, F., Brown, K.M., Brown, S.H., Golightly, E.J., Halkier, T., Kauppinen, S., Pederson, A. y Schneider, P. (**1996**) The identification and characterization of four laccases from the plant pathogenic fungus *Rhizoctonia solani*. *Curr. Genet.* 29: 395-403.

Wang, C.Q., Eufemi, M., Turano, C. y Giartosio, A. (**1996**) Influence of the carbohydrate moiety on the stability of glycoproteins. *Biochemistry* 35: 7299-7307.

Wang, L.J., Kong, X.D., Zhang, H.Y., Wang, X.P. y Zhang, J. (**2000**) Enhancement of the activity of L-aspartase from *Escherichia coli* W by directed evolution. *Biochem. Bioph. Res. Co.* 276**:** 346-349.

Wang, M., Si, T. y Zhao, H. (**2012**) Biocatalyst development by directed evolution. *Bioresource Technol.* 115: 117-125.

Watanabe, K., Ohkuri, T., Yokobori, S. y Yamagishi, A. (**2006**) Designing thermostable proteins: Ancestral mutants of 3-isopropylmalate dehydrogenase designed by using a phylogenetic tree. *J. Mol. Biol.* 355: 664-674.

Widsten, P. y Kandelbauer, A. (**2008**) Laccase applications in the forest products industry: A review. *Enzyme Microb. Technol.* 42: 293-307.

Witayakran, S. y Ragauskas, A.J. (**2009**) Synthetic applications of laccase in green chemistry. *Adv. Synth. Catal.* 351: 1187-1209.

Wong, T.S., Arnold, F.H. y Schwaneberg, U. (**2004a**) Laboratory evolution of cytochrome P450 BM-3 monooxygenase for organic cosolvents. *Biotechnol. Bioeng.* 85: 351-358.

Wong, T.S., Tee, K.L., Hauer, B. y Schwaneberg, U. (**2004b**) Sequence saturation mutagenesis (SeSaM): a novel method for directed evolution. *Nucleic Acids Res.* 32: e26.

Wong, T.S., Zhurina, D. y Schwaneberg, U. (**2006**) The diversity challenge in directed protein evolution. *Comb. Chem. High T. Scr.* 9: 271-288.

Wong, T.S., Roccatano, D. y Schwaneberg, U. (**2007**) Steering directed protein evolution: strategies to manage combinatorial complexity of mutant libraries. *Environ. Microbiol.* 9: 2645-2659.

Wood, D.A. (**1980**) Production, purification and properties of extracellular laccase of *Agaricus bisporus*. *J. Gen. Microbiol.* 117: 327-338.

Wymer, N., Buchanan, L.V., Henderson, D., Mehta, N., Botting, C.H., Pocivavsek, L., Fierke, C. A., Toone, E.J. y Naismith, J.H. (**2001**) Directed evolution of a new catalytic site in 2-keto-3-deoxy-6-phosphogluconate aldolase from *Escherichia coli*. *Structure* 9: 1-9.

Xu, F. (**1996a**) Catalysis of novel enzymatic iodide oxidation by fungal laccase. *Appl. Biochem. Biotech.* 59: 221-230.

Xu, F. (**1996b**) Oxidation of phenols, anilines, and benzenethiols by fungal laccases: Correlation between activity and redox potentials as well as halide inhibition. *Biochemistry* 35: 7608-7614.

Xu, F. (**1997**) Effects of redox potential and hydroxide inhibition on the pH activity profile of fungal laccases. *J. Biol. Chem.* 272: 924-928.

Xu, F. (**2001**) Dioxygen reactivity of laccase - Dependence of laccase source, pH, and anion inhibition. *Appl. Biochem. Biotech.* 95: 125-133.

Xu, F. (**2005**) Applications of oxidoreductases: recent progress. *Industrial Biotechnol.* 1: 38-50.

Xu, F., Berka, R.M., Wahleithner, J.A., Nelson, B.A., Shuster, J.R., Brown, S.H., Palmer, A.E. y Solomon, E.I. (**1998**) Site-directed mutations in fungal laccase: effect on redox potential, activity and pH profile. *Biochemical J.* 334: 63-70.

Xu, F., Palmer, A.E., Yaver, D.S., Berka, R.M., Gambetta, G.A., Brown, S.H. y Solomon, E.I. (**1999**) Targeted mutations in a *Trametes villosa* laccase - Axial perturbations of the T1 copper. *J. Biol. Chem.* 274: 12372-12375.

Yaropolov, A.I., Skorobogatko, O.V., Vartanov, S.S. y Varfolomeyev, S.D. (**1994**) Laccase - Properties, catalytic mechanism, and applicability. *Appl. Biochem. Biotech.* 49: 257-280.

Yaver, D.S., Overjero, A.I., Xu, F., Nelson, B.A., Brown, K.M., Halkier, T., Bernauer, S., Brown, S.H. y Kauppinen, S. (**1999**) Molecular characterization of laccase genes from the basidiomycete *Coprinus cinereus* and heterologous expression of the laccase Lcc1. *Appl. Environ. Microbiol.* 65: 4943-4948.

Yoon, S.H., Kim, S.K. y Kim, J.F. (**2010**) Secretory production of recombinant proteins in *Escherichia coli*. *Recent Pat. Biotechnol.* 4: 23-29.

Yoshida, H. (**1883**) LXIII.-Chemistry of lacquer (Urushi). Part I. Communication from the Chemical Society of Tokio. *J. Chem. Soc. Trans.* 43: 472-486.

You, L. y Arnold, F.H. (**1996**) Directed evolution of subtilisin E in *Bacillus subtilis* to enhance total activity in aqueous dimethylformamide. *Protein Eng.* 9: 77-83.

Zafar, M.N., Beden, N., Leech, D., Sygmund, C., Ludwig, R. y Gorton, L. (**2012**) Characterization of different FAD-dependent glucose dehydrogenases for possible use in glucose-based biosensors and biofuel cells. *Anal. Bioanal. Chem.* 402: 2069-2077.

Zhao, H.M., Giver, L., Shao, Z. X., Affholter, J. A. y Arnold, F.H. (**1998**) Molecular evolution by staggered extension process (StEP) *in vitro* recombination. *Nat. Biotechnol.* 16: 258-261.

Zhao, H.M. y Arnold, F.H. (**1999**) Directed evolution converts subtilisin E into a functional equivalent of thermitase. *Protein Eng.* 12: 47-53.

Zhu, X. D. y Williamson, P. R. (**2004**) Role of laccase in the biology and virulence of *Cryptococcus neoformans*. *FEMS Yeast Res.* 5: 1-10.

Zouari, N., Romette, J.L. y Thomas, D. (**1988**) A continuous-flow method for the rapid-determination of sanitary quality of grape must at industrial-scales. *J. Chem. Technol. Biot.* 41: 243-248.

Zsebo, K.M., Lu, H.S., Fieschko, J.C., Goldstein, L., Davis, J., Duker, K., Suggs, S.V, Lai, P.H. y Bitter, G.A. (**1986**) Protein secretion from *Saccharomyces cerevisiae* directed by the prepro-α-factor leader region. *J. Biol. Chem.* 261:5858-5865.

Zumárraga, M., Bulter, T., Shleev, S., Polaina, J., Martínez-Arias, A., Plou, F.J., Ballesteros, A. y Alcalde, M. (**2007a**) *In vitro* evolution of a fungal laccase in high concentrations of organic cosolvents. *Chem. Biol.* 14: 1052-1064.

Zumárraga, M., Plou, F.J., García-Arellano, H., Ballesteros, A. y Alcalde, M. (**2007b**) Bioremediation of polycyclic aromatic hydrocarbons by fungal laccases engineered by directed evolution. *Biocatal. Biotransfor.* 25: 219-228.

Zumárraga, M., Camarero, S., Shleev, S., Martínez-Arias, A., Ballesteros, A., Plou, F.J. y Alcalde, M. (**2008a**) Altering the laccase functionality by *in vivo* assembly of mutant libraries with different mutational spectra. *Proteins* 71: 250-260.

Zumárraga, M., Domínguez, C.V., Camarero, S., Shleev, S., Polaina, J., Martínez-Arias, A., Ferrer, M., De Lacey, A.L., Fernandez, V., Ballesteros, A., Plou, F.J. y Alcalde, M. (**2008b**) Combinatorial saturation mutagenesis of the *Myceliophthora thermophila* laccase T2 mutant: the connection between the C-terminal plug and the conserved $_{509}$VSG$_{511}$ tripeptide. *Comb. Chem. High T. Scr.* 11: 807-816.

5. ANEXOS

5.1. ANEXO I

I. Publicaciones científicas

1. Maté, D., García-Burgos, C., García-Ruiz, E., Ballesteros, A.O., Camarero, S. y Alcalde, M. (**2010**). Laboratory evolution of high-redox potential laccases. *Chem. Biol.* 17: 1030-1041. **Capítulo 1 de la Tesis**.

2. García-Ruiz, E., Maté, D., Ballesteros, A., Martinez, A.T. y Alcalde, M. (**2010**). Evolving thermostability in mutant libraries of ligninolytic oxidoreductases expressed in yeast. *Microb. Cell. Fact.* 9: 17. **Capítulo 2 de la Tesis**.

3. Maté, D., García-Burgos, C., García-Ruiz, E., Ballesteros, A. O., Camarero, S. y Alcalde, M. (**2010**). High-redox potential laccases engineered by directed evolution. En *Proceedings of the oxidative enzymes as sustainable industrial biocatalysts*. Eds. G. Feijoo y M.T. Moreira. Santiago de Compostela. ISBN: 978-84-614-2824-3. pág. 115-119.

4. Maté, D., García-Ruiz, E., Camarero, S. y Alcalde, M. (**2011**). Directed evolution of fungal laccases. *Curr. Genomics* 12: 113-122. **Capítulo 3 de la Tesis**.

5. Pardo, I., Vicente, A.I., Mate, D.M., Alcalde, M. y Camarero, S. (**2012**). Development of chimeric laccases by directed evolution. *Biotechnol. Bioeng.* 109: 2978-2986.

6. Mate, D.M., Garcia-Ruiz, E., Camarero, S., Shubin, V.V., Falk, M., Shleev, S., Ballesteros, A.O. y Alcalde, M. (**2013**) Switching from blue to yellow: altering the spectral properties of a high redox potential laccase by directed evolution. *Biocatal. Biotransfor.* 31: 8-21. **Capítulo 4 de la Tesis**.

7. Mate, D.M., Gonzalez-Perez, D., Falk, M., Kittl, R., Pita, M., De Lacey, A.L., Ludwig, R., Shleev, S. y Alcalde, M. (**2013**) Blood tolerant laccases by directed evolution. *Chem. Biol.* 20: 223-231. **Capítulo 5 de la Tesis**.

8. Mate, D.M., Gonzalez-Perez, D., Kittl, R., Ludwig, R. y Alcalde, M. Functional expression of a blood tolerant laccase in *Pichia pastoris*. *BMC Biotechnol*. 13: 38. **Capítulo 6 de la Tesis**.

9. Torres-Salas, P., Mate, D.M., Ghazi, I., Plou, F.J., Ballesteros, A.O. y Alcalde, M. (**2013**) Widening the pH activity profile of a fungal laccase by directed evolution. *ChemBioChem*. DOI: 10.1002/cbic.201300102.

II. Patentes

1. Maté, D., Valdivieso, M., Fernández, L. y Alcalde, M. Laccase with high redox potential. Patente internacional WO 2011/144784.

2. Maté, D., González, D., Falk, M., Kittl, R., Pita, M., López, A., Ludwig, R., Shleev, S. y Alcalde, M. Lacasa de alto potencial redox funcional en sangre mediante evolución dirigida, método de obtención y sus aplicaciones. Patente española P201330222.

III. Trabajos presentados en congresos

1. Maté, D., Fernández, L., García-Burgos, C., Valdivieso, M., Plou, F.J., Ballesteros, A. y Alcalde, M. (**2009**) Directed evolution of a high redox potential laccase. *ProStab 2009: 8th International Conference on Protein Stabilisation.* Graz (Austria). 14-17 Abril.

2. Maté, D., García-Burgos, C., García-Ruiz, E., Ballesteros, A., Camarero, S. y Alcalde, M. (**2010**) High redox potential laccases engineered by directed evolution. *Oxidative Enzymes as Sustainable Industrial Biocatalysts.* Santiago de Compostela (España). 14-15 Septiembre.

3. Maté, D., García-Ruiz, E., Moshtaghioun, M., Camarero, S. y Alcalde, M. (**2010**) Directed evolution of a high redox potential laccase in *Saccharomyces cerevisiae*: improving functional expression, thermostability and kinetic properties. *III Congreso de Microbiología Industrial y Biotecnología Microbiana (CMIBM2010).* Alcalá de Henares (España). 17-19 Noviembre.

4. Maté, D., Shleev, S. y Alcalde, M. (**2011**) Altering the spectral properties of a high redox potential laccase by directed evolution: from blue to yellow. *Biotrans 2011: 10th International Symposium on Biocatalysis and Biotransformations.* Giardini Naxos (Italia). 2-6 Octubre.

5. Garcia-Ruiz, E., Mate, D., Gonzalez-Perez, D., Roman, A., Molina, P., Torres, P., Zumarraga, M., Camarero, S., Ballesteros, A., Plou, F.J. y Alcalde, M. (**2011**) *Saccharomyces cerevisiae* in directed evolution: an efficient tool to improve enzymes. *Biotrans 2011: 10th International Symposium on Biocatalysis and Biotransformations.* Giardini Naxos (Italia). 2-6 Octubre.

6. Pardo, I., Mate, D., Alcalde, M. y Camarero, S. (**2011**) Obtaining chimeric laccases by directed evolution. *Biotrans 2011: 10th International Symposium on Biocatalysis and Biotransformations.* Giardini Naxos (Italia). 2-6 Octubre.

7. Camarero, S., Pardo, I., Mate, D. y Alcalde, M. (**2011**) Engineering platforms for the directed evolution of ligninolytic laccases. *Biotrans 2011: 10th International Symposium on Biocatalysis and Biotransformations.* Giardini Naxos (Italia). 2-6 Octubre.

8. Molina-Espeja, P., Garcia-Ruiz, E., Gonzalez-Perez, D., Mate, D.M. y Alcalde, M. (**2012**) Directed evolution of α-factor prepro-leader fusion genes for functional expression in *Saccharomyces cerevisiae*. *Multistep Enzyme-Catalyzed Processes 2012.* Graz (Austria). 10-13 Abril.

9. Ballesteros, A.O., Plou, F.J., Alcalde, M., Fernandez-Arrojo, L., Torres-Salas, P., Rodriguez-Colinas, B., Garcia-Ruiz, E., Mate, D.M., Lozano, R., Gonzalez-Perez, D., Molina, P., Sandoval, G. y Santos, P. (**2012**) Applications of biocatalysts in sustainable chemistry. Directed evolution and semi-rational approaches. *Biocat 2012: 6th International Congress on Biocatalysis.* Hamburgo (Alemania). 2-6 Septiembre.

IV. Comunicaciones orales presentadas en congresos

Maté, D., Plou, F.J. y Alcalde, M. (**2011**) Biocatalysts improved by directed evolution: laccases for green chemistry. *VIII Simposio de Jóvenes Investigadores RSEQ-Sigma Aldrich.* Torremolinos (España). 25-28 Octubre.

5.2. ANEXO II

Secuencia completa del gen de la lacasa PM1 fusionado con el prepro-líder del factor α de *S. cerevisiae*. Las mutaciones introducidas en los mutantes OB-1 y ChU-B aparecen subrayadas.

pre-líder del factor α (57 pb, 19 aminoácidos); **pro-líder del factor α** (192 pb, 64 aminoácidos); **sitio de corte de *KEX2*** (6 pb, 2 aminoácidos); **sitio de corte de *STE13*** (12 pb, 4 aminoácidos); **sitio de corte de *Eco*RI** (6 pb, 2 aminoácidos); proteína madura (1488 pb, 496 aminoácidos); **mutaciones de OB-1** (presentes también en ChU-B); **mutaciones exclusivas de ChU-B**.

```
1     ATG AGA TTT CCT TCA ATT TTT ACT GCT GAT TTA TTC GCA GCA TCC   45
1      M   R   F   P   S   I   F   T   A   D   L   F   A   A   S   15

46    TCC GCA TTA GCT GCT CCA GTC AAA ACT ACA ACA AAA GAT GAA ACG   90
16     S   A   L   A   A   P   V   K   T   T   T   K   D   E   T   30

91    GCA CAA ATT CCG GCT GAA GCT GTC ATC GGT TAC TCA GAT TTA GAA   135
31     A   Q   I   P   A   E   A   V   I   G   Y   S   D   L   E   45

136   GGG GAT TTC GAC GTT GCT GTT TTG CCA TTT TCC AAC AGC ACA AAT   180
46     G   D   F   D   V   A   V   L   P   F   S   N   S   T   N   60

181   AAC GGA TTA TTG TTT ATG AAT ACT ACT ATT GCC AGC ATT GCT GCT   225
61     N   G   L   L   F   M   N   T   T   I   A   S   I   A   A   75

226   AAA GAA GAA GGG GTA TCT CTC GAG AAA AGA GAG ACT GAA GCT GAG   270
76     K   E   E   G   V   S   L   E   K   R   E   T   E   A   E   90

271   TTC AGC ATT GGG CCA GTC GCA GAC CTC ACC ATC TCC AAC GGT GCT   315
91     F   S   I   G   P   V   A   D   L   T   I   S   N   G   A   105

316   GTC AGT CCC GAT GGT TTC TCT CGG CAG GCC ATC CTG GTC AAC GAC   360
106    V   S   P   D   G   F   S   R   Q   A   I   L   V   N   D   120

361   GTC TTC CCC AGT CCC CTC ATT ACG GGG AAC AAG GGT GAT CGT TTC   405
121    V   F   P   S   P   L   I   T   G   N   K   G   D   R   F   135

406   CAA CTC AAT GTC ATC GAC AAC ATG ACC AAC CAC ACC ATG TTG AAG   450
136    Q   L   N   V   I   D   N   M   T   N   H   T   M   L   K   150

451   TCC ACC AGT ATC CAT TGG CAC GGC TTC TTC CAG CAC GGC ACC AAC   495
151    S   T   S   I   H   W   H   G   F   F   Q   H   G   T   N   165

496   TGG GCC GAC GGC CCC GCC TTC GTG AAC CAG TGC CCG ATT TCT ACC   540
166    W   A   D   G   P   A   F   V   N   Q   C   P   I   S   T   180

541   GGG CAT GCG TTC CTT TAC GAC TTC CAG GTC CCT GAC CAA GCT GGT   585
181    G   H   A   F   L   Y   D   F   Q   V   P   D   Q   A   G   195

586   ACT TTC TGG TAC CAC AGT CAC TTG TCC ACT CAA TAC TGT GAC GGT   630
196    T   F   W   Y   H   S   H   L   S   T   Q   Y   C   D   G   210
```

```
631   CTC AGG GGT CCG ATT GTT GTC TAT GAC CCT CAA GAT CCC CAC AAG   675
211    L   R   G   P   I   V   V   Y   D   P   Q   D   P   H   K    225

676   AGC CTT TAC GAT GTT GAT GAC GAC TCC ACT GTA ATC ACT CTC GCG   720
226    S   L   Y   D   V   D   D   D   S   T   V   I   T   L   A    240

721   GAT TGG TAC CAC TTG GCT GCC AAA GTC GGC CCG GCG GCC CCG ACT   765
241    D   W   Y   H   L   A   A   K   V   G   P   A   A   P   T    255

766   GCC GAT GCT ACT CTT ATC AAC GGC CTC GGT CGC AGC ATC AAC ACG   810
256    A   D   A   T   L   I   N   G   L   G   R   S   I   N   T    270

811   CTC AAC GCC GAT TTG GCT GTC ATC ACG GTC ACG AAG GGC AAG CGC   855
271    L   N   A   D   L   A   V   I   T   V   T   K   G   K   R    285

856   TAT CGC TTC CGC CTG GTG TCG CTG TCA TGC GAC CCG AAT TAC ACG   900
286    Y   R   F   R   L   V   S   L   S   C   D   P   N   Y   T    300

901   TTC AGC ATT GAT GGT CAC TCT CTG ACC GTC ATC GAG GCG GAC GGC   945
301    F   S   I   D   G   H   S   L   T   V   I   E   A   D   G    315

946   GTG AAT CTC AAG CCC CAG ACT GTC GAC TCC ATC CAG ATC TTC CCT   990
316    V   N   L   K   P   Q   T   V   D   S   I   Q   I   F   P    330

991   GCC CAG CGG TAC TCG TTT GTG CTC AAC GCA GAT CAG GAT GTG GAC   1035
331    A   Q   R   Y   S   F   V   L   N   A   D   Q   D   V   D    345

1036  AAC TAC TGG ATC CGT GCC CTT CCC AAC TCC GGG ACC AGG AAC TTC   1080
346    N   Y   W   I   R   A   L   P   N   S   G   T   R   N   F    360

1081  GAC GGC GGC GTT AAC TCC GCC ATC CTT CGC TAC GAA GGT GCT GCG   1125
361    D   G   G   V   N   S   A   I   L   R   Y   E   G   A   A    375

1126  CCC GTT GAG CCC ACC ACG ACC CAG ACG CCG TCG ACG CAG CCT TTG   1170
376    P   V   E   P   T   T   T   Q   T   P   S   T   Q   P   L    390

1171  GTG GAG TCC GCC CTG ACC ACT CTC GAA GGC ACC GCT GCG CCC GGC   1215
391    V   E   S   A   L   T   T   L   E   G   T   A   A   P   G    405

1216  AAC CCG ACC CCT GGC GGT GTC GAC CTG GCT CTC AAC ATG GCT TTC   1260
406    N   P   T   P   G   G   V   D   L   A   L   N   M   A   F    420

1261  GGC TTT GCC GGC GGC AGG TTC ACC ATC AAC GGC GCG AGC TTC ACC   1305
421    G   F   A   G   G   R   F   T   I   N   G   A   S   F   T    435

1306  CCG CCC ACC GTC CCC GTC CTC CTG CAG ATC CTG AGC GGC GCG CAG   1350
436    P   P   T   V   P   V   L   L   Q   I   L   S   G   A   Q    450

1351  TCG GCG CAG GAC CTC CTC CCC TCT GGA AGT GTA TAC TCG CTC CCT   1395
451    S   A   Q   D   L   L   P   S   G   S   V   Y   S   L   P    465

1396  GCG AAC GCG GAC ATT GAA ATC TCC CTC CCC GCC ACC TCC GCC GCC   1440
466    A   N   A   D   I   E   I   S   L   P   A   T   S   A   A    480

1441  CCC GGC TTC CCG CAC CCC ATC CAC TTG CAC GGG CAC ACC TTC GCC   1485
481    P   G   F   P   H   P   I   H   L   H   G   H   T   F   A    495
```

```
1486  GTC GTG CGC AGC GCC GGC TCG TCG ACA TAC AAC TAC GCG AAC CCG   1530
496    V   V   R   S   A   G   S   S   T   Y   N   Y   A   N   P    510

1531  GTC TAC CGC GAC GTC GTC AAC ACG GGC TCG CCC GGG GAC AAC GTC   1575
511    V   Y   R   D   V   V   N   T   G   S   P   G   D   N   V    525

1576  ACG ATC CGG TTC AGG ACG GAC AAC CCC GGC CCG TGG TTC CTC CAC   1620
526    T   I   R   F   R   T   D   N   P   G   P   W   F   L   H    540

1621  TGC CAC ATC GAC GAG CAC CTT GAG GCT GGG TTC ACG GTC GTC ATG   1665
541    C   H   I   D   E   H   L   E   A   G   F   T   V   V   M    555

1666  GCC GAG GAC ATT CCC GAC GTC GCC GCT ACG AAC CCG GTC CCG CAA   1710
556    A   E   D   I   P   D   V   A   A   T   N   P   V   P   Q    570

1711  GCA TGG TCG GAT CTG TGC CCG ACC TAT GAT GCG CTC TCG CCT GAC   1755
571    A   W   S   D   L   C   P   T   Y   D   A   L   S   P   D    585

1756  GAC CAG TAA  1764
586    D   Q   *
```